ZooKeys 685: 1–14 (2017)
doi: 10.3897/zookeys.685.11341
http://zookeys.pensoft.net

RESEARCH ARTICLE

A peer-reviewed open-access journal
ZooKeys
Launched to accelerate biodiversity research

# A new species of deep-sea sponge-associated shrimp from the North-West Pacific (Decapoda, Stenopodidea, Spongicolidae)

Peng Xu[1], Yadong Zhou[1], Chunsheng Wang[1,2]

**1** *Laboratory of Marine Ecosystem and Biogeochemistry, Second Institute of Oceanography, State Oceanic Administration, Hangzhou, 310012, China* **2** *State Key Laboratory of Satellite Ocean Environment Dynamics, Second Institute of Oceanography, State Oceanic Administration, Hangzhou, 310012, China*

Corresponding author: *Chunsheng Wang* (wangsio@sio.org.cn)

Academic editor: *I. Wehrtmann* | Received 27 November 2016 | Accepted 31 May 2017 | Published 13 July 2017

*http://zoobank.org/22713130-2770-47E2-A29D-12C3A9BBB5F6*

**Citation:** Xu P, Zhou Y, Wang C (2017) A new species of deep-sea sponge-associated shrimp from the North-West Pacific (Decapoda, Stenopodidea, Spongicolidae). ZooKeys 685: 1–14. https://doi.org/10.3897/zookeys.685.11341

## Abstract

A new species of the deep-sea spongicolid genus *Spongicoloides* Hansen, 1908 is described and illustrated based on material from the northwestern Pacific. *Spongicoloides weijiaensis* **sp. n.** was found inside a hexactinellid sponge, *Euplectella* sp., sampled by the Chinese manned submersible "Jiaolong" at depths of 2279 m near the Weijia Guyot, in the Magellan Seamount Chain. The new species can be distinguished from all congeneric species by several morphological features, involving gill formula, spination of the carapace, antennal scale, third pereiopod, telson and uropod, posteroventral teeth of the pleura, and dactyli of the fourth and fifth pereiopods. An identification key to the Pacific species of *Spongicoloides* is provided.

## Keywords

Hexactinellida, Magellan Seamount Chain, *Spongicoloides*, Weijia Guyot

## Introduction

The stenopodidean shrimp family Spongicolidae is a relatively small group of marine decapod crustaceans. Based on its gill formula and external morphological features, the genus *Spongicoloides* Hansen, 1908 represents the most derived group

among spongicolid genera (Saito and Takeda 2003). Although de Saint Laurent and Cleva (1981) synonymized *Spongiocaris* Bruce & Baba, 1973 with *Spongicoloides* and emended the generic diagnosis of *Spongicoloides*, Holthuis (1993) maintained *Spongiocaris* as a valid genus and his classification was followed by subsequent workers (e.g., Berggren 1993, Ortiz et al. 2007, Komai and Saito 2006, Saito and Komai 2008, Goy 2015, González et al. 2016, Komai et al. 2016). The presence of the exopod on the second maxilliped is the major characteristic used to distinguish *Spongiocaris* from *Spongicoloides*, so Saito (2008) transferred *Spongicoloides koehleri* (Caullery, 1896) to *Spongiocaris*. Chen et al. (2016) attempted to solve the controversial higher taxonomy of infraorder Stenopodidea using sequence data from both mitochondrial and nuclear genes. All their findings indicated that the morphological characters currently adopted to define genera are mostly invalid and substantial taxonomic revisions are required. Although they suggested that the genera such as *Spongicola* de Haan, 1844, *Spongicoloides* and *Spongiocaris* need to be redefined and revised with particular caution in the future, we accept *Spongicoloides* as a valid genus for the time being in this study. Eight species are currently known in *Spongicoloides*, and the loss of gills and the loss of spination on some body parts (carapace, pereiopods, pleon and tail fan) are thought to be secondarily derived in relation to the shrimps' highly specialized sponge-dwelling habits.

In May of 2016, during Dive 106 of the Chinese manned submersible "Jiaolong", one specimen of a hexactinellid sponge, *Euplectella* sp. (Fig. 1A, B), was sampled at a depth of 2279 m near Weijia Guyot, part of the Magellan Seamount Chain in the northwestern Pacific. On board of the vessel, a pair of spongicolid shrimps (Fig. 1C, D) was found inside this sponge. Since the absence of exopods on the second and third maxillipeds is one of the most important characteristics of *Spongicoloides*, the shrimps were assigned to that genus. After a careful comparison with all congeneric species, they were confirmed to be a new species, which is described and illustrated in this study, representing the ninth species of the genus.

## Materials and methods

The type specimens were preserved in 80% ethanol and deposited in the Sample Repository of Second Institute of Oceanography (SRSIO), State Oceanic Administration, Hangzhou, China.

Marginal spines of the telson are counted as: spines on the lateral margin; spine on the posterolateral angle, at the termination point of the dorsolateral carina; and spines on the posterior margin. Postorbital carapace length (in mm) is abbreviated as **cl** in the text. In the laboratory, photographs were taken using a dissecting microscope (Zeiss Discovery V20) equipped with a camera (AxioCam ICc5). Line drawings were made with the aid of a drawing tube mounted on a LEICA M205 C stereomicroscope. Setae have been omitted from illustrations for clarity.

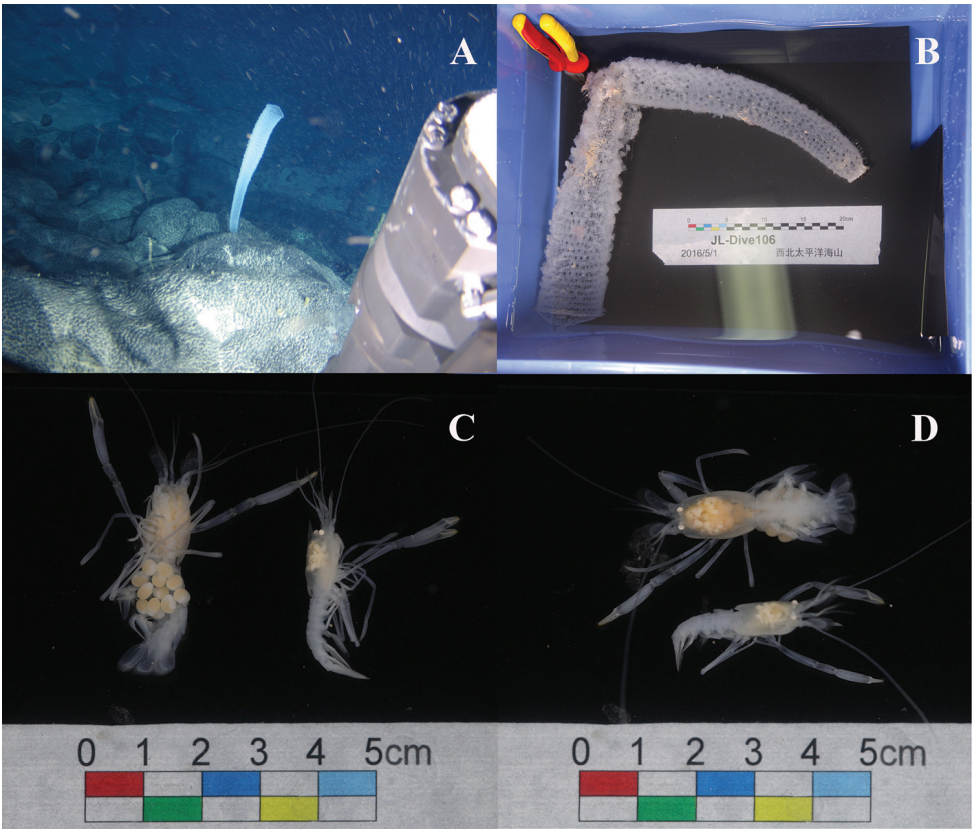


**Figure 1.** Hexactinellid sponge, *Euplectella* sp., *in situ* (**A**) and shortly after collection (**B**) **C, D** *Spongicoloides weijiaensis* sp. n., ovigerous female and male shortly after extraction from the host sponge.

## Systematics

**Family Spongicolidae Schram, 1986**
**Genus *Spongicoloides* Hansen, 1908**

***Spongicoloides weijiaensis* sp. n.**
http://zoobank.org/7BB95D26-0799-4078-B8F2-8C0AB4883D79
Figs 2–5

**Material examined.** Holotype: ovigerous female, cl 11.1 mm, 13°01.01'N, 156°56.71'E, near Weijia Guyot, Magellan Seamount Chain, North West Pacific, depth: 2279 m, associated with hexactinellid sponge, coll. team of "Jiaolong" submersible, 1 May 2016, sample 37I-JL106-1, SRSIO16050001.

Paratype: male, cl 9.3 mm, same collection data as for holotype, sample 37I-JL106-2, SRSIO16050002.

**Diagnosis.** Rostrum nearly horizontal, reaching to distal margin of basal article of antennular peduncle; rostral base triangular in dorsal view, each ventrolateral ridge armed with a minute spine. Carapace with distinct cervical groove; anterolateral margin with branchiostegal and pterygostomial spines, and several spinules situated posterior to them; postorbital region armed with one short longitudinal row of spinules; groups of similar spinules also present on posterior portion of cervical groove and rostrum. Second to fourth pleura each with one articular knob; first to third pleura broadly rounded and fourth to sixth pleura each with several posteroventral teeth. Telson quadrangular, with two conspicuous dorsolateral carinae each bearing 7–10 posteriorly directed spines. Eye devoid of dark pigment; eyestalk armed with minute spines. Lateral margin of antennal scale slightly concave, armed with 10–12 spines. Fixed finger of third pereiopod without row of small teeth on distoventral margin; ischium of third pereiopod with one row of 2–4 small teeth on flexor margin. Dactyli of fourth and fifth pereiopods biunguiculate primarily, bearing several much smaller accessory teeth arising from bases of ventral and dorsal ungues.

**Description of holotype female.** *Rostrum* (Fig. 2A) nearly horizontal, 0.26 times as long as carapace, reaching to distal margin of basal article of antennular peduncle; dorsal margin armed with eight small teeth; ventral margin armed with two small teeth on distal half; rostral base triangular in dorsal view, each ventrolateral ridge armed with a minute spine.

*Carapace* (Fig. 2A) fairly inflated; cervical groove distinct. Antennal spine blunt. Anterolateral margin with two branchiostegal spines and three (right) or five (left) pterygostomial spines; several spinules situated posterior to them. Postorbital region armed with one short longitudinal row of spinules; groups of similar spinules also present on posterior portion of cervical groove and rostrum.

Sixth *thoracic sternite* (Fig. 5A) with paired triangular plates, ventral surface concave. Seventh and eighth sternites with bilobed prominences, ventral surface concave.

*Pleomeres* (Fig. 2B) glabrous. First to third pleura broadly rounded, unarmed, and setose on ventral margin. Second to fourth pleura each with one articular knob. First somite short, divided in two sections by distinct transverse carina; posterior section of pleuron rounded. Second and third somites with shallow transverse grooves on terga. Fourth pleura with five (right) or seven (left) minute posteroventral teeth. Fifth pleura with eight (right) or nine (left) minute posteroventral teeth. Sixth pleura with six (right) or three (left) minute posteroventral teeth; posterolateral process terminating acutely.

*Telson* (Fig. 2C) quadrangular, almost twice as long as broad, slightly constricted near base, with two conspicuous dorsolateral carinae, each armed with nine (right) or ten (left) posteriorly directed spines; constricted part of each lateral margin with a single proximal submarginal spine; lateral marginal spines distinct. Setiferous posterior margin broadly rounded, with thirteen spines.

*Eyes* (Fig. 3A) moderate in size; cornea globular, devoid of dark pigment, broader than eyestalk. Eyestalk armed with three minute spines.

*Antennular peduncle* (Fig. 3B) reaching mid-length of antennal scale; first article distinctly longer than both distal articles combined, with a blunt spine distolaterally;

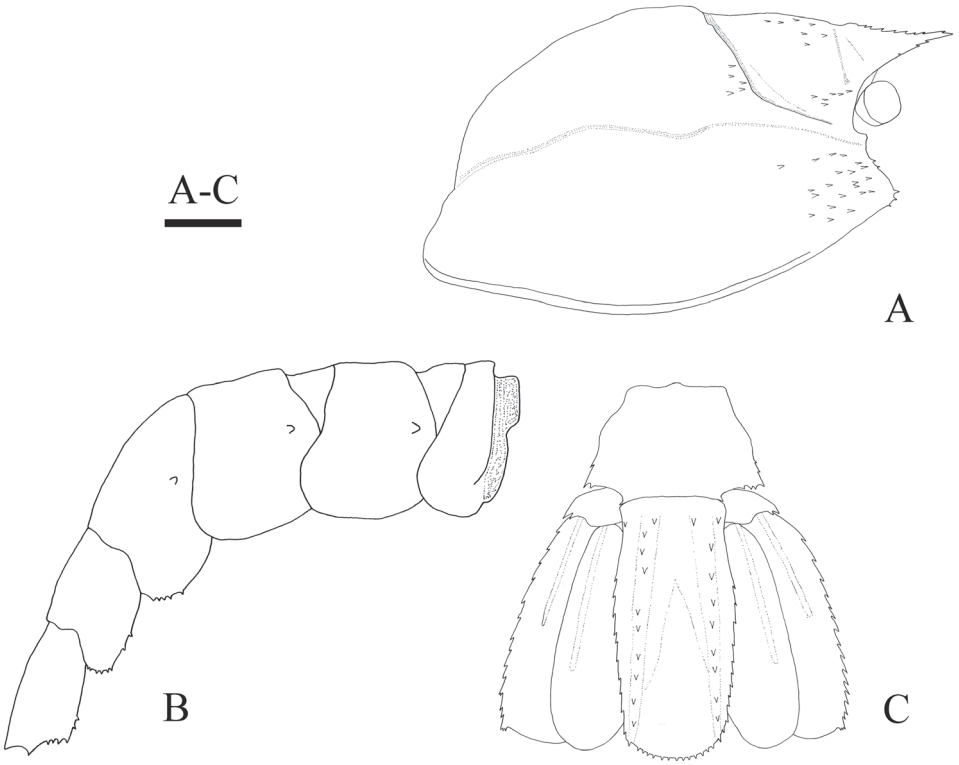


**Figure 2.** *Spongicoloides weijiaensis* sp. n. Holotype female: **A** carapace, lateral view **B** pleon, lateral view **C** telson and uropods, dorsal view. Scale bar 2 mm.

stylocerite small, subacutely pointed; second article longer than distal article, bearing a single distal spinule on inner margin; distal article unarmed.

*Antenna* with stout basicerite, bearing four (right) or three (left) large spines at distolateral angle, additional four (right) or three (left) small spines on ventrodistal margin, and two (right) or three (left) small spines on ventral surface proximally. Carpocerite overreaching first article of antennular peduncle. Antennal scale (Fig. 3C) broad; twice as long as rostrum, 2.7 times as long as wide; lateral margin slightly concave, not setiferous, with ten (right) or twelve (left) spines; distolateral bifid spine slightly falling short of or just reaching rounded distal margin of lamella; inner margin convex, Both inner and distal margins with long setae; dorsal surface with single longitudinal carina. Basal article of antennal peduncle armed with three (right) or two (left) terminal spines laterally.

*Mandible* (Fig. 3D) with 3-jointed palp; distal article oval, subequal in length to intermediate article; molar and incisor processes separated.

*Maxillule* (Fig. 3E) with simple palp bearing a pair of terminal setae; distal endite broad, its mesial margin straight; proximal endite suboval, tapering distally.

*Maxilla* (Fig. 3F) with palp tapering distally; distal and proximal endites both deeply bilobed; scaphognathite well developed.

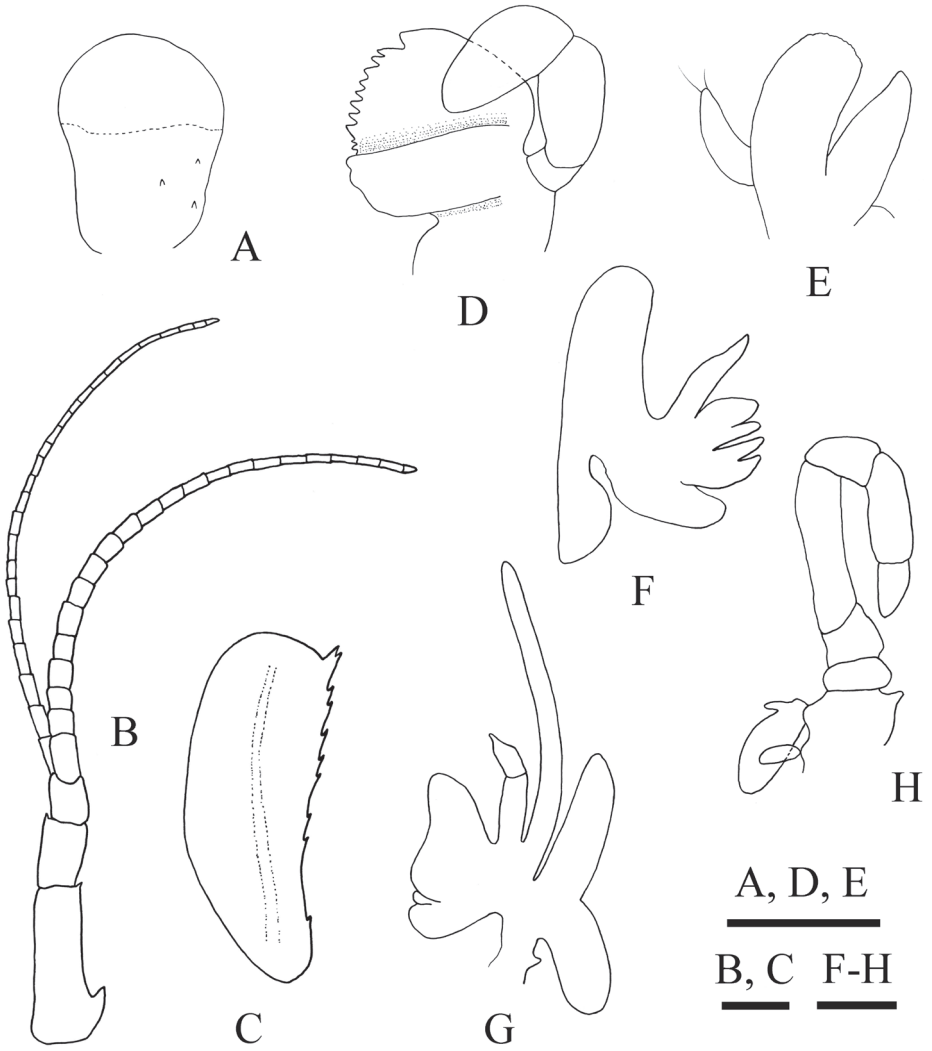


**Figure 3.** *Spongicoloides weijiaensis* sp. n. Holotype female: **A** right eye, outer view **B** right antennule, dorsal view **C** right antennal scale, dorsal view **D** right mandible, inner view **E** right maxillule, outer view **F** right maxilla, outer view **G** left first maxilliped, outer view **H** left second maxilliped, inner view. Setae omitted. Scale bars 1 mm.

First *maxilliped* (Fig. 3G) with bi-jointed palp; proximal article broad, 1.5 times of distal article in length; distal endite large, rounded anteriorly; proximal endite bilobed; exopod well developed; epipod large, subequally bilobed.

Second maxilliped (Fig. 3H) with endopod composed of seven articles; dactylus triangular, approximately 1.5 times as long as broad; propodus subquadrate, nearly 1.9 times of dactylus in length; carpus short, widening distally, 0.6 times as long as propo-

dus; merus long, 2.3 times as long as carpus; ischium not fused with basis, 0.2 times as long as merus; epipod oval, with rudimentary podobranch; exopod absent.

Third maxilliped (Fig. 4A) with 7-jointed endopod, slender, slightly overreaching mid-length of antennal scale in full extension; dactylus tapering distally; propodus 1.8 times as long as dactylus; carpus 1.1 times of propodal length; merus 1.7 times of carpal length; ischium subequal to merus; basis shortest, approximately 0.2 times length of ischium; coxa with epipod; exopod absent.

First *pereiopod* (Fig. 4B) reaching distal margin of antennal scale; dactylus half as long as palm; palm subcylindrical, with some grooming setae; carpus longest, nearly 2.4 times as long as palm, distal part of flexor margin of carpus with tuft of grooming setae; merus 0.7 times as long as carpus; ischium 0.5 times as long as merus; coxa and basis short, unarmed.

Second pereiopod (Fig. 4C) generally similar in shape to first pereiopod, longer, overreaching distal margin of antennal scale by length of chela; dactylus 0.4 times as long as palm; carpus 1.9 times as long as palm; merus 0.8 times as long as carpus; ischium 0.4 times as long as merus; coxa and basis short, unarmed.

Third pereiopod (Fig. 4D) strongest and longest, overreaching distal margin of antennal scale by length of chela. Fingers terminating each in strongly curved, corneous claw, tips crossing; fixed finger with deep longitudinal concavity proximally, bearing single rounded tooth at nearly mid-length of cutting edge and with short row of small teeth on proximal cutting edge, distoventral margin without row of teeth; dactylus 0.6 times of palm length, protruded at proximal 0.4 of length, with concavity on distal half portion; palm almost equal to merus in length, subcylindrical; some minute teeth present on distal half of flexor margin of propodus (Fig. 4E); carpus widening distally, nearly half as long as palm; merus of right third pereiopod unarmed; merus of left third pereiopod bearing minute tooth at approximately distal 0.2 of its length on flexor margin; ischium 0.9 times as long as carpus, flexor margin with row of 3–4 small teeth, distolateral margin also with similar teeth; basis and coxa short, unarmed.

Fourth and fifth pereiopods similar, moderately long and slender. Fourth pereiopod (Fig. 4F) overreaching distal margin of antennal scale by length of dactylus and propodus; dactylus (Fig. 4H) short, compressed laterally, biunguiculate primarily, ventral unguis shorter than dorsal unguis, both clearly demarcated, with some much smaller accessory teeth arising from bases of both ventral and dorsal ungues; propodus approximately 0.4 times length of carpus, armed with single row of eleven or twelve movable spines on flexor margin; carpus longest; merus 0.8 times length of carpus; ischium half-length of merus, unarmed; coxa and basis short and stout.

Fifth pereiopod (Fig. 4G) overreaching distal margin of antennal scale by dactylus and half-length of propodus; propodus 0.4 times length of carpus, armed with single row of twelve or thirteen movable spines on flexor margin; merus 0.7 times length of carpus; ischium 0.4 times length of merus, unarmed; coxa and basis short and stout.

All pereiopods with small and blunt protrusions on proximal parts of ischial flexor margins.

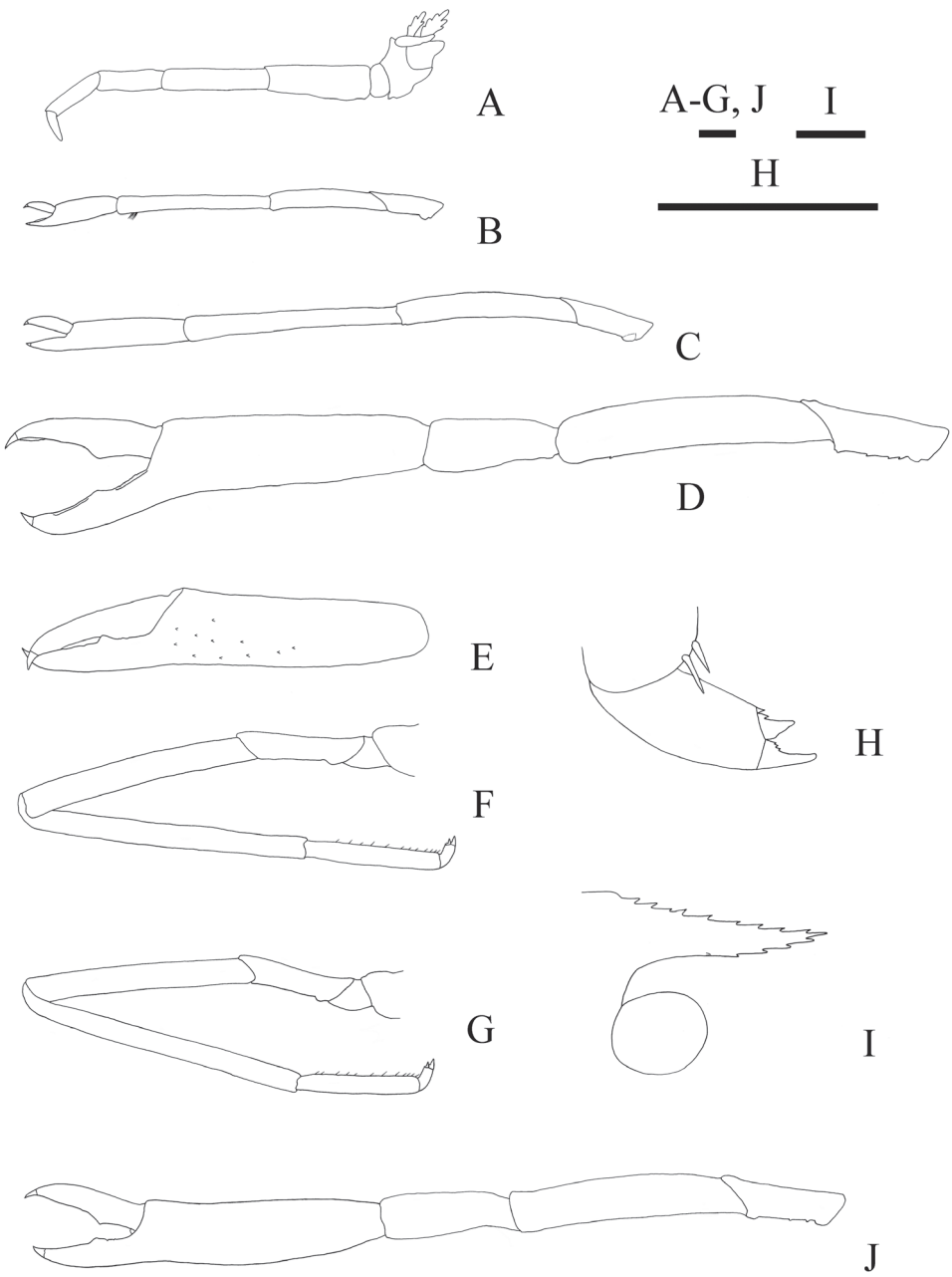


**Figure 4.** *Spongicoloides weijiaensis* sp. n. Holotype female: **A** left third maxilliped, lateral view **B** left first pereiopod, lateral view **C** left second pereiopod, lateral view **D** left third pereiopod, lateral view **E** flexor margin of right third pereiopod chela, lateral view **F** left fourth pereiopod, lateral view **G** left fifth pereiopod, lateral view **H** dactylus of left fourth pereiopod, lateral view. Paratype male: **I** rostrum, lateral view **J** left third pereiopod, lateral view. Scale bars 1 mm.

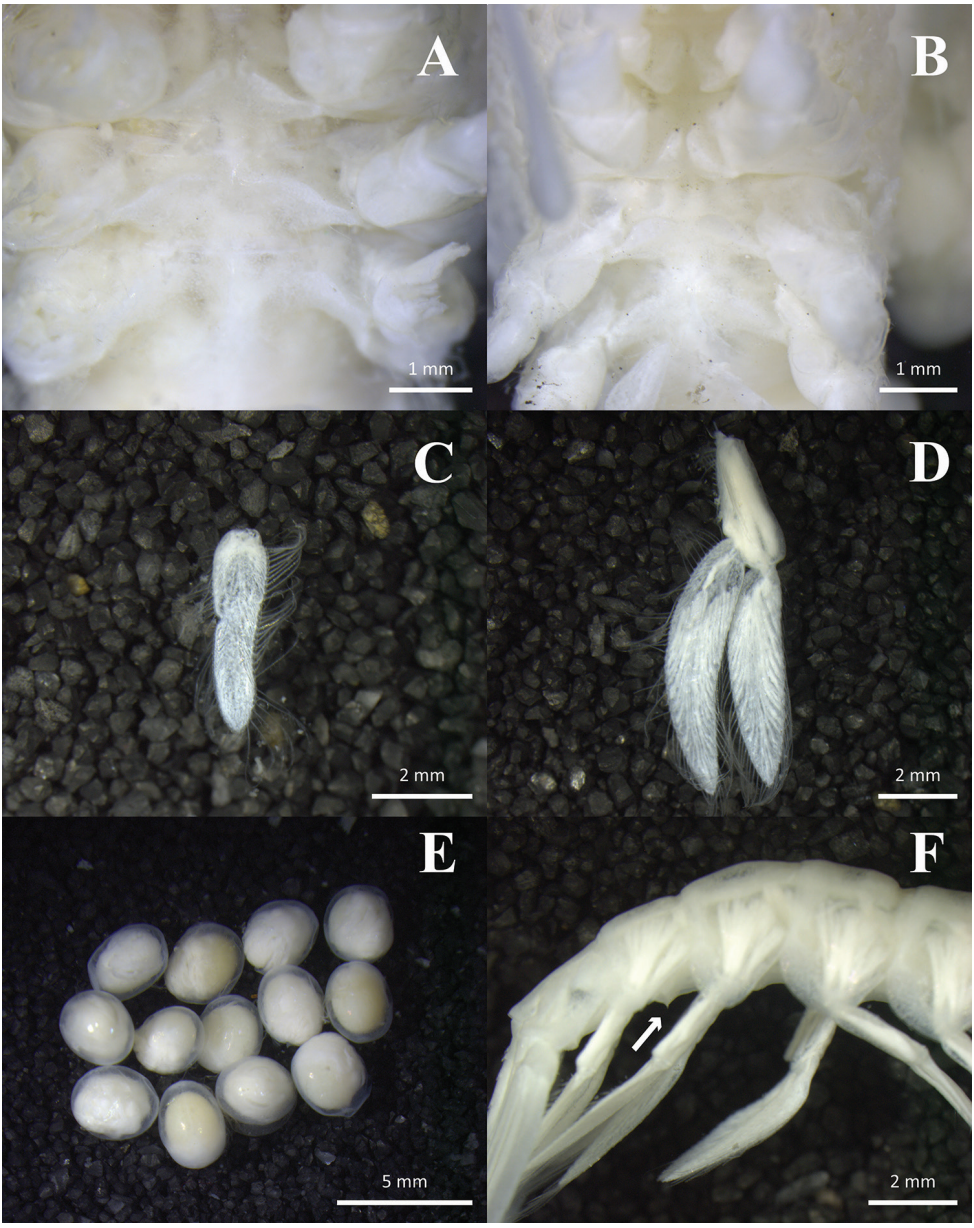


**Figure 5.** *Spongicoloides weijiaensis* sp. n. Holotype female: **A** thoracic sternites, ventral view **C** first pleopod, lateral view **D** second pleopod, lateral view **E** eggs, outer view. Paratype male: **B** thoracic sternites, ventral view **F** second to sixth pleonites, showing spine of fifth sternite, lateral view.

First *pleopod* (Fig. 5C) smallest, uniramous. Second to fifth pleopods biramous. Second pleopod (Fig. 5D) with protopod shorter than rami, bearing ovipositing setae on dorsal and ventral margins; mesial surface with ridge bearing ovipositing setae.

Third to fifth pleopods generally similar, decreasing in size posteriorly; fourth and fifth pleopods lacking ovipositing setae.

Uropod (Fig. 2C) with stout protopod; lateral margin terminating in two spines. Endopod and exopod each with single weak dorsal carina. Lateral margin of exopod slightly convex with row of fourteen (left) or fifteen (right) acute teeth, excluding broad trilobed tooth on distolateral angle. Endopod ovate, falling short of posterior margin of telson.

Holotype female carrying thirteen eggs (Fig. 5E). Pleonal sternites unarmed. Branchial formula summarized in Table 1.

**Main characters of paratype male.** Rostrum (Fig. 4I) nearly horizontal, reaching to distal margin of basal article of antennular peduncle, dorsal margin armed with nine small teeth; ventral margin armed with four small teeth on distal half; rostral base triangular in dorsal view, each ventrolateral ridge armed with a minute spine. Thoracic sternites (Fig. 5B) much narrower than in female; sixth thoracic sternite lacking paired distinct spines anteromesially. Fifth pleonal sternite (Fig. 5F) with one spine. Dorsolateral carinae of telson conspicuous, armed with seven (right) or eight (left) posteriorly directed spines. Left antennal scale with bifid distolateral spine, right antennal scale with simple distolateral spine. Fingers of third pereiopod (Fig. 4J) relatively shorter than in female, 0.3 times length of chela; fixed finger without row of small teeth on distoventral margin; ischium flexor margin with two small teeth. Dactyli of fourth and fifth pereiopods biunguiculate, ventral unguis shorter than dorsal unguis, bearing some much smaller accessory teeth. Distolateral angles of uropodal exopods with single blunt tooth (possibly abraded) or with bifid tooth.

**Etymology.** The specific name, *weijiaensis*, refers to the type locality, the Weijia Guyot, part of the Magellan Seamount Chain in the northwestern Pacific.

**Color in life.** Body whitish, translucent; corneas, some intrathoracic organs and eggs pale yellow.

**GenBank accession numbers.** KY404237 (16S rRNA), KY404238 (COI).

**Discussion.** One of the most important taxonomic features of species assigned to *Spongicoloides* is the branchial formula. Although some gills are rather fragile and easily detachable structures, and their development may be variable (rudimentary, simple or well-developed), the total number of gills is still one of the first and main characters to examine when one is dealing with *Spongicoloides*.

*Spongicoloides weijiaensis* sp. n. shares the presence of two arthrobranchs on the third maxilliped and first through fourth pereiopod with *Spongicoloides novaezelandiae* Baba, 1979 from Chatham Rise east of New Zealand, *S. hawaiiensis* Baba, 1983 from Hawaii, and *S. iheyaensis* Saito, Tsuchida & Yamamoto, 2006 from southern Japan (Baba 1979, 1983, Saito et al. 2006).

The other five species of *Spongicoloides* can be distinguished in having substantial differences in the gill formulae, such as the third maxilliped bears a single arthrobranch in *S. evolutus* (Bouvier, 1905a) and the first through fourth pereiopod each bear a single arthrobranch in *S. galapagensis* Goy, 1980, *S. inermis* (Bouvier, 1905b), *S. profundus* Hansen, 1908 and *S. tabachnicki* Burukovsky, 2009.

The new species can be separated from *S. novaezelandiae* by the fourth pleuron bearing several minute teeth on the posteroventral margin (vs fourth pleuron broadly

**Table 1.** Branchial formula of *Spongicoloides weijiaensis* sp. n. (r = rudimentary).

| | **Maxillipeds** | | | **Pereiopods** | | | | |
|---|---|---|---|---|---|---|---|---|
| | **I** | **II** | **III** | **I** | **II** | **III** | **IV** | **V** |
| Pleurobranchs | 0 | 0 | 1 | 1 | 1 | 1 | 1 | 1 |
| Arthrobranchs | r | 1 | 2 | 2 | 2 | 2 | 2 | 0 |
| Podobranchs | 0 | r | 0 | 0 | 0 | 0 | 0 | 0 |
| Epipods | 1 | 1 | 1 | 0 | 0 | 0 | 0 | 0 |
| Exopods | 1 | 0 | 0 | 0 | 0 | 0 | 0 | 0 |

rounded in *S. novaezelandiae*); the flexor margin of the third pereiopod ischium armed with a row of 2-4 small teeth (vs unarmed in *S. novaezelandiae*); the second maxilliped with a single arthrobranch (vs with paired arthrobranchs in *S. novaezelandiae*); and the fourth and fifth pereiopod dactyli with accessory teeth at the bases of the ungues (vs absent or at most with small angle in *S. novaezelandiae*) (cf. Baba 1979).

The new species can be also distinguished from *S. hawaiiensis*, e.g. by the carapace bearing groups of spinules posterior to the rostrum, orbits, cervical groove and pterygostomian angle (vs almost spineless in *S. hawaiiensis*); the more numerous spines on the lateral and posterior margins of the telson and the lateral margin of the antennal scale; the flexor margin of the third pereiopod ischium armed with some small teeth (vs unarmed in *S. hawaiiensis*); and the dorsal surface of the antennal scale and uropodal exopod each with a single mesial or submesial longitudinal carina (vs with two longitudinal carinae in *S. hawaiiensis*) (cf. Baba 1983).

*Spongicoloides weijiaensis* sp. n. differs from *S. iheyaensis* by the sixth pleonite unarmed dorsally (vs armed with one spine or a longitudinal row of small spines on dorsal midline in *S. iheyaensis*); the fixed finger of the third pereiopod unarmed on distoventral margin (vs bearing a short row of small teeth on the distoventral margin in *S. iheyaensis*); the third pereiopod ischium armed with a row of 2-4 small teeth on flexor margin (vs unarmed in *S. iheyaensis*); the dorsal surface of the antennal scale and uropodal exopod with one mesial or submesial longitudinal carina (vs with two longitudinal carinae in *S. iheyaensis*); and the ovigerous female with much smaller number of eggs (13 eggs in holotype female of *S. weijiaensis* sp. n. vs 229 eggs in holotype female of *S. iheyaensis*) (cf. Saito et al. 2006).

## Key to the known Pacific species of *Spongicoloides*

1 Third maxilliped and first through fourth pereiopod each with single arthrobranch; propodus and ischium of third maxilliped armed with spines on mesial margins; dorsal median carina of uropodal endopod with a single spine ..... ..... ***S. galapagensis* Goy, 1980**

– Third maxilliped and first through fourth pereiopod each with two arthrobranchs; propodus and ischium of third maxilliped unarmed on mesial margins; dorsal median carina of uropodal endopod unarmed ..... **2**

2 Sixth pleonite armed with one spine or longitudinal row of small spines on midline; fixed finger of third pereiopod armed with several (3-9) teeth on distoventral margin ..... ***S. iheyaensis*** **Saito, Tsuchida & Yamamoto, 2006**

– Sixth pleonite unarmed on midline; fixed finger of third pereiopod unarmed on distoventral margin ..... **3**

3 Carapace with spinules on postrostral and postorbital regions; third pereiopod ischium with row of 2-4 small teeth on flexor margin ..... ***S. weijiaensis*** **sp. n.**

– Carapace without spinules on postrostral and postorbital regions; flexor margin of third pereiopod ischium unarmed ..... **4**

4 Carapace with scattered spinules on anterolateral region; third pereiopod ischium with prominent process on distoventral margin; posterior margin of telson with eight spines ..... ***S. novaezelandiae*** **Baba, 1979**

– Carapace without scattered spinules on anterolateral region, third pereiopod ischium without distoventral process; posterior margin of telson with three spines ..... ***S. hawaiiensis*** **Baba, 1983**

## Acknowledgements

We are very grateful to all the scientists and crew of the R/V "Xiangyanghong 9" and the team of the submersible "Jiaolong" for their help in the collection of interesting deep-sea material. We sincerely thank Dr Joseph W. Goy (Department of Biology, Harding University, USA), who helped us to check morphological characters of the new species and provided valuable guidance in the taxonomy of stenopodidean shrimps. We express our appreciation to Dr Tomoyuki Komai (Natural History Museum and Institute, Chiba, Japan), Dr Mary K. Wicksten (Department of Biology, Texas A&M University, USA) and the anonymous reviewer for commenting upon and improving the manuscript patiently and meticulously. We specially acknowledge Dr Dongsheng Zhang (SIOSOA) for helping sequence the 16S rRNA and COI barcoding gene segments of the new species. This study was supported by the National Basic Research Program of China (No. 2015CB755901), foundation of China Ocean Mineral Resources R & D Association (No. DY125-13-E-01), Scientific Research Fund of the Second Institute of Oceanography, SOA (No. JG1613), and the National Natural Science Foundation of China (NSFC) (No. 41606155).

## References

Baba K (1979) A new stenopodidean shrimp (Decapoda, Natantia) from the Chatham Rise, New Zealand. Pacific Science 33: 311–314.

Baba K (1983) *Spongicoloides hawaiiensis*, a new species of shrimp from the Hawaiian Islands. Journal of Crustacean Biology 3: 477–481. https://doi.org/10.2307/1548148

Berggren M (1993) *Spongiocaris hexactinellicola*, a new species of stenopodidean shrimp (Decapoda: Stenopodidae) associated with hexactinellid sponges from the Tartar Bank, Bahamas. Journal of Crustacean Biology 13: 784–792. https://doi.org/10.2307/1549108

Bouvier EL (1905a) Sur les Pénéides et les Sténopides recueillis par les expéditions françaises et monégasques dans l'Atlantique oriental. Comptes Rendus Hebdomadaires des Séances de l'Academie des Sciences 140: 980–983. https://doi.org/10.5962/bhl.part.10354

Bouvier EL (1905b) Sur les macroures nageurs (abstraction faite des Carides), recueillis par les expéditions américaines du Hassler et du Blake. Comptes Rendus Hebdomadaires des Séances de l'Academie des Sciences 141: 746–749. https://doi.org/10.5962/bhl.part.28551

Bruce AJ, Baba K (1973) *Spongiocaris*, a new genus of stenopodidean shrimp from New Zealand and South African waters, with a description of two new species (Decapoda, Natantia, Stenopodidea). Crustaceana 25: 153–170. https://doi.org/10.1163/156854073X00803

Burukovsky RN (2009) A description of the shrimp *Spongicoloides tabachnicki* (Decapoda, Spongicolidae) from the glass sponge *Euplectella jovis*. Zoologicheskii Zhurnal 88: 498–503.

Caullery M (1896) Crustacés Schizopodes et Décapodes. In: Koehler R (Ed.) Résultats scientifiques de la campagne du "Caudan" dans le Golfe de Gascogne, aout-septembre 1895. Annales de l'Université Lyons 26: 365–419.

Chen CL, Goy JW, Brackengrissom HD, Felder DL, Tsang LM, Chan TY (2016) Phylogeny of Stenopodidea (Crustacea: Decapoda) shrimps inferred from nuclear and mitochondrial genes reveals non-monophyly of the families Spongicolidae and stenopididae and most of their composite genera. Invertebrate Systematics 30: 479–490. https://doi.org/10.1071/IS16024

González JA, Triay-Portella R, Santana JI (2016) Southernmost record of *Spongiocaris koehleri* (Decapoda, Stenopodidea, Spongicolidae) off the Canary Islands. Crustaceana 89: 1233–1238. https://doi.org/10.1163/15685403-00003598

Goy JW (1980) *Spongicoloides galapagensis*, a new shrimp representing the first record of the genus from the Pacific Ocean (Crustacea: Decapoda: Stenopodidea). Proceedings of the Biological Society of Washington 93: 760–770.

Goy JW (2015) Stenopodidean shrimps (Crustacea: Decapoda) from New Caledonian waters. Zootaxa 4044: 301–344. https://doi.org/10.11646/zootaxa.4044.3.1

Haan W de (1844) Crustacea. Fascicle 6–7. In: Siebold PF von (Ed.) Fauna Japonica, sive descriptioanimalium, quae in itinere per Japonicum, jussu et auspiciis superiorum in India Batava Imperium tenant, suscepto, annis 1823–1830 collegit, notis, observationobus et adumbrationibus illustravit. Müller J & Co., Amsterdam, 244 pp.

Hansen HJ (1908) Crustacea Malacostraca. I. The Danish Ingolf-Expedition 3: 1–120.

Holthuis LB (1993) The recent genera of the caridean and stenopodidean shrimps (Crustacea, Decapoda) with an appendix on the order Amphionidacea. Nationaal Natuurhistorisch Museum, Leiden, 328 pp.

Komai T, De Grave S, Saito T (2016) Two new species of the stenopodidean shrimp genus *Spongiocaris* Bruce & Baba, 1973 (Crustacea: Decapoda: Spongicolidae) from the Indo-West Pacific. Zootaxa 4111: 421–447. https://doi.org/10.11646/zootaxa.4111.4.5

Komai T, Saito T (2006) A new genus and two new species of Spongicolidae (Crustacea, Decapoda, Stenopodidea) from the South-West Pacific. In: Richer de Forges B, Justine JL (Eds) Tropical Deep-Sea Benthos, vol. 24. Mémoires du Muséum national d'Histoire naturelle 193: 265–284.

Ortiz M, Lalana R, Varela C (2007) Una nueva especie de camarón del género *Spongiocaris* (Pleocyemata, Stenopodidea) asociado a una esponja (Hexactinellida) colectada por la expedición del B/I "Atlantis", en las aguas profundas del Sur de Cuba, en 1939. Avicennia 19: 25–30.

Saint Laurent Mde, Cleva R (1981) Crustacés Décapodes: Stenopodidea. In: Crosnier A (Ed.) Résultats des Campagnes MUSORSTOM. 1. Philippines. Mémoires du Muséum national d'Histoire naturelle 91: 151–188.

Saito T (2008) An overview of taxonomy of the family Spongicolidae (Crustacea: Decapoda: Stenopodidea). Taxa, Proceedings of the Japanese Society Systematic Zoology 24: 33–46.

Saito T, Komai T (2008) A review of species of the genera *Spongicola* de Haan, 1844 and *Paraspongicola* de Saint Laurent & Cleva, 1981 (Crustacea, Decapoda, Stenopodidea, Spongicolidae). Zoosystema 30: 87–147.

Saito T, Takeda M (2003) Phylogeny of the family Spongicolidae (Crustacea: Stenopodidea): evolutionary trend from shallow-water free-living to deep-water sponge-associated habitat. Journal of the Marine Biological Association of the United Kingdom 83: 119–131. https://doi.org/10.1017/S002531540300688Xh

Saito T, Tsuchida S, Yamamoto T (2006) *Spongicoloides iheyaensis*, a new species of deep-sea sponge-associated shrimp from the Iheya Ridge, Ryukyu Islands, southern Japan (Decapoda: Stenopodidea: Spongicolidae). Journal of Crustacean Biology 26: 224–233. https://doi.org/10.1651/C-2650.1

Schram FR (1986) Crustacea. Oxford University Press, New York, 606 pp.

ZooKeys 685: 15–47 (2017)
doi: 10.3897/zookeys.685.13890
http://zookeys.pensoft.net

RESEARCH ARTICLE

A peer-reviewed open-access journal
ZooKeys
Launched to accelerate biodiversity research

# Three new species of *Heteromysis* (Mysida, Mysidae, Heteromysini) from the Cape Peninsula, South Africa, with first documentation of a mysid-cephalopod association

Karl J. Wittmann[1], Charles L. Griffiths[2]

**1** *Abteilung für Umwelthygiene, Zentrum für Public Health, Medizinische Universität Wien, Kinderspitalgasse 10, A-1090 Vienna, Austria* **2** *Department of Biological Sciences and Marine Research Institute, University of Cape Town, Rondebosch 7701, Republic of South Africa*

Corresponding author: *Karl J. Wittmann* (karl.wittmann@meduniwien.ac.at)

Academic editor: *T. Horton* | Received 30 May 2017 | Accepted 3 July 2017 | Published 13 July 2017

*http://zoobank.org/DF60153C-7D8F-448C-9274-CFF507523092*

**Citation:** Wittmann KJ, Griffiths CL (2017) Three new species of *Heteromysis* (Mysida, Mysidae, Heteromysini) from the Cape Peninsula, South Africa, with first documentation of a mysid-cephalopod association. ZooKeys 685: 15–47. https://doi.org/10.3897/zookeys.685.13890

## Abstract

Faunistic studies in sublittoral and littoral marine habitats on the Cape Peninsula, South Africa, have yielded three new species belonging to the genus *Heteromysis*, subgenus *Heteromysis*: *H. cancelli* **sp. n.** associated with the diogenid hermit crab *Cancellus macrothrix* Stebbing, 1924, and *H. fosteri* **sp. n.** extracted from 'empty' urchin and gastropod shells. The first documented mysid-cephalopod association is reported for *H. octopodis* **sp. n.** which was found in dens occupied by *Octopus vulgaris* Cuvier, 1797, but was also captured from tide pools. The three new species differ from previously known E. Atlantic species, among other characters, by a single spine on the endopods of uropods in combination with large cornea and absence of median sternal processes on thoracic somites. They are also characterized by a white stripe along the dorso-lateral terminal margin of the eyestalks in living specimens. The new species appear quite similar to each other, but are distinguished by different depths of the telson cleft, different distributions of spines on the lateral margins of the telson, different numbers of segments on thoracic endopod 4, and by differently modified setae on the carpus of the third thoracic endopod, as well as on the carpopropodus of the fourth endopod. An updated key to the species of *Heteromysis* known from the E. Atlantic is given.

## Keywords

Crustacea, hermit crab association, octopus association, ectocommensals, taxonomy, key to species, SE. Atlantic

## Introduction

Ongoing taxonomic surveys of littoral and sublittoral habitats along the coasts of the Cape Peninsula (South Africa) have yielded a number of previously unreported Mysidae species, of which one, *Mysidopsis zsilaveczi*, has already been described as new by Wittmann and Griffiths (2014). The examination of this material is now continued with descriptions of three new species of *Heteromysis* S.I. Smith, 1873. Not counting doubtful species and non-nominotypical subspecies, but including the new ones described here, as many as 88 species of this genus are currently acknowledged on a world-wide scale and lots of additional new ones may be expected. Four subgenera are distinguished. However, as many as 28 species have so far not been assigned to any subgenus (Mees 2017), particularly due to missing data. This is also the case for two E. Atlantic species given in the key below. Including the three new ones, all 11 currently known species from the E. Atlantic are from cold-temperate to subtropical climates. Elsewhere, the main bulk of species comes from subtropical to tropical climates. In this view, the coastal waters of the tropical E. Atlantic appear as practically unexplored for this genus. This is true also for the temperate SE. Atlantic, as no *Heteromysis* species have been previously described from South Africa, although for the sake of completeness we note that Connell (1974) reported a single specimen of *Heteromysis* sp., without giving any further details, from the Mtentu River Estuary on the Indian Ocean coast of South Africa.

The distributions and habitats occupied by species belonging to this genus were reviewed by Fukuoka (2005). Most species were found in cryptic habitats, such as dense vegetation, microcaves, empty gastropod shells, etc. Many species are also associated with benthic invertebrates, some are known even as obligate commensals, at least during daytime. The present paper adds one species associated with hermit crabs, an additional one from empty shells, and a third one associated with octopus, with this last association documented as the first known facultative ectocommensal symbiosis between mysids and cephalopods.

## Material and methods

The three species described below were collected at four stations in 0-20 m depth within 5.5 km of the False Bay coastline (34°11'S 18°27'E to 34°14'S 18°28'E), Cape Peninsula, South Africa, using different methods, as detailed below:

The first species was extracted from a gastropod shell occupied by a hermit crab, as part of a separate taxonomic study on the regional hermit crab fauna. Although numerous shells, occupied by a variety of hermit crab species, were collected individually by SCUBA diving or by hand-collecting on the shore at this and many other sites, mysids were only found associated with a single individual of the rarely-recorded hermit *Cancellus macrothrix* Stebbing, 1924.

The second, shell-occupying species was discovered during a separate and mysid-directed sampling operation, in which roughly 1 kilo of dead urchin and gastropod

shells, without hermit crabs, were sampled from sublittoral habitats near Miller's Point, False Bay, then put into a bucket of seawater, into which a small amount of formalin was added, just enough to expel any infauna from the recesses, but not to kill them. The sample was then rinsed with seawater and each shell shaken out back into the bucket. The seawater was then poured through a 1 mm mesh net. Only the single mysid species described below was obtained in this way (although along with numerous amphipods, isopods and other small crustaceans).

The third species described here was visually sighted and photographed in sublittoral dens occupied by octopus and in intertidal rock pools by a local underwater photographer, who then captured specimens with a small hand net, or by coaxing them into an open jar, and submitted them to us for identification.

Fixation, preservation, preparation, measurements, and examination of materials was carried out as described in Wittmann (2000); and examination of statolith structure as detailed in Wittmann et al. (1993). Terminology of larval stages is given according to Wittmann (1981). With certain modifications, as stated by Wittmann (2000), appendage terminology is according to Tattersall and Tattersall (1951), and for non-sensory cuticle structures according to Klepal and Kastner (1980). Holotypes and slides of dissected paratypes were deposited at the Natural History Museum of Vienna (NHMW), vial paratypes at the Iziko South African Museum, Cape Town (SAM).

## Systematics

**Order Mysida Boas, 1883**
**Family Mysidae Haworth, 1825**
**Subfamily Heteromysinae Norman, 1892**
**Tribe Heteromysini Norman, 1892**
**Genus *Heteromysis* S.I. Smith, 1873**
**Subgenus *Heteromysis* S.I. Smith, 1873**

***Heteromysis* (*Heteromysis*) *cancelli* Wittmann & Griffiths, sp. n.**
http://zoobank.org/A2B8C8A8-CC29-4464-8E01-841454C06837
Figs 1–5

**Type series.** Holotype, adult male with 6.9 mm body length, in vial at NHMW-25903; paratypes in vial at SAM-MB-A067550: adult male 5.3 mm, adult female 6.1 mm, subadult female 6.0 mm, one immature female, one juvenile; dissected paratypes on slides at NHMW-25904: adult female 6.4 mm and adult male 6.9 mm; Roman Rock, off Simonstown, on the False Bay coastline of the Cape Peninsula, South Africa, 34°10.95'S, 18°27.50'E, 20 m depth; all eight specimens from the same gastropod shell inhabited by the hermit crab *Cancellus macrothrix* Stebbing, 1924, 3 May 2015, leg. Jannes Landschoff.

**Diagnosis.** Carapace produced into well projecting, broadly-subtriangular rostrum with rounded apex. Eyes well developed; cornea occupies 40–55% of eye surface;

eyestalks with small, distally directed, blunt extension of (obliquely anterior facing) inner margin. Antennular trunk with a number of smooth and barbed setae, but no particularly modified setae; inner distal corner of its terminal segment with anteriorly directed apophysis carrying two large, smooth setae. Antennal scale moderately stout and short, extending shortly beyond distal half of terminal segment of antennular trunk; outer margin feebly convex. First thoracic sternite with anteriorly projecting, terminally rounded median lobe; sternites 2–8 without lobes in both sexes. Carpopropodus of thoracic endopods 1–8 with 2, 2, 2, 3-4, 5, 6, 6, or 5-6 segments, respectively. Third thoracic endopod not dimorphic, without any spines or spine-like setae; carpus not swollen (with respect to merus). Carpus of third thoracic endopod with series of 2–3 subbasally spiny (i.e. with modified barbs) and medially to subterminally pectinate setae near outer margin. Carpopropodus of fourth thoracic endopod with series of 2–4 subbasally more strongly spiny setae near outer margin, these 'spines' thick but not tooth-like; no such modified setae in endopods 5–8. Penes long and slender, twice length of merus of eighth thoracic endopod; tip with three rounded lobes, each wider than long. Pleopods reduced to small, setose, bilobate plates, without any spines in both sexes. Exopods of uropods extend distinctly beyond endopods. Endopods with only one spine on inner margin, in subbasal position near statocyst. Telson subtriangular, though terminally transversely truncate; lateral margins weakly sigmoid, along their distal 56–60% furnished with continuous series of 18–21 spines each. Telson with apical cleft that forms a narrow, proximally rounded 'V', cleft four times deeper than wide, its depth 27–36% telson length. Cleft densely furnished with total of 29–33 acute laminae (= laminar processes) along basal 81–84% of its margins. Two latero-apical lobes of telson show transverse apical margins, each carrying 2–3 large spines of subequal size.

**Description.** General appearance is that of mysids with intermediate proportions. Cephalothorax comprises 39–42% of body length without telson, pleon 58–61%, and carapace 33–37%, when measured along dorsal median line (Fig. 1). First thoracic sternite with median lobe showing a number of minute bristles on its well-rounded apex (Fig. 3B). Each of first to fifth abdominal somites measures 0.7–0.9 times length of sixth somite. Terminal margin of sixth pleonite with sinusoidal lateral shields covering the basis of uropods in females (Fig. 5F) versus (sub)triangular ones in males (Fig. 5E).

***Carapace*** (Fig. 2A, D). Non-dimorphic, antero-lateral edges evenly rounded. Cervical sulcus well marked, no cardial sulcus visible. Posterior margin rounded, emarginated, leaving the ultimate and part of penultimate thoracic segment dorsally exposed. Carapaces dissected and mounted on slides in only a single specimen for each sex: 10–11 pores (Fig. 2D) of about 1 μm diameter are in roughly butterfly-shaped arrangement in front of the posterior margin, surrounding a larger, less distinct pore, as in the Mediterranean *H. arianii* Wittmann, 2000, and NE. Atlantic *H. dardani* Wittmann, 2008. An additional group with 18–20 pores (Fig. 2C), in strongly flattened 'V'-shaped arrangement, is in median position, closely in front of cervical sulcus.


**Figure 1.** Ex-situ microphotographs of *Heteromysis cancelli* sp. n. from False Bay, Simonstown, Cape Peninsula, South Africa; adult males with 6–7 mm body length in lateral (**A**) or in dorsal view (**B**), respectively. Aquarium photos by C.L. Griffiths.

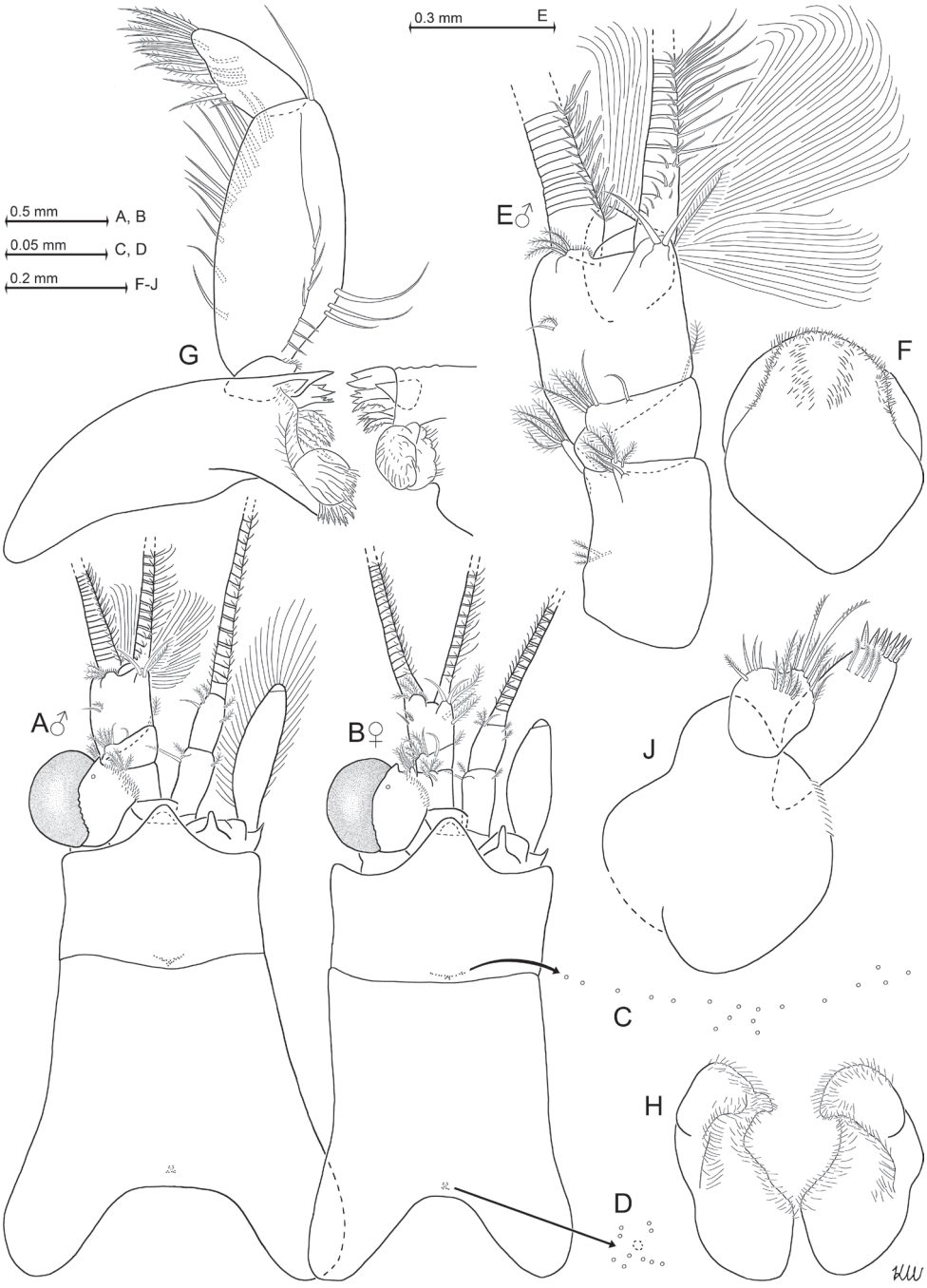


**Figure 2.** *Heteromysis cancelli* sp. n., paratype male with 6.9 mm body length (**A, E–H**), paratype female 6.4 mm (**B–D, J**). **A, B** cephalic region plus carapace in male (**A**) versus female (**B**), dorsal view, details show pore groups (**C, D**) on carapace **E** male antennula, dorsal **F** labrum, obliquely ventral **G** mandibles with right palpus, caudal **H** labium, ventral **J** maxillula, caudal.

***Eyes*** (Figs 1; 2A, B). Thick, shaped in form of dorsoventrally compressed globoids. Cornea appears calotte-shaped to sub-reniform in dorsal and in ventral view, oval in lateral view. Comparatively large group of scales distributed along inner, obliquely anteriorly facing margin of eyestalks. Ocular symphysis with broadly-rounded, smooth, subrostral process (as dashed lines in Fig. 2A, B).

***Antennulae*** (Fig. 2A, B, E). Basal segment 42–47% length of trunk, middle is 12–19% and terminal segment is 36–42%, when measured along dorsal midline of trunk (only Fig. 2E shows entire extension of basal segment). Trunk stouter in males, with basal segment 1.4–1.5 times longer than broad, compared to 1.7–1.8 in females. A small dorsal apophysis and a longer outer ventral lobe (exite) extend (obliquely) forwards from end of basal segment. Dorsal apophysis bears 1–2 smooth setae and a number of barbed setae, ventral lobe bears four plumose setae at its tip. Median segment obliquely truncate, its anterior margin dorsally with a smooth seta in median position and more laterally an additional smooth seta, together with several barbed setae. Two small barbed setae antero-ventrally near outer margin. These last setae not visible in dorsal view (Fig. 2A, B, E). Inner distal corner of terminal segment ventrally with a large, obliquely inwards-forwards directed, plumose seta, this seta larger in females compared to males, and dorsally with an apophysis as described in the diagnosis. In sublateral to submedian position on anterior margin of terminal segment there is a lobe with 3–5 medium-sized barbed setae and a dense series of short bristles. Only females with additional, large plumose setae, also obliquely inwards-forwards directed in Fig. 2B, on terminal segment of trunk, one half-way on inner margin, the second on ventral surface proximally from inner flagellum, at about 25% segment length from anterior margin of terminal segment. Appendix masculina terminally bilobate, forming a medium-sized, forwards directed extension distally on ventral surface of terminal segment, and bearing a large and dense brush of setae extending obliquely downwards (Figs 1; 2A, E). Outer antennular flagellum 1.3–1.5 times as thick as inner flagellum, when measured near basis.

***Antennae*** (Fig. 2A, B). Length of antennal scale 3.2–3.9 times its maximum width; without spines, setose all around. A small apical segment with five plumose setae separated from basal part by an essentially transverse, though slightly-oblique suture; apical segment broader than long, contributing 4–7% to total scale length. Antennal sympod with forwards-projecting tongue-like, terminally rounded lobe; posteriorly with a broad, terminally weakly-bilobate lobe containing end sac of antennal gland. Peduncle three-segmented, clearly shorter than scale. Basal segment 17–22% length of peduncle, second 40–48% and third 34–38%.

***Mouth parts*** (Figs 2F–J, 3A). Labrum, labium, maxillulae and maxillae as normal in this genus. Mandibular palp normal, three-segmented. Median segment with normal setae along inner and outer margins. Pars molaris of both mandibles with strong grinding surface. Pars incisivus with 2–3 large teeth, and digitus mobilis with 2–3 large, plus two small, teeth. Pars centralis ('spine row' in terminology of Tattersall and Tattersall 1951) with 5–7 spiny teeth. Distal segment of maxillula terminally with 7–10 strong, inconspicuously serrated spines, subterminally with transverse row of 4–5

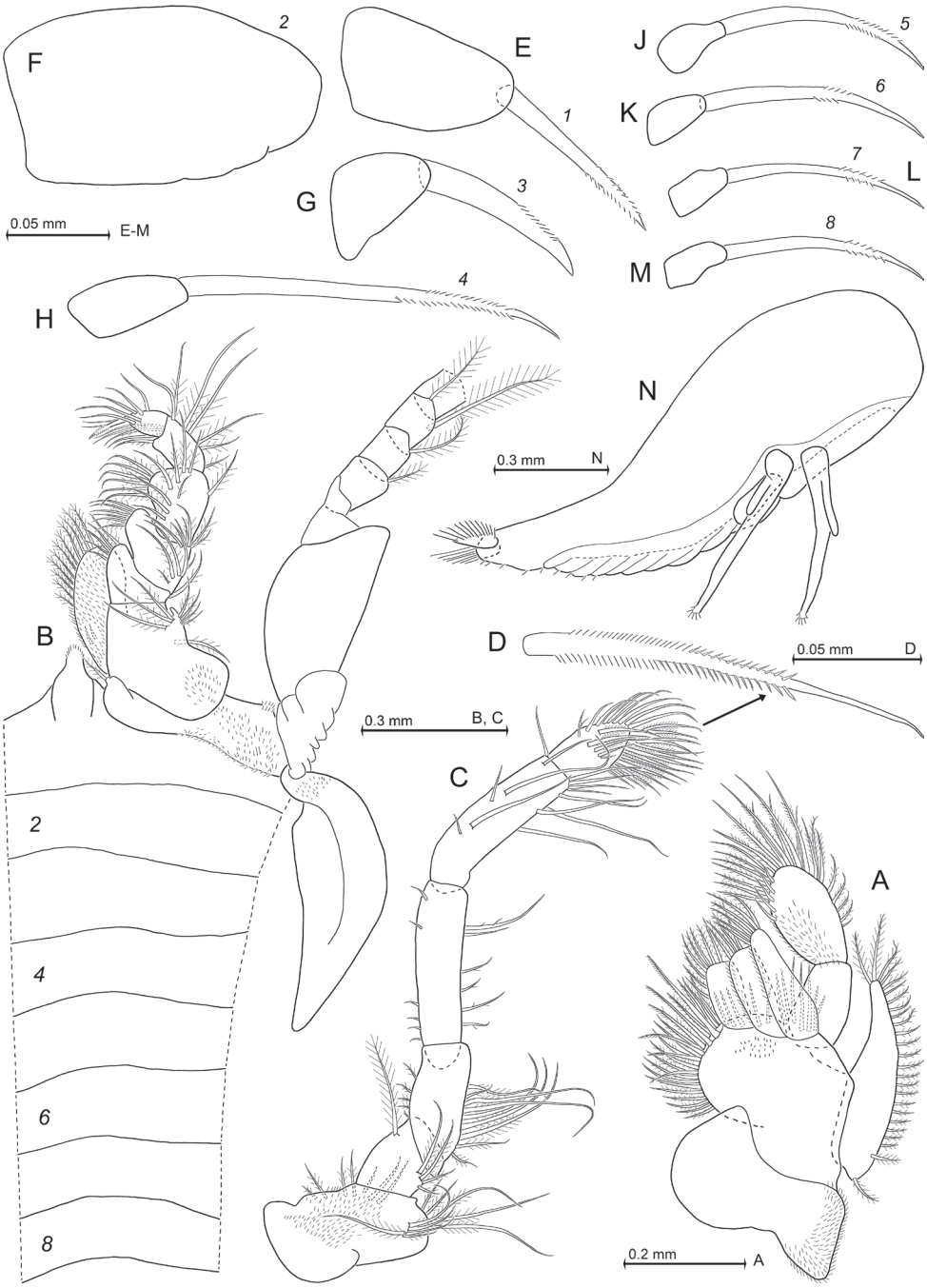


**Figure 3.** *Heteromysis cancelli* sp. n., paratype female with 6.4 mm body length (**A, C, D, H, J, L, M**) with one of its larvae (**N**), paratype male 6.9 mm (**B, E–G, K**). **A** maxilla, caudal **B** first thoracopod, caudal aspect, with thoracic sternites 1-8, ventral **C** second maxilliped, ventral, detail (**D**) shows modified seta **E–M** series of dactylus in thoracic endopods 1-8 with claw (if present), caudal **N** nauplioid larva at late substage 2, lateral.

weakly barbed setae. Endite of maxillula with two large, distally spinose setae, and total of 12–17 smaller, smooth or barbed setae.

***Thoracopods in general*** (Figs 3B–M; 4A–F; 5A, B). Sizes increase from exopod 1 to 5 or 6 and decrease from 6 to 8. Homologous exopods larger in males than in females. Flagellum of first to eighth exopods with 8, 9, 9, 9, 9, 9, 9, 9 segments in males, or 8, 9, 9, 9, 9, 9, 9, 8 segments in females, respectively, not counting the large intersegmental joint between basis and flagellum. Exopods with basal plate 1.4–2.2 times longer than broad in males, versus 1.8–2.5 in the mostly less broad exopods of females. Lateral expansion distinct in both sexes, outer margin ending in rounded edge. Endopods: for segmental numbers of carpopropodus see diagnosis. Distinct dactylus present in all thoracic endopods. Size of dactylus (Fig. 3E–M) decreases in order of endopod 2 > 1 > 3 > 4 > (5–8). Claws present in endopods 1 and 3–8, but absent in endopod 2. Claws do not differ between sexes.

***Maxillipeds*** (first and second thoracic endopods; Fig. 3B–F). First endopod with sympod bearing large fields of minute hairs, mainly on its outer half. Inner portions of sympod representing basis of endopod. First thoracic epipod large, leaf-like, without setae or hairs, but with small field of minute scales near insertion with sympod (Fig. 3B). Basis of first endopod with short, conical endite ending in one plumose, basally-thick seta. Basis with additional, large prominent endite, ischium and merus with feebly-projecting endites, carpus with again shorter, almost indistinct endite: these endites densely setose on their inner margins. Large endite of basis strongly hairy, that of ischium weakly hairy only at and near its inner margin, that of merus again less hairy in this position, that of carpus not hairy at all. Dactylus with strong, subapically, bilaterally microserrated claw (Fig. 3E). Basis of second endopod with weakly-projecting, subterminally setose endite (Fig. 3C). Merus slender, slightly longer than combined praeischium and ischium, but distinctly shorter than combined carpopropodus and dactylus. Dactylus without claw (Fig. 3F), bearing only a dense brush of setae (Fig. 3C). Among these setae are 9–13 modified setae, each bearing bilateral series of stiff, partly-acute micro-barbs in their subbasal to median portions (Fig. 3D).

***Gnathopods*** (third thoracic endopod; Fig. 4A, B). Endopod weakly powerful, somewhat subchelate. Its carpopropodus in both sexes comparatively slender among species of *Heteromysis*, 4.4–5.7 times longer than broad; length 0.9 times that of merus, and 1.0–1.1 times that of ischium. Modified setae on outer margin of carpus as in diagnosis. Claw smooth, powerful, showing only weak curvature; microserrated in subapical portions of only its outer margin (Fig. 3G). Most setae of endopod smooth or barbed to different degrees.

***Pereiopods*** (fourth to eighth thoracic endopods; Figs 3H–M; 4D–F; 5A, B) all moderately long and slender. Their claws microserrated on two opposite sides of their subapical portions (Fig. 3H–M). Fourth endopod with modified setae on outer margin of its carpopropodus, as in diagnosis. Its moderately small dactylus bearing long, thin, weakly-bent claw (Fig. 3H). Fifth to eighth endopods equipped with again smaller dactylus bearing much shorter claw that shows a stronger, distally-increasing curvature (Fig. 3J–M). Fifth endopod, when stretched, extends well beyond eyes.

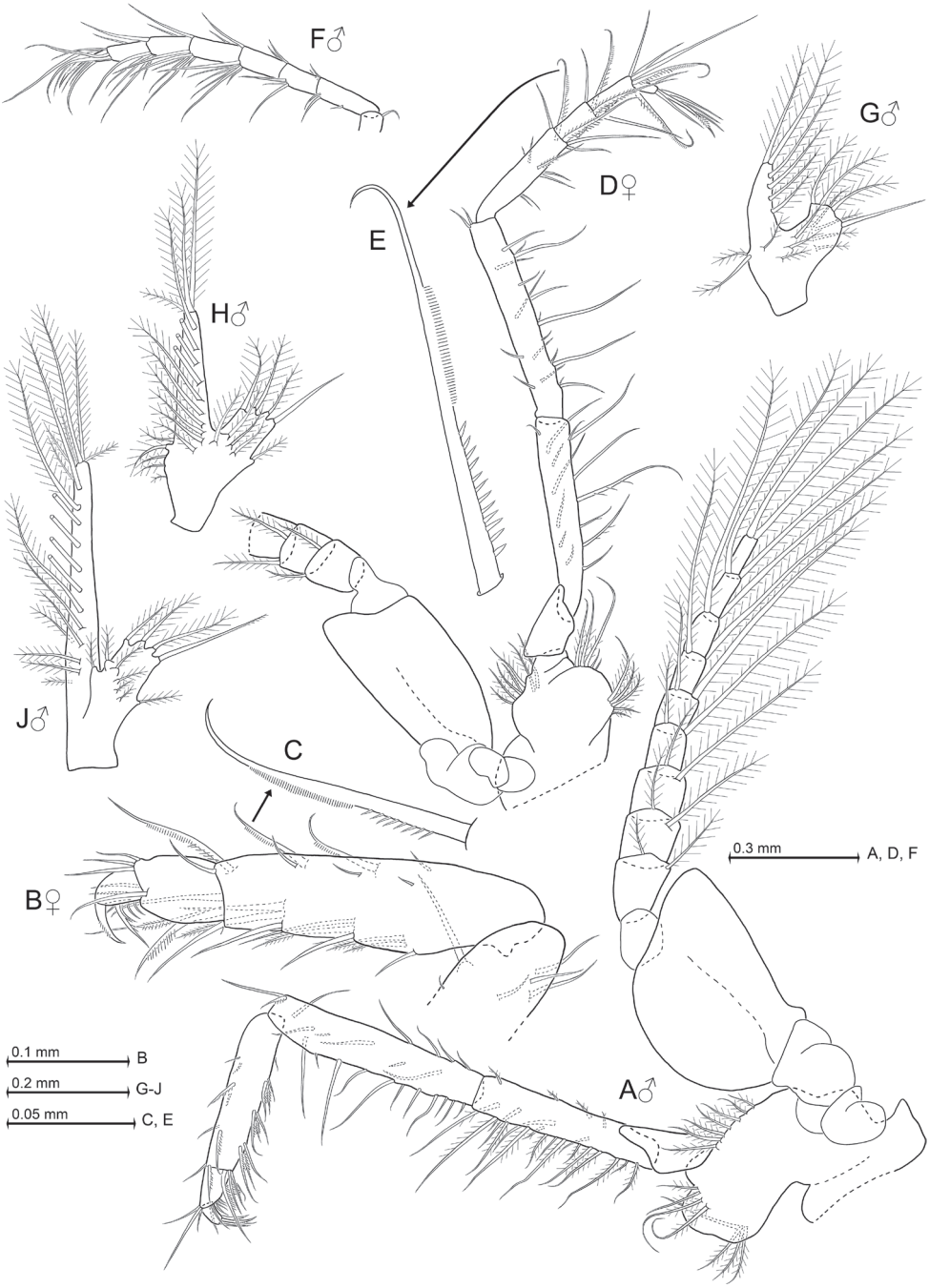


**Figure 4.** *Heteromysis cancelli* sp. n., paratype male with 6.9 mm body length (**A, F–J**), paratypes female 6.1 mm (**B, C**) and 6.4 mm (**D, E**). **A** male third thoracopod, caudal aspect **B** tarsus of female thoracic endopod 3, rostral, detail (**C**) shows modified seta **D** fourth thoracopod, rostral, detail (**E**) shows modified seta **F** tarsus of sixth thoracic endopod, rostral **G–J** series of male pleopods 1, 4, 5, rostral.

***Marsupium.*** Females with large marsupial plates on seventh and eighth thoracopods. Sixth thoracopod with rudimentary oostegite representing a small lobe, on its inner margin with three proximally weakly-barbed setae.

***Penes*** (Fig. 5A). Shape roughly that of rod-like, straight tubes, facing obliquely in anterior direction up to basis of second thoracopod. Each penis very long, stiff, with smooth cuticle; series of three small, barbed setae subterminally on exterior face.

***Pleopods*** (Fig. 4G–J). Length and structure of pleopods do not differ between sexes, with rod-like exopodal portion and shorter lobe-like endopodal portion. The long seta at inner, terminal edge of endopod smooth or almost smooth, all remaining setae well barbed or plumose. Total length of pleopod 5 about twice (198–214%) that of pleopod 1 (n = 4). This increase is not continuous: starting with pleopods 1 versus 2, the length increase between subsequent pleopods is 22–27%, 3–5%, 5–7%, and 41–65%, respectively.

***Uropods*** (Fig. 5C). Exopods reach with 12–21% of their length beyond endopods and 25–33% beyond telson, endopods 15–18% of their length beyond telson. Exopod length 4.1–5.0 times maximum width, inner margin more strongly convex than outer one. Endopods basally with large statocyst, containing discoidal, in dorsal view slightly ellipsoid, statolith of average size. Statoliths with indistinct fundus and distinct tegmen, composed of fluorite; diameter 130–143 μm (n = 4); statolith formula is 2 + 3 + 1 + (7–12) + (7–12) = 21–30. Uropods with densely setose lateral margins, except for their most basal portions.

***Telson*** (Fig. 5D). Length 1.2–1.4 times ultimate abdominal somite, or 0.8–0.9 times exopod of uropods. Length of telson 1.7–1.8 times maximum width. Laminae of cleft show about half average length of lateral spines. Basal half of telson as well as distal portions of its cleft with smooth margins. Lateral spines with almost equal length, their size not increasing distally.

***Colour*** (Fig. 1). General appearance of living specimens light red. Cornea brown-golden; eyestalks mainly light red, except for a light spot near inner anterior corner and a narrow white ribbon along posterior, dorsal portions of the inner margin of the cornea (best visible in left eye of upper male in Fig. 1B). Red chromatophore centres scattered over eyestalks, antennae, carapace, pleon, uropods, and telson. Transverse double series of chromatophores near posterior margin of each thoracomere 8 and pleomere 1-6; additional chromatophores on pleomere 6. Uropods with chromatophores over entire length. Telson with the greatest density of chromatophores. These colours disappeared within a few weeks of fixation, except for some dark brown pigment in cornea. White ribbon on eyestalks persisted longer than red colour on remaining parts of stalk.

***Nauplioid stage*** (Fig. 3N). Breeding female of 6.4 mm body length carried three nauplioid larvae at late substage 2, length 1.2–1.3 mm (n = 3). The female of 6.1 mm showed 11 naupliods at substage 3, length 1.0–1.1 mm (n = 8). Besides features typical of the respective state of development, one finds small setae near tip of antennulae and antennae and a pair of cercopods flanking end of larval abdomen. Each cercopod bears 10–15 acute spines with apically-increasing size (n = 11). A number of additional very small spines (or bristles) present on terminal tip of body, a few also more anteriorly on ventral face of larval abdomen.

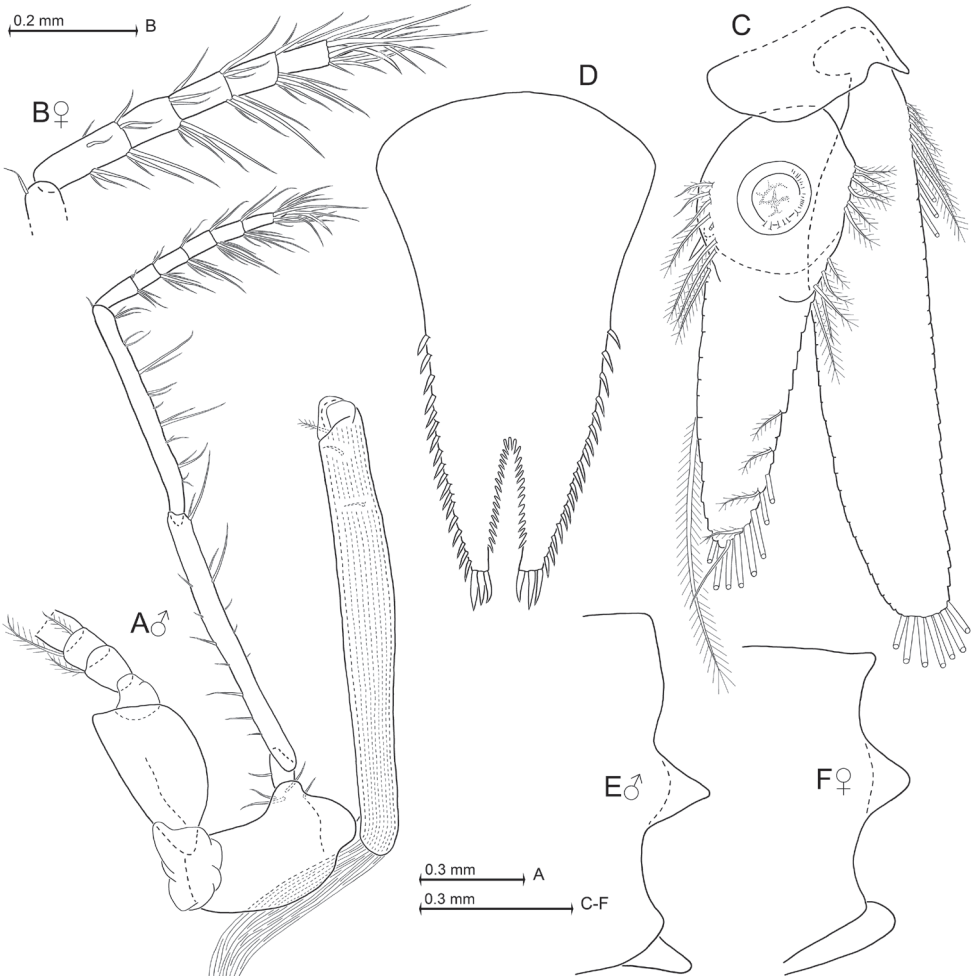


**Figure 5.** *Heteromysis cancelli* sp. n., paratype male with 6.9 mm body length (**A, C–E**), paratype female 6.4 mm (**B, F**) **A** eighth thoracopod with penis, caudal aspect **B** tarsus of female eighth thoracic endopod, caudal **C** uropods, dorsal **D** telson, dorsal **E, F** terminal margin of sixth pleonite, lateral, in male (**E**) versus female (**F**).

**Etymology.** The species name is a noun in genitive singular, adopted from the hermit crab host *Cancellus*.

**Type locality.** Sublittoral marine coastal waters at Roman Rock, off Simonstown, on the False Bay coastline of the Cape Peninsula, South Africa, 34°10.95'S, 18°27.50'E, 20 m depth. *H. cancelli* sp. n. was only found in a single gastropod shell inhabited by the hermit *Cancellus macrothrix* Stebbing, 1924, although four other *Cancellus* specimens and numerous other hermit crabs, mainly *Paguristes gamianus* (H. Milne-Edwards, 1836), were collected and examined from this and nearby sites.

***Heteromysis* (*Heteromysis*) *fosteri* Wittmann & Griffiths, sp. n.**
http://zoobank.org/15D6AFA7-B148-4474-B348-C7F011A0D3E7
Figs 6A, 7, 8

**Type series.** Holotype, adult male with 6.7 mm body length, in vial at NHMW-25905; paratypes adult female 7.0 mm, adult male 6.6 mm, 2 subadult males 3.6, 4.6 mm in vial at SAM-MB-A067551; dissected paratypes on slides at NHMW-25906: adult female 8.0 mm, subadult female 5.9 mm, adult male 6.0 mm; sublittoral marine coastal waters, Miller's Point, on the False Bay coastline of the Cape Peninsula, South Africa, 34°13.78'S, 18°28.47'E, 5 m depth; extracted from empty urchin and gastropod shells without hermit crabs, 25 Jan. 2017, leg. Craig Foster.

**Diagnosis.** Carapace produced into well-projecting, triangular rostrum with narrow rounded apex. Eyes well developed; cornea occupies 35–50% of eye surface; eyestalks with inconspicuous, distally-directed, blunt extension of (obliquely anterior facing) inner margin. Antennular trunk with a number of smooth and barbed setae, but no particularly modified setae; inner distal corner of its terminal segment with anteriorly directed apophysis carrying two large, smooth setae. Antennal scale stout, extending to 0-10% below tip of antennular trunk; outer margin convex. First thoracic sternite with anteriorly-projecting, terminally-rounded median lobe; sternites 2–8 without lobes in both sexes. Carpopropodus of thoracic endopods 1–8 with 2, 2, 2, 3, 6, 6, 6, or 5-6 segments, respectively. Third thoracic endopod weakly dimorphic, without any spines or spine-like setae; carpus not swollen in female, slightly swollen in male (with respect to merus). Carpus of third thoracic endopod with series of three subbasally toothed setae (i.e. with modified barbs) near outer margin. Carpopropodus of fourth thoracic endopod with series of 2–3 subbasally toothed setae near outer margin; no such modified setae in endopods 5–8. Penes long and slender, twice length of merus of eighth thoracic endopod; tip with three rounded lobes, each wider than long. Pleopods reduced to small setose, bilobate plates, without any spines in both sexes. Exopods of uropods extend distinctly beyond endopods. Endopods with only one spine on inner margin, in subbasal position near statocyst. Telson subtriangular, terminally truncate; lateral margins weakly-sigmoid, along their distal 83–93% furnished with slightly discontinuous series of 17–20 spines each. Telson with apical cleft forming proximally poorly rounded 'V'. This cleft slightly deeper than wide, its depth 14–18% telson length. Cleft densely furnished with 16–24 acute laminae all along its margins. Two latero-apical lobes of telson show narrow, transverse apical margins, each bearing a large latero-apical spine plus much smaller medio-apical spine.

**Description.** As described above for *H. cancelli* sp. n. unless stated otherwise in the following. Cephalothorax comprises 41–44% of body length without telson, pleon 56–59%, and carapace 30–38%, when measured along dorsal median line. First thoracic sternite with median lobe showing a smooth, rounded apex. Terminal margin of sixth pleonite with lateral shields more evenly rounded in females (Fig. 7L) versus males (Fig. 7K).


**Figure 6.** Microphotographs of adult female of *Heteromysis fosteri* sp. n. with 7 mm body length (**A**) and of adult male of *Heteromysis octopodis* sp. n. with 9 mm (**B**), each from Miller's Point, Cape Peninsula, South Africa. **A** laboratory photo by C.L. Griffiths **B** in situ image by Craig Foster, this last with background cleaned with electronic tools.

***Carapace*** (Figs 6A, 7A). Non-dimorphic, antero-lateral edges evenly rounded. Anterior pore group with 25–34 pores, in strongly flattened 'U'-shaped arrangement. Posterior pore group with 12–16 pores.

***Eyes*** (Figs 6A, 7A). Anterior, basal, and posterior margins of eyestalks densely covered by scales. Ocular symphysis with broadly-rounded, smooth, subrostral process (dashed line in Fig. 7A).

***Antennulae*** (Fig. 7A, B). Basal segment 41–48% the length of trunk, middle 14–18% and terminal segment 37–43%, when measured along dorsal midline of trunk. Trunk stouter in males, with basal segment 1.1–1.2 times longer than broad, compared to 1.3 times in females. Basal segment with three barbed and one smooth seta at its dorsal apophysis; four plumose setae at tip of outer ventral lobe (exite). Anterior margin of median segment dorsally with a smooth seta and larger barbed seta; and more laterally another smooth seta together with three barbed setae in both sexes. Two small barbed setae anteroventrally near outer margin, visualized by dashed lines in Fig. 7B. Anterior margin of terminal segment in about median position with a lobe bearing 3–4 medium-sized barbed setae plus a dense series of short bristles. Only females with additional, large plumose setae on terminal segment of trunk, one inserting ventrally half-way near inner margin, the second, forward directed in Fig. 7A, on the ventral surface proximally from the inner flagellum at about 9–19% segment length from anterior margin of terminal segment. Outer antennular flagellum 1.5–1.7 times as thick as inner flagellum, when measured near basis.

***Antennae*** (Fig. 7A). Length of antennal scale 2.7–3.0 times its maximum width. Basal segment 24–29% length of peduncle, second 33–39% and third 34–38%.

***Mouth parts*** (not figured). Pars incisivus of mandibles with 3–4 large teeth, and digitus mobilis with 3–4 large plus 1–3 small teeth. Pars centralis with 4–5 spiny teeth. Distal segment of maxillula terminally with 8–10 strong, inconspicuously serrated spines, subterminally with a transverse row of 5–6 barbed setae. Endite of maxillula with three large, distally-spinose setae, and a total of 15–20 smaller, smooth or barbed setae.

***Thoracopods in general*** (Figs 7D–J, 8A–F). Sizes increase from exopod 1 to 4 and then show no clear trend from 4 to 8. Homologous exopods are not clearly different between sexes. Flagellum of first to eighth exopods with 8, 9, 9, 9, 9, 9, 9, 8–9 segments. Exopods with basal plate 1.4–2.0 times longer than broad in both sexes. Claw of third endopod more strongly serrated in males (Fig. 7J) versus females (Fig. 7E), to a minor degree also in fourth endopod, not so in remaining endopods.

***Maxillipeds*** (first and second thoracic endopods; Fig. 7C, D). First endopod with hairs on outer half of sympod. Its epipod large, leaf-like, with comparatively long field of minute scales near insertion with sympod, and subbasally with a large seta densely barbed along its distal 60–75%. Dactylus of second endopod with dense brush of setae, among these 10–15 modified ones.

***Gnathopods*** (Figs 7E, J; 8A–C). Carpopropodus of endopod comparatively slender, four times longer than broad in males, versus five times in females; length is 0.8–0.9 times that of merus and 0.9–1.0 times that of ischium in both sexes. Subbasally toothed setae (Fig. 8C): three on carpus plus two in (sub)apical position near outer margin on merus (Fig. 8A, B).

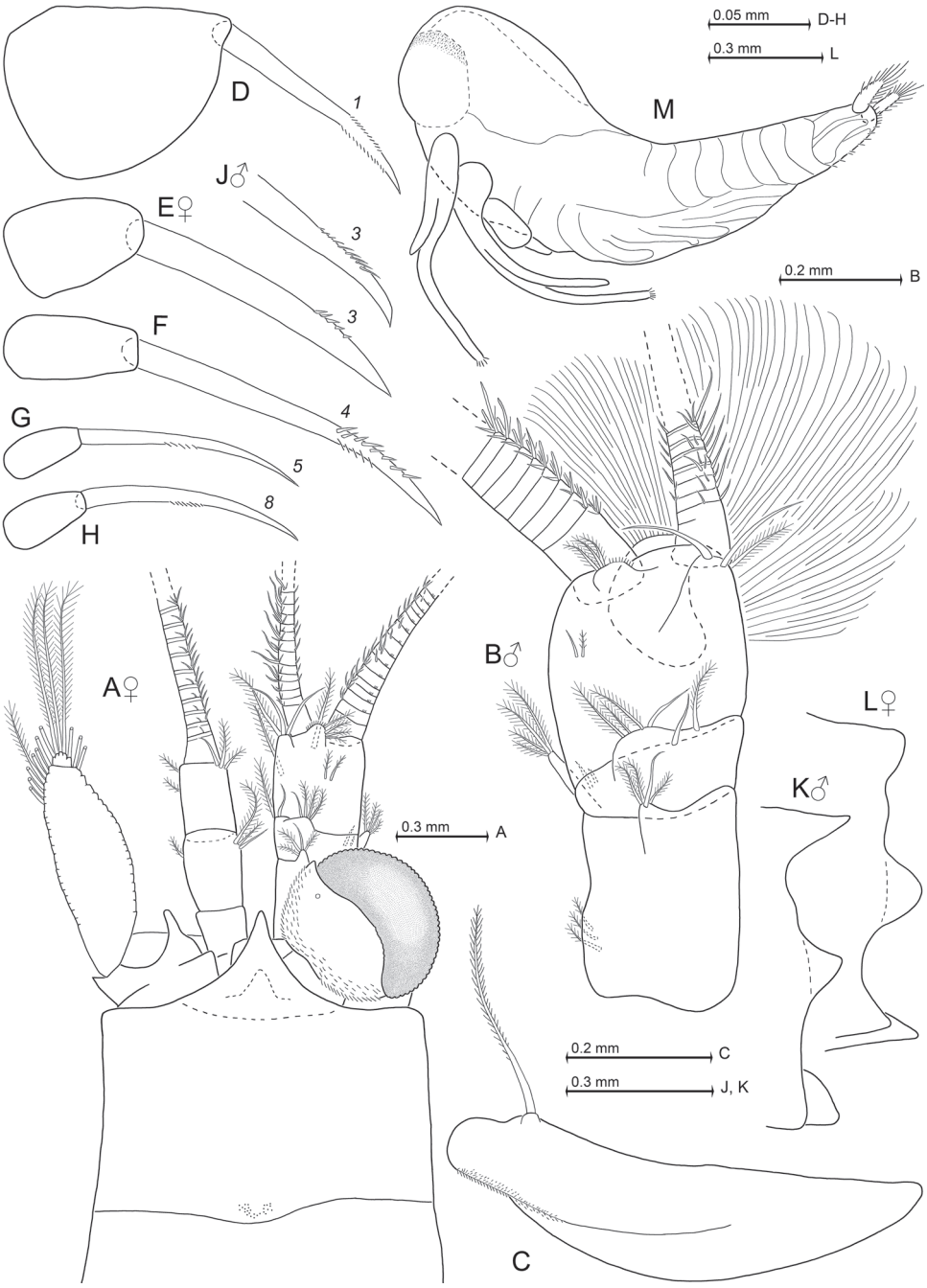


**Figure 7.** *Heteromysis fosteri* sp. n., paratype females with 7.0 mm (**A**) and 8.0 mm (**C–H, L**) body length, paratype male 6.0 mm (**B, J, K**). **A** cephalic region plus anterior part of carapace in female, dorsal view **B** male antennula, dorsal **C** epipod of first thoracopod, caudal **D–H** series of dactylus with claw in thoracic endopods 1, 3-5, 8 of female, caudal **J** tip of claw of third thoracic endopod in male **K, L** terminal margin of sixth pleonite, lateral, in male (**K**) versus female (**L**) **M** nauplioid larva at substage 3, lateral.

***Pereiopods*** (Figs 7F–H, 8D–F). Carpus of fourth endopod (Fig. 8D, E) with longer, subbasally toothed setae compared to third endopod (Fig. 8A–C). Fourth endopod with moderately small dactylus bearing long, strong, weakly-bent claw, microserrated on two opposite sides of subapical portions (Fig. 7F). Fifth to eighth endopods equipped with again smaller dactylus bearing a much shorter claw that shows slightly stronger, distally-increasing curvature; this claw unilaterally microserrated only in median portions of its inner margin (Fig. 7G, H). Sixth thoracopod of females with rudimentary oostegite representing a small lobe, on its inner margin with 0–2 proximally weakly barbed setae.

***Penes*** (Fig. 8F) as above in diagnosis. Presence of small, barbed setae: 1–2 subterminally on exterior face plus 4–5 ones scattered anywhere between 3% and 70% penis length from basis.

***Pleopods*** (Fig. 8G). The seta at inner terminal edge of endopod shows only minor number of barbs, all remaining setae well-barbed or plumose. Total length of pleopod 5 is 177–190% that of pleopod 1 (n = 4). Starting with pleopods 1 versus 2, length increase between subsequent pleopods is 19–32%, 0–13%, 1–18%, and 22–33%, respectively.

***Uropods*** (not figured). The exopods reach with 21–30% of their length beyond endopods and 17–25% beyond telson, the endopods 6–11% of their length beyond telson. Exopod length 4.3–4.4 times maximum width. Statoliths composed of fluorite; diameter 145–181 µm (n = 4); statolith formula is 2 + 3 + 1 + (8–13) + (16–19) = 31–38.

***Telson*** (Fig. 8H). Length 1.2 times that of ultimate abdominal somite or 0.7–0.8 times exopod of uropods. Length of telson 1.2–1.5 times its maximum width. Laminae of cleft show 0.6–0.8 times average length of lateral spines. Length of lateral spines distally discontinuously increasing in size by a factor of about 1.6, arming almost all outer margin.

***Colour*** (Fig. 6A). General appearance of living specimens light red with orange tinge. The stronger orange tinge of the thorax in Fig. 6A is due to yolk in the ovarian tubes. Cornea yellow-golden; eyestalks mainly light red, except for a white ribbon along posterior, dorsal portions of the inner margin of the cornea. Red chromatophore centres scattered over eyestalks, antennae, pleon, uropods, and most densely over carapace, thoracomere 8, and telson. Two transverse series of chromatophores, one in about the middle and the second near posterior margin of pleomeres 1–2, and less regularly arranged also on pleomeres 3–6. Starting with pleomere 3, additional chromatophores are scattered with increasing density up to pleomere 6. Uropods with chromatophores only over proximal 70%. Persistence of colours as in *H. cancelli* sp. n.

***Nauplioid stage*** (Fig. 7M). One female with body length 8.0 mm carried 13 nauplioid larvae at substage 3, length 1.1–1.3 mm. At that same state of development one finds the same external morphological features as in *H. cancelli* sp. n. (Fig. 3N shows substage 2). Each cercopod bears 10–14 acute spines with apically increasing size.

**Etymology.** The species name is a noun in genitive singular, named after well-know underwater-photographer and diver Craig Foster, who has accompanied and assisted the second author in many collecting expeditions and who made all in situ photographs and sampled all specimens of both this species and the one following.

**Type locality.** Sublittoral marine coastal waters at Miller's Point, on the False Bay coastline of the Cape Peninsula, South Africa, 34°13.78'S, 18°28.47'E. This is only 5.5

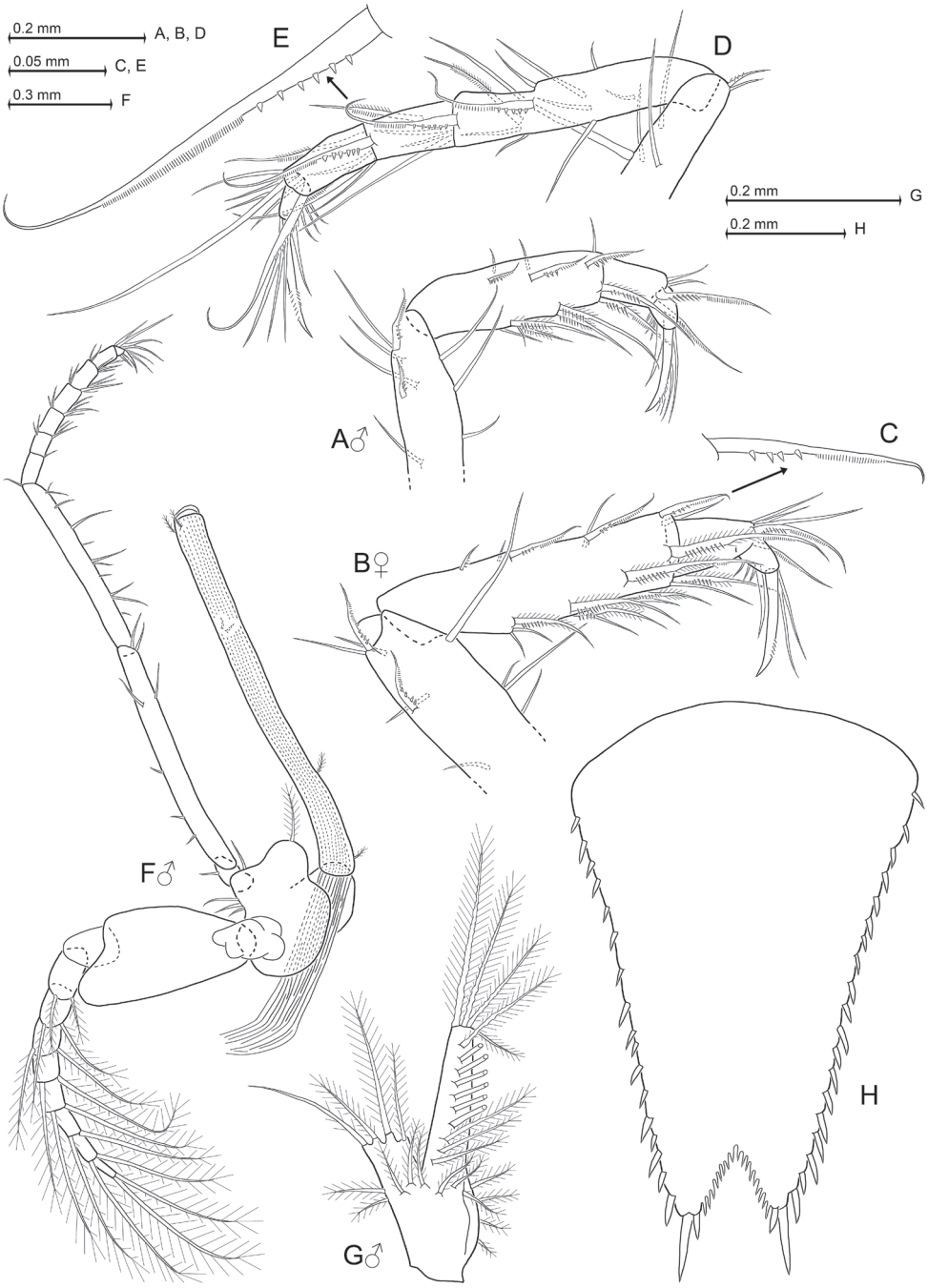


**Figure 8.** *Heteromysis fosteri* sp. n., paratype male (**A, F–H**) with 6.0 mm body length and paratype female 8.0 mm (**B–E**). **A** male tarsus with part of merus pertaining to third thoracic endopod, caudal aspect **B** the same for female, detail (**C**) shows subbasally toothed seta **D** tarsus of fourth thoracic endopod, caudal, detail (**E**) shows subbasally toothed seta **F** eighth thoracopod with penis, caudal **G** third male pleopod, rostral **H** telson, dorsal.

km to the SSE of the type locality of *H. cancelli* sp. n. (above). Materials were extracted from mixed collection of dead shells mainly belonging to the whelk *Argobuccinum pustulosum* (Lightfood, 1786), the winkle *Turbo cidaris* Gmelin, 1791, and the urchin *Parechinus angulosus* (Leske, 1778).

### *Heteromysis* (*Heteromysis*) *octopodis* Wittmann & Griffiths, sp. n.

http://zoobank.org/6C36EF49-CECB-4506-BD82-0B49ACCBD83B
Figs 6B, 9–11

**Type series.** All materials from Miller's Point, on the False Bay coastline of the Cape Peninsula, South Africa, leg. Craig Foster. Holotype, adult male with 7.0 mm body length, in vial at NHMW-25907; paratypes immature female 6.2 mm and immature male 6.1 mm, in vial at SAM-MB-A067552; dissected paratypes adult male 6.8 mm, subadult female 10.8 mm, immature female 7.8 mm, on slides at NHMW-25908, associated with *Octopus vulgaris* inside den in 3 m depth, 34°13.77'S, 18°28.45'E, 15°C, 26 March 2017; paratype adult male 8.8 mm (dissected, slides at NHMW-25909) from euhaline intertidal pool, 34°13.79'S, 18°28.43'E, 10 Aug. 2014; paratypes 2 subadult females (9.4 mm entire, 9.0 mm in 2 parts, both in vial at SAM-MB-A067553) plus damaged subadult female (estimated original size 8.8 mm, head missing, dissected, slides at NHMW-25910), from same pool as before, at a few cm depth upon low tide, 8 Sept. 2015.

**Diagnosis.** Based only on adult males and subadult females. Carapace produced into well-projecting, (sub)triangular rostrum with rounded apex. Eyes well-developed; cornea occupies 60–70% of eye surface; eyestalks with inconspicuous, distally-directed, blunt extension of (obliquely anterior facing) inner margin. Antennular trunk with a number of smooth and barbed setae, but no particularly modified setae; inner distal corner of its terminal segment with apophysis carrying two medium-sized, smooth setae. Antennal scale stout, extending to 0–20% below tip of antennular trunk; outer margin convex. First thoracic sternite with anteriorly-projecting, terminally-rounded median lobe; sternites 2-8 without lobes. Carpopropodus of thoracic endopods 1-8 with 2, 2, 2-3, 4-6, 5-7, 5-8, 6-8, or 6-8 segments, respectively. Third thoracic endopod without any spines or spine-like setae; carpus not swollen with respect to merus. Carpus with series of three weakly-modified setae near outer margin; these setae subbasally furnished with bristles. Merus (sub)terminally with two subbasally toothed setae. Fourth thoracic endopod with series of 2–3 such toothed setae near outer margin of carpopropodus; no such modified setae in endopods 5–8. Penes long and slender, 1.6–1.7 times length of merus of eighth thoracic endopod; tip with three rounded lobes, each wider than long. Pleopods reduced to small setose, bilobate plates, without any spines. Exopods of uropods extend distinctly beyond endopods. Endopods with only one spine on inner margin, in subbasal position near statocyst. Telson subtriangular, terminally truncate; lateral margins weakly sigmoid, along their distal 46–53% furnished with almost continuous series of 13–17 spines each. Telson with apical cleft forming a proximally rounded 'V'. Cleft slightly deeper than wide, its depth 17–23%


**Figure 9. A** subadult female of *Heteromysis octopodis* sp. n. with 11 mm body length from tide pool **B** multi-species association inside den in 3 m depth, occupied by *Octopus vulgaris*, to the right with the crab *Guinusia chabrus*; upper arrow points to a mysid school of what we assume to be *H. octopodis* sp. n., lower arrow to a different but undetermined mysid species. **A, B** from Miller's Point, Cape Peninsula, South Africa; in situ images by Craig Foster **B** image is taken of the same octopus den from which the samples were collected, but on a different date.

telson length. Cleft densely furnished with a total of 26–37 acute laminae all along its margins. Two latero-apical lobes of telson show narrow transverse apical margins, each bearing a large latero-apical spine, plus much smaller medio-apical spine.

**Description.** As described above for *H. cancelli* sp. n. unless stated otherwise in the following. Cephalothorax comprises 37–44% of body length without telson, pleon 54–63%, and carapace 32–38%, when measured along dorsal median line. First thoracic sternite with median lobe showing smooth rounded apex. Each of first to fifth abdominal somites measure 0.8–1.1 times length of sixth somite. Terminal margin of sixth pleonite with lateral shields triangular, with tip more rounded in subadult females (Fig. 10L) than in males (Fig. 10K).

***Carapace*** (Figs 6B, 9, 10A). Non-dimorphic, antero-lateral edges evenly rounded. Cervical sulcus well marked, cardial sulcus weak but distinct. Anterior pore group of carapace with 29–32 pores in strongly flattened 'U'-shaped arrangement; posterior group with 12–15 pores (n = 6).

***Eyes*** (Figs 6B, 9, 10A). Anterior and posterior margins of eyestalks densely covered by scales, but not so the basal portions. Ocular symphysis with subtriangular to sinusoid, in any case terminally rounded, smooth, subrostral process (dashed line in Fig. 10A).

***Antennulae*** (Fig. 10A, B). Basal segment 41–49% length of trunk, middle 14–18% and terminal segment 34–44%. Trunk on the average stouter in males, with basal segment 0.9–1.4 times longer than broad, compared to 1.2–1.5 times in subadult females. Terminal portion of basal segment with bifid dorsal apophysis bearing 4–5 barbed setae on its more median projection, plus two smooth setae on its outer projection. Outer ventral lobe of basal segment bears four plumose setae at its tip plus a small barbed seta in subbasal position. Anterior margin of median segment dorsally with apophysis bearing a smooth seta together with several barbed setae; inner margin anteriorly with medium-sized to large barbed seta together with smooth seta. Two small barbed setae antero-ventrally close to outer margin (not visible in Fig. 10A). Terminal segment ventrally with 1–2 large, obliquely forwards-directed, plumose setae and 0–2 additional plumose setae dorsally at inner distal corner in both sexes. Lobe with four medium-sized barbed setae plus a dense series of short bristles in about median position on anterior margin of terminal segment. Outer antennular flagellum 1.3–1.5 times as thick as inner flagellum, when measured near basis.

***Antennae*** (Fig. 10A). Length of antennal scale 2.8–3.2 times its maximum width. Apical segment contributing 5–7% to total scale length. Basal segment 21–28% length of peduncle, second 36–40% and third 34–40%.

***Mouth parts*** (not figured). Pars incisivus of mandible with 3–4 large teeth, and digitus mobilis with 3–4 large plus 2–3 small teeth. Pars centralis with 3–4 spiny teeth. Distal segment of maxillula terminally with 9–12 weakly serrated spines, subterminally with a transverse row of 5–6 barbed setae. Endite of maxillula with three large, distally spinose setae, and 18–28 smaller, smooth or barbed setae.

***Thoracopods in general*** (Figs 10D–H; 11A–F). Sizes increase from exopod 1 to (4–6) and decrease from 6 to 8. Flagellum of first to eighth exopods with 8, 9, 9, 9, 9, 9, 9, 9 segments. Exopods with basal plate 1.3–2.2 times longer than broad. Claws of endopods 1, 3, 4 more strongly serrated in male versus subadult female, not so in endopods 5–8.

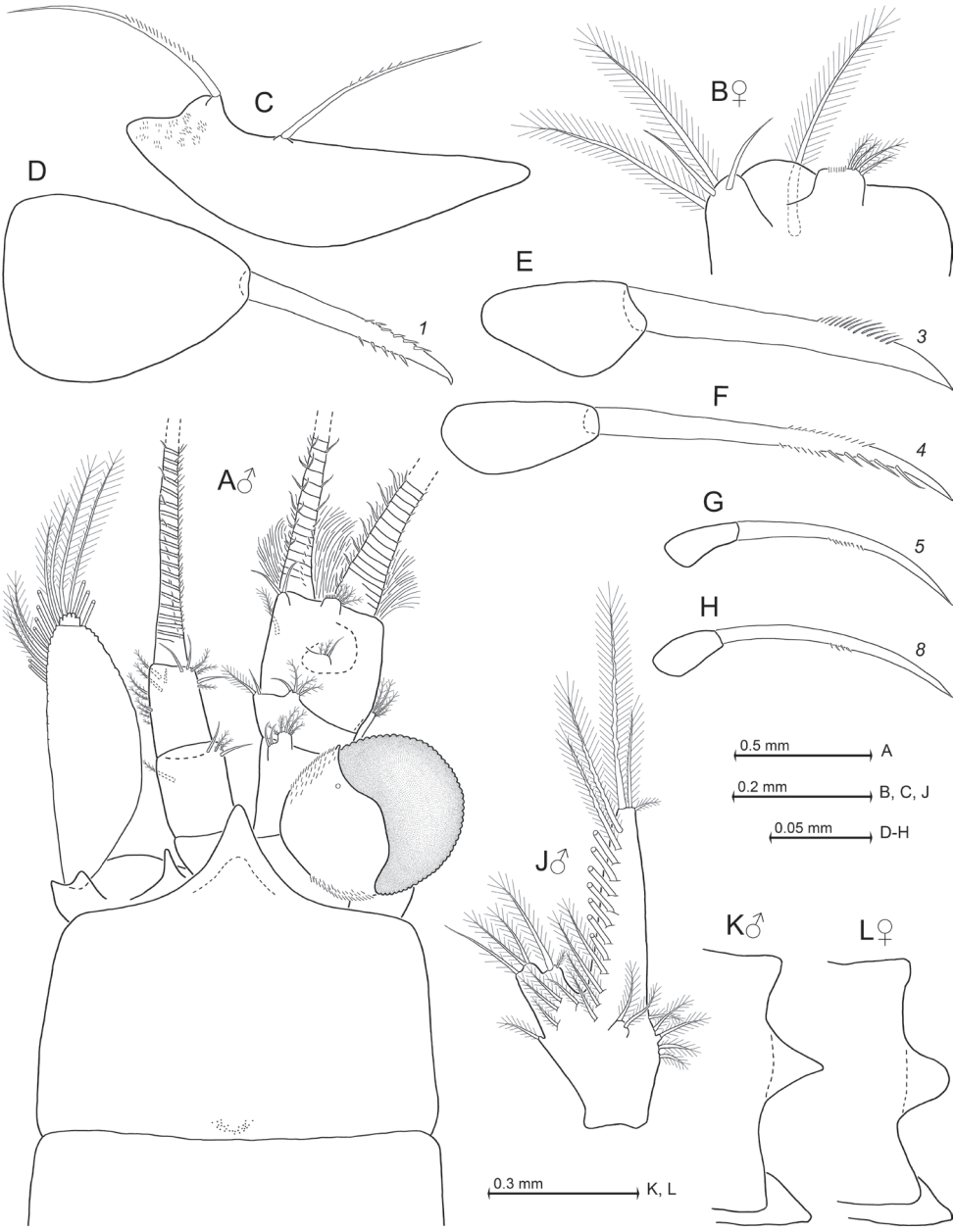


**Figure 10.** *Heteromysis octopodis* sp. n., paratype adult male with 8.8 mm body length (**A, D–K**), paratype subadult females with 9.0 mm (**B, L**) and 8.8 mm (**C**). **A** cephalic region plus anterior part of carapace in male, dorsal view **B** anterior margin of antennular trunk in subadult female, dorsal **C** epipod of first thoracopod, caudal **D–H** series of dactylus with claw in thoracic endopods 1, 3-5, 8, caudal **J** fourth male pleopod, rostral **K, L** terminal margin of sixth pleonite, lateral, in male (**K**) versus subadult female (**L**).

***Maxillipeds*** (Fig. 10C, D). Sympod of first endopod with hairs on outer half. First thoracic epipod large, leaf-like, with small field of minute scales near insertion with sympod, and (sub)basally with 1–2 large, sparsely barbed setae (Fig. 10C). Dactylus of first endopod with strong, subapically, bilaterally-microserrated claw (Fig. 10D). Dactylus of second endopod with dense brush of setae, among these 16–19 modified ones.

***Gnathopods*** (Figs 10E, 11A–C). Endopod with comparatively slender carpopropodus, 4.9–5.5 times longer than broad; length 0.8–1.0 times that of merus, and 0.9–1.0 times that of ischium.

***Pereiopods*** (Figs 10F–H, 11D–F). Fourth endopod with moderately-small dactylus bearing a long, weakly-bent claw, microserrated on two opposite sides of its subapical portions (Fig. 10F). Fifth to eighth endopods equipped with again smaller dactylus bearing much shorter claw that shows a stronger, distally increasing curvature; this claw unilaterally microserrated only in median portions of inner margin (Fig. 10G, H).

***Penes*** (Fig. 11F) long, facing obliquely in anterior direction up to basis of fourth thoracopod. Five to six small, barbed setae scattered all along the penis.

***Oostegites.*** The subadult females already have eggs in the ovaries, visible in Fig. 9A by yellow complexion through the semi-transparent, essentially red carapace (best visible at the rostrum). The subadults show well-formed but still immature marsupial plates on the seventh and eighth thoracopods, plus rudimentary oostegites on the sixth thoracopods.

***Pleopods*** (Fig. 10J). The seta at inner, terminal edge of endopod weakly barbed, remaining setae well-barbed or plumose. Part of plumose setae of exopod with wave-like series of weak constrictions along shaft. Total length of pleopod 5 is 173–207% that of pleopod 1 (n = 7). Starting with pleopods 1 versus 2, the length increase between subsequent pleopods is 14–31%, 3–12%, 0–15%, and 21–58%, respectively.

***Uropods.*** The exopods reach with 15–38% of their length beyond endopods and 33–43% beyond telson, endopods 6–17% of their length beyond telson. Exopod length 3.8–4.2 times maximum width. Statoliths composed of fluorite; diameter 120–196 μm (n = 12); statolith formula 2 + 3 + (0–1) + (8–16) + (12–19) = 27–39.

***Telson*** (Fig. 11G). Length 1.2–1.5 times that of ultimate abdominal somite, or 0.7–0.9 times exopod of uropods. Length of telson 1.5–1.6 times its maximum width. Laminae of cleft show about 0.5–0.7 times average length of lateral spines. Basal half of outer margins smooth. Length of lateral spines distally (somewhat discontinuously) increasing in size by a factor of 1.3–1.7 .

***Colour*** (Figs 6B, 9). General appearance of living specimens red-orange to blazing red. Cornea brown to yellow-golden; eyestalks red, except for a white ribbon along posterior, dorsal portions of the inner margin of the cornea (best visible in Fig. 6B). Chromatophores could only partly be discerned individually due to their strong expansion (stronger in Fig. 6B than in Fig. 9A) in three specimens micro-photographed alive. Red spots scattered over eyestalks, antennae, carapace, pleon, uropods, and telson. Transverse double series of spots near posterior margin of each pleomere, not well distinguishable in thoracomeres; a broader posterior red band on pleomere 6. Uropods and telson most intensively red. Compared with that of the male in Fig. 6B, the more orange tinge of the female thorax in Fig. 9A comes from yellow yolk in the ovarian tubes. Persistence of colours as in *H. cancelli*.

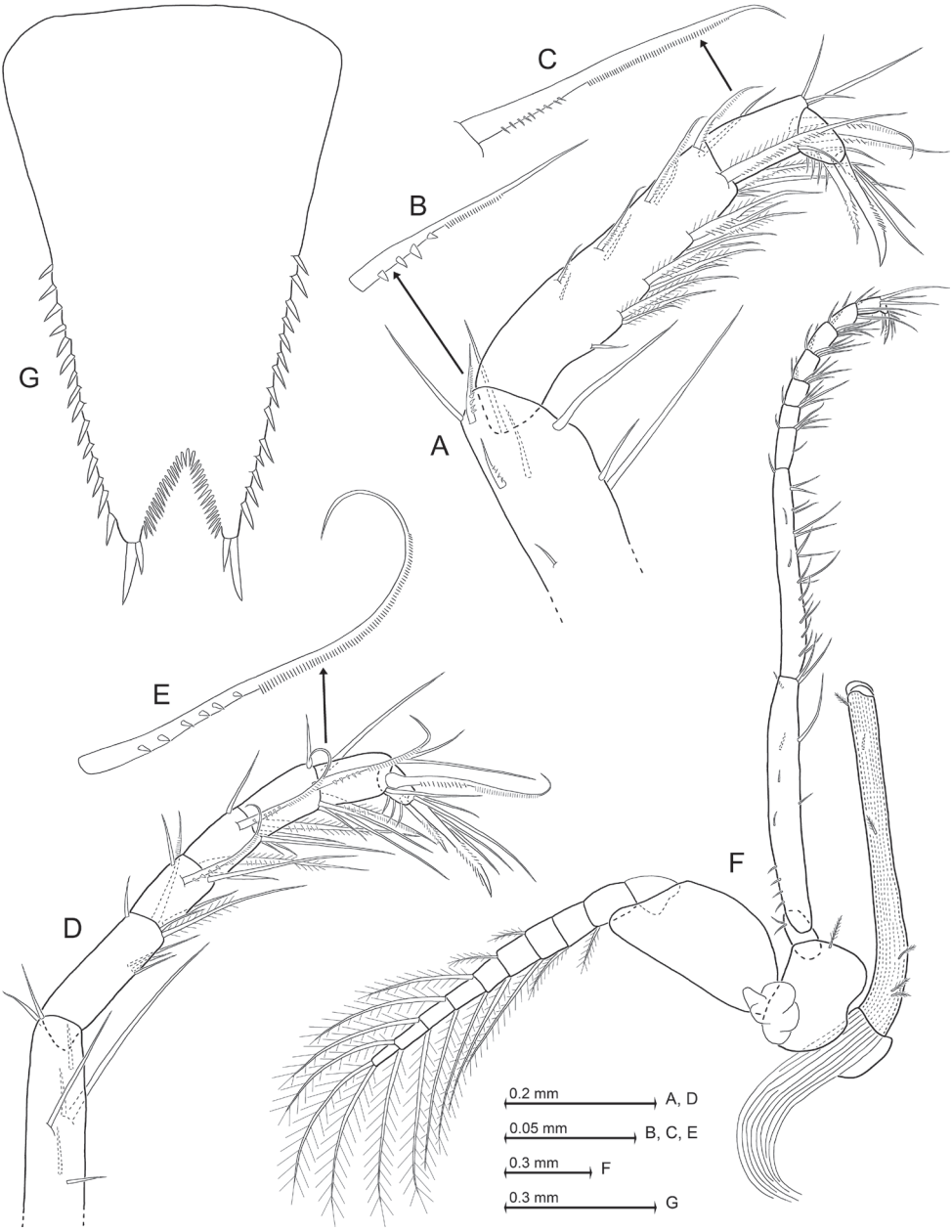


**Figure 11.** *Heteromysis octopodis* sp. n., paratype adult male with 8.8 mm body length. **A** tarsus with part of merus pertaining to third thoracic endopod, caudal aspect, details show subbasally toothed seta on merus (**B**) versus subbasally barbed seta on carpus (**C**) **D** tarsus with part of merus pertaining to fourth thoracic endopod, caudal, detail (**E**) shows subbasally toothed seta **F** eighth thoracopod with penis, caudal **G** telson, dorsal.

**Etymology.** The species name *octopodis* is a noun in genitive singular, derived from the substantive octopus by using the third declension of New Latin.

**Type locality.** Octopus den (Fig. 9B) in 3 m depth at Miller's Point, on the False Bay coastline of the Cape Peninsula, South Africa, 34°13.79'S, 18°28.43'E. This is closely adjacent to the type locality of *H. fosteri* sp. n. (above).

**Microdistribution.** Schools of this mysid were encountered during daytime in shallow sublittoral waters inside dens occupied by *Octopus vulgaris* (in case of Fig. 9B together with a crab and an additional, undetermined mysid species). Association with octopus appears a regular phenomenon as *H. octopodis* was found there nine times between 14 May 2016 and 26 March 2017. Nonetheless, this mysid species was also found upon low tide in a few cm depth in rocky tide pools (Figs 6B, 9A). Also this kind of microdistribution appears to be a regular phenomenon since it occurred there upon various excursions, namely 10 Aug. 2014, 14 Aug. 2014, and 8 Sept. 2015.

## Discussion

### Relationships of the new species

There is a close morphological relationship between the three new *Heteromysis* species from the Cape Peninsula, which share most details described above for the eyes, antennula, mouth parts, carapace, and uropods. This regards also colour as the new species are essentially red, but share a white stripe along the dorso-lateral terminal margin of the eyestalks. As major differences from *H. cancelli* sp. n., *H. fosteri* sp. n. shows relatively shorter telson cleft, different distribution of laminae within the telson cleft, shorter spine-free basal portion of the lateral margins of the telson, as well as differently modified setae on merus and carpus of thoracic endopod 3 and on carpopropodus of endopod 4. *H. octopodis* sp. n. is most similar to *H. fosteri*, but is distinguished mainly by a longer spine-free basal portion of the lateral margins of the telson, by more segments at the carpopropodus of thoracic endopod 4, and by differently modified setae on carpus of endopod 3. It differs from *H. cancelli* by relatively shorter telson cleft, different distribution of laminae within the telson cleft, and by more segments together with differently modified setae on carpopropodus of endopod 4. Both, *H. forsteri* and *H. octopodis*, differ from *H. cancelli* by endopod 4 with shorter and less slender claw, and by endopods 5–8 with claws serrated on only their inner margin, while the outer margin is smooth.

### Subgeneric assignment

The three new species described here are concordant with the original definition of the subgenus *Heteromysis* S.I. Smith, 1873, by non-dimorphic, rudimentary pleopods without spines or spine-setae. Among the eleven species of the genus *Heteromysis* listed for the E. Atlantic in the key below, six belong to this subgenus. Three species show

dimorphic pleopods together with a subapically flagellate, modified seta near the inner distal corner of the antennular trunk, typical of the subgenus *Olivemysis* Băcescu, 1968, according to the diagnosis of Price and Heard (2011). For two species the available data do not suffice for subgeneric assignment.

Among the three previously described E. Atlantic species of the subgenus *Heteromysis*, only *H.* (*Heteromysis*) *microps* (G.O. Sars, 1877) shares a single spine on the endopods of uropods with the three additional, new species described here for this subgenus. However, *H. microps* differs clearly from each new species by eyes with smaller cornea, by median sternal processes present on the last five thoracic somites, and by a single spine on basal third of each lateral margin of the telson. Single spines on the endopods of uropods are also found outside the E. Atlantic (two species without subgeneric assignment): in *H. nouveli* Brattegard, 1969, and *H.* (*Heteromysis*) *spottei* Price & Heard, 2000, from W. Atlantic; *H.* (*Heteromysis*) *australica* Băcescu & Bruce, 1980, *H.* (*Olivemysis*) *kushimotensis* Murano & Fukuoka, 2003, *H.* (*Olivemysis*) *meenakshiae* Bamber, 2000, and *H.* (*Olivemysis*) *panamaensis* O.S. Tattersall, 1967, from Pacific; and *H. proxima* W.M. Tattersall, 1922, from Indian Ocean. One to four spines are found in *H.* (*Olivemysis*) *mayana* Brattegard, 1970, from W. Atlantic. The three new species differ from members of the subgenus *Olivemysis* by absence of flagellate, modified setae on antennular trunk and by male pleopods without spines (spine-setae); and from the remaining five species listed above, including *H. microps*, by absence of spines or spine-like setae on carpopropodus of third thoracic endopod.

## Larval morphology

The nauplioids of *Heteromysis cancelli* sp. n. and *H. fosteri* sp. n. share setae at the tip of antennulae and antennae, so far known, with certain other species of Heteromysini, for example with *H. wirtzi* Wittmann, 2008, *H. ekamako* Wittmann & Chevaldonne, 2016, and *Ischiomysis peterwirtzi* Wittmann, 2013. Among these five species, *H. cancelli* and *H. fosteri* are the only ones showing cercopods close to the tip of the nauplioid abdomen. Including the new findings for *Heteromysis* (Figs 3N, 7M) cercopods or furcal spines, respectively, are currently known from diverse species belonging to only eight genera within the Mysida, all genera pertaining to the family Mysidae: *Acanthomysis*, *Hemimysis*, *Heteromysis*, *Metamysidopsis*, *Mysidium*, *Mysis*, *Neomysis*, and *Praunus* (Nusbaum 1887, Bergh 1893, Manton 1928, Davis 1966, Green 1970, Modlin 1979, Wittmann 1981, Carreño et al. 1989, Jirikowski et al. 2015; taxonomy in part updated, data in part derived from drawings). These genera belong to the subfamilies Heteromysinae, Leptomysinae, and Mysinae, respectively, while no caudal furcae are so far known from at least six out of the ten currently acknowledged subfamilies of the Mysidae. The situation is not clear for Boreomysinae, where Jepsen (1965) found "polyspinal appendages" on the abdomen of nauplioids of *Boreomysis arctica* (Krøyer, 1861), however in much more anterior position compared to normal caudal furcae. A caudal furca is well known from 'lower' Crustacea, according to Wittmann et al. (2014) suggesting that the presence of a furca found in nauplioid larvae of a limited number of Mysidae, represents a case of plesiomorphism.

## Microhabitat

As in most species of *Heteromysis*, the three new species show a strictly benthic mode of live. The occurrence of *H. fosteri* in empty shells is in line with other five *Heteromysis* species reported by San Vicente and Monniot (2014) from this and mostly also from other free-living habitats. A major number of species hovers in cryptic habitats during the day (may emerge during the night), such as dense vegetation, gravel, empty shells, coralloid habitats, microcaves or larger marine caves.

As for *H. cancelli* and *H. octopodis*, benthic invertebrates may serve for many species as cryptic habitats in a broader sense, such as sponges, stony corals, gorgonians, sea anemones, brittle stars, tubes of annelids, and shells inhabited by hermit crabs (see list in Fukuoka 2005). The occurrence of *H. octopodis* in tide pools is shared with only few species of *Heteromysis* (Tattersall and Tattersall 1951, Bousfield 1958, Băcescu 1986, Fukuoka 2005). Such microdistribution regards mainly a minor fraction within or among populations as in the well known E. Atlantic and Mediterranean species *Heteromysis norvegica* G.O. Sars, 1883, that hides in tide pools under stones at low tide. It may shelter also in gastropod shells or in dense vegetation. During daytime it is (epi)-benthic in 0-400 m depth (Lagardère and Nouvel 1980, Frutos and Sorbe 2013) and may be planktonic during the night (Tattersall and Tattersall 1951: reported as *H. formosa* S.I. Smith, 1874). Shallow water species of diverse other mysid genera are often found in rocky tide pools or among weed at low tide (Tattersall and Tattersall 1951). Intertidal distribution as a component of normal life habit is mainly found in species of the subfamily Gastrosaccinae, which are sand-burrowing during low tide and/or during daytime and may emerge into the water column during the night (Takahashi and Kawaguchi 1997).

## Commensalism with invertebrates

The facultative ectocommensal association reported here of *Heteromysis octopodis* with *Octopus vulgaris* represents the first documented regular association between mysids and cephalopods. On the first glance it sounds surprising that a commensal of sublittoral invertebrates may be also found in tide pools. However, there is a comparable case already known from *Heteromysis*: the E. Atlantic and Mediterranean *H. microps* G.O. Sars, 1877, is usually found on sublittoral mud flats, pebble bottoms, and in seagrass stands (Tattersall and Tattersall 1951, Zouhiri et al. 1998, Wittmann 2001), but also occurs on intertidal mud flats where it hovers in burrows of the mud shrimp *Upogebia pusilla* (Petagna, 1792) during low tide (Lavesque et al. 2016). The Y-shaped burrows penetrate up to 1 m into the sediment and serve as shelter to a diversity of invertebrate and fish species (listed by Lavesque et al. 2016). In analogy, there is several crustacean species associated with *Octopus* as is shown in Fig. 9B: in addition to *H. octopodis* there are an yet undetermined mysid species and the crab *Guinusia chabrus* (Linnaeus, 1758). So far, we did not examine whether these last crustaceans may regularly occur in such associations.

*H. cancelli* sp. n. follows *H. dardani* Wittmann, 2008, as the second association between mysids and hermit crabs documented from the E. Atlantic Ocean. The new species was found only in a large gastropod shell inhabited by *Cancellus macrothrix*, and not in any other type of microhabitat, although a variety of sampling methods was used. In order to test whether this commensalism may be obligate, a number of dead gastropod and sea urchin shells were collected 5.5 km from the type locality and then brought to the lab where the mysids were extracted and photographed still alive. Surprisingly, the shells yielded no *H. cancelli*, but only a different species described above as *H. fosteri* sp. n. (i.e. finding mysids in these empty shells was not surprising, but the exclusive occurrence of a different congeneric species in such shells was surprising). This points to obligate commensalism of the former species with hermit crabs, but insufficient data are available at present to demonstrate this, in that all specimens so far known derive from a single hermit specimen (among only five of this rare hermit crab species examined). The species has not, however, been observed amongst hundreds of hermit crabs of other species examined both at this site and in the broader region. With this new species a total of eight *Heteromysis* species have been reported as commensals of hermit crabs at a worldwide scale (Bonnier and Pérèz 1902, Clarke 1955, Tattersall 1967, Vannini et al. 1993, 1994, Fukuoka 2005, Wittmann 2008). As far as known, five *Heteromysis* species appear to be obligate commensals, at least two species are less host specific and are also found in microhabitats other than shells inhabited by hermit crabs. Based on morphological comparison Wittmann (2008) concluded that commensalism with hermit crabs may have independently evolved in the shelf areas of the Indo-Pacific, E. Pacific, and Atlantic oceans.

## Key to the *Heteromysis* species of the E. Atlantic

Modified and updated from the key given by Wittmann and Wirtz (2017). Certain heterogeneities in the structure of the key are due to missing data.

> Heteromysini with normal eyes and a well-developed cornea. Males without mediocaudal lobe on appendix masculina of the antennular trunk; both sexes without a pair of backwards-oriented modified setae on inner terminal angle of antennular trunk, only forwards-oriented setae are present, not modified or modified in different ways. Gnathopod moderately to strongly stout, propodus separated from carpus by an oblique or a transverse articulation or not separated (propodus not always stouter than merus as in the three species described above). Thoracic endopod 4 with entire, apically not bifid claw. Thoracic endopod 8 in both sexes without flagellate spine on ischium and without spiniform extension of praeischium. Penes terminally not or only weakly widened by lobes. Females without sternal plate transversely projecting behind marsupium. Pleopods rudimentary and dimorphic or non-dimorphic. Genus *Heteromysis* S.I. Smith, 1873 ..... **1**

1 Eyestalks without spiniform extension, or distally with small blunt extension of inner margin. All pleopods of male (if known) without spines or spine-setae.....**5**

– Eyestalks distally with small spiniform extension of the inner margin. At least one among third and fourth (usually both) pleopods of male with flagellate spines (spine-setae) distally on outer margin of endopodal portion .....**2**

2 Apical cleft 22-23% telson length. Antennular trunk with two forwards-directed, smooth setae on inner, distal corner of terminal segment; no flagellate seta present. Endopod of uropods with 3-4 spines near statocyst. Only one damaged male known .....***H. tattersalli* H. Nouvel, 1942** (Cape Verde Islands, 91 m)

– Apical cleft longer than 23% telson length. One flagellate, strong, modified seta on inner distal corner of terminal segment of antennular trunk.....**3**

3 Second male pleopod without spines. Endopod of uropods with 2–3 spines on inner margin near statocyst..... ***H.* (*Olivemysis*) *sabelliphila* Wittmann & Wirtz, 2017** (Cape Verde Islands, 6–18 m, associated with sabellids, also on gravel bottom or in submarine cave)

– Second male pleopod with one or more flagellate spines. Endopod of uropods with 3–4 spines.....**4**

4 Fifth to seventh thoracic endopods with (4-6)-segmented carpopropodus. Endopod of uropods with three spines on inner margin near statocyst .....***H.* (*Olivemysis*) *dardani* Wittmann, 2008** (Madeira, 10–20 m, commensal of hermit crab)

– Fifth to seventh thoracic endopods with seven-segmented carpopropodus. Endopod of uropods with four spines on inner margin near statocyst...***H.* (*Olivemysis*) *wirtzi* Wittmann, 2008** (Madeira, 28 m, commensal of sea anemone)

5 Telson with spines along distal 80-100% of the lateral margins.....**10**

– Telson with spines mainly on distal half; without spines, or at most one spine, on basal third of each lateral margin .....**6**

6 Telson cleft wider than deep. Endopod of uropods with four spines on inner margin near statocyst. Powerful gnathopod with stout carpus. Only one female specimen known.....***H. atlantidea* O.S. Tattersall, 1961** (Cape Verde Islands, 8 m)

– Telson cleft at least about as deep as wide, in most species deeper than wide .....**7**

7 Telson with one spine on basal third of each lateral margin, followed by a naked portion and then 8-13 spines on distal half; medio-apical spines distinctly shorter than latero-apical spines. Endopod of uropods with only one spine, which is near statocyst..... ***H.* (*Heteromysis*) *microps* (G.O. Sars, 1877)** (NE Atlantic and Mediterranean: N Adriatic, Gulf of Naples, Sardinia, Tunisia, 0–16 m, mud flats, gravel bottoms, seagrass stands, burrows of mud shrimp, meso- to metahaline)

– Telson without spines on basal third of lateral margins .....**8**

8 Telson on each side with one medio-apical spine being distinctly shorter than latero-apical spine; cleft with a total of 26–37 laminae all along its margins.

Endopod of uropods with only one spine below statocyst ..... ..... ***H.* (*Heteromysis*) *octopodis* sp. n.** (South Africa: Cape Peninsula, 0-3 m, associated with octopus or in tide pools)

– Telson with the 1–2 medio-apical spines on each side longer or subequal compared to latero-apical spines ..... **9**

9 Endopod of uropods with only one spine below statocyst. Telson cleft densely furnished with a total of 29–33 laminae along basal 81–84% of its margins..... ***H.* (*Heteromysis*) *cancelli* sp. n.** (South Africa: Cape Peninsula, 20 m, associated with hermit crab)

– Endopod of uropods with 17-30 spines along inner margin between statocyst and tip. Telson cleft densely furnished with a total of 11–21 laminae along basal 50–70% of its margins ..... ***H.* (*Heteromysis*) *norvegica* G.O. Sars, 1882** (NE Atlantic and Mediterranean, west coast of Norway, British Isles, English Channel, north and west coasts of France, Portugal, Madeira, Atlantic coast of Morocco, Mediterranean: off Monaco, Malta, 0–400 m)

10 Endopod of uropods with only one spine below statocyst. Telson cleft with 16-24 laminae all along its margins..... ***H.* (*Heteromysis*) *fosteri* sp. n.** (South Africa: Cape Peninsula, 4 m, in empty shells)

– Endopod of uropods with 20–24 spines in dense series along inner margin. Telson cleft with 10-12 laminae only on its proximal half ..... .....***H.* (*Heteromysis*) *armoricana* H. Nouvel, 1940** (coast of Brittany, Galicia, Mediterranean, shallow coastal waters, muddy sand bottom, brown algae)

## Acknowledgements

We are greatly indebted to diver and photographer Craig Foster for initially sampling two of the three new *Heteromysis* species described herein and for providing some of the photographs of these. Also to Jannes Landschoff of the Department of Biological Sciences, University of Cape Town, for collecting and providing us with specimens of *H. cancelli* sp. n. Financial support for the work undertaken in South Africa was provided via a National Research Foundation Incentive Grant to C.L. Griffiths.

## References

Băcescu M (1986) Two new species of *Heteromysis* from the coral reefs of northern Australia. Travaux du Muséum d´Histoire Naturelle "Grigore Antipa" 28: 19–24. https://www.travaux.ro/web/pdf/28-TMNHNGA-19-24.pdf [accessed on 2015-12-19]

Bergh RS (1893) Beiträge zur Embryologie der Crustaceen. 1. Zur Bildungsgeschichte des Keimstreifens von *Mysis*. Zoologische Jahrbücher, Abtheilung für Anatomie und Ontogenie der Thiere 6: 491–528, pls 26–29.

Bonnier J, Pérez C (1902) Sur un Crustacé commensal des Pagures, *Gnathomysis Gerlachei*, nov. sp., type d'une famille nouvelle des Schizopodes. Comptes Rendus Hebdomadaires des Séances de l´Académie des Sciences 134: 117–119.

Bousfield EL (1958) Littoral marine arthropods and mollusks collected in Western Nova Scotia, 1956. Proceedings of the Nova Scotian Institute of Science 24(3): 303–325. http://hdl.handle.net/10222/13549 [accessed on 2017-05-14]

Carreño I, Pujol S, Zoppi de Roa E (1989) *Metamysidopsis insularis* Brattegard (Mysidacea): Field study of the larval cycle. Crustaceana 56(2): 127–131. https://doi.org/10.1163/156854089X00022

Clarke WD (1955) A new species of the genus *Heteromysis* (Crustacea, Mysidacea) from the Bahama Islands, commensal with a sea-anemone. American Museum Novitates 1716: 1–13. http://hdl.handle.net/2246/4712 [accessed on 2017-05-14]

Connell AD (1974) Mysidacea of the Mtentu River Estuary, Transkei, South Africa. Zoologica Africana 9(2): 147–159. https://doi.org/10.1080/00445096.1974.11448522

Davis CC (1966) A study of the hatching process in aquatic invertebrates. XXII. Multiple membrane shedding in *Mysidium columbiae* (Zimmer) (Crustacea: Mysidacea). Bulletin of marine Science 16(1): 124–131. http://www.ingentaconnect.com/contentone/umrsmas/bullmar/1966/00000016/00000001/art00007 [accessed on 2017-05-14]

Frutos I, Sorbe JC (2013) Bathyal suprabenthic assemblages from the southern margin of the Capbreton Canyon ("Kostarrenkala" area), SE Bay of Biscay. Deep-Sea Research Part II: Topical Studies in Oceanography 102: 291–309. https://doi.org/10.1016/j.dsr2.2013.09.010i

Fukuoka K (2005) A new species of *Heteromysis* (Mysida, Mysidae) associated with sponges, from the Uraga Channel, central Japan, with notes on distribution and habitat within the genus *Heteromysis*. Crustaceana 77(11): 1353–1373. https://doi.org/10.1163/1568540043165976

Green JM (1970) Observations on the behavior and larval development of *Acanthomysis sculpta* (Tattersall, Mysidacea). Canadian Journal of Zoology 48: 289–292. https://doi.org/10.1139/z70-047

Jepsen J (1965) Marsupial development of *Boreomysis arctica* (Krøyer, 1861). Sarsia 20: 1–8. https://doi.org/10.1080/00364827.1965.10409550

Jirikowski GJ, Wolff C, Richter S (2015) Evolution of eumalacostracan development — new insights into loss and reacquisition of larval stages revealed by heterochrony analysis. EvoDevo 6(4): 1–30. https://doi.org/10.1186/2041-9139-6-4

Klepal W, Kastner RT (1980) Morphology and differentiation of non-sensory cuticular structures in Mysidacea, Cumacea and Tanaidacea (Crustacea, Peracarida). Zoologica Scripta 9: 271–281. https://doi.org/10.1111/j.1463-6409.1980.tb00667.x

Lagardère JP, Nouvel H (1980) Les mysidacés du talus continental du golfe de Gascogne. II. Familles des Lophogastridae, Eucopiidae et Mysidae (Tribu des Erythropini exceptée). (Suite et fin). Bulletin du Muséum national d'Histoire naturelle, 4ème série, section A (Zoologie, Biologie, Écologie animale) 2(3): 845–887. http://www.vliz.be/imisdocs/publications/282458.pdf [accessed on 2017-05-05]

Lavesque N, Pascal L, Gouilleux G, Sorbe J-C, Bachelet G, Maire O (2016) *Heteromysis* (*Heteromysis*) *microps* (Crustacea, Mysidae), a commensal species for *Upogebia pusilla* (Crustacea, Upogebiidae) in Arcachon Bay (NE Atlantic Ocean). Marine Biodiversity Records 9(14): 1–6. https://doi.org/10.1186/s41200-016-0001-1

Manton SM (1928) On the embryology of a mysid crustacean, *Hemimysis lamornae*. Philosophical Transactions of the Royal Society. B. Biological Sciences 216: 363–463. [pls 21–25] https://doi.org/10.1098/rstb.1928.0008

Mees J [Ed.] (2017) Mysida. World Register of Marine Species. http://www.marinespecies.org/aphia.php?p=taxlist [accessed on 2017-05-28]

Modlin RF (1979) Development of *Mysis stenolepis* (Crustacea: Mysidacea). The American Midland Naturalist 101(1): 250-254. https://doi.org/10.2307/2424923

Nusbaum J (1887) L'embryologie de *Mysis chameleo* (Thompson). Archives de Zoologie expérimentale et générale, ser. 2: 5: 123–202. [pls V-XII] http://gallica.bnf.fr/ark:/12148/bpt6k5455965b.image.langEN [accessed on 2012-01-08]

Price WW, Heard RW (2011) Two new species of *Heteromysis* (*Olivemysis*) (Mysida, Mysidae, Heteromysinae) from the tropical northwest Atlantic with diagnostics on the subgenus *Olivemysis* Băcescu, 1968. Zootaxa 2823: 32–46. https://doi.org/10.5281/zenodo.207036

San Vicente C, Monniot F (2014) The ascidian-associated mysid *Corellamysis eltanina* gen. nov., sp.nov. (Mysida, Mysidae, Heteromysinae): a new symbiotic relationship from the Southern Ocean. Zootaxa 3780(2): 323–346. https://doi.org/10.11646/zootaxa.3780.2.6

Takahashi K, Kawaguchi K (1997) Diel and tidal migrations of the sand-burrowing mysids, *Archaeomysis kokuboi*, *A. japonica* and *Iiella ohshimai*, in Otsuchi Bay, northeastern Japan. Marine Ecology Progress Series 148: 95–107. http://www.jstor.org/stable/24857475 [accessed on 2017-05-05]

Tattersall OS (1967) A survey of the genus *Heteromysis* (Crustacea: Mysidacea) with descriptions of five new species from tropical coastal waters of the Pacific and Indian Ocean, with a key for the identification of the known species of the genus. Transactions of the Zoological Society of London 31: 157–193. https://doi.org/10.1111/j.1096-3642.1967.tb00366.x

Tattersall WM, Tattersall OS (1951) The British Mysidacea. Ray Society, London, monograph no. 136, 460 pp. http://www.pisces-conservation.com/softmys.html [accessed on 2010-04-27]

Vannini M, Innocenti G, Ruwa RK (1993) Family group structure in mysids, commensals of hermit crabs (Crustacea). Tropical Zoology 6: 189–205. https://doi.org/10.1080/03946975.1993.10539219

Vannini M, Ruwa RK, Innocenti G (1994) Notes on the behaviour of *Heteromysis harpax*, a commensal mysid living in hermit crab shells. Ethology Ecology & Evolution (Spec. Issue) 3: 137–142. https://doi.org/10.1080/03949370.1994.10721987

Wittmann KJ (1981) Comparative biology and morphology of marsupial development in *Leptomysis* and other Mediterranean Mysidacea (Crustacea). Journal of experimental marine Biology and Ecology 52(2-3): 243–270. https://doi.org/10.1016/0022-0981(81)90040-X

Wittmann KJ (2000) *Heteromysis arianii* sp.n., a new benthic mysid (Crustacea, Mysidacea) from coralloid habitats in the Gulf of Naples (Mediterranean Sea). Annalen des Naturhistorischen Museums in Wien 102 (B): 279–290. http://www.zobodat.at/pdf/ANNA_102B_0279-0290.pdf [accessed on 2013-07-15]

Wittmann KJ (2001) Centennial changes in the near-shore mysid fauna of the Gulf of Naples (Mediterranean Sea), with description of *Heteromysis riedli* sp. n. (Crustacea, Mysidacea). Marine Ecology 22(1–2): 85–109. https://doi.org/10.1046/j.1439-0485.2001.00741.x

Wittmann KJ (2008) Two new species of Heteromysini (Mysida, Mysidae) from the Island of Madeira (N.E. Atlantic), with notes on sea anemone and hermit crab commensalisms in the genus *Heteromysis* S. I. Smith, 1873. Crustaceana 81(3): 351–374. https://doi.org/10.1163/156854008783564037

Wittmann KJ, Ariani AP, Lagardère JP (2014) Orders Lophogastrida Boas, 1883, Stygiomysida Tchindonova, 1981, and Mysida Boas, 1883 (also known collectively as Mysidacea). In: von Vaupel Klein JC, Charmantier-Daures M, Schram FR (Eds) Treatise on Zoology - Anatomy, Taxonomy, Biology. The Crustacea. Revised and updated, as well as extended from the Traité de Zoologie 4 Part B (54): 189–396. [colour plates: 404–406] https://doi.org/10.1163/9789004264939_006

Wittmann KJ, Griffiths CL (2014) Description of the 'stargazer mysid' *Mysidopsis zsilaveczi* sp. nov. (Mysida: Mysidae: Leptomysinae) from the Cape Peninsula, South Africa. Crustaceana 87(11): 1411–1429. https://doi.org/10.1163/15685403-00003364

Wittmann KJ, Schlacher TA, Ariani AP (1993) Structure of Recent and fossil mysid statoliths (Crustacea, Mysidacea). Journal of Morphology 215: 31–49. https://doi.org/10.1002/jmor.1052150103

Wittmann KJ, Wirtz P (2017) *Heteromysis sabelliphila* sp. nov. (Mysida: Mysidae: Heteromysinae) in facultative association with sabellids from the Cape Verde Islands (subtropical N.E. Atlantic). Crustaceana 90(2): 131–151. https://doi.org/10.1163/15685403-00003542

Zouhiri S, Vallet C, Mouni P, Dauvin J-C (1998) Spatial distribution and biological rhythms of suprabenthic mysids from the English Channel. Journal of the Marine Biological Association of the United Kingdom 78: 1181–1202. https://doi.org/10.1017/S0025315400044416

ZooKeys 685: 49–64 (2017)
doi: 10.3897/zookeys.685.13552
http://zookeys.pensoft.net

RESEARCH ARTICLE

A peer-reviewed open-access journal
ZooKeys
Launched to accelerate biodiversity research

# Revision of the genus *Amphirhachis* Townes, 1970 (Hymenoptera, Ichneumonidae, Banchinae) from Japan

Kyohei Watanabe[1]

1 *Kanagawa Prefectural Museum of Natural History, Iriuda 499, Odawara, Kanagawa 250–0031, Japan*

Corresponding author: *Kyohei Watanabe* (watanabe-k@nh.kanagawa-museum.jp)

Academic editor: *J. Fernandez-Triana* | Received 5 May 2017 | Accepted 26 May 2017 | Published 13 July 2017

*http://zoobank.org/3D61C25A-CF1D-4CA2-BADB-DC2223BCB6AB*

**Citation:** Watanabe K (2017) Revision of the genus *Amphirhachis* Townes, 1970 (Hymenoptera, Ichneumonidae, Banchinae) from Japan. ZooKeys 685: 49–64. https://doi.org/10.3897/zookeys.685.13552

## Abstract

The Japanese species of the genus *Amphirhachis* Townes, 1970 are revised. Four species are found from Japan and two them, *A. fujiei* **sp. n.** and *A. miyabi* **sp. n.** are here described as new. A key to world species of this genus is provided.

## Keywords

Atrophini, Far East Asia, new species, parasitoid, taxonomy

## Introduction

The genus *Amphirhachis* Townes, 1970, is a small-sized genus of the tribe Atrophini (subfamily Banchinae), consisting of five species from the Eastern Palaearctic and Oriental regions (Yu et al. 2012, 2016). To the best of my knowledge, little is known of the biology of this genus. The species might be koinobiont endoparasitoids of lepidopterous larvae, similar to other genera of Atrophini.

In Japan, two species have been recorded, i.e. *A. nigra* Townes, 1970, from Honshu and *A. tertia* (Momoi, 1970) from Amamioshima Island and Tsushima Island (Townes 1970, Watanabeand Maeto 2012). I found some specimens of an unknown species, including many males, during a recent investigation. In the present study, I revise the Japanese species of *Amphirhachis*.

## Materials and methods

Materials used were from the collections of

| | |
|---|---|
| **KPMNH** | Kanagawa Prefectural Museum of Natural History, Odawara, Japan |
| **MNHAH** | Museum of Nature and Human Activities, Hyogo, Sanda, Japan |
| **MU** | Laboratory of Entomology, Meijyo University, Nagoya, Japan |
| **NIAES** | National Institute of Agro-Environmental Sciences, Tsukuba, Japan |
| **SEHU** | Laboratory of Systematic Entomology, Hokkaido University, Sapporo, Japan |
| **AEIC** | American Entomological Institute, Logan, Utah, USA |
| **ZISP** | Zoological Institute, Russian Academy of Sciences, St. Petersburg, Russia |

The holotype and paratype of *A. fasciata* Chandra & Gupta, 1977, deposited in Swedish Museum of Natural History, Sweden, and a paratype of *A. rubriventris* Chandra & Gupta, 1977, deposited in AEIC were also examined. *Fintona nigripalpis* Cameron, 1909, was classified as *Amphirhachis* by a recent database (Yu et al. 2016), although I did not examine the specimen of that species. Thus I referred the character states of this species based on Chandra and Gupta (1977).

A stereomicroscope (Nikon S800) was used for observations. Photographs were taken by OLYMPUS TG-4 digital camera joined with the stereo microscope. Digital images were edited using Adobe Photoshop® CS6.

Morphological terminology mainly follows that established by Gauld (1991) and Gauld et al. (2002). Eady (1968) is referred for microsculpture description. The following abbreviations are used in the descriptions: **BWM** Basal mandibular width, **MSL** Length of malar space, **F** Segment of flagellum, **OOL** Ocello-ocular line, **POL** Postocellar line, **TS** Tarsal segment, **T** Metasomal tegite and **HT** Holotype.

The following abbreviations are used in the material data and distribution: **F** Female, **M** Male, **LT** Light trap (or came to light), **FIT** Flight interception trap, **MsT** Malaise trap and * New distributional record.

## Results

The Japanese *Amphirhachis* are classified into four species. Two of them, *A. nigra* and *A. tertia*, have been previously recorded, whereas the remaining ones, which are novel species, *A. fujiei* sp. n. and *A. miyabi* sp. n., are described below. In addition, the male of *A. nigra* is described and illustrated for the first time. All the specimens could be clearly distinguished based on morphological characters (see the key below).

## Taxonomy

### Subfamily Banchinae Wesmael, 1845
### Tribe Atrophini Seyrig, 1932

### Genus *Amphirhachis* Townes, 1970

*Amphirhachis* Townes, 1970: 33. Type species: *Amphirhachis nigra* Townes, 1970. Original designation.

**Description.** Body covered with short setae. Head and mesosoma mat, covered with dense punctures. Ventral margin of clypeus blunt, without a median notch. Occipital carina complete. Lower end of occipital carina connected to hypostomal carina distant from base of mandible. Antenna with tyloid-like carina on ventral surface of basal 9–14 segments in female. Mesoscutum without a raised anterolateral area on each side. Epomia absent. Epicnemial carina present laterally and ventrally. Hind rim of metanotum without a sublateral triangular projection. Fore wing with: junction of vein *Cu1* and vein *Cu-a* slightly distant or opposite to junction of *Rs*+*M* and *M*+*Cu*; *Cu-a* more or less inclivous; large areolet, receiving vein 2*m-cu* near or at its outer corner; 2*m-cu* with a single narrow bulla that is ca. 0.2 as wide as the portion of 2*m-cu* behind the bulla. Hind wing with distal abscissa of *Cu*1 meeting cu-a slightly closer to 1*A* than *M*. Tarsal claws pectinate. Posterior transverse carina of propodeum largely absent, only represented by a weak or faint vertical ridge at apex of each side and/or on median part. T1 with basal half more or less stout, its spiracle in front of middle. Median dorsal and dorsolateral carinae of T1 absent. Ovipositor sheath shorter than 0.6 times as long as hind tibia. Subgenital plate pentagonal, posterior margin weakly concave medially. Apex of paramere not projected beyond apex of aedeagus, apical margin round. Basal apodeme of aedeagus 0.3–0.4 times of total length of aedeagus.

**Distribution.** Eastern Palaearctic and Oriental regions.

**Remarks.** The above description is partly referred from diagnosis provided by Townes (1970), Chandra and Gupta (1973) and Kuslitzky (1995). The world species of *Amphirhachis* can be identified by the key presented below. The antennal tyloid-like carina was recognized in all Japanese species and was not found in other genera of Japanese Atrophini. These points support the hypothesis proposed by Kuslitzky (1995), i.e., that carina is one of the generic characters of *Amphirhachis*. In all Japanese species, the number of segments with that carina are varied between basal 9 to 14 segments. This number is usually 12 and the apex of the carina is never surpassed at apex of white band.

**Key to World species of the genus *Amphirhachis***

1 Base of T1 with a conspicuous yellow area or spots (Figs 16, 18, 19). Hind femur largely reddish brown (Figs 16, 19).....**2**

– Base of T1 without yellow area or spots (Figs 1, 3, 4, 6, 9, 10, 12, 13, 15). Hind femur various in colouration.....**4**

2 Base of T1 with a pair of lateral yellow spots. Posterior segments of metasoma reddish brown. Antenna with 52 flagellomeres. Scutellum black with two yellow spots. Ovipositor sheath 0.4 times as long as hind tibia. Male unknown. Myanmar and India ..... *A. rubriventris* Chandra & Gupta, 1977

– Base of T1 with a wide yellow area or if with a pair of lateral yellow spots, propodeum with four yellow spots anteriorly and posteriorly (Fig. 21). Posterior segments of metasoma black and white (Figs 16, 18, 19, 21). Antenna with 47–49 flagellomeres. Scutellum entirely yellow (Figs 18, 21). Ovipositor sheath 0.4–0.5 times as long as hind tibia.....**3**

3 Propodeum with four yellow spots anteriorly and posteriorly in both sexes (Figs 18, 21). Mesopleuron with two (in female, Fig. 16) or one (in male, Fig. 19) large yellow spot(s). MSL 0.5–0.6 (in female) and 0.4 (in male) times as long as BWM. T1 2.0–2.2 times as long as maximum width. Ovipositor sheath 0.4 times as long as hind tibia. Japan, Far East Russia and Kazakhstan..... ***A. tertia*** **(Momoi, 1970)**

– Propodeum with two posterior yellow spots. Mesopleuron without two large yellow spots in female. MSL 0.7 times as long as BWM. T1 2.3 times as long as maximum width. Ovipositor sheath 0.4–0.5 times as long as hind tibia. Male unknown. Myanmar ..... ***A. fasciatus*** **Chandra & Gupta, 1977**

4 T2-T7 entirely red. T1 ca. 2.0 times as long as maximum width ..... .....***A. nigripalpis*** **(Cameron, 1909)**

– T2-T7 black with or without white band(s), without red area. T1 various in length .....**5**

5 Body large and elongate. T1 2.2–2.8 times as long as maximum width. T2 1.1–1.3 times as long as maximum width (Figs 12, 15). Face black, usually with a pair of yellow stripes or spot(s) along inner orbit in female (Fig. 11), or yellow with a median longitudinal black stripe in male (Fig. 14). Antenna with 54–58 flagellomeres. Metasomal tergites with a posterior white band on some segments in female (Fig. 12). Ovipositor sheath 0.3–0.4 times as long as hind tibia. Japan and Far East Russia .....***A. nigra*** **Townes, 1970**

– Body small and not elongate. T1 1.8–2.1 times as long as maximum width. T2 0.9–1.0 times as long as maximum width (Figs 3, 6, 9). Face sometimes without a pair of yellow stripes along inner orbit in female (Fig. 8), or entirely yellow in male (Fig. 5). Antenna with 45–50 flagellomeres. Metasomal tergites with (Fig. 9) or without (Fig. 3) a posterior white band in female. Ovipositor various in length .....**6**

6 Ovipositor sheath 0.3 times as long as hind tibia. Clypeus 0.5 times as long as wide. Face 0.6 times as long as wide, without a narrow longitudinal depression between eye and antennal socket (Figs 2, 5). Hind femur 5.7–6.1 times as long as maximum depth in lateral view, black. Metasomal tergite nearly entirely black in female (Figs 1, 3). Japan..... ***A. fujiei* sp. n.**

– Ovipositor sheath 0.4–0.5 times as long as hind tibia. Clypeus 0.4 times as long as wide. Face 0.5 times as long as wide, with a narrow longitudinal depression between eye and antennal socket (Fig. 8). Hind femur 6.4–6.9 times as long as maximum depth in lateral view, black or reddish brown. Each metasomal tergite with a posterior white band (Figs 7, 9). Male unknown. Japan ..... ***A. miyabi* sp. n.**

***Amphirhachis fujiei* sp. n.**

http://zoobank.org/47BB2E0E-EEB6-4946-816E-954337D32012

Figs 1–6

**Diagnosis.** Clypeus 0.5 times as long as wide. Face 0.6 times as long as wide, without a narrow longitudinal depression between eye and antennal socket. Antenna with 45–47 flagellomeres. Hind femur 5.7–6.1 times as long as maximum depth in lateral view, black. T1 1.8–1.9 times as long as maximum width. Base of T1 without yellow area or spots. T2 0.9–1.0 times as long as maximum width. T2-T7 black with or without white band(s), without red area. Ovipositor sheath 0.3 times as long as hind tibia. Face sometimes without a pair of yellow stripes along inner orbit in female, or entirely yellow in male. Metasomal tergite nearly entirely black in female.

**Description. Female** (n = 18). Body length 7.5–11.0 (HT: 9.0) mm.

*Head* 0.6 times as long as wide. Clypeus 0.5 times as long as wide. Face slightly convex medially, 0.6 times as long as wide, without a narrow longitudinal depression between eye and antennal socket (Fig. 2). Frons without a longitudinal area before anterior ocellus without punctures. POL 1.0 times as long as OOL. MSL 0.6–0.7 (HT: 0.7) times as long as BWM. Antenna with 45–47 (HT: 45) flagellomeres. F1 1.5–1.8 (HT: 1.8) times as long as F2.

*Mesosoma*. Mesopleuron without a speculum. Pleural carina present anteriorly, absent posteriorly. Fore wing length 8.0–9.5 (HT: 8.5) mm. Hind femur 5.7–6.1 (HT: 6.0) times as long as maximum depth in lateral view. Hind TS1 2.0 times as long as TS2.

*Metasoma*. T1 1.8–1.9 (HT: 1.8) times as long as maximum width. T2 0.9–1.0 (HT: 0.95) times as long as maximum width. Ovipositor sheath 0.3 times as long as hind tibia.

*Colouration* (Figs 1–3). Body (excluding wings and legs) black, except for: ventral part of clypeus, a pair of spots along inner orbit of face, vertex with a pair of spots between lateral ocellus and eye, mandible excluding apex and base, a median band of flagellum, and a pair of median spots of collar white to whitish yellow. The spot of

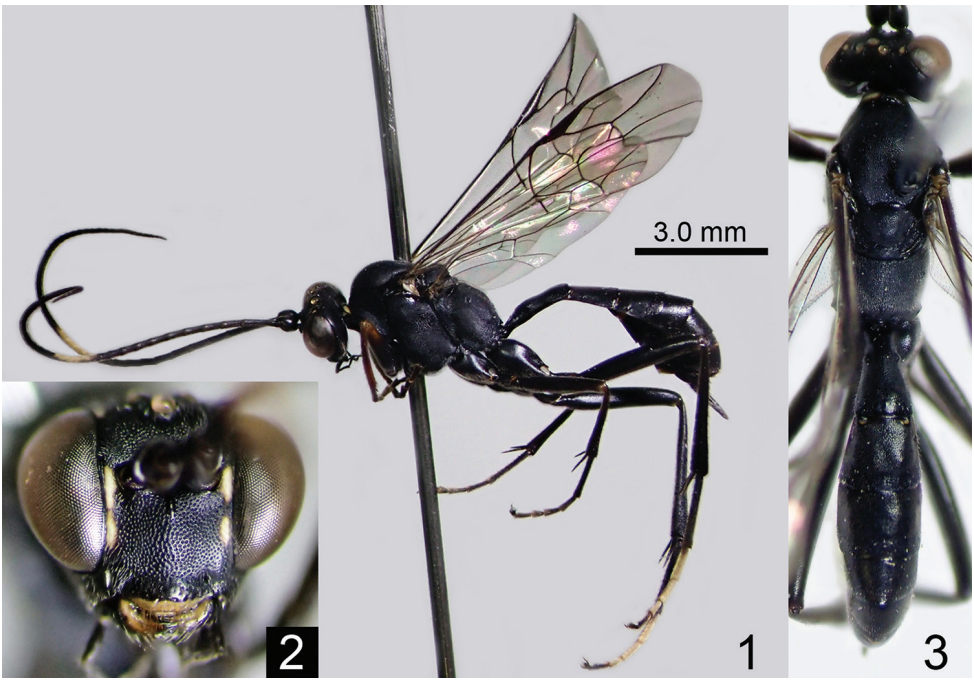


**Figures 1–3.** *Amphirhachis fujiei* sp. n., female (holotype). **1** lateral habitus **2** head, anterior view **3** head, mesosoma and metasoma, dorsal view.

face sometimes elongated along orbit. Wings hyaline; veins and pterostigma blackish brown to brown except for yellow wing base. Legs black except for: fore and mid femora, tibiae and tarsi partly blackish brown to reddish brown and hind TS2-TS4 white to whitish yellow.

**Male** (n = 9). In body structure, similar to female except for: POL 1.1–1.4 times as long as OOL, MSL 0.5–0.6 times as long as BWM, antenna with 45-50 flagellomeres, F1 1.4–1.6 times as long as F2, hind femur 5.4–6.2 times as long as maximum depth in lateral view, hind TS1 1.9–2.0 times as long as TS2, and T1 1.9–2.1 times as long as maximum width. In colouration, similar to the pattern of female but largely differed (Figs 4–6). Clypeus, face and malar space entirely yellow. Vertex with a pair of yellow spots between lateral ocellus and eye. Palpi, ventral spot of scape and pedicel, median band of flagellum yellow. Collar, posterodorsal corner of pronotum, subalar prominence, dorsal area of mesepimeron and posterior transverse stripe of T2-T7 whitish yellow to yellow. Mesoscutum sometimes with a pair of yellow anterolateral spots. Scutellum sometimes with a pair of yellow spots. Fore and mid legs whitish yellow to reddish yellow. Hind leg black to blackish brown except for whitish yellow trochanter and trochantellus, basal yellowish area of tibia, and TS2-TS5.

**Specimens examined.** JAPAN: [Holotype] F, Wakayama Pref., Tanabe City, Ryujin Vil., Ryujin, 23. VI. 2012, S. Fujie leg. (KPMNH). [Paratypes] 1 F, Hokkaido, Sapporo City, Mt. Soranuma-dake, 14. VI. – 4. VII. 2007, A. Ueda leg. (MsT)

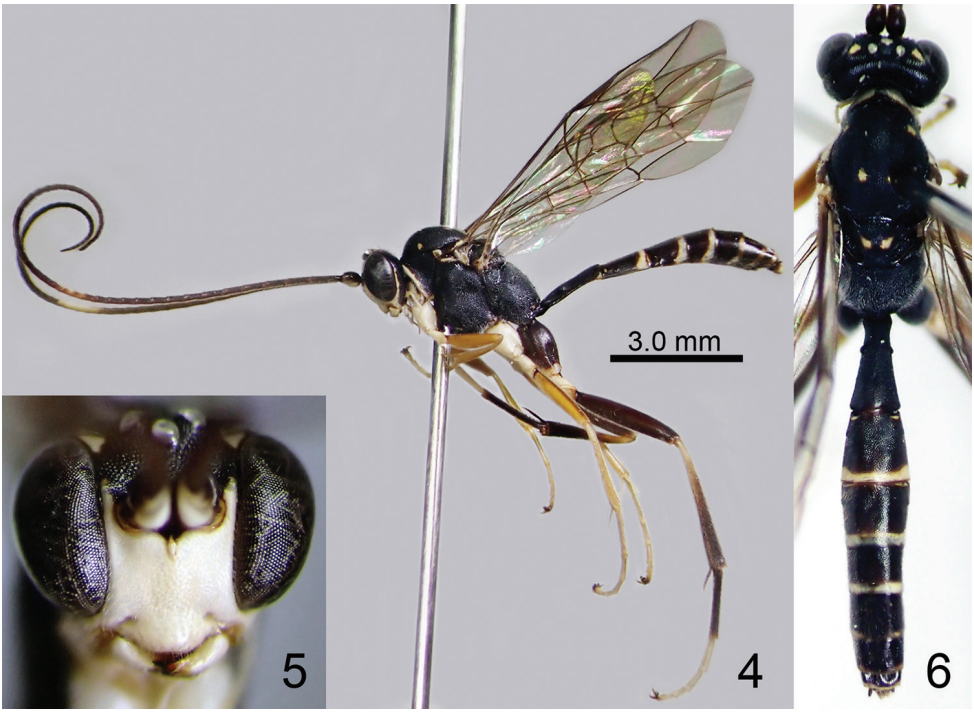


**Figures 4–6.** *Amphirhachis fujiei* sp. n., male (paratype). **4** lateral habitus **5** head, anterior view **6** head, mesosoma and metasoma, dorsal view.

(KPMNH); 1 M, Hokkaido, Kuriyama Town, 31. VIII. – 13. IX. 2007, A. Ueda leg. (MsT) (KPMNH); 1 M, Hokkaido, Yubari City, Oyubari, 31. VIII. – 13. IX. 2007, A. Ueda leg. (MsT) (KPMNH); 1 M, Hokkaido, Horikanai Town, Moshiri, Uryu, 11–17. VII. 2012, K. Watanabe et al. leg. (MsT) (KPMNH); 1 M, Hokkaido, Mt. Tarumae-san, 12–21. VII. 1998, K. Konishi leg. (MsT.) (NIAES); 1 F, Ibaraki Pref., Kitaibaraki, Ogawa, 27. VI. – 9. VII. 1996, K. Maeto leg. (MsT) (NIAES); 2 F, same locality and collector, 9–25. IX. 1996 (MsT) (NIAES); 1 M, same locality and collector, 20. VIII. – 4. IX. 1996 (MsT) (NIAES); 3 M, Tochigi Pref., Yaita, 30. VI. – 15. VII. 1989, K. Konishi leg. (MsT) (NIAES); 1 F, Kanagawa Pref., Odawara, 4. VI. 1987, H. Makihara leg. (NIAES); 1 F, Kanagawa Pref., Mt. Tanzawa-san, 6. VI. 2013, T. Taniwaki leg. (FIT) (KPMNH); 1 F, Kanagawa Pref., Mt. Oomuro-yama, 16. VI. 2013, T. Taniwaki leg. (FIT) (KPMNH); 1 F, Kanagawa Pref., Mt. Komotsurushi-yama, 21. VI. 2013, T. Taniwaki leg. (FIT) (KPMNH); 1 M, Yamanashi Pref., Hokuto City, Masutomi, Biwakubo-sawa, 28. VII. 2007, T. Ban leg. (KPMNH); 1 F, Yamanashi Pref., Tsuru City, Matsuhime-toge, 28. VII. – 9. VIII. 2008, T. Sakurai & T. Zakoji leg. (KPMNH); 1 F, Yamanashi Pref., Koushu City, Yamato Town, Tokusa, 7. VIII. 2008, T. Muraki leg. (KPMNH); 1 F, Nagano Pref., Shimashima-dani, 28. VII. 1980, H. Takemoto leg. (NIAES); 1 F, Nagano Pref., Outaki Vil., Mt. Ontake-san, Hakkaisan, 8–9. VIII. 2014, S. Shimizu leg. (MsT.) (KPMNH); 1 F, Hyogo

Pref., Kami Town, Niiya, Mikata-kogen (710 m alt.), 26. VI. – 18. VII. 2011, S. Fujie leg. (MsT) (KPMNH); 1 F, Tottori Pref., Mt. Daisen, 24. VI. 1978, Y. Yoneda leg. (NIAES); 1 F, Tottori Pref., Wakasa Town, Mt. Hyonosen, Oodanganaru, 6. VIII. 2011, K. Watanabe leg. (LT) (KPMNH); 1 F, Ehime Pref., Odamiyama, 25. VII. 1995, E. Yamamoto leg. (LT) (NIAES); 1 F, Fukuoka Pref., Mt. Hiko, 5–6. VII. 1979, K. Maeto leg. (NIAES).

**Distribution.** Japan (Hokkaido, Honshu, Shikoku and Kyushu).

**Etymology.** The specific name is from my friend, Mr. Shunpei Fujie, who is a taxonomist of Japanese Braconidae and a collector of types.

**Bionomics.** Host is unknown. The specimens collected from Hyogo (Mt. Hyonosen) and Shikoku were collected by light trap.

**Remarks.** This species resembles *A. nigra* in the body colouration, but it can be distinguished by the T1 1.8–2.1 times as long as maximum width (2.2–2.8 times in *A. nigra*), T2 0.9–1.0 times as long as maximum width (1.1–1.3 times in *A. nigra*), the body length 7.0–7.5 mm (54–58 flagellomeres in *A. nigra*) and T2 without a posterior white band in female (usually with a white band in female of *A. nigra*). Males were collected only from Hokkaido and Honshu.

### *Amphirhachis miyabi* sp. n.

http://zoobank.org/CEDF0413-1954-4DCE-A9C6-353DB0CB7A68
Figs 7–9

**Diagnosis.** Clypeus 0.4 times as long as wide. Face 0.5 times as long as wide, with a narrow longitudinal depression between eye and antennal socket. Antenna with 46–49 flagellomeres. Hind femur 6.4–6.9 times as long as maximum depth in lateral view, black or reddish brown. T1 1.9–2.0 times as long as maximum width. Base of T1 without yellow area or spots. T2 0.9–1.0 times as long as maximum width. Each metasomal tergite with a posterior white band. Ovipositor sheath 0.4–0.5 times as long as hind tibia.

**Description. Female** (n = 18). Body length 10.0–11.0 (HT: 10.0) mm.

*Head* 0.6 times as long as wide. Clypeus 0.4 times as long as wide. Face slightly convex medially, 0.5 times as long as wide, with a narrow longitudinal depression between eye and antennal socket (Fig. 8). Frons with a longitudinal area before anterior ocellus without punctures. POL 0.8–1.0 (HT: 0.8) times as long as OOL. MSL 0.7–0.8 (HT: 0.7) times as long as BWM. Antenna with 46–49 (HT: 46) flagellomeres. F1 1.6–1.7 (HT: 1.6) times as long as F2.

*Mesosoma*. Mesopleuron with a very small speculum. Pleural carina present but trace-like in entire length. Fore wing length 9.0–10.0 (HT: 9.0) mm. Hind femur 6.4–6.9 (HT: 6.9) times as long as maximum depth in lateral view. Hind TS1 2.0–2.1 (HT: 2.1) times as long as TS2.

*Metasoma*. T1 1.9–2.0 (HT: 1.9) times as long as maximum width. T2 0.9–1.0 (HT: 0.9) times as long as maximum width. Ovipositor sheath 0.4–0.5 (HT: 0.5) times as long as hind tibia.

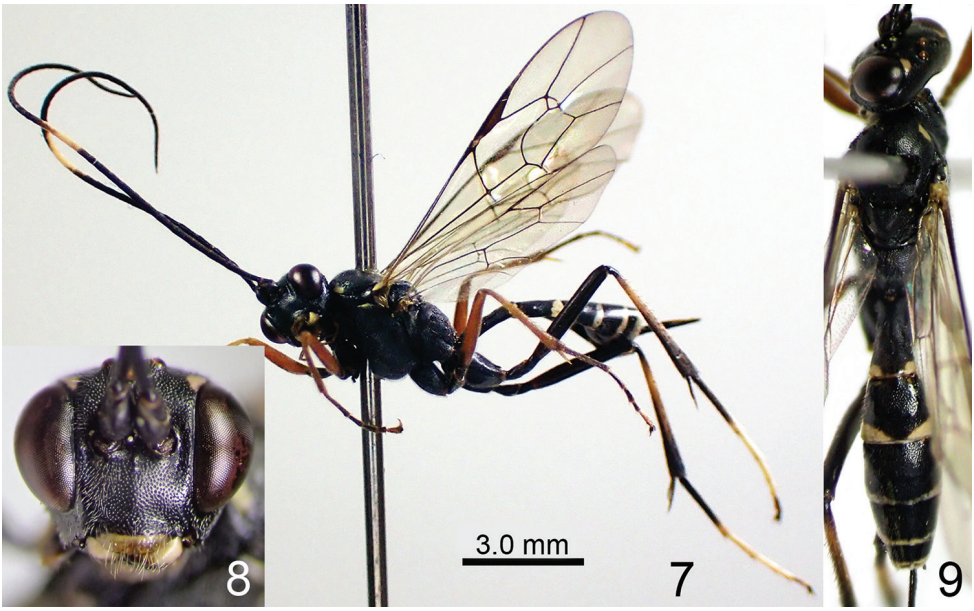


**Figures 7–9.** *Amphirhachis miyabi* sp. n., female (holotype). **7** lateral habitus **8** head, anterior view **9** head, mesosoma and metasoma, dorsal view.

*Colouration* (Figs 7–9). Body (excluding wings and legs) black, except for: clypeus excluding dorsal part, vertex with a pair of spots between lateral ocellus and eye, mandible excluding apex and base, a median band of flagellum, anterolateral spots of mesoscutum, subalar prominence, apical spots of T1, apical transverse stripe of T2-T7 white to whitish yellow; palpi brown; metasomal sternites blackish brown brown basally, whitish brown apically. Wings hyaline; veins and pterostigma blackish brown to brown except for yellow wing base. Coxae, trochanters and trochantelli black. Fore and mid femora, tibiae and tarsi reddish brown to brown. Hind femur, base and apical part of hind tibia, basal 0.7–0.8 (HT: 0.8) of hind TS1, and TS5 black to blackish brown. Subbasal area of hind tibia reddish brown. Apical 0.2 of hind TS1 and TS2-TS4 whitish yellow. In some paratypes with: collar with yellow spot medially, mesoscutum with a indistinct, median yellow spot, scutellum with a pair of small yellow spots, and propodeum with a pair of small yellow spots near the socket of hind coxa. The apical yellow spot of T1 usually united into a single transverse stripe. In specimens collected in Yakushima Is., hind femur sometimes tinged with reddish brown. Ovipositor reddish brown.

**Male**. Unknown.

**Specimens examined.** JAPAN: [Holotype] F, Nagasaki Pref., Tsushima Is., Kamitsushima Town, Izumi, Shitazaki (ca. 10 m alt.), 8. V. 2015, T. Kurihara leg. (KPMNH). [Paratypes] 2 F, Aichi Pref., Nagoya City, Higashiyama Park, 1–10. V. 2001, M. Watanabe leg. (MsT) (MU); 2 F, same locality and collector, 11–20. V. 2001 (MsT) (MU); 5 F, Aichi Pref., Toyota City, Takiwaki, 30. IV. – 6. V. 2002, Y. Kurahashi leg. (MsT) (MU); 2 F, Aichi Pref., Toyota City, Sanage, 30. IV. – 6. V. 2002, M. Kiyota leg. (MsT)

(MU); 1 F, Miyazaki Pref., Mt. Wanizuka, 23. V. 1966, K. Kusigemati leg. (SEHU); 1 F, Kagoshima Pref., Yakushima Is., Kosugidani, 2. VI. 1969, K. Kusigemati leg. (SEHU); 1 F, same locality and collector, 3. VI. 1969 (SEHU); 3 F, Kagoshima Pref., Yakushima Is., Shiratani (600 m alt.), 6. V. – 20. VI. 2000, T. Murata leg. (MsT) (MU).

**Distribution.** Japan (Honshu, Kyushu, Tsushima Is. and Yakushima Is.),

**Etymology.** The specific name is from a Japanese term "Miyabi", which means elegant.

**Bionomics.** Host is unknown.

**Remarks.** This species resembles *A. fujiei* sp. n. in the body structures, but it can be distinguished by ovipositor sheath 0.4–0.5 times as long as hind tibia (0.3 times in *A. fujiei* sp. n.) and the each metasomal tergite with a posterior white band (entirely black in female of *A. fujiei* sp. n.).

### *Amphirhachis nigra* Townes, 1970

Figs 10–15

*Amphirhachis nigra* Townes, 1970: 33.

**Description. Female** (n = 32). Body length 10.0–12.5 mm.

*Head* 0.6 times as long as wide. Clypeus 0.5 times as long as wide. Face slightly convex medially, 0.6 times as long as wide, without a narrow longitudinal depression between eye and antennal socket (Fig. 11). Frons densely punctate with rugae above each antennal socket, without a longitudinal area before anterior ocellus without punctures. POL 0.8–1.0 times as long as OOL. MSL 0.7 times as long as BWM. Antenna with 56-57 flagellomeres. F1 1.5–1.6 times as long as F2.

*Mesosoma*. Mesopleuron without a speculum. Pleural carina present but trace-like in entire length. Fore wing length 9.0–12.5 mm. Hind femur 7.1–8.1 times as long as maximum depth in lateral view. Hind TS1 1.9–2.0 times as long as TS2.

*Metasoma*. T1 2.2–2.8 (usually 2.2–2.3) times as long as maximum width. T2 1.1–1.3 times as long as maximum width. Ovipositor sheath 0.3–0.4 (usually 0.3) times as long as hind tibia.

*Colouration* (Figs 10–12). Body (excluding wings and legs) black, except for: clypeus except for dorsal part, longitudinal stripes along orbit except for ventral part of face and dorsal part of gena, mandible excluding apex and base, a median band of flagellum, a pair of median spot of collar, a pair of small spot of scutellum, anterolateral small spots of T1, posterior transverse stripe of T2, narrow posterior margin of T3-T6, base and apex of S1, posterior transverse stripe of S2-S6 whitish yellow; palpi, ventral surface of scape and pedicel, posterodorsal corner of pronotum, subalar prominence, and dorsal area of mesepimeron tinged with brown to reddish brown. The marking along orbit sometimes partly reduced. Scutellum sometimes without yellow markings. Stripes of metasomal tergites sometimes reduced but usually present on T2. Wings hyaline; veins and pterostigma blackish brown to brown except for yellow wing base.


**Figures 10–12.** *Amphirhachis nigra* Townes, 1970, female from Japan. **10** lateral habitus **11** head, anterior view **12** head, mesosoma and metasoma, dorsal view.

Legs black except for: fore and mid femora, tibiae and tarsi partly blackish brown to reddish brown and hind TS2-TS4 white to whitish yellow. Hind femur and tibia sometimes tinged with reddish brown. Hind TS2 sometimes black basally.

**Male** (n = 24). In body structure, similar to female except for: MSL 0.4–0.6 times as long as BWM, antenna with 54-58 flagellomeres, F1 1.4–1.6 times as long as F2, anterior part of pleural carina well-developed, T1 relatively longer than female (usually 2.5–2.6 times as long as maximum width), hind femur 6.5–7.7 times as long as maximum depth in lateral view, hind TS1 1.8–1.9 times as long as TS2 and T2 1.4–1.8 times as long as maximum width. In colouration, similar to the pattern of female but largely differed (Figs 13–15). Clypeus and malar space entirely yellow. Face yellow except for median longitudinal black stripe. Palpi, ventral spot of scape and pedicel, and median band of flagellum whitish yellow to yellow. Collar, posterodorsal corner of pronotum, anterolateral spots of mesoscutum, subalar prominence, dorsal area of mesepimeron and posterior transverse stripe of T1-T7 whitish yellow to yellow. Propleuron sometimes with a whitish yellow to yellow spot. Mesoscutum sometimes with a median yellow spot. Mesopleuron usually along mesosternum with a longitudinal whitish yellow stripe. Mesepimeron sometimes entirely whitish yellow. Propodeum

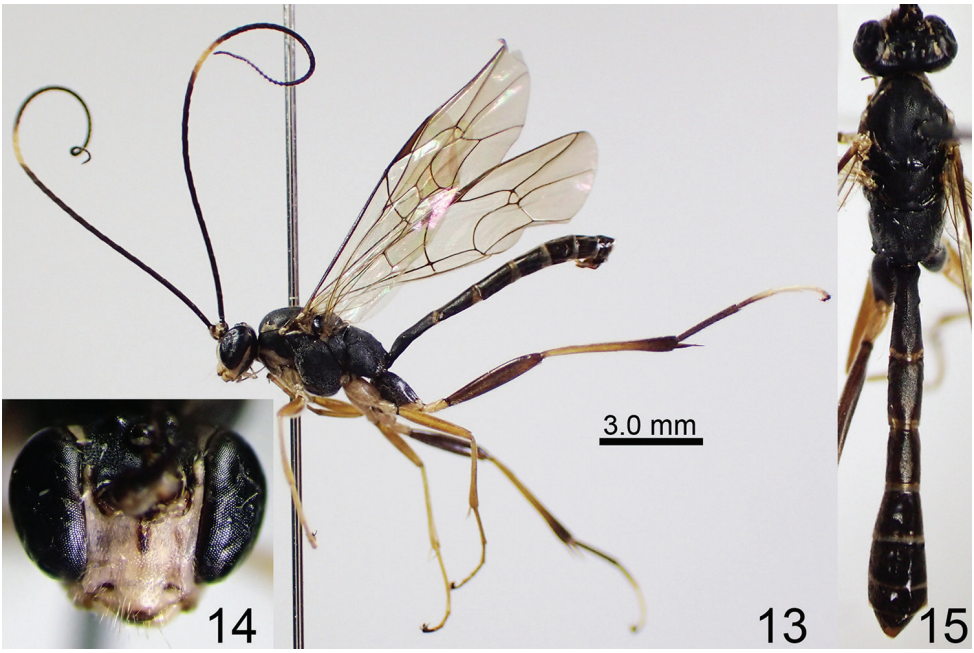


**Figures 13–15.** *Amphirhachis nigra* Townes, 1970, male from Japan. **13** lateral habitus **14** head, anterior view **15** head, mesosoma and metasoma, dorsal view.

sometimes with a pair of small yellow spots near the socket of hind coxa. Fore and mid legs whitish yellow to reddish yellow. Hind coxa partly tinged with whitish yellow. Hind trochanter and trochantellus whitish yellow. Hind femur, tibia and tarsus more or less paler than female especially basal part of tibia largely reddish brown.

**Specimens examined.** JAPAN: 1 M, Hokkaido, Mt. Tarumae-san, 12–21. VII. 1998, K. Konishi leg. (MsT.) (NIAES); 1 F, same locality and collector, 21–26. VII. 1998 (MsT) (NIAES); 8 M, Hokkaido, Sapporo City, Mt. Soranuma-dake, 14. VI. – 4. VII. 2007, A. Ueda leg. (MsT) (KPMNH); 1 F, same locality and collector, 27. VII. – 21. VIII. 2007 (MsT) (KPMNH); 2 M, Hokkaido, Hidaka Town, Uenzaru-gawa, 21. VI. – 10. VII. 2007, A. Ueda leg. (MsT) (KPMNH); 1 M, same locality and collector, 10. VII. – 1. VIII. 2007 (MsT) (KPMNH); 1 M, Hokkaido, Eniwa City, Izari, Ichankoppe-zawa, 20–30. VI. 1995, T. Ito leg. (MsT) (NIAES); 1 M, same locality and collector, 12–20. VII. 1995 (MsT) (NIAES); 1 F, same locality and collector, 21–31. VII. 1995 (MsT) (NIAES); 1 M, Kanagawa Pref., Atsugi City, Mt. Oyama (1250 m alt.), 7. VI. 1997, M. Kato leg. (KPMNH); 1 F, Kanagawa Pref., Mt. Tanzawa-san, 16. V. 2013, T. Taniwaki leg. (FIT) (KPMNH); 1 M, same locality and collector, 20. VI. 2013 (FIT) (KPMNH); 1 M, Kanagawa Pref., Mt. Oomuro-yama, 16. VI. 2013, T. Taniwaki leg. (FIT) (KPMNH); 2 M, Kanagawa Pref., Mt. Hinokiboramaru, 23. V. 2013, T. Taniwaki leg. (FIT) (KPMNH); 2 M, Kanagawa Pref., Mt. Hinokiboramaru, 6. VI. 2013, T. Taniwaki leg. (FIT) (KPMNH); 1 F, Shizuoka Pref., Kanaya City, Fukuyo, 16. XI. 1952, J. Minamikawa leg. (NIAES); 1 F, Shizuoka Pref., Kanaya, 1.

XII. 1955, J. Minamikawa leg. (NIAES); 1 F (holotype), Nagano Pref., Kamikochi, 31. VII. 1954, Townes family leg. (AEIC); 1 F, Nagano Pref., Mt. Shiroumayari, 29. VII. 1972, T. Aoki leg. (NIAES); 1 F, Nagano Pref., Outaki Vil., Mt. Ontake-san, Hakkaisan, 16. IX. 2011, S. Fujie leg. (KPMNH); 1 M, same locality, 8–9. VIII. 2014, S. Shimizu leg. (MsT.) (KPMNH); 1 M, Ishikawa Pref., Mt. Hakusan, 5. VIII. 1993, I. Togashi leg. (NIAES); 1 M, same locality and collector, 8. IX. 1996 (NIAES); 1 F, Mie Pref., Owase, 16. XI. 1958, S. Ishida leg. (NIAES); 1 F, "Odaigahara", 6. VI. 2004, A. Kawazoe leg. (KPMNH); 1 F, Nara Pref., Odaigahara (1500 m alt.), 25. VI. 1984, K. Konishi leg. (NIAES); 1 F, Ehime Pref., Odamiyama, 15. VI. 1990, E. Yamamoto leg. (NIAES); 1 F, same locality and collector, 13. V. 1994 (NIAES); 1 F, same locality and collector, 27. V. 1994 (NIAES); 1 F, same locality and collector, 28. V. 1994 (NIAES); 1 F, same locality and collector, 26. VI. 1994 (NIAES); 2 F, same locality and collector, 1. VI. 1995 (NIAES); 1 F, same locality and collector, 5. VI. 1995 (NIAES); 1 F, same locality and collector, 11. VI. 1995 (NIAES); 2 F, same locality and collector, 25. VI. 1995 (NIAES); 1 F, same locality and collector, 10. VII. 1995 (NIAES); 1 F, Tokushima Pref., Mt. Tsurugisan, 19. VI. 1981, I. Kanazawa leg. (LT) (NIAES); 2 F, Kumamoto Pref., Mt. Aso, 12. VI. 1978, H. Makihara leg. (LT) (NIAES); same locality and collector, 18. VI. 1978 (LT) (NIAES); 1 F, Kumamoto Pref., Izumi Vil., Mt. Shiratori-yama (1300 m alt.), 6. VI. 1980, K. Ohara leg. (NIAES); 1 F, Kumamoto Pref., Izumi Vil., "Mt. Hakuchō-zan" (= Mt. Shiratori-yama ??), 14. V. 1983, K. Ohara leg. (NIAES); 1 F, same locality, 14–21. V. 1983, K. Ohara & T. Goto leg. (MsT) (NIAES); 1 F, Kumamoto Pref., Shiiya-toge (1400 m alt.), 15. VI. 1985, K. Konishi et al. leg. (LT) (NIAES).

**Distribution.** Japan (Hokkaido, Honshu, Shikoku and Kyushu); Far East Russia.

**Bionomics.** Host is unknown. Some specimens collected from Shikoku and Kyushu were collected by light trap.

**Remarks.** This is the first record of the male. Males were collected only from Hokkaido and Honshu.

### *Amphirhachis tertia* (Momoi, 1970)

Figs 16–21

*Fintona tertia* Momoi, 1970: 375.
*Amphirhachis quadripunctata* Kuslitskiy, 1995: 674.

**Description. Female** (n = 4). Body length 10.0–11.0 mm.

*Head* 0.6 times as long as wide. Clypeus 0.4 times as long as wide. Face slightly convex medially, 0.6–0.7 times as long as wide, without a narrow longitudinal depression between eye and antennal socket (Fig. 17). Frons densely punctate with transverse creases above each antennal socket, with a longitudinal area before anterior ocellus without punctures. POL 0.9 times as long as OOL. MSL 0.5–0.6 times as long as BWM. Antenna with 47–50 flagellomeres. F1 1.5–1.8 times as long as F2.

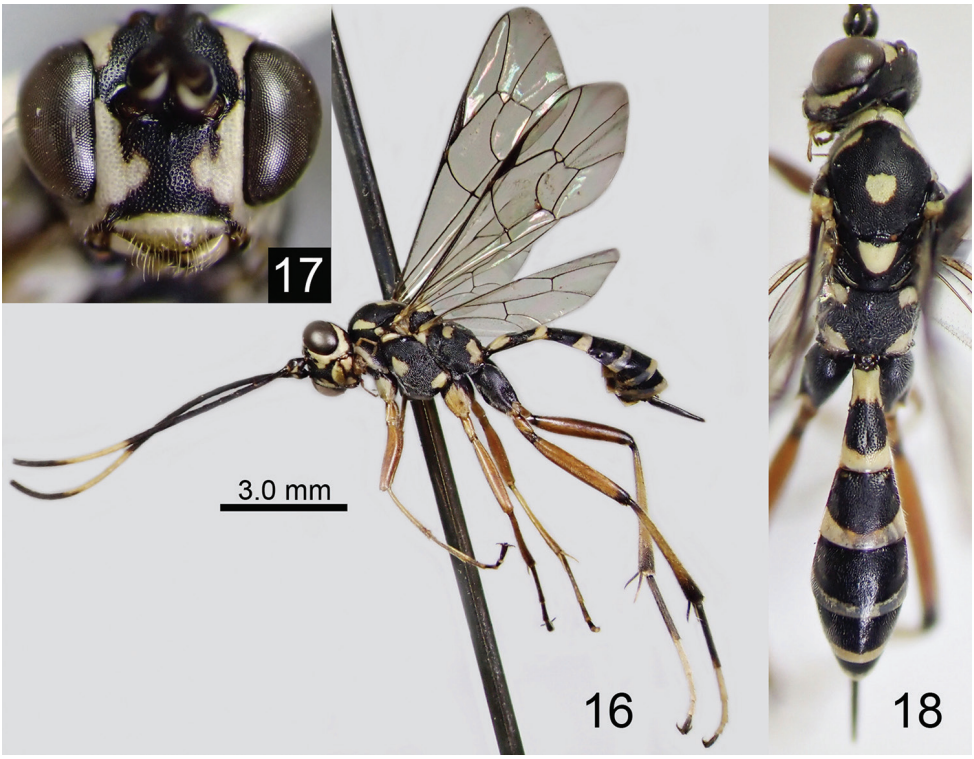


**Figures 16–18.** *Amphirhachis tertia* Momoi, 1970, female from Japan. **16** lateral habitus **17** head, anterior view **18** head, mesosoma and metasoma, dorsal view.

*Mesosoma*. Mesopleuron without speculum. Pleural carina present but trace-like in entire length. Fore wing length 8.0–8.5 mm. Hind femur 6.1–6.4 times as long as maximum depth in lateral view. Hind TS1 2.0–2.1 times as long as TS2.

Metasoma. T1 2.0–2.2 times as long as maximum width. T2 0.9–1.0 times as long as maximum width. Ovipositor sheath 0.4 times as long as hind tibia.

*Colouration* (Figs 16–18). Body (excluding wings and legs) black with some whitish yellow markings. The yellow area on head are: mandible except for base and apex, clypeus except for dorsal margin, stripe along orbit except for dorsal part of gena, ventral spot of scape and pedicel, and a median band of flagellum. Yellow stripe on face widened medially. The yellow area on mesosoma are: collar and posterodorsal corner of pronotum, anterolateral longitudinal spots and a median spot of mesoscutum, scutellum, subalar prominence, dorsal area of mesepimeron, two large spots on mesopleuron, four spots on propodeum. Wings hyaline; veins and pterostigma blackish brown to brown except for yellow wing base. Fore and mid coxae whitish yellow, with small black area. Fore and mid trochanters, trochanteli and tarsi yellowish brown. Fore and mid femora and tibiae reddish brown. Hind coxa, base and apex of hind femur, base and apical part of hind tibia, hind TS1 and TS5 black to blackish brown. Hind trochanter, trochantellus, femur and tibia except for black area reddish brown. Hind

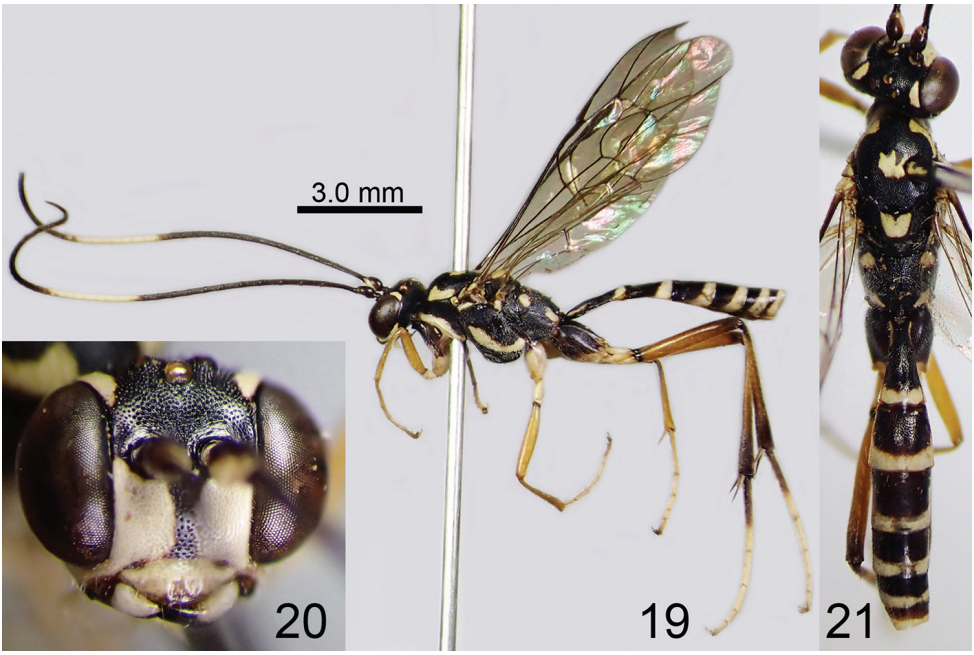


**Figures 19–21.** *Amphirhachis tertia* Momoi, 1970, male from Japan. **19** lateral habitus **20** head, anterior view **21** head, mesosoma and metasoma, dorsal view.

TS2-TS4 white. The yellow area on mesosoma are: basal spot and apical transverse stripe of T1, apical transverse stripe of T2-T7. Metasomal sternites blackish brown brown basally, whitish brown apically. Ovipositor reddish brown.

**Male**. Similar to female (Figs 19–21) except for: MSL 0.4 times as long as BWM, face largely white except blackish areas along each antennal socket and median longitudinal line, yellowish spots on mesopleuron united as transverse band, blackish areas on fore and middle coxae reduced, hind TS5 white; basal white area of first metasomal tergite reduced, and only longitudinal line between spiracle and base present.

**Specimens examined.** JAPAN: 1 F (holotype of *Fintona tertia*), Kagoshima Pref., Amamioshima Is., 6. V. 1959, K. Kamijo leg. (MNHAH; 1 F, Kagoshima Pref., Amamioshima Is., Mt. Yuidake, 1. IV. 1989, Y. Takematsu leg. (NIAES); 1 F, Kagoshima Pref., Amamioshima Is., Yuwan, 29. III. 2015, Y. Fujisawa leg. (KPMNH); 1 M, Nagasaki Pref., Tsushima Is., Mt. Mitake, 3. V. 1989, K. Konishi leg. (NIAES). KAZAKHSTAN: 1 F (holotype of *Amphirhcachis quadripunctata*), Andreyevka, 3. VIII. 1985, S. Belokobylskij leg. (ZISP).

**Distribution.** Japan (Tsushima Is. and Amamioshima Is.); Far East Russia (Primorye Kray) and Kazakhstan.

**Bionomics.** Host is unknown.

**Remarks.** The distribution data for this species is relatively sparse as compared to other species. The locality of Kazakhstan is distant from Japan and Far East Russia (Primorye Kray) while no differences of character states were found between both specimens.

## Acknowledgements

The author would like to express his cordial thanks to David Wahl (AEIC), Kenzou Yamagishi (MU), Shin-ichi Yoshimatsu and Hiraku Yoshitake (NIAES), Dmitry Kasparyan, Andrey Khalaim, Konstantin Samartsev and Sergei Belokobylskij (ZISP) for their kind support in researching their collections and to Editage (http://www.editage.jp) for English language editing. This study was partly supported by the Grant-in-Aid for JSPS KAKENHI Grant numbers 26840134 and 17K15185 for the author.

## References

Chandra G, Gupta VK (1977) Ichenumonologia Orientalis, VII. The Tribes Lissonontini & Banchini. Oriental Insects Monograph 7: 1–290.

Eady RD (1968) Some illustrations of microsculpture in the Hymenoptera. Proceedings of the Royal Entomological Society of London 43: 66–72. https://doi.org/10.1111/j.1365-3032.1968.tb01029.x

Gauld ID (1991) The Ichneumonidae of Costa Rica, 1. Memoirs of the American Entomological Institute 47: 1–589.

Gauld ID, Godoy C, Ugalde J, Sithole (2002) The Ichneumonidae of Costa Rica, 4. Memoirs of the American Entomological Institute 66: 1–768.

Kuslitzkiy VS (1995) New genera and species of Ichneumonid wasps of the tribe Lissonotini (Hymenoptera, Ichneumonidae) of the fauna of Russia. Entomologicheskoye Obozreniye 74: 673–676. [In Russian, English translation in Entomological Review 75: 24–28]

Momoi S (1970) Ichneumonidae (Hymenoptera) of the Ryukyu Archipelago. Pacific Insects 12: 327–399.

Townes H (1970) The genera of Ichneumonidae, part 3. Memoirs of the American Entomological Institute 13: 1–307.

Watanabe K, Maeto K (2012) Taxonomic position of *Fintona tertia* Momoi, 1970, with a new synonym and description of male (Hymenoptera, Ichneumonidae, Banchinae). Japanese Journal of Systematic Entomology 18: 53–56.

Yu DSK, van Achterberg C, Horstmann K (2012) Taxapad 2012 – World Ichneumonoidea 2011. Taxonomy, Biology, Morphology and Distribution. On USB Flash drive. Ottawa, Ontario. http://www.taxapad.com

Yu DSK, van Achterberg C, Horstmann K (2016) Taxapad 2016, Ichneumonoidea 2015. Database on flash-drive. Nepean, Ontario. http://www.taxapad.com

ZooKeys 685: 65–81 (2017)
doi: 10.3897/zookeys.685.12152
http://zookeys.pensoft.net

RESEARCH ARTICLE

A peer-reviewed open-access journal
ZooKeys
Launched to accelerate biodiversity research

# *Bryophryne phuyuhampatu* sp. n., a new species of Cusco Andes frog from the cloud forest of the eastern slopes of the Peruvian Andes (Amphibia, Anura, Craugastoridae)

Alessandro Catenazzi[1,2], Alex Ttito[3,4], M. Isabel Diaz[3,4], Alexander Shepack[1]

**1** *Department of Zoology, Southern Illinois University, Carbondale, USA* **2** *Centro de Ornitología y Biodiversidad, Lima, Perú* **3** *Museo de Historia Natural de la Universidad Nacional de San Antonio Abad del Cusco, Plaza de armas s/n (Paraninfo universitario), Cusco, Perú* **4** *Museo de Biodiversidad del Perú, Urbanización Mariscal Gamarra A-61, Zona 2, Cusco, Perú*

Corresponding author: *Alessandro Catenazzi* (acatenazzi@gmail.com)

Academic editor: *J. Penner* | Received 7 Februrary 2017 | Accepted 8 June 2017 | Published 13 July 2017

*http://zoobank.org/310FD77C-029A-45F5-9AE4-C59772CA1F83*

**Citation:** Catenazzi A, Ttito A, Diaz MI, Shepack A (2017) *Bryophryne phuyuhampatu* sp. n., a new species of Cusco Andes frog from the cloud forest of the eastern slopes of the Peruvian Andes (Amphibia, Anura, Craugastoridae). ZooKeys 685: 65–81. https://doi.org/10.3897/zookeys.685.12152

## Abstract

A new species of *Bryophryne* from the humid montane forest of the Department of Cusco, Peru, is described. Specimens were collected at 2795–2850 m a.s.l. in the Área de Conservación Privada Ukumari Llaqta, Quispillomayo valley, in the province of Paucartambo. The new species is readily distinguished from all other species of *Bryophryne* by having green coloration on dorsum, and blue flecks on flanks and ventral parts. Specimens are characterized by lacking a distinct tympanic annulus, tympanic membrane, and dentigerous processes of vomers, and by having dorsal skin shagreen, discontinuous dorsolateral folds, skin tuberculate on flanks, skin areolate on ventral surfaces of the body, and fingers and toes without lateral fringes or webbing. The new species has a snout–vent length of 14.2–16.9 mm in three males and 22.2–22.6 mm in two females, and is smaller than all other congeneric species except for *B. abramalagae*. Generic allocation is supported by low genetic distances of the 16S mitochondrial gene and morphological similarity with other species of *Bryophryne*, and geographic distribution. *Bryophryne phuyuhampatu* **sp. n.** is only known from the type locality, a cloud forest along the Quispillomayo River in the upper Nusiniscato watershed.

**Resumen**

Se describe una nueva especie de *Bryophryne* de los bosques nublados del Departamento de Cusco en Perú. Los especímenes fueron colectados a una elevación de 2795–2850 m en el Área de Conservación Privada Ukumari Llaqta, valle del río Quispillomayo, provincia de Paucartambo. La nueva especie se diferencia fácilmente de todas las demás especies de *Bryophryne* por tener coloración verde en la espalda y manchitas azuladas en los flancos y las superficies ventrales. Los especímenes se caracterizan por carecer de procesos vomerianos y de anillo y membrana timpánicos, y por poseer piel dorsal finamente granulada, pliegues dorsolaterales discontinuos, piel en los flancos verrugosa, y cubierta de verrugas en areola en las partes ventrales, y por carecer de membrana basal y quillas laterales en los dedos. La nueva especie tiene una longitud hocico–cloaca (LHC) de 14.2–16.9 mm en tres machos y de 22.2–22.6 mm en dos hembras, siendo menor que todas las demás especies de *Bryophryne* excepto por *B. abramalagae*. Distancias genéticas bajas para el gen mitocondrial 16S, similitud morfológica con otras especies de *Bryophryne* y distribución geográfica indican que la nueva especie forma parte del género *Bryophryne*. *Bryophryne phuyuhampatu* **sp. n.** se conoce únicamente de su localidad tipo, un bosque nublado en el valle del torrente Quispillomayo, en la parte alta de la cuenca del río Nusiniscato.

**Keywords**

leaf litter amphibian, montane forest, Paucartambo, taxonomy

**Palabras clave**

anfibio de hojarasca, Paucartambo, bosque nublado, taxonomía

## Introduction

The frog genus *Bryophryne* currently includes nine species, all endemic to the southern Peruvian Department of Cusco, and distributed across the humid highland grasslands and forests from 2350 to 4000 m a.s.l. in the Amazonian slopes of the Andes (Chaparro et al. 2015; Duellman and Lehr 2009; Frost 2017; Padial et al. 2014). Molecular phylogenies support placement of the genus within the Holoadeninae in the family Craugastoridae (Hedges et al. 2008; Padial et al. 2014). High-Andean genera of Holoadeninae are characterized by having narrow terminal digits on the fingers and toes and by lacking circumferential grooves, but are generally indistinguishable on the basis of morphological traits (Duellman and Lehr 2009; Hedges et al. 2008).

Knowledge of the diversity of this genus has improved dramatically over the past decade (Chaparro et al. 2015), contributing to Peru's high rate of new species discoveries (Catenazzi 2015). Whereas only the type species of the genus, *B. cophites* (Lynch), was known until 2007, all other congeneric species have been discovered since 2007 (Chaparro et al. 2007; Chaparro et al. 2015; Lehr and Catenazzi 2008; Lehr and Catenazzi 2009a; Lehr and Catenazzi 2010). These recent discoveries confirm that species of *Bryophryne* are predominantly mountaintop species, and that each mountain pass is occupied by up to three different species of seemingly restricted geographic distribution (Lehr and Catenazzi 2009a; Lehr and Catenazzi 2010). Mountain passes as close as 50 km share no species of *Bryophryne*, suggesting high levels of beta diversity.

During May and June of 2015 and 2016 we explored two valleys of the eastern side of the Cordillera de Paucartambo within the Área de Conservación Privada Ukumari Llaqta (Catenazzi and Ttito 2016), a protected area recognized by a Peruvian environmental ministerial decree in 2011. This private area is owned and managed by local communities, whose members permitted our work and guided us through the high-elevation grasslands, montane scrub, and down to the higher reaches of the humid montane forest. Our work in the Japumayo Valley in 2015 led to the discovery of *Psychrophrynella chirihampatu* (Catenazzi and Ttito 2016). In 2016 we surveyed the adjacent Quispillomayo Valley, where we found specimens of a new species of *Bryophryne* in the humid montane forest. Here we report on these recent surveys, and describe the new species.

## Materials and methods

The format of the diagnosis and description follows Duellman and Lehr (2009) and Lynch and Duellman (1997), except that the term dentigerous processes of vomers is used instead of vomerine odontophores (Duellman et al. 2006). We follow Hedges et al. (2008) for taxonomy, except for family placement (Pyron and Wiens 2011). We derived meristic traits of similar species from specimens examined, published photographs, or species descriptions.

Specimens were fixed and preserved in 70% ethanol. Sex and maturity of specimens were determined by observing sexual characters and gonads through dissections. We measured the following variables (Table 1) to the nearest 0.1 mm with digital calipers under a stereomicroscope:

**SVL** snout–vent length
**TL** tibia length
**FL** foot length (distance from proximal margin of inner metatarsal tubercle to tip of Toe IV)
**HL** head length (from angle of jaw to tip of snout)
**HW** head width (at level of angle of jaw)
**ED** eye diameter
**TY** tympanum diameter
**IOD** interorbital distance
**EW** upper eyelid width
**IND** internarial distance
**E–N** eye–nostril distance (straight line distance between anterior corner of orbit and posterior margin of external nares)

Hand length was measured as the distance from the proximal margin of thenar tubercle to tip of Finger III. Fingers and toes are numbered preaxially to postaxially from I–IV and I–V respectively. We determined comparative lengths of toes III and V

**Table 1.** Genetic distances (uncorrected p-distances) estimated from the non-coding 16S rRNA mitochondrial fragment (GenBank accession codes in parentheses) between *Bryophryne phuyuhampatu* and related taxa (in boldface the most closely related species) of the subfamily Holoadeninae (Craugastoridae).

| | *Barycholos pulcher* (EU186709) | *Bryophryne bakersfield* (KT276289) | *Br. bustamantei* (KT276293) | *Br. cophites* (EF493537) | *Br. phuyuhampatu* CORBIDI 18224 (MF419254) | *Br. phuyuhampatu* MUBI 14654 (MF419259) | *Br. phuyuhampatu* CORBIDI 18225 (MF419255) | *Br. phuyuhampatu* CORBIDI 18226 (MF419256) | *Br. phuyuhampatu* CORBIDI 18227 (MF419257) | *Br. phuyuhampatu* CORBIDI 18228 (MF419258) | *Br. phuyuhampatu* MUBI 14655 (MF419260) | *Holoaden luederwaldti* (EU186710) | *Noblella lochites* (EU186699) | *Psychrophrynella chirihampatu* (KU884559) | *P. guillei* (AY843720) | *P. usurpator* (EF493714) | *P. wettsteini* (EU186696) |
|---|---|---|---|---|---|---|---|---|---|---|---|---|---|---|---|---|---|
| *Barycholos pulcher* (EU186709) | | | | | | | | | | | | | | | | | |
| *Bryophryne bakersfield* (KT276289) | 0.19 | | | | | | | | | | | | | | | | |
| *Br. bustamantei* (KT276293) | 0.26 | 0.05 | | | | | | | | | | | | | | | |
| *Br. cophites* (EF493537) | 0.24 | 0.04 | 0.15 | | | | | | | | | | | | | | |
| *Br. phuyuhampatu* CORBIDI 18224 (MF419254) | 0.19 | **0.04** | **0.06** | **0.06** | | | | | | | | | | | | | |
| *Br. phuyuhampatu* MUBI 14654 (MF419259) | 0.20 | **0.04** | **0.06** | **0.06** | 0.00 | | | | | | | | | | | | |
| *Br. phuyuhampatu* CORBIDI 18225 (MF419255) | 0.20 | **0.04** | **0.07** | **0.06** | 0.00 | 0.00 | | | | | | | | | | | |
| *Br. phuyuhampatu* CORBIDI 18226 (MF419256) | 0.20 | **0.04** | **0.06** | **0.06** | 0.00 | 0.00 | 0.00 | | | | | | | | | | |
| *Br. phuyuhampatu* CORBIDI 18227 (MF419257) | 0.20 | **0.04** | **0.06** | **0.06** | 0.00 | 0.00 | 0.00 | 0.00 | | | | | | | | | |
| *Br. phuyuhampatu* CORBIDI 18228 (MF419258) | 0.20 | **0.04** | **0.06** | **0.06** | 0.00 | 0.00 | 0.00 | 0.00 | 0.00 | | | | | | | | |
| *Br. phuyuhampatu* MUBI 14655 (MF419260) | 0.21 | **0.04** | **0.06** | **0.06** | 0.00 | 0.00 | 0.00 | 0.00 | 0.00 | 0.00 | | | | | | | |
| *Holoaden luederwaldti* (EU186710) | 0.27 | 0.18 | 0.23 | 0.21 | 0.17 | 0.17 | 0.17 | 0.19 | 0.19 | 0.19 | 0.20 | | | | | | |
| *Noblella lochites* (EU186699) | 0.25 | 0.20 | 0.26 | 0.24 | 0.20 | 0.19 | 0.20 | 0.18 | 0.19 | 0.18 | 0.19 | 0.23 | | | | | |
| *Psychrophrynella chirihampatu* (KU884559) | 0.21 | 0.19 | 0.19 | 0.19 | 0.17 | 0.17 | 0.18 | 0.18 | 0.18 | 0.18 | 0.17 | 0.17 | 0.21 | | | | |
| *P. guillei* (AY843720) | 0.24 | 0.14 | 0.12 | 0.22 | 0.13 | 0.12 | 0.14 | 0.13 | 0.13 | 0.13 | 0.13 | 0.23 | 0.27 | 0.15 | | | |
| *P. usurpator* (EF493714) | 0.29 | 0.20 | 0.24 | 0.24 | 0.20 | 0.19 | 0.20 | 0.20 | 0.20 | 0.20 | 0.20 | 0.22 | 0.27 | 0.05 | 0.21 | | |
| *P. wettsteini* (EU186696) | 0.26 | 0.17 | 0.20 | 0.21 | 0.16 | 0.15 | 0.15 | 0.15 | 0.15 | 0.15 | 0.15 | 0.21 | 0.24 | 0.17 | 0.13 | 0.21 | |

by adpressing both toes against Toe IV; lengths of fingers I and II were determined by adpressing these fingers against each other. In two female specimens, the ovaries were dissected, the eggs extracted, and their diameter measured under a stereomicroscope to the nearest 0.01 with a digital caliper.

Standard protocols were used to extract, amplify and sequence the non-coding 16S rRNA mitochondrial fragment (Catenazzi and Ttito 2016), and new sequences were deposited in GenBank (Table 1). Variation in coloration was described on the basis of field notes and photographs of live frogs. Photographs taken by A. Catenazzi of live specimens, including types and non-collected specimens, and of preserved types have been deposited at the Calphoto online database (http://calphotos.berkeley.edu). Locality names follow the spelling of the Carta Nacional "Chontachaca" (27-t), Instituto Geográfico Nacional, Lima. Elevation data for the map (Figure 1) were obtained from http://www.diva-gis.org.

Specimens examined are listed in Appendix I; codes of collections are:

| | |
|---|---|
| **CORBIDI** | Herpetology Collection, Centro de Ornitología y Biodiversidad, Lima, Peru |
| **MUBI** | Museo de Biodiversidad del Perú, Cusco |
| **KU** | Natural History Museum, The University of Kansas, Lawrence, Kansas, USA |
| **MUSM** | Museo de Historia Natural Universidad Nacional Mayor de San Marcos, Lima, Peru |
| **MHNG** | Muséum d'Histoire Naturelle, Genève, Switzerland |

Research was approved by Institutional Animal Care and Use Committees of Southern Illinois University Carbondale (protocol #13–027). The permit to carry on this research has been issued by the Peruvian Ministry of Agriculture (permit #292–2014-MINAGRI-DGFFS-DGEFFS). The Comunidad Campesina Japu Q'eros authorized our work on their land.

***Bryophryne phuyuhampatu* sp. n.**
http://zoobank.org/BB13FD82-3470-4E31-A6EF-87606B0CC356

**Holotype.** (Figs 1–3, Table 2). CORBIDI 18226, an adult male (Figs 2, 3) from 13°22'12.14"S; 71°6'49.82"W (WGS84), 2795–2850 m a.s.l., Quispillomayo valley, Área de Conservación Privada (ACP) Ukumari Llaqta, Distrito Paucartambo, Provincia Paucartambo, Departamento de Cusco, Peru, collected by A. Catenazzi, A. Shepack, M. I. Diaz and A. Ttito on 27 May 2016.

**Paratopotypes.** (Fig. 4, Table 2). Four specimens: two females, CORBIDI 18224 and MUBI 14654, and one male, CORBIDI 18225, collected with the holotype on 27 May 2016; and one male, MUBI 14655 collected on 28 May 2016.

**Referred specimens.** Three juveniles, CORBIDI 18227, 18228, and MUBI 14665, collected with the holotype and paratopotypes on 27 May 2016.

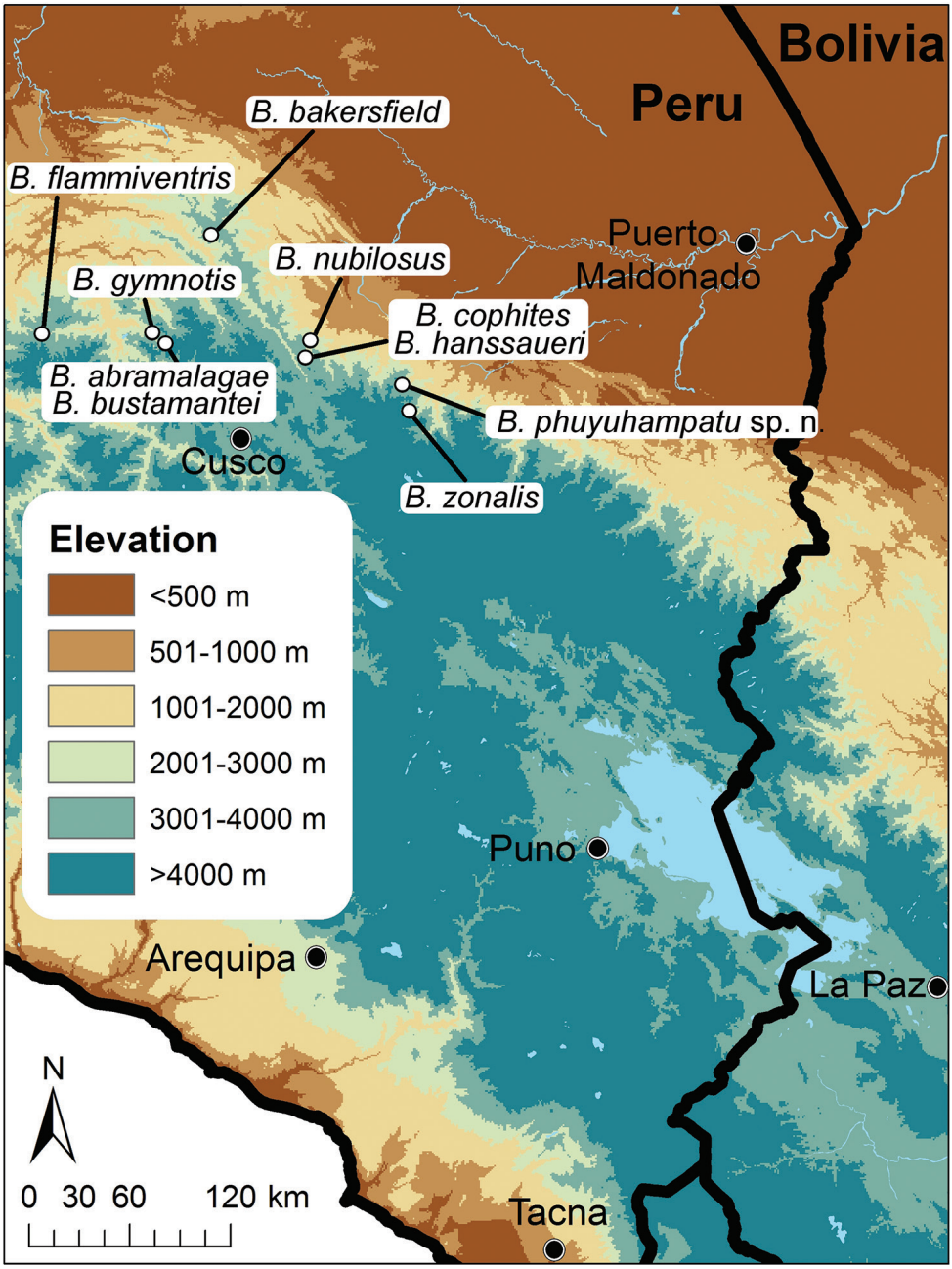


**Figure 1.** Map of Peru indicating the type localities of species of *Bryophryne*.

**Generic placement.** A new species of *Bryophryne* as defined by Duellman and Lehr (2009), Hedges et al. (2008), and Padial et al. (2014). Frogs of the genus *Bryophryne* are morphologically similar and closely related to *Barycholos*, *Holoaden*, *No-*

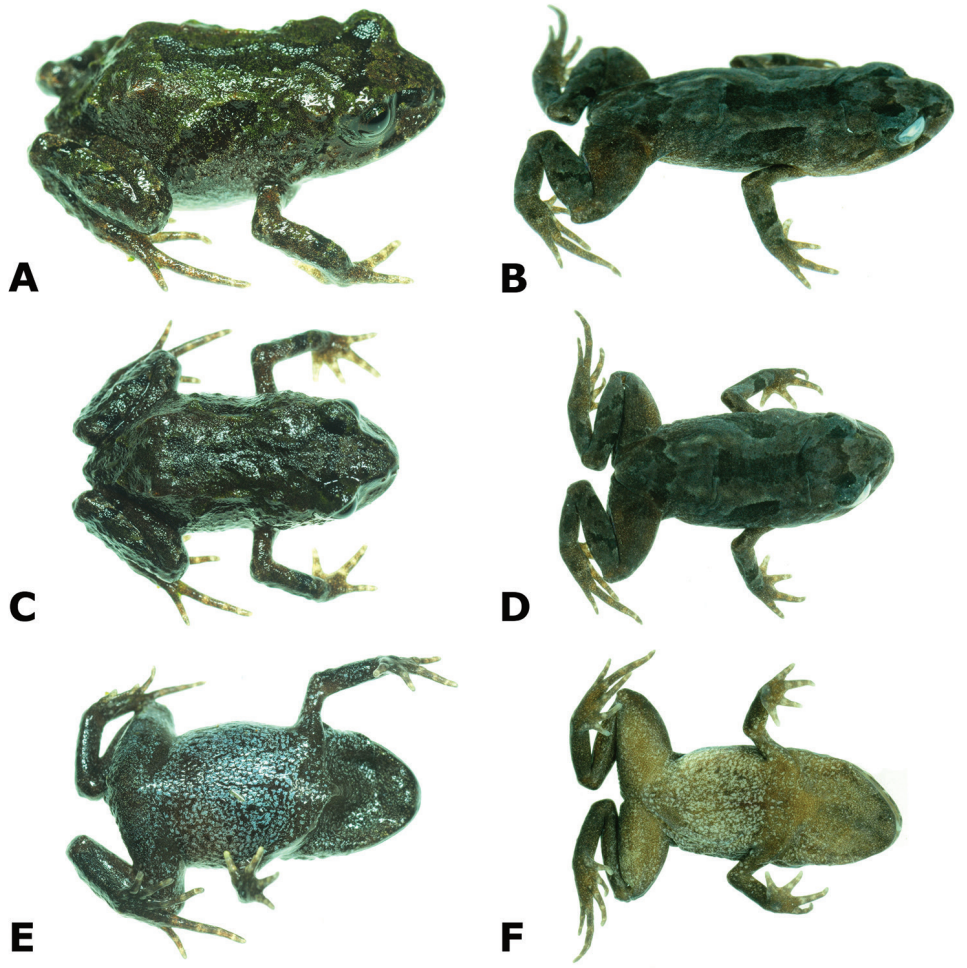


**Figure 2.** Live (left column) and preserved (right column) specimen of the holotype of *Bryophryne phuyuhampatu* sp. n., male CORBIDI 18226 (SVL 16.9 mm) in dorsolateral **A, B** dorsal **C, D** and ventral **E, F** views. Photographs by A. Catenazzi.

*blella* and *Psychrophrynella* (Chaparro et al. 2015; Hedges et al. 2008; Heinicke et al. 2007; Padial et al. 2014). Genetic data confirm generic placement of the new species within *Bryophryne* (Table 1). We found substantial genetic distances (uncorrected p-distances from 3.7–6.7%; Table 1) between *B. phuyuhampatu* and congeneric species for which mitochondrial sequence data were available (*B. bakersfield*, *B. bustamantei*, and *B. cophites*). The most closely related species is *B. bakersfield* (16S uncorrected p-distance: 3.7–4.1%), followed by *B. cophites* (5.6–6.2%) and *B. bustamantei* (5.6–6.7%). Regarding species from other genera, *B. phuyuhampatu* had genetic distances ranging from 12.4% (*Psychrophrynella guillei*) to 20.8% (*Barycholos pulcher*). In addition to the molecular data, the new species is assigned to *Bryophryne* rather than any of

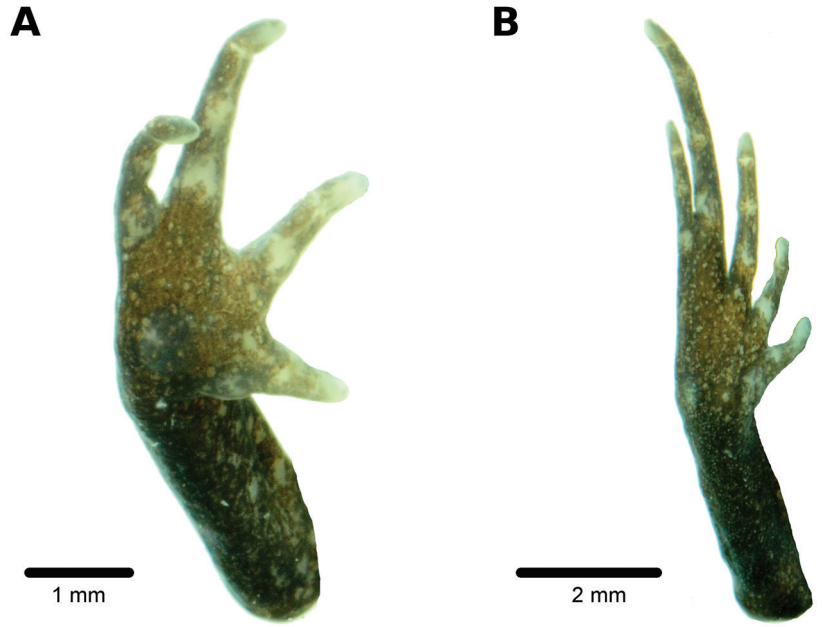


**Figure 3.** Ventral views of hand **A** and foot **B** of holotype, CORBIDI 18226 (hand length 4.1 mm, foot length 6.6 mm) of *Bryophryne phuyuhampatu* sp. n. Photographs by A. Catenazzi.

the other genera on the basis of overall morphological resemblance with the type species *B. cophites*, including head narrower than body, short limbs, and tympanic membrane and annulus usually absent (absent in most species of *Bryophryne*, except for *B. flammiventris* and *B. gymnotis*), and geographic distribution within the Departamento Cusco, where all other species of *Bryophryne* occur.

**Diagnosis.** A new species of *Bryophryne* characterized by: (1) skin on dorsum shagreen; skin on venter areolate, discoidal fold absent, thoracic fold present; dorsolateral folds irregular and discontinuous; (2) tympanic membrane and tympanic annulus absent; (3) snout rounded in dorsal view and in profile; (4) upper eyelid with two small tubercles, narrower than IOD; cranial crests absent; (5) dentigerous process of vomers absent; (6) vocal sac and slits absent; nuptial pads absent; (7) Finger I much shorter than Finger II; tips of digits slightly pointed; (8) fingers lacking lateral fringes; (9) outer edge of forearm bearing small tubercles; (10) heel bearing minute tubercles; inner tarsal fold absent; outer edge of tarsus bearing small tubercles; (11) inner metatarsal tubercle prominent, ovoid, of similar relief and slightly larger than ovoid, outer metatarsal tubercle; supernumerary plantar tubercles indistinct; (12) toes lacking lateral fringes; webbing absent; toes III and V about equal in length; tips of digits slightly pointed; (13) in life, dorsum tan to green and brown with dark brown markings, greenish blue on lower flanks; some specimens with a yellow middorsal line extending from tip of snout to cloaca and to the posterior surface of thighs; interorbital bar present; chest, belly and ventral parts of forearms and legs dark brown with grayish blue

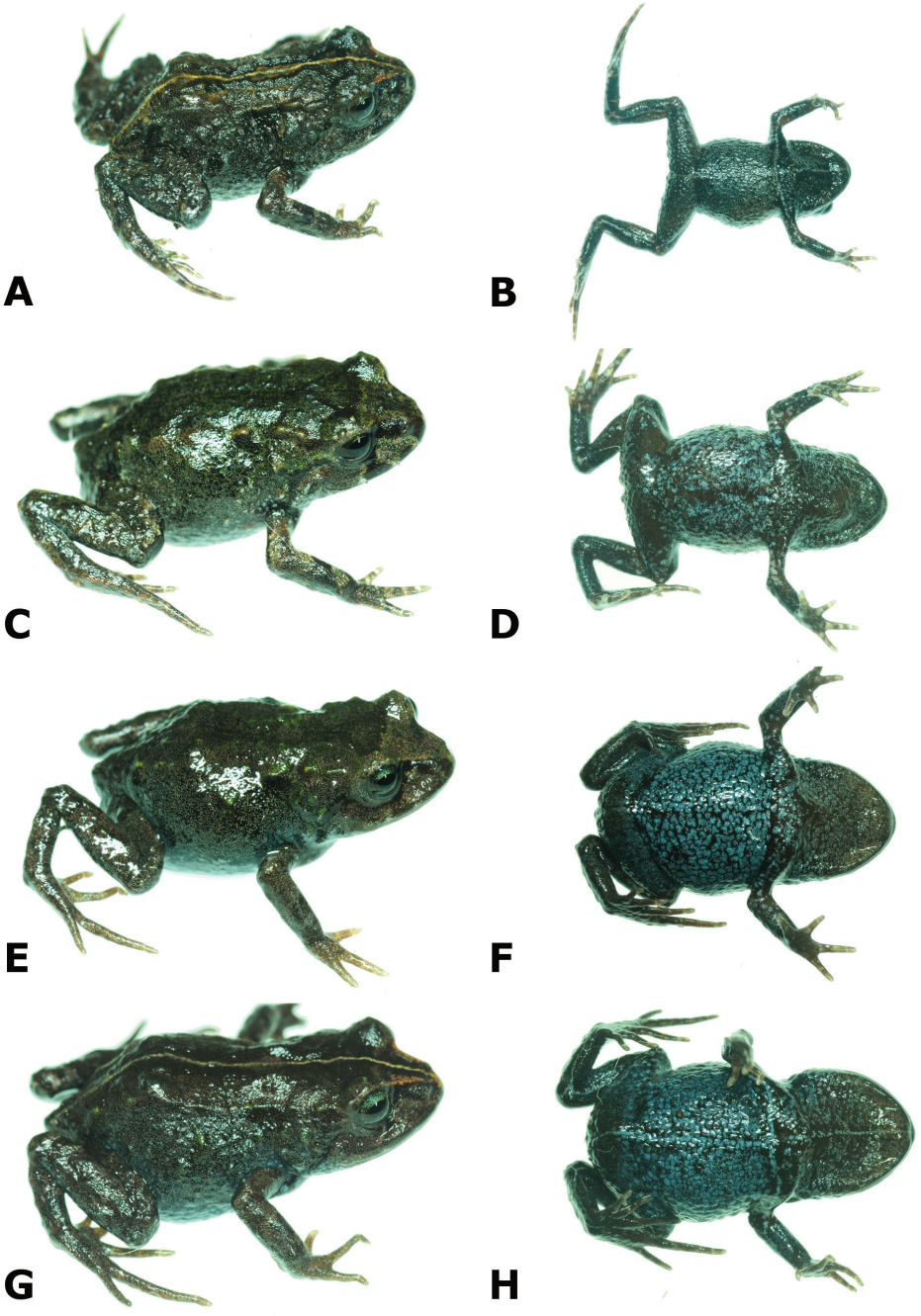


**Figure 4.** Dorsolateral and ventral views of four paratypes of *Bryophryne phuyuhampatu* sp. n. showing variation in dorsal and ventral coloration. Male CORBIDI 18225, SVL = 14.2 mm **A, B** Male MUBI 14655, SVL = 15.9 mm **C, D** Female CORBIDI 18224, SVL = 22.6 mm **E, F**. Female MUBI 14654, SVL = 22.2 mm **G, H** Photographs by A. Catenazzi.

**Table 2.** Range and average (± standard deviation) measurements (in mm) of type series of *Bryophryne phuyuhampatu* sp. n.

| Characters | Females (n = 2) | Males (n = 3) |
|---|---|---|
| SVL | 22.2–22.6 | 14.2–16.9 (15.7 ± 0.8) |
| TL | 8.1–8.4 | 5.6–6.5 (6.1 ± 0.3) |
| FL | 9.2–9.9 | 5.8–6.6 (6.3 ± 0.3) |
| HL | 8.1–8.9 | 4.8–5.5 (5.1 ± 0.2) |
| HW | 7.0–7.6 | 4.4–5.4 (5.0 ± 0.3) |
| ED | 2.1 | 1.6–1.8 (1.7 ± 0.1) |
| IOD | 3.6–3.7 | 2.2–2.6 (2.4 ± 0.1) |
| EW | 1.4–1.6 | 1.0–1.1 (1.1 ± 0.0) |
| IND | 2.0–2.1 | 1.4–1.5 (1.5 ± 0.0) |
| E–N | 1.5–2.0 | 1.3 (1.3 ± 0.0) |
| TL/SVL | 0.36–0.38 | 0.38–0.39 |
| FL/SVL | 0.41–0.45 | 0.39–0.41 |
| HL/SVL | 0.36–0.40 | 0.31–0.34 |
| HW/SVL | 0.31–0.34 | 0.31–0.33 |
| HW/HL | 0.85–0.86 | 0.92–1.06 |
| E–N/ED | 0.71–0.95 | 0.72–0.81 |
| EW/IOD | 0.38–0.44 | 0.38–0.50 |

flecks; throat brown with flecks turning from gray-blue to copper near tip of mouth; palmar and plantar surfaces brown with lighter fingers and toes; (14) SVL 14.2–16.9 in males (n = 3), 22.2–22.6 in females (n = 2).

**Comparisons.** The new species differs from other members of the genus by having green coloration on dorsum and blue coloration on flanks and ventral parts. Furthermore, *B. phuyuhampatu* differs from other species by the following combination of characters (condition for comparing species in parenthesis): from *B. abramalage* by having proportionally longer feet with FL/SVL from 0.41–0.45 (0.37–0.42), narrower head with HW/HL from 0.85–0.86 (0.97–1.07), and inner metatarsal tubercle larger than outer metatarsal (inner half the size of outer metatarsal tubercle); *B. flammiventris* and *B. gymnotis* by lacking a tympanum (present), from *B. bakersfield* and *B. bustamantei* by having discontinuous dorsolateral folds (continuous), from *B. cophites* by females being much smaller (22.6 mm vs. 35.8 mm), from *B. hanssaueri* by lacking bright orange coloration on throat (present), from *B. nubilosus* by having toes III and V similar in length (toe V > III), and from *B. zonalis* by having blue-gray mottled coloration on belly (distinctive black mottled coloration, variably confined to lower portion of belly). The new species further differs from *B. gymnotis* by having vomers lacking dentigerous processes (present), from *B. cophites* by males lacking nuptial pads (present), and from *B. bakersfield*, *B. bustamantei*, *B. flammiventris* and *B. gymnotis* for males lacking vocal slits (present).

*Bryophryne phuyuhampatu* (max. SVL 22.6 mm) is much smaller than *B. bakersfield* (31.1 mm), *B. cophites* (35.8 mm; pers. obs.), *B. hanssaueri* (29.3 mm; pers. obs.), and

*B. zonalis* (32.4 mm), smaller than *B. bustamantei* (23.4 mm), *B. flammiventris* (24.1), *B. hanssaueri* (24.6 mm), and about the same size of *B. abramalagae* (20.1 mm) and *B. nubilosus* (26.0 mm; pers. obs.). Five other small species of craugastorid frogs of the subfamily Holoadeninae are known to occur in montane forests and high Andean grasslands south of the Apurimac canyon in Peru: *Noblella madreselva*, *N. pygmaea*, *Psychrophrynella bagrecito*, *P. chirihampatu* and *P. usurpator*, which all possess a visible tympanic annulus.

**Description of holotype.** Adult male (16.9 mm SVL); head narrower than body, its length 33% of SVL; head wider than long, head length 83% of head width; head width 32% of SVL; snout short, rounded in dorsal and lateral views (Fig. 2), eye diameter 35% of head length, its diameter 1.2 times as large as its distance from the nostril; nostrils slightly protuberant, close to snout, directed dorsolaterally; canthus rostralis slightly straight in dorsal view, rounded in profile; loreal region slightly concave; lips rounded; upper eyelids with two small tubercles; upper eyelid width 46% of interorbital distance; interorbital region flat, lacking cranial crests; eye-nostril distance 81% of eye diameter; supratympanic fold short and weak; tympanic membrane and tympanic annulus absent; postrictal tubercles absent. Vocal sac and vocal slits absent. Choanae ovoid, small, positioned far anteriorly and laterally, widely separated from each other; dentigerous processes of vomer and vomerine teeth absent; tongue large, ovoid, about 2.5 times as long as wide, not notched posteriorly.

Skin on dorsum shagreen with small, scattered tubercles; dorsolateral folds discontinuous, extending from posterior margin of upper eyelid to sacral region; skin on flanks tuberculate; skin on throat smooth, skin on chest, and belly areolate; thoracic fold present, discoidal fold absent; cloaca slightly protuberant, cloacal sheath short, cloacal region without tubercles. Outer surface of forearm with minute tubercles; palmar tubercle flat and oval, approximately same length but twice the width of elongate, thenar tubercle; few supernumerary tubercles low, ovoid; subarticular tubercles prominent, ovoid in ventral view, rounded in lateral view, largest at base of fingers; fingers lacking lateral fringes; Finger I much shorter than Finger II; relative lengths of fingers 3 > 4 = 2 > 1 (Fig. 3); tips of digits slightly pointed, lacking circumferential grooves (Fig. 3); forearm lacking tubercles.

Hindlimbs short and robust, tibia length 38% of SVL; foot length 39% of SVL; upper surfaces of hindlimbs shagreen with scattered, minute tubercles; posterior surface of thighs tuberculate to areolate, ventral surface areolate; heel with minute tubercles (not visible in preservative); inner edge of tarsus without tubercles, outer edge of tarsus with small tubercles; inner metatarsal tubercle prominent, ovoid, of similar relief and slightly larger than ovoid, outer metatarsal tubercle; supernumerary plantar tubercles indistinct; subarticular tubercles low, ovoid in dorsal view; toes lacking lateral fringes, not webbed; toe tips weakly pointed, not expanded laterally, about as large as those on fingers; relative lengths of toes: 4 > 3 = 5 > 2 > 1 (Fig. 3); foot length 32% of SVL.

Measurements of holotype (all in mm): SVL 16.9, TL 6.5, FL 6.6, HL 5.5, HW 5.4, ED 1.6, IOD 2.4, EW 1.1, IND 1.5, E–N 1.3.

**Coloration of holotype in life. (Fig. 2)**. Dorsum green and brown with a dark brown marking extending from the interorbital bar to a mid-dorsal longitudinal band,

a horizontal dark mark near the sacral region, and an oblique dark band on each flank. Dorsal surfaces of arms and legs dark brown, with transverse dark bars on forearms and hind limbs. Lower flanks with greenish blue flecks. Chest, belly and ventral parts of forearms and legs dark brown with grayish blue flecks. Iris grayish blue with a medial copper band. Throat brown with flecks turning from gray-blue to copper near the tip of the mouth. Palmar and plantar surfaces brown; tips of fingers and toes light brown to yellow.

**Coloration of holotype in alcohol. (Fig. 2)**. Similar to coloration in life, but dorsal surfaces grayish tan with higher contrast of dorsal markings. Ventral surfaces beige to brown with cream flecks.

**Variation.** Coloration in life is based on field notes and photographs taken by A. Catenazzi of the paratopotypes (Fig. 4; photographs available through Calphoto database). The amount of dorsal green coloration varies among specimens. While juvenile MUBI 14665 and male MUBI 14655 are similar to the holotype in having a generally greenish dorsum, all other specimens have dark tan to brown dorsum, with just a few tubercles colored green. Female MUBI 14654, male CORBIDI 18225 and juvenile CORBIDI 18228 have a yellow middorsal line extending from the tip of the snout to the cloaca and to the posterior surface of the thighs.

The summary of measurements of all types is reported in Table 2.

**Etymology.** The specific name *phuyuhampatu* is a combination of Quechua words used in apposition meaning "toad" ("hampa'tu") that lives in the "fog" ("phuyu").

**Distribution, natural history, and threats.** *Bryophryne phuyuhampatu* was discovered during a rapid amphibian survey in the upper Quispillomayo Valley (Fig. 5A) from 22 to 31 May 2016. The Quispillomayo torrent (Fig. 5B) is a tributary of the Nusiniscato River, which reaches the Araza River downstream of Quincemil, in the upper Madre de Dios drainage. During the inventory high-Andean grasslands (puna; 3350–4515 m a.s.l.), a forest patch of tasta (*Escallonia myrtillioides*), kishuar (*Buddleja incana*) and qeñua (*Polylepis incana*) at 4280 m a.s.l., montane scrub, disturbed areas and other transitional formations along the treeline around 3350 m a.s.l., and the montane cloud forest from 2780–3350 m a.s.l. were sampled. Frogs were searched for under rocks, logs, mosses, and in the leaf litter and the understory in the montane forest. All but one specimens of *B. phuyuhampatu* were found under mosses in the cloud forest around 2850 m a.s.l. (Fig. 5C). Male MUBI 14655 was found ~250 m from this site, under rocks and mosses under the riparian vegetation at the confluence of a small stream at 2795 m a.s.l. Two sympatric frogs, *Gastrotheca* cf. *excubitor* and *Psychrophrynella chirihampatu*, were found under rocks in disturbed habitats (i.e., along streams, landslides) but not in the cloud forest. Two additional amphibian species, *Bryophryne* sp. and *B.* cf. *zonalis*, were found along with *G.* cf. *excubitor* in the grasslands from 3100–3650 m a.s.l.

Both female paratopotypes had large eggs in their ovaries, indicative of terrestrial breeding and direct development: CORBIDI 18224 contained 15 eggs averaging 1.58 ± 0.05 mm in diameter (range 1.20–1.80 mm), while MUBI 16654 contained 16 eggs averaging 2.44 ± 0.03 mm in diameter (range 2.30–2.60 mm).

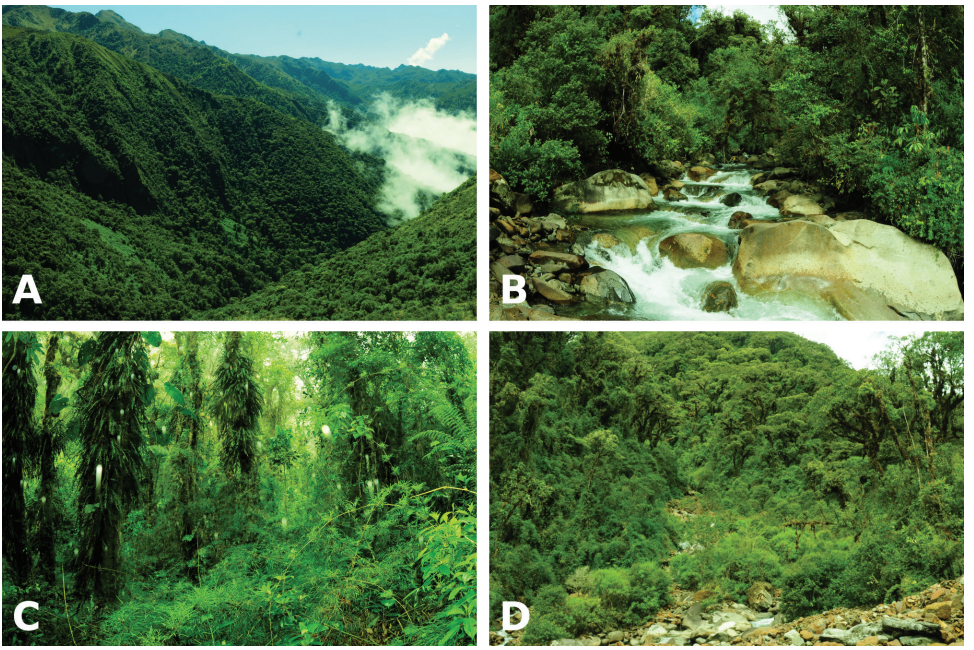


**Figure 5.** Collection localities of *Bryophryne phuyuhampatu* sp. n. in the upper Quispillomayo River valley **A** lookout from 3050 m a.s.l.: frogs were found under mosses, leaves and rocks in the cloud forest along the Quispillomayo River **B** such as the type locality at 2850 m a.s.l. **C** and disturbed forest at the confluence with a stream at 2795 m a.s.l. **D** Photographs by A. Catenazzi.

The type locality (and known distribution range) of the new species lies within the Área de Conservación Privada Ukumari Llaqta (Catenazzi and Ttito 2016), a protected area recognized by Peruvian environmental ministerial decree N° 301–2011-MINAM in December 2011. The upper puna and transitional habitats, as well as a narrow elevational band around the treeline are used for agriculture (potato cultivation), livestock (llamas grazing), fishing (exotic trout), and timber extraction. These land use patterns appear sustainable, and the grasslands at Patawasi (3350–3450 m a.s.l.) are in excellent conditions, with large bunchgrasses supporting large populations of *Bryophryne* sp. and *B.* cf. *zonalis*. There is little indication of human disturbance in the cloud forest, and the main use seems to be limited to trout fishing.

## Discussion

We assign the new species to *Bryophryne* on the basis of molecular data, shared meristic traits, general body shape and appearance, and overall similarity with the type species *B. cophites*, as well as with other species of *Bryophryne*. These frogs share robust bodies, short limbs, and usually lack a tympanic membrane and annulus (but they are present in *B. flammiventris* and *B. gymnotis*). Although no synapomorphy has been

identified for external morphological characters, the geographic distribution within the Cusco region along with the molecular data support allocation of the new species to *Bryophryne*. Many recent descriptions within Holoadeninae have used molecular data as evidence supporting genus allocation (Catenazzi and Ttito 2016; Chaparro et al. 2015; Padial et al. 2012).

The diversity of high-elevation, small terrestrial-breeding frogs in the Department of Cusco has increased sharply over the past decade (Catenazzi and Ttito 2016; Catenazzi et al. 2015; Chaparro et al. 2007; Chaparro et al. 2015; De la Riva et al. 2008; Lehr and Catenazzi 2008; Lehr and Catenazzi 2009a; Lehr and Catenazzi 2009b; Lehr and Catenazzi 2010), mostly due to the addition of new species of *Bryophryne*. With the present description, three species of *Bryophryne* are known to occur in the region surrounding Abra (= mountain pass) Hualla Hualla and the upper Marcapata and adjacent valley (the other two being *Bryophryne* sp. and *B. zonalis*), equal to the number of species found around Abra Acjanaco (*B. cophites*, *B. hanssaueri*, and *B. nubilosus*) and Abra Málaga (*B. abramalagae*, *B. bustamantei*, and *B. gymnotis*). No other mountain pass has been surveyed as exhaustively as these three, and surveys in other mountain passes are likely to further increase the known diversity of the genus. Similarly to congeneric forms, *B. phuyuhampatu* appears to have a small geographic range, although it should be noted that the exact geographic and elevational range of forest dwelling species is poorly known at the moment. Two ecologically similar species occupy elevational ranges from 3195–3475 m a.s.l. (*B. hanssaueri*) and from 2340–3215 m a.s.l. (*B. nubilosus*) in the forests of the Kosñipata Valley (Catenazzi et al. 2013; Lehr and Catenazzi 2008; Lehr and Catenazzi 2009b), while *B. gymnotis* has been found from 3272–3354 m a.s.l. in the cloud forest near Abra Málaga.

*Bryophryne phuyuhampatu* occurs in a remote and protected area where no threats have been observed. Therefore, and according to the IUCN Red List criteria and categories (IUCN 2013), we propose to assign this species to the "Least Concern" category of the Red List. Although the amphibian pathogenic fungus *Batrachochytrium dendrobatidis* (Bd) has been reported in several frogs from the nearby region of Abra Hualla Hualla and Coline (~22 km S by airline from the type locality of *B. phuyuhampatu*) (Catenazzi et al. 2011), and is known to have caused the local extinction of many stream-breeding species in the montane forests of Manu NP (58 km NW of Quispillomayo), terrestrial-breeding frogs such as *Bryophryne* do not appear to be threatened by chytridiomycosis, and their populations have persisted during Bd epizootics (Catenazzi et al. 2011; Catenazzi et al. 2014; Warne et al. 2016). A survey of Bd infection in the nearby Japumayo Valley in 2015 found no infected frogs along an elevational transect from 2650–4600 m a.s.l. (Catenazzi and Ttito 2016). With the discovery of *Psychrophrynella chirihampatu* (Catenazzi and Ttito 2016) and *B. phuyuhampatu*, the Ukumary Llaqta protected area now boasts two endemic species not found in nationally protected areas, demonstrating the beneficial contribution of private protected areas to amphibian conservation (Catenazzi et al. 2015; Catenazzi and von May 2014; von May et al. 2008).

## Acknowledgements

We thank the Comunidad Campesina Japu Qeros for their hospitability, for granting us access to and guiding us through the Quispillomayo valley; special thanks to Juan Samata Apaza, and Juan Marcos and Daniel Samata Huillca. We thank the Asociación para la Conservación de la Cuenca Amazónica for logistical support, and especially Marlene Mamani for coordinating our visit to Ukumari Llaqta. We thank E. Lehr, S. Serrano Rojas, and an anonymous reviewer for comments on an earlier version of the manuscript. This research was supported by grants from the Sabin Family Foundation, the Eppley Foundation, the bin Zayed Species Conservation Fund, and Southern Illinois University startup funds to AC.

## References

Catenazzi A (2015) State of the world's amphibians. Annual Review of Environment and Resources 40: 91–119. https://doi.org/10.1146/annurev-environ-102014-021358

Catenazzi A, Lehr E, Rodriguez LO, Vredenburg VT (2011) *Batrachochytrium dendrobatidis* and the collapse of anuran species richness and abundance in the upper Manu National Park, southeastern Peru. Conservation Biology 25: 382–391.

Catenazzi A, Lehr E, von May R (2013) The amphibians and reptiles of Manu National Park and its buffer zone, Amazon basin and eastern slopes of the Andes, Peru. Biota Neotropica 13: 269–283. https://doi.org/10.1590/S1676-06032013000400024

Catenazzi A, Lehr E, Vredenburg VT (2014) Thermal physiology, disease and amphibian declines in the eastern slopes of the Andes. Conservation Biology 28: 509–517. https://doi.org/10.1111/cobi.12194

Catenazzi A, Ttito A (2016) A new species of *Psychrophrynella* (Amphibia, Anura, Craugastoridae) from the humid montane forests of Cusco, eastern slopes of the Peruvian Andes. Peerj 4: e1807.

Catenazzi A, Uscapi V, von May R (2015) A new species of *Noblella* from the humid montane forests of Cusco, Peru. Zookeys 516: 71–84. https://doi.org/10.3897/zookeys.516.9776

Catenazzi A, von May R (2014) Conservation status of amphibians in Peru. Herpetological Monographs 28: 1–23. https://doi.org/10.1655/HERPMONOGRAPHS-D-13-00003

Chaparro JC, De la Riva I, Padial JM, Ochoa JA, Lehr E (2007) A new species of *Phrynopus* from Departamento Cusco, southern Peru (Anura : Brachycephalidae). Zootaxa 1618: 61–68.

Chaparro JC, Padial JM, Gutiérrez RC, De la Riva I (2015) A new species of Andean frog of the genus *Bryophryne* from southern Peru ( Anura: Craugastoridae) and its phylogenetic position, with notes on the diversity of the genus. Zootaxa 3994: 94–108. https://doi.org/10.11646/zootaxa.3994.1.4

De la Riva I, Chaparro JC, Padial JM (2008) A new, long-standing misidentified species of *Psychrophrynella* Hedges, Duellman & Heinicke from Departamento Cusco, Peru (Anura: Strabomantidae). Zootaxa 1823: 42–50.

Duellman WE, Lehr E (2009) Terrestrial-breeding frogs (Strabomantidae) in Peru. Natur und Tier Verlag, Münster, 382 pp.

Duellman WE, Lehr E, Venegas PJ (2006) Two new species of *Eleutherodactylus* (Anura: Leptodactylidae) from the Andes of northern Peru. Zootaxa 1285: 51–64.

Frost DR (2017) Amphibian Species of the World: an Online Reference. Version 6.0. http://research.amnh.org/herpetology/amphibia/index.html [accessed 12 May 2017]

Hedges SB, Duellman WE, Heinicke MP (2008) New World direct-developing frogs (Anura: Terrarana): molecular phylogeny, classification, biogeography, and conservation. Zootaxa 1737: 1–182.

Heinicke MP, Duellman WE, Hedges SB (2007) Major Caribbean and Central American frog faunas originated by ancient oceanic dispersal. Proceedings of the National Academy of Sciences of the United States of America 104: 10092–10097. https://doi.org/10.1073/pnas.0611051104

IUCN (2013) Guidelines for using the IUCN Red List categories and criteria. – Version 10.1. Prepared by the Standards and Petitions Subcommittee. IUCN.

Lehr E, Catenazzi A (2008) A new species of *Bryophryne* (Anura: Strabomantidae) from southern Peru. Zootaxa 1784: 1–10

Lehr E, Catenazzi A (2009a) Three new species of *Bryophryne* (Anura: Strabomantidae) from the Region of Cusco, Peru. South American Journal of Herpetology 4: 125–138. https://doi.org/10.2994/057.004.0204

Lehr E, Catenazzi A (2009b) A new species of minute *Noblella* (Anura: Strabomantidae) from southern Peru: The smallest frog of the Andes. Copeia 2009: 148–156. https://doi.org/10.1643/CH-07-270

Lehr E, Catenazzi A (2010) Two new species of *Bryophryne* (Anura: Strabomantidae) from high elevations in southern Peru (Region of Cusco). Herpetologica 66: 308–319. https://doi.org/10.1655/09-038.1

Lynch JD, Duellman WE (1997) Frogs of the genus *Eleutherodactylus* in western Ecuador. Systematics, ecology, and biogeography. The University of Kansas Special Publication 23: 1–236.

Padial JM, Chaparro JC, Castroviejo-Fisher S, Guayasamin JM, Lehr E, Delgado AJ, Vaira M, Teixeira M, Jr., Aguayo R, De la Riva I (2012) A revision of species diversity in the Neotropical genus *Oreobates* (Anura: Strabomantidae), with the description of three new species from the Amazonian slopes of the Andes. American Museum Novitates 3752: 1–55. https://doi.org/10.1206/3752.2

Padial JM, Grant T, Frost DR (2014) Molecular systematics of terraranas (Anura: Brachycephaloidea) with an assessment of the effects of alignment and optimality criteria. Zootaxa 3825: 1–132. https://doi.org/10.11646/zootaxa.3825.1.1

Pyron RA, Wiens JJ (2011) A large-scale phylogeny of Amphibia including over 2800 species, and a revised classification of extant frogs, salamanders, and caecilians. Molecular Phylogenetics and Evolution 61: 543–583. https://doi.org/10.1016/j.ympev.2011.06.012

von May R, Catenazzi A, Angulo A, Brown JL, Carrillo J, Chávez G, Córdova JH, Curo A, Delgado A, Enciso MA, Gutiérrez R, Lehr E, Martínez JL, Medina-Müller M, Miranda A, Neira DR, Ochoa JA, Quiroz AJ, Rodríguez DA, Rodríguez LO, Salas AW, Seimon T, Seimon A, Siu-Ting K, Suárez J, Torres C, Twomey E (2008) Current state of conservation

knowledge on threatened amphibian species in Peru. Tropical Conservation Science 1: 376–396. https://doi.org/10.1177/194008290800100406

Warne RW, LaBumbard B, LaGrange S, Vredenburg VT, Catenazzi A (2016) Co-Infection by chytrid fungus and Ranaviruses in wild and harvested frogs in the Tropical Andes. PLoS ONE 11: e0145864. https://doi.org/10.1371/journal.pone.0145864

## Appendix 1. Specimens examined

*Bryophryne bustamantei*: PERU: Cusco: Provincia La Convención: Abra de Málaga: MUSM 24537–38.

*Bryophryne cophites*: PERU: Cusco: Provincia de Paucartambo: Distrito Kosñipata: S slope Abra Acanaco, 14 km NNE Paucartambo, 3400 m: KU 138884 (holotype); N slope Abra Acanaco, 27 km NNE Paucartambo, 3450 m: KU 138885–908, 138911–5 (all paratypes); 2 km NE of Abra Acanaco, 3280 m: MHNG 2698.24, 5.5 km N of Abra Acanacu, 3523 m: MUSM 27895, Tres Cruces, 8.5 km N of Abra Acanaco, 3590 m: MUSM 20855–56, 26283–84, 26264, 26266–67, 26313, 26315, 27896, 30414–17, Pillco Grande, 3865 m, near border of Manu NP: CORBIDI 11919.

*Bryophryne gymnotis*: PERU: Cusco: Provincia de La Convención, Distrito de Huayopata: 1 km east of San Luis at elevations of 3272–3354 m: MUSM 24543 (holotype), MHNG 2710.28, 2710.29, MTD 46860–64, 47288, 47291–92, 47297, MUSM 24541–42, 24544–45, 24546–56, MVZ 258407–10 (all paratypes).

*Bryophryne hanssaueri*: PERU: Cusco: Provincia de Paucartambo, Distrito de Kosñipata: Acjanaco, Manu National Park, 3266 m elevation: MUSM 27567 (holotype); from near Acjanaco, Manu National Park at elevations of 3280–3430 m: MHNG 2698.25, MTD 46865–66, 46887–89, MUSM 24557, 27568–69, 27607–11, MVZ 258411–13 (all paratypes).

*Bryophryne nubilosus:* PERU: Cusco: Provincia de Paucartambo: Distrito de Kosñipata, 500 m NE of Esperanza, 2712 m: MUSM 26310 (holotype), MUSM 26311; near the type locality, 13°11'33.21"S, 71°35'25.17"W, 3065 m: MTD 47294; near Hito Pillahuata, 2600 m: MUSM 20970; Quebrada Toqoruyoc, 3097 m: MUSM 26312, MTD 47293; Esperanza, 2800 m: MHNSM 26316–17; 13°11'20.2"S, 71°35'07.3"W, 2900 m: MUSM 24539–40.

*Bryophryne* sp.: PERU: Cusco: Provincia de Quispicanchis: Distrito de Marcapata: Coline, 3672 m: MUSM 27571, 27573.

*Bryophryne zonalis*: PERU: Cusco: Provincia de Quispicanchis, Distrito de Marcapata, Kusillochayoc at 3129 m elevation: MUSM 27570 (holotype), MTD 46867, 46869–70, MUSM 27572, 27574–75, 27861, MVZ 258414 (all paratpyes); at Puente Coline, 3285 m elevation: MVZ 258415 (paratype).

ZooKeys 685: 83–89 (2017)
doi: 10.3897/zookeys.685.13625
http://zookeys.pensoft.net

RESEARCH ARTICLE

A peer-reviewed open-access journal
ZooKeys
Launched to accelerate biodiversity research

# Proposal for an index to evaluate dichotomous keys

Nguyen Van Sinh[1,2], Martin Wiemers[3], Josef Settele[3,4]

**1** *Institute of Ecology and Biological Resources (IEBR), Vietnam Academy of Science and Technology (VAST), 18 Hoang Quoc Viet, Nghia Do, Cau Giay, Ha Noi, Vietnam* **2** *Graduate School of Science and Technology, Vietnam Academy of Science and Technology (VAST), 18 Hoang Quoc Viet, Nghia Do, Cau Giay, Ha Noi, Vietnam* **3** *Helmholtz Centre for Environmental Research – UFZ, Dept. Community Ecology, Theodor-Lieser-Str. 4, 06120 Halle, Germany* **4** *Institute of Biological Sciences, University of the Philippines Los Baños, College of Arts and Sciences, Laguna 4031, Philippines*

Corresponding author: *Nguyen Van Sinh* (vansinh.nguyen@iebr.vast.vn)

Academic editor: *P. Stoev* | Received 10 May 2017 | Accepted 3 July 2017 | Published 17 July 2017

*http://zoobank.org/A0BD7648-1A92-45A4-B27D-60E30EABCC67*

**Citation:** Van Sinh N, Wiemers M, Settele J (2017) Proposal for an index to evaluate dichotomous keys. ZooKeys 685: 83–89. https://doi.org/10.3897/zookeys.685.13625

## Abstract

Dichotomous keys are the most popular type of identification keys. Studies have been conducted to evaluate dichotomous keys in many aspects. In this paper we propose an index for quantitative evaluation of dichotomous keys ($E_{dicho}$). The index is based on the evenness and allows comparing identification keys of different sizes.

## Keywords

index, dichotomous key, evaluation

## Introduction

A taxonomic key is a method used to identify organisms. Dichotomous keys are the most popular type of identification keys. Dichotomous keys are single entry identification keys. They consist of nested questions or couplets, and each question provides two choices or leads (Thesis and Antithesis). These choices contain descriptions of key characteristics of an organism. The paired statements or choices consider the differenc-

es between items. After choosing the statement that best matches the object, the user proceeds to another pair of statements until the name of the taxon is identified. There may be several keys for a group of taxa. This prompts the question, which key has a better performance, provided that all the used characters are good ones which allow an unambiguous identification? How can we evaluate quantitatively the performance of the keys? As a key is intended for identification of each of the taxa in the group, the key will achieve the highest performance when the mean number of steps to their identification is minimal. If the number of steps to identification of the taxa in a key become more even, the mean number of steps to their identification is decreasing, and the mean number of steps to identification of the taxa is minimal when the number of steps to their identification are most even (Fig. 1). These considerations lead us to the evenness index of Pielou (1966). This paper proposes an index that is based on Pielou's evenness index for quantitative evaluation of dichotomous keys.

## Methods

We use Pielou's evenness index as a prototype for our index. Pielou's evenness index (J) can be calculated using the following formula (Help et al. 1998):

$$J = H' / Hmax = H' / \ln S$$

where:

- H' is the Shannon diversity index. This measure was originally proposed by Shannon (1948) to quantify the entropy (uncertainty or information content) in strings of text. The idea is that the more different the letters are, and the more equal their proportional abundances in the string of interest, the more difficult it is to correctly predict which letter will be the next one in the string. The index can be calculated using the following formula:

$$H' = -\sum_{i=1}^{S} (p_i \ln p_i)$$

In which $p_i$ is the proportion of characters belonging to the $i$th type of letter in the string of interest and $S$ the number of types of letter.

- $H_{max}$ is the maximum value of H' and equal to:

$$H_{max} = -\sum_{i=1}^{S} \frac{1}{S} \ln \frac{1}{S} = \ln S$$

As result, Pielou's evenness index can be calculated according to the following formula:

$$J = -\sum_{i=1}^{S} (p_i \ln p_i) / \ln S$$

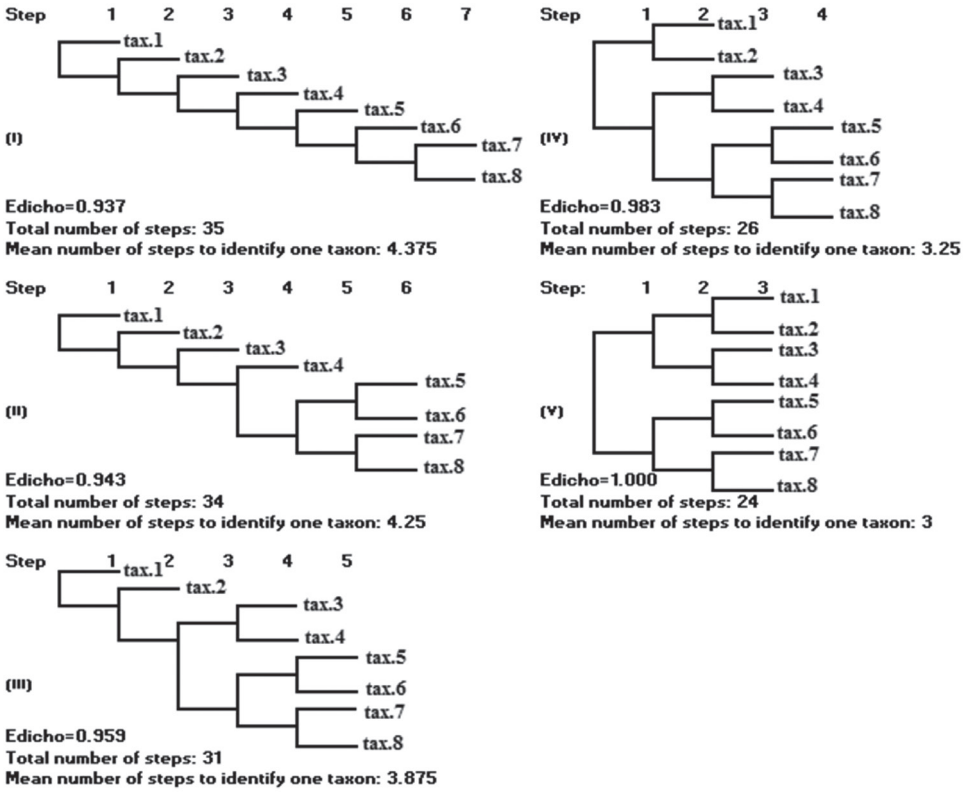


**Figure 1.** Schematic presentation of 5 dichotomous keys for a group of 8 taxa.

## Results and discussion

If the number of steps we have to pass to come to a decision (a taxon) is $N_i$ and the total steps when we identify all the taxa is N, the proportion of the steps to identify the *i*th taxon is equal:

$$p_i = N_i/N$$

As can be inferred from the scheme of a dichotomous key (Fig. 2), the number of taxa in a dichotomous key corresponds to S – the number of types of letters in the formula of Pielou's evenness index.

We call the index for dichotomous keys $E_{Dicho}$ (because of its origin from evenness index). As a result, $E_{Dicho}$ is equal:

$$E_{Dicho} = -\sum_{i=1}^{s}(p_i \ln p_i)/\ln S$$

Where: S is the number of taxa of the key, and $p_i$ is the proportion of steps to identify the *i*th taxon.

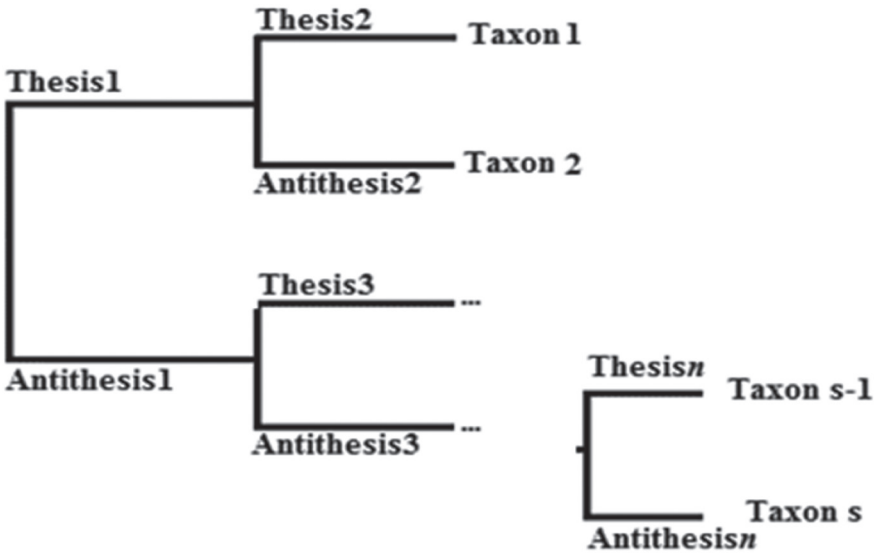


**Figure 2.** Schematic presentation of a dichotomous key.

Many attempts have been undertaken in order to evaluate identification keys (e.g. Lobanov 1975, 1983, 2015, Pankhurst 1978, Leuschner and Sviridov 1986, Leuschner 1991). Generally, these are methods that are based on the same concept of average length of taxon definition in a key and comparison of this number with the theoretical minimum. However, these attempts do not consider the length evenness of taxon definitions.

Several studies have been conducted to evaluate dichotomous keys in practice of key use (Morse et al. 1996) or to improve the key based on the user-tracking method (Schmidt et al. 2010). According to Osborne (1963), in principle, a simple dichotomous key used by an accurate observer must always lead to correct identification provided that the specimen in hand does actually belong to one of the taxa covered by the key and is not missing any crucial characters. Sandvik (1976) came to the conclusion that keys in which all taxa are gathered on the last two levels (so the number of steps of their identification is relatively equal) have the maximum probability of right determination. So our proposed index ($E_{Dicho}$) can both evaluate the speed and the quality of the determination of a dichotomous key, provided that all else (e.g. choice of characters) being equal.

The $E_{Dicho}$ index in its nature is an evenness index, therefore it has all the properties of a normal evenness index and is constrained between 0 and 1. The higher the variation in the number of steps we have to pass to come to the determination of the taxa, the lower is the $E_{Dicho}$ index, and the asymptotic lowest value is 0. The highest value of 1 can be achieved in case of all the taxa having the same number of identification steps (Fig. 1.V). As we can see in the Figure 1, the two versions of the dichotomous key (1.I

and 1.V) have the same number of taxa (8) and the same number of paired statements (7), but $E_{Dicho}$ of the version '1.I' is smaller than that of the version '1.V', because the variation in the length of path of identification steps in the version '1.I' is higher. Thus, the higher the $E_{Dicho}$ index is, the "better" is the dichotomous key in the aspect of identification speed and in the aspect of right determination.

## An example of calculation of $E_{Dicho}$ - the index for dichotomous keys

Let us consider five dichotomous keys as shown in the Figure 1.

Here, the number of taxa (S) equals 8. The number of steps or paired statements (Thesis + Antithesis) for identification of each taxon, the total number of steps for identification of all the taxa, and the proportion of steps to identify each taxon are the data for calculation of $H'_{Dicho}$ of the dichotomous key and are presented in Table 1 for the five versions of the dichotomous key.

The calculation of $H'_{Dicho}$ and $E_{dicho}$ of five versions of the dichotomous key is presented in Table 2.

**Table 1.** The data for calculation of $H'_{Dicho}$ for the keys in Figure 1.

| Key version | The number of steps for identification of each taxon | The total number of steps for identification of all the taxa | The proportion of steps to identify each taxon |
|---|---|---|---|
| 1.I | 1,2,3,4,5,6,7,7 | 35 | 1/35,2/35,3/35,4/35,5/35,6/35,7/35,7/35 |
| 1.II | 1,2,3,4,6,6,6,6 | 34 | 1/34,2/34,3/34,4/34,6/34,6/34,6/34,6/34 |
| 1.III | 1,2,4,4,5,5,5,5 | 31 | 1/31,2/31,4/31,4/31,5/31,5/31,5/31,5/31 |
| 1.IV | 2,2,3,3,4,4,4,4 | 26 | 2/26,2/26,3/26,3/26,4/26,4/26,4/26,4/26 |
| 1.V | 3,3,3,3,3,3,3,3 | 24 | 3/24,3/24,3/24,3/24,3/24,3/24,3/24,3/24 |

**Table 2.** Calculation of $H'_{Dicho}$ and $E_{dicho}$.

| Key version | $H'_{Dicho}$ | $E_{Dicho} = H'_{Dicho}/\ln(8)$ |
|---|---|---|
| 1.I | -{(1/35).ln(1/35)+(2/35).ln(2/35)+(3/35).ln(3/35)+(4/35).ln(4/35)+ (5/35).ln(5/35)+(6/35).ln(6/35)+(7/35).ln(7/35)+(7/35).ln(7/35)} | 0.937 |
| 1.II | -{(1/34).ln(1/34)+(2/34).ln(2/34)+(3/34).ln(3/34)+(4/34).ln(4/34)+ (6/34).ln(6/34)+(6/34).ln(6/34)+(6/34).ln(6/34)+(6/34).ln(6/34)} | 0.943 |
| 1.III | -{(1/31).ln(1/31)+(2/31).ln(2/31)+(4/31).ln(4/31)+(4/31).ln(4/31)+ (5/31).ln(5/31)+(5/31).ln(5/31)+(5/31).ln(5/31)+(5/31).ln(5/31)} | 0.959 |
| 1.IV | -{(2/26).ln(2/26)+(2/26).ln(2/26)+(3/26).ln(3/26)+(3/26).ln(3/26)+ (4/26). ln(4/26)+(4/26).ln(4/26)+(4/26).ln(4/26)+(4/26).ln(4/26)} | 0.983 |
| 1.V | -{(3/24).ln(3/24)+(3/24).ln(3/24)+(3/24).ln(3/24)+(3/24).ln(3/24)+ (3/24). ln(3/24)+(3/24).ln(3/24)+(3/24).ln(3/24)+(3/24).ln(3/24)} | 1.000 |

## Conclusions

By using computer software it is possible to create many dichotomous keys for a group of taxa with the same set of pairs of dichotomous characters. It would be desirable to have a sound basis for choosing one or another key version. The $E_{Dicho}$ index developed here is suitable for a quantitative evaluation of dichotomous keys. It can serve well as the mathematical basis for the task of choosing the dichotomous key with the best performance. Because the index is based on the evenness, it can be used to compare the identification keys of different sizes.

## Acknowledgement

This work has been supported by the VAST04.06/16-17 project and the IEBR-UFZ joint research LEGATO project.

## References

Help CHR, Herman PMJ, Soetaert K (1998) Indices of diversity and evenness. Oceanis 24(4): 61–87.

Leuschner D, Sviridov AV (1986) The Mathematical Theory of Taxonomic Keys. Biometrical Journal 28: 109–113. https://doi.org/10.1002/bimj.4710280120

Leuschner DA (1991) Mathematical Model for Classification and Identification. Journal of Classification 8: 99–113. https://doi.org/10.1007/BF02616250

Lobanov AL (1975) A mathematical apparatus for calculation, an assessment and comparison design data of identification keys. Zoologicheskiy Zhurnal 54(4): 485–497. [In Russian]

Lobanov AL (1983) The principles of creation of insects keys with use electronic computers. The abstract of the thesis on the scientist's competition degrees of Doct. Biol. Sci. Leningrad: ZIN of Sci. Acad. USSR, 19 pp. [In Russian]

Lobanov AL (2015) The Diagnostic Value of Qualitative and Quantitative Characters in Computer Identification Keys. Entomological Review 95(2): 285–288. https://doi.org/10.1134/S0013873815020128

Morse DR, Tardival GM, Spicer J (1996) A Comparison of the Effectiveness of a Dichotomous Key and a Multi-Access Key to Woodlice. Technical report. UKC, University of Kent, Canterbury, UK.

Osborne DV (1963) Some aspects of the theory of dichotomous keys. New Phytologist 62(2): 144–160. https://doi.org/10.1111/j.1469-8137.1963.tb06322.x

Pankhurst RJ (1978) Biological Identification. The Principles and Practice of Identification Methods in Biology. Edward Arnold, London, 104 pp.

Pielou EC (1966) The measurement of diversity in different types of biological collections. Journal of Theoretical Biology 13: 131–144. https://doi.org/10.1016/0022-5193(66)90013-0

Sandvik L (1976) A note on the theory of dichotomous keys. New Phytologist 76: 555–558. https://doi.org/10.1111/j.1469-8137.1976.tb01492.x

Schmidt G, Giurgiu M, Hetzner S, Neumann F (2010) Improvement of identification keys by user-tracking. In: Nimis PL, Vignes Lebbe R (Eds) Tools for Identifying Biodiversity: Progress and Problems, 137–143.

Shannon CE (1948) A mathematical theory of communication. The Bell System Technical Journal 27: 379–423, 623–656. https://doi.org/10.1002/j.1538-7305.1948.tb00917.x

ZooKeys 685: 91–103 (2017)
doi: 10.3897/zookeys.685.12700
http://zookeys.pensoft.net

RESEARCH ARTICLE

A peer-reviewed open-access journal
ZooKeys
Launched to accelerate biodiversity research

# A new species of *Leiochrides* from the Korean subtidal waters with notes on the taxonomic status of the genus *Pseudomastus* (Annelida, Capitellidae)

Man-Ki Jeong[1], Jin Hee Wi[2], Hae-Lip Suh[1]

**1** *Department of Oceanography, Chonnam National University, Yongbong-ro, Buk-gu, Gwangju 61186, Korea* **2** *School of Environmental Science and Engineering, Gwangju Institute of Science and Technology, Cheomdangwagi-ro, Buk-gu, Gwangju 61005, Korea*

Corresponding author: *Hae-Lip Suh* (suhhl@chonnam.ac.kr)

Academic editor: *C. Glasby* | Received 14 March 2017 | Accepted 8 June 2017 | Published 17 July 2017

*http://zoobank.org/223781CE-DD6E-4087-94B2-FD5550B2E502*

**Citation:** Jeong M-K, Wi JH, Suh H-L (2017) A new species of *Leiochrides* from the Korean subtidal waters with notes on the taxonomic status of the genus *Pseudomastus* (Annelida, Capitellidae). ZooKeys 685: 91–103. https://doi.org/10.3897/zookeys.685.12700

## Abstract

*Leiochrides yokjidoensis* **sp. n.**, collected from the sublittoral muddy bottom in southern Korea, is described as a new species. The taxonomic status of the monospecific genus *Pseudomastus* has been a subject of controversy for many years, as its characteristics overlap those given in recent generic definitions of *Leiochrides*. The results of a comprehensive review and comparison regarding the two genera, based on previous records showed minor differences. In this study, a detailed description of *L. yokjidoensis* **sp. n.** is given and a comparison with closely related species is tabulated and discussed.The taxonomic status of *Pseudomastus* is discussed and the genus placed in synonymy with *Leiochrides*.

## Keywords

Korea, *Leiochrides yokjidoensis* sp. n., morphology, Polychaeta, Scolecida, Sedentaria

## Introduction

Polychaetes are an important component of the macrobenthic community and they play a crucial role in the functioning of benthic communities in the recycling and reworking of the benthic sediments, bioturbation, and in the burial of organic matter

(Hutchings 1998). The Capitellidae Grube, 1862 are found in many types of sediments from the intertidal region to the deep sea and is a frequently dominant component of the benthic infaunal communities, especially in organically enriched sediments (Blake 2000). Owing to their accessibility and their importance in sedimentary environments, capitellids have been the subject of numerous ecological studies (Blake 2000). Despite their ecological importance, the taxonomy of Capitellidae has been largely ignored (Dean 2001). Since the first designation by Grube (1862), the family Capitellidae is currently composed of 48 genera, including 24 monospecific genera (Read 2017). The genera in this family have been defined by the number of segments with capillary chaetae or hooded hooks or mixtures of both (Blake 2000, Fauchald 1977). However, several previous records of Capitellidae include incorrect taxonomic information due to the ontogenetic variations in the chaetal arrangement and an indistinct demarcation of the peristomium or the transitional segment (Blake 2000, Green 2002, García-Garza and León-González 2011). Moreover, the high percentage of monospecific genera and the use of the insufficient characters in identification keys (i.e. based mostly on segmental distribution and chaetal composition) have steadily raised questions about taxonomic concepts of many Capitellidae (Ewing 1991, Blake 2000).

The genus *Leiochrides* was established by Augener (1914) with the description of *L. australis* Augener, 1918 from southwest Australia. The additional seven described species in the genus are *L. africanus* Augener, 1918 from western Africa, *L. pallidior* (Chamberlin, 1918) and *L. biceps* Hartman, 1954 from California, *L. hemipodus* from Southern California, *L. norvegicus* Fauchald, 1972 from western Norway, and *L. branchiatus* Hartman, 1976 and *L. andamanus* Green, 2002 from the Indian Ocean. The genus *Leiochrides* was formerly defined as having 12 thoracic chaetigers with only capillaries, abdominal chaetigers with only hooks, an indistinct boundary between the thorax and the abdomen, and the absence of branchiae (Augener 1914). However, the generic definition has continuously been modified for several decades. Hartman (1963, 1974) described *L. branchiatus* and *Leiochrides* sp. from California and revealed that some species of *Leiochrides* had transitional chaetigers in the thorax as a unique characteristic that had not been noted in previous studies. The genus *Leiochrides* is represented by having 12 chaetigers with capillary chaetae and only one or two species have the transitional chaetigers with capillary notochaetae and neurohooks. On the other hand, Day (1967) and Fauchald (1977) did not accept the new character proposed by Hartman (1963, 1974) and followed the original generic definition of Augener (1914). Recently, Blake (2000) and Green (2002) reconfirmed the existence of the transitional thoracic chaetigers in *Leiochrides* species and emended the generic definition in the light of Hartman (1963, 1974). We follow the expanded generic definition of Green (2002) in this study.

The genus *Pseudomastus* established by Capaccioni-Azzati and Martin (1992) was defined by the 12 thoracic chaetigers, which comprised 11 thoracic chaetigers with capillaries and the last thoracic chaetiger with capillary notochaetae and neuropodial hooks. The chaetal arrangement of *Pseudomastus* coincides with the expanded generic definition of *Leiochrides* by Blake (2000) and Green (2002). The taxonomic relation-

ship for these two genera, however, has never been precisely defined since the erection of *Pseudomastus* as a new monospecific genus.

This study provides a detailed description of a new species of *Leiochrides* from southern Korea and reveals its morphological distinctiveness through comprehensive comparisons with closely related species. Additionally, the taxonomic status of the genus *Pseudomastus* is discussed.

## Materials and methods

Sediment samples were obtained from the sublittoral muddy-sand bottom of the southern coast of Korea with a 0.05 $m^2$ Van Veen grab followed by elutriation on a 0.35 mm sieve in a 30 L seawater container. The remaining organisms on the sieve were transferred to a 1 L collecting jar with a 7% $MgCl_2$ solution for anesthesia. The relaxed samples were initially fixed in a 10% formalin solution for an hour before they were preserved in 90% ethanol for subsequent analysis. For the identification of the morphological features, the samples were stained with Shirlastain A (SDLATLAS, Inc.) for three seconds and sorted under a zoom stereomicroscope (Nikon SMZ745T). Line drawings were conducted using a differential interference contrast microscope (Eclipse Ci-L, Nikon) and a digital pen display (Cintiq 22HD, Wacom). The MGSP of the examined specimens were described and photographed as described in Jeong et al. (2017). A Scanning Electron Microscopy (SEM) analysis was carried out to confirm the detailed morphological structure. The specimens were placed in an ultrasonic chamber with distilled water for 30–60 seconds to remove the hoods of the hooded hooks. The treated specimens were dehydrated through a series of increasing concentrations of ethanol ending with two changes of absolute ethanol, followed by critical point drying. The dehydrated specimens were coated with gold and then photographed using the Hitachi S-3000N.

The type materials were deposited in the collections of the Marine Biodiversity Institute of Korea (MABIK) in Seocheon, Korea.

## Systematics

### Family Capitellidae Grube, 1862

### Genus *Leiochrides* Augener, 1914

*Pseudomastus* Capaccioni-Azzati & Martin, 1992: 247–249, figs 1a–h, 2a–f. **Syn. n.**

**Type species.** *Leiochrides australis* Augener, 1914

**Type locality.** Western Australia

**Generic diagnosis** (modified after Green 2002). Thorax with 13 segments including an achaetous peristomium and 12 chaetigers with capillary chaetae. Chaetiger 11 and 12 may have capillary chaetae in both rami or may be transitional with capillary chaetae in notopodia and hooded hooks in neuropodia. Remaining chaetigers with hooded hooks. Parapodia reduced. Retractile branchiae may be present.

***Leiochrides yokjidoensis* sp. n.**
http://zoobank.org/996ABB3E-3E71-452F-9A3E-BEE6F3015A9D
Figs 2A–F, 3A–H

**Material examined.** Holotype (complete specimen): MABIKNA00145754, sex uncertain, Yokjido, 34°31.1'N, 128°21.6'E (DDM), subtidal, sandy mud bottom, 53 m depth, April 2016, collector: Man-Ki Jeong. Paratypes (3 incomplete specimens): MABIKNA00145755–NA00145757, same information as holotype.

**Diagnosis.** Thorax with achaetigerous peristomium and 12 chaetigers. First chaetiger without neuropodia. Chaetigers 1–11 with capillary chaetae only, chaetiger 12 with notopodial capillaries and neuropodial hooks. Abdominal chaetigers with hooded hooks only. Branchiae present on posterior abdominal segments as 2–4 digitate filaments near notopodia. Approximately ten preanal chaetigers without branchiae. Pygidium with four anal cirri.

**Description.** One complete specimen and eight incomplete specimens. Largest specimen 27 mm long, 0.34 mm wide for 159 chaetigers. Smallest specimens 7 mm long, 0.25 mm wide for 34 chaetigers. Body thread-like, cylindrical, widest in anterior thoracic chaetigers, tapering from abdomen to pygidium. Color in alcohol yellowish or reddish brown.

*Prostomium* short, conical, wider than long, with blunt anterior end; presence of nuchal organs indistinct, eyespots not observed in preserved specimen (Figs 2A–C, 3A). Everted proboscis with numerous short, rounded, papillae, without cilia on tip of papillae (Figs 2C, 3A). Peristomium achaetigerous, wider than long, weakly biannulated and tessellated, subequal or slightly longer than first chaetiger (Figs 2A–C, 3A).

*Thorax* with 13 segments including single peristomium and 12 chaetigers (Fig. 2A–B). Thoracic segments biannulate, wider than long, with shallow intra- and inter-segmental grooves (Figs 2A–B, 3A). Anterior thoracic segments 1–5 slightly expanded and tessellated. First chaetiger uniramous with only notochaetae, both parapodia of chaetigers 1–11 and notopodia of chaetiger 12 each with 8–12 capillaries per fascicle; neuropodia of chaetiger 12 with 8 hooded hooks per fascicle (Fig. 2A). All capillary chaetae unilimbate, with narrow wing, whip-like, broad basally, and narrow apically; dorsal notochaetae without spinules on distal region of chaeta (Fig. 3B). Notopodia dorso-lateral and neuropodia ventro-lateral (Fig. 2A–B). Lateral organs distinct, oval shape, not protruding; present between notopodia and neuropodia, nearer to notopodia (Figs 1A, 2B, D). Genital pores not observed.

*Transition* between thoracic and abdominal region distinguished by change in position and type of chaetae and length of segments; abdominal segments longer and

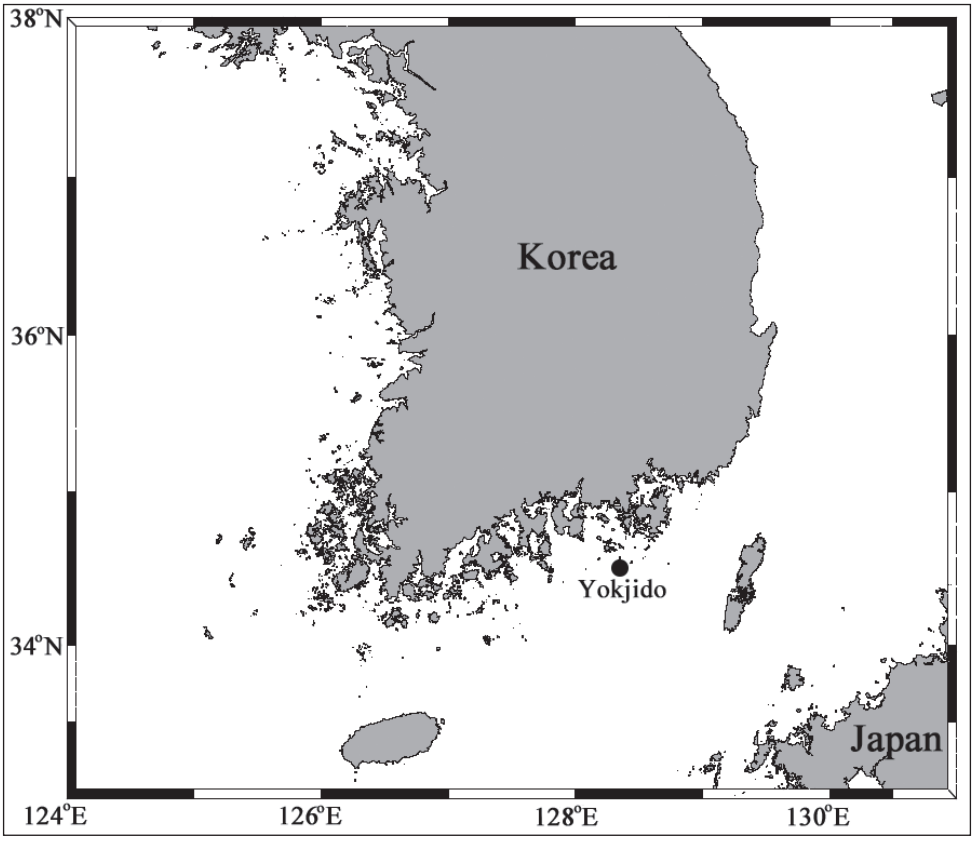


**Figure 1.** Map of study area with main collection stations indicated.

slightly narrower than thoracic segments, gradually smaller posteriorly; notopodial hooded hooks first present on chaetiger 13 (first abdominal chaetiger) (Fig. 2A–B). Abdominal chaetigers with hooded hooks on posterior end of segment; thoracic chaetigers with capillary chaetae or neuropodial hooks in center of segment (Fig. 2A–B).

*Abdominal parapodial lobes* slightly developed, located in posterior half of segment, well separated from each other; parapodial lobe gradually reduced posteriorly (Fig. 2A–B, D). Abdominal notopodia with 5–6 hooded hooks per fascicle; neuropodia with 8–10 hooded hooks per fascicle, 2–3 hooks on terminal segments (Fig. 2A–B).

*Hooded hooks* short, with main fang extending slightly beyond hoods; hood flared; shaft slightly enlarged like manubrium (Figs 2F, 3E). Hooks with three rows of small teeth above main fang; two in basal row, three in middle row, and 3–5 in superior rows (Figs 2E, 3F).

*Branchiae* digitiform, cylindrical, retractile; abdominal chaetiger 120–150 each with 3–5 branchiae per fascicle emerging from notopodia which lack hooks in this region; eight preanal 8 segments without branchiae (Figs 2D, 3H). Pygidium an oval ring, with four digitate caudal cirri (Figs 2D, 3H).

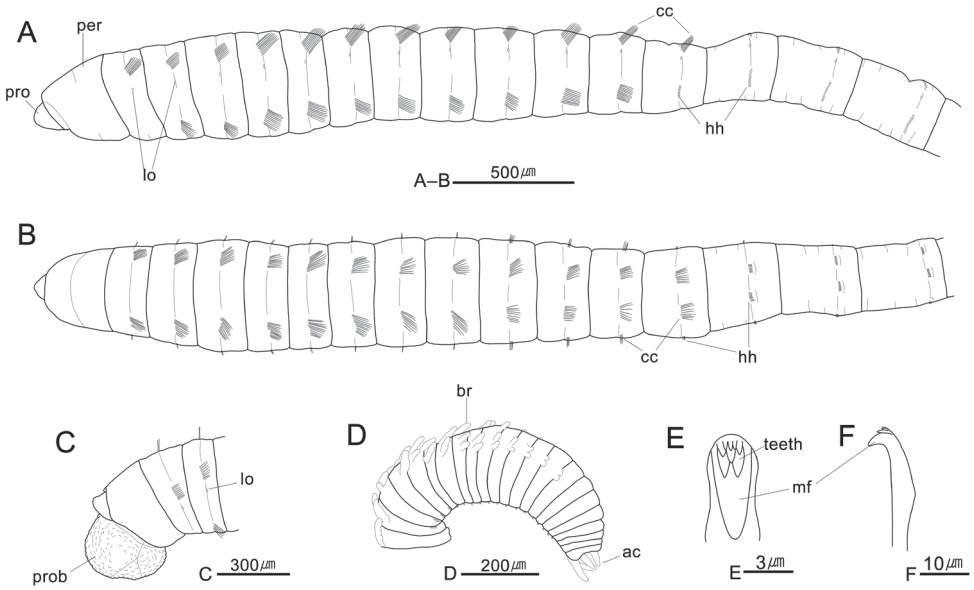


**Figure 2.** *Leiochrides yokjidoensis* sp. n. **A** anterior end, left lateral view **B** same, dorsal view **C** anterior end with proboscis (MABIKNA00145754), left lateral view **D** posterior end (MABIKNA00145754), left lateral view **E–F** hooded hooks from anterior abdominal notopodium. Abbreviations: ac, anal cirri; br, branchia; cc, capillary chaeta; hh, hooded hook; lo, lateral organ; mf, main fang; per, peristomium; pro, prostomium; prob, proboscis.

**Methyl green staining pattern.** Prostomium not stained. Peristomium and thoracic chaetigers 1–5 slightly stained in blue but rapidly fades. Chaetigers 6–9 stained blue, with narrow transverse blue speckled band near intra-segmental furrow (Fig. 3G). Post-chaetal region of chaetiger 10 and pre-chaetal region of chaetiger 11 with intense blue speckles on epidermis (Fig. 3G). Abdominal segments without distinct staining pattern.

**Etymology.** The new species is named for its occurrence in Yokjido, Korea.

**Distribution.** *Leiochrides yokjidoensis* sp. n. is distributed in the subtidal habitat (53 m) of the southern part of Korea.

**Ecology.** The surface sediment is mainly composed of sandy mud with fragmented shells. *Mediomastus* Hartman, 1944 and *Notomastus* M. Sars, 1851, also belonging to the Capitellidae, also occurred at the same location.

**Remarks.** *Leiochrides yokjidoensis* sp. n. is distinct in the morphological combination of 12 thoracic chaetigers, chaetigers 1–11 with only capillary chaetae, and the last thoracic chaetiger with the notopodial capillaries and neuropodial hooks. Among the genera of Capitellidae the presence of 12 thoracic chaetigers and neurohooks in last thoracic chaetiger are shared with *Leiochrides*, *Pseudomastus*, and *Scyphoproctus* Gravier, 1904. However, *Scyphoproctus* is clearly separated from the new species by the presence of the unique anal plaque, acicular spines in the posterior abdomen, and two achaetous segments in the anterior part of the thorax. In this study, the new species

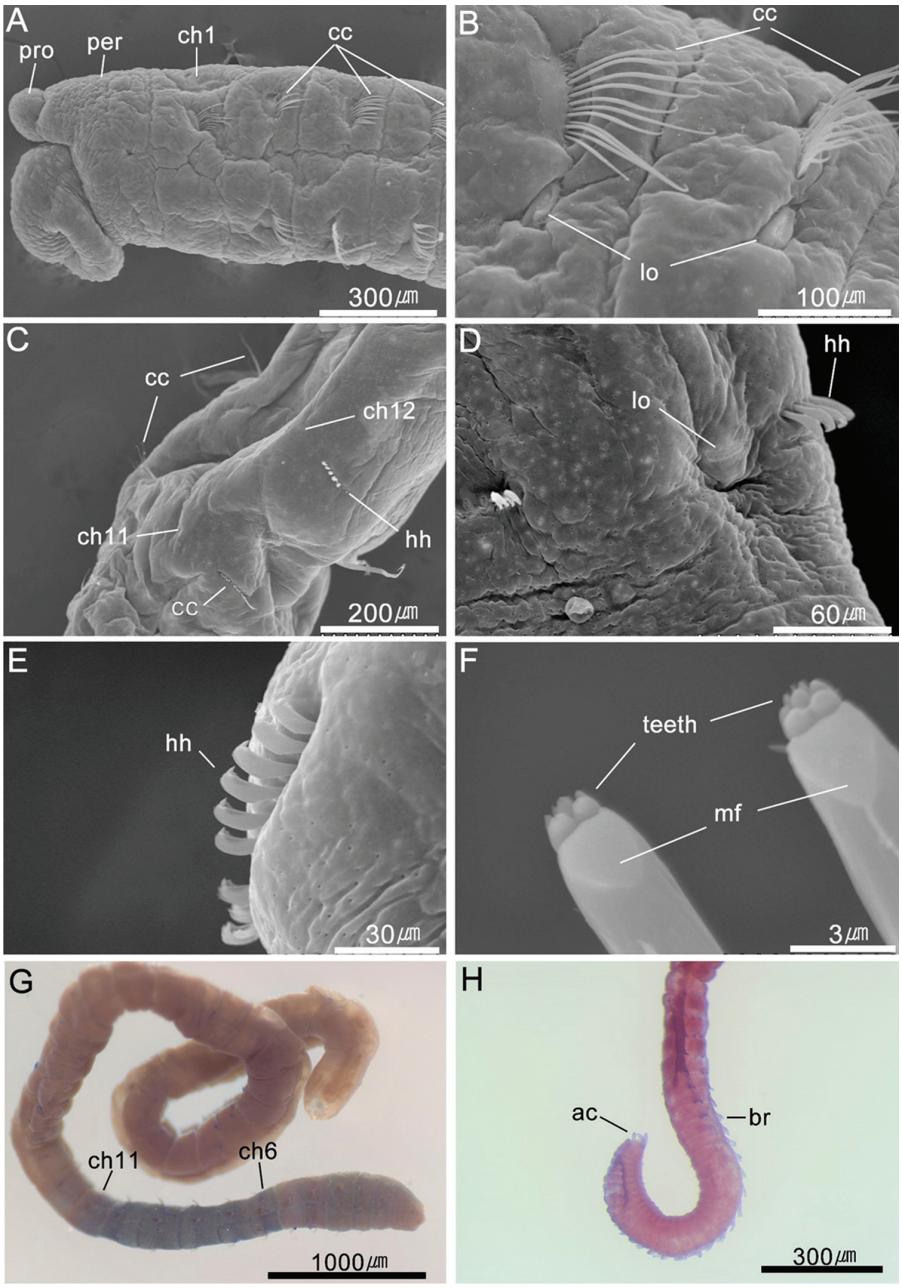


**Figure 3.** *Leiochrides yokjidoensis* sp. n. **A–F** scanning electron micrographs **A** anterior end in left lateral view **B** chaetigers 4–5 in left dorsolateral view **C** chaetigers 11–12 in left lateroventral view **D** chaetiger 15 in left lateral view **E** notopodial hooded hooks of chaetiger 16 **F** neuropodial hooded hooks of chaetiger 16 in frontal view **G–H** photomicrographs **G** thorax and anterior abdomen, right lateral view showing methyl green staining reaction **H** posterior end of body in left lateral view (MABIKNA00145754). Abbreviations: ac, anal cirri; br, branchia; cc, capillary chaeta; ch, chaetiger; hh, hooded hook; lo, lateral organ; mf, main fang; per, peristomium; pro, prostomium

was placed under the genus *Leiochrides*, because the generic diagnosis of *Pseudomastus* mostly agreed with that of *Leiochrides* (see details in discussion section). *Leiochrides yokjidoensis* sp. n. closely resembles *L. hemipodus* and *P. deltaicus* in the presence of the neurohooks in the thorax, the uniramous first chaetiger, the two distinct basal teeth above the main fang, and the presence of the branchiae in the posterior abdomen (Table 1). In particular, *L. yokjidoensis* sp. n. and *P. deltaicus* correspond in the presence of multiple cirri on the pygidium (Table 1). However, the new species is discriminated from *P. deltaicus* by the following morphological characteristics: the absence of eyespots in the preserved materials, dorsal notochaetae without distal spinules, a proboscis without cilia on the tip of the papillae, the number of capillary chaetae (8–12 vs. 13–20) and neurohooks (8–10 vs. 11–12) per fascicle, the number of teeth above the main fang (8–10 vs. 7), the absence of neuropodial hooks in chaetiger 11, and the number of anal cirri (4 vs. 3). On the other hand, the holotype of *L. hemipodus* has identical chaetal arrangement to *L. yokjidoensis* sp. n., but it differs in the number of teeth above the main fang (3 vs. 8–10), the maximum number of branchiae per fascicle (12 vs. 5), and the species-specific MGSP (chaetigers 1–12 vs. 6–11, Table 1). In addition, *L. hemipodus* has been reported only in deep basin near California, but *L. yokjidoensis* sp. n. was found in shallow waters of southern Korea (Table 1). The paratype of *L. hemipodus* has a different chaetal arrangement (chaetigers 11–12 with neuropodial hooks) to the holotype of *L. hemipodus*, however these type specimens were almost identical in the remaining characteristics (Blake 2000, Green 2002, Table 1). Generally, capitellids have developmental variation in the chaetal arrangement on the thorax, and the hooded hooks are replaced by capillaries with development (Fredette 1982, Blake 2009). Thus, the differences in chaetal arrangement between the type specimens of *L. hemipodus* may be associated with the developmental variation within a species. Blake (2000) had reported *L. hemipodus* from Santa Maria basin (603 m) and compared his specimens with the characteristics of the paratype of *L. hemipodus* Hartman, 1960. According to his description, *L. hemipodus* also differs from *L. yokjidoensis* sp. n. in the presence of a band of glands on chaetiger 6 and the shape of the branchiae (Table 1).

## Discussion

Capaccioni-Azzati and Martin (1992) established the genus *Pseudomastus* to accommodate the only species, *P. deltaicus* characterized by 12 thoracic chaetigers, the first chaetiger with only notochaetae, chaetigers 1–10 with capillaries, the last two thoracic chaetigers with notopodial capillaries and neuropodial hooks, the posterior end of each notopodium with 2–4 digitate branchiae on chaetigers 205–210 to chaetigers 255–260, and the pygidium with three anal cirri. At this point, the genus *Leiochrides* was earlier assigned with morphological characteristics that coincided with *Pseudomastus*. However, Capaccioni-Azzati and Martin (1992) did not detect the close relationship in morphology between *Leiochrides* and their new genus, *Pseudomastus*. Hartman (1963, 1974) had proposed the presence of transitional chaetigers, with capillary notochaetae

**Table 1.** Morphological comparison between *L. yokjidoensis* sp. n. and most related species. A: absent; P: present; C: capillary chaeta; H: hooded hook; L: length; W: width; Ch: chaetiger; incomp: incomplete specimen; no: notopodia; neu: neuropodia; NM: not mentioned.

| Species | Overall size (L/W, mm) | Eyes | Thoracic chaetal arrangement | No. of chaetae per fascicle | | Dental structure of hooks | Special character | No. of branchiae per fascicle | No. of anal cirri | Methyl green staining pattern | Locality | References |
|---|---|---|---|---|---|---|---|---|---|---|---|---|
| | | | | Thorax | Abdomen | | | | | | | |
| *L. hemipodus* (Holotype) | 30–40/1–2 (incomp.) | A | no: 12C neu: 11C+1H | NM | NM | 2 rows (2/1) | | 3–12 (sometimes bifurcated) | NM | Ch 1–12 | San Pedro basin, California (887m) | Hartman (1960); Green (2002) |
| *L. hemipodus* (Paratype & its related sp.) | ?/1 | A | no: 12C neu: 10C+2H | NM | NM | 2 rows (2/1) | Glands on chaetiger 6 | ca. ~15 (in fig. 4.9; branched) | 0 | Ch 1–12 | Santa Maria basin, California (603m) | Blake (2000) |
| *L. yokjidoensis* sp. n. | 27/0.34 | A | no: 12C neu: 11C+1H | 8–12(C) 8(H) | no: 5–6(H) neu: 8–10(H) | 3 rows (2/3/3–5) | | 3–5 (palmate) | 4 | Ch 6–11 | Korea (~43m) | This study |
| *P. deltaicus* | 50/0.7 | P | no: 12C neu: 10C+2H | 13–20(C) 12(H) | 11–12(H) | 3 rows (2/1/4) | Distal spinules on notopodial capillaries | 2–4 | 3 | NM | Spain (~6m) | Capaccioni-Azzati and Martin (1992) |

and neurohooks, as an important characteristic of *Leiochrides* but it was not accepted as a generic diagnosis by Fauchald (1977). Blake (2000) later added this characteristic to the generic definition, which was redefined as 12 chaetigers with capillary chaetae but sometimes one or two of the chaetigers having notopodial capillaries and neurohooks. According to this expanded generic definition, the characteristics of *Pseudomastus* also matched those of *Leiochrides*. In addition, the uniramous first chaetiger, the multiple branchiae in the posterior part of abdomen, the two distinct basal teeth above the main fang of the hooks, and the presence of multiple anal cirri are also identical features that are found in some members of *Leiochrides*. Although *P. deltaicus* is unique in having spinules on the distal edge of the dorsal capillary notochaetae and cilia on the papillae of the proboscis, these seem to be species level characteristics within the Capitellidae. Thus, we regard the monospecific *Pseudomastus* as a junior synonym of *Leiochrides*.

This study provides the detailed morphological features of *L. yokjidoensis* sp. n. including the presence/absence of the lateral organ and genital pore, the number of chaetae per fascicle, MGSP, and the number of anal cirri. Green (2002) used variations in the thoracic chaetal distribution and the details of the hooded hooks among six of the described *Leiochrides* species in an identification key to species. Nevertheless, the use of additional taxonomic information on the distribution of the lateral organs, nephridia or genital pores, MGSP, and characteristics of the pygidium are still insufficient to distinguish many of the previously described *Leiochrides* species, including *L. hemipodus*. Therefore, a precise examination of the morphological details and a re-examination of existing *Leiochrides* species is needed in the future and may prove useful in a clarification of the taxonomic relationship between *Leiochrides* species.

**Key to species of genus *Leiochrides* (modified from Green 2002)**

| | | |
|---|---|---|
| 1 | First chaetiger biramous; chaetigers 1–12 with capillary chaetae only | **2** |
| – | First chaetiger uniramous | **4** |
| 2 | Prostomium deeply bifid; hooded hooks with small teeth above main fang in 3 rows | ***L. biceps*** |
| – | Prostomium without dorsal furrow; hooded hooks with small teeth above main fang in 2 rows | **3** |
| 3 | Hooded hooks with 4–6 teeth above main fang | ***L. africanus*** |
| – | Hooded hooks with 8–10 teeth above main fang | ***L. pallidior*** |
| 4 | Chaetigers 1–12 with capillary chaetae | **5** |
| – | One or more transitional chaetigers with capillary notochaetae and neurohooks | 7 |
| 5 | First two abdominal segments with notopodial capillaries; pygidium with 4 anal cirri; branchiae present | ***L. norvegicus*** |
| – | Abdominal segments without capillary chaetae | **6** |
| 6 | Hooded hooks with 5 teeth above main fang in 3 rows | ***L. andamanus*** |
| – | Hooded hooks with 10–11 teeth above main fang in 3 rows | ***L. australis*** |

7 Chaetiger 12 transitional with capillary notochaetae and neurohooks ..... **8**
– Chaetigers 11–12 transitional with capillary notochaetae and neurohooks .... **9**
8 Hooded hooks with 8–10 teeth above main fang in 3 rows; posterior abdomen with 3–5 branchiae per fascicle; pygidium with 4 anal cirri ..... ***L. yokjidoensis* sp. n.**
– Hooded hooks with 3 teeth above main fang in 2 rows; posterior abdomen with 3–12 branchiae per fascicle; pygidium without anal cirri... ***L. hemipodus***
9 Hooded hooks with 3 teeth above main fang in 2 rows..... ***L. branchiatus***
– Hooded hooks with 7 teeth above main fang in 3 rows; posterior abdomen with 2–4 branchiae per fascicle; pygidium with 3 anal cirri..... ***P. deltaicus***

## Acknowledgements

We would like to thank the editor and anonymous reviewers who made constructive and invaluable suggestions. This study was a part of the project titled 'Long-term change of structure and function in marine ecosystems of Korea', funded by the Ministry of Oceans and Fisheries, Korea. This work was supported by National Marine Biodiversity Institute Research Program (2017M01100).

## References

Augener H (1914) Polychaeta. II. Sedentaria. In: Michaelsen W, Hartmeyer R (Eds) Die fauna Südwest-Australiens. Ergebnisse der Hamburger südwest-australischen Forschungsreise. Gustav Fischer, Jena, 170 pp.

Augener H (1918) Polychaeta. Beitrage zur Kenntnis der Meeresfauna Westafrikas. L. Friederichsen & Co., Hamburg, 625 pp. http://www.biodiversitylibrary.org/page/7172671#pa-ge/79/mode/1up

Blake JA (2009) Redescription of *Capitella capitata* (Fabricius) from West Greenland and designation of a neotype (Polychaeta, Capitellidae). Zoosymposia 2: 55–80. http://www.mapress.com/zoosymposia/content/2009/v2/f/v002p055-080.pdf

Blake JA (2000) Chapter 4. Family Capitellidae Grube, 1862. In: Blake JA, Hilbig B, Scott PV (Eds) Taxonomic Atlas of the Santa Maria Basin and Western Santa Barbara Channel. Annelida Part 4. Polychaeta: Flabelligeridae to Sternaspidae. Santa Barbara Museum of Natural History, California, 47–96.

Capaccioni-Azzati R, Martín D (1992) *Pseudomastus deltaicus* gen. et sp. n. (Polychaeta: Capitellidae) from a shallow water bay in the north-western Mediterranean Sea. Zoologica Scripta 21: 247–250. doi: 10.1111/j.1463-6409.1992.tb00328.x

Chamberlin RV (1918) Polychaetes from Monterey Bay. Proceedings of the Biological Society of Washington 31: 173–180. http://www.biodiversitylibrary.org/part/39134#/summary

Day JH (1967) A Monograph on the Polychaeta of Southern Africa. Part 2. Sedentaria. Trustees of the British Museum (Natural History), London, 878 pp. http://www.biodiversitylibrary.org-/part/92954#/summary

Dean HK (2001) Capitellidae (Annelida: Polychaeta) from the Pacific coast of Costa Rica. Revista de Biologia Tropical 49: 69–84. https://doi.org/10.15517/rbt.v49i2.26293

Ewing RM (1991) Review of monospecific genera of the family Capitellidae (Polychaeta) (abstract). In: Petersen ME, Kirkegaard JB (Eds) Systematics, Biology, and Morphology of World Polychaeta. Proceedings of the 2nd International Polychaete Conference (Copenhagen), August 1986. Ophelia Supplement, Denmark, 692–693. http://www.annelida.net/ipcpub.html

Fauchald K (1977) The Polychaete Worms: Definitions and Keys to the Orders, Families and Genera. Natural History Museum of Los Angeles County, Los Angeles, 188 pp. https://repository.si.edu/bitstream/handle/10088/3435/PinkBookplain.pdf?sequence=1&isAllowed=y

Fauchald K (1972) Some polychaetous annelids from the deep basins in Sognefjorden, western Norway. Sarsia 49: 89–106. https://doi.org/10.1080/00364827.1972.10411211

Fredette T (1982) Evidence of ontogenetic setal changes in *Heteromastus filiformis* (Polychaeta: Capitellidae). Proceedings of the Biological Society of Washington 95: 194–197. http://www.biodiversitylibrary.org/part/48248#/summary

García-Garza ME, De León-González JA (2011) Review of the Capitellidae (Annelida, Polychaeta) from the eastern tropical Pacific region, with notes on selected species. Zookeys 151: 17–52. https://doi.org/10.3897/zookeys.151.1964

Gravier C (1904) Sur un type nouveau de la famille des Capitelliens: *Scyphoproctus* nov. gen. *djiboutiensis* nov. sp. Bulletin Museum History Natural 10: 557–561. http://www.biodiversitylibrary.org/item/27180#page/584/mode/1up

Green K (2002) Capitellidae (Polychaeta) from the Andaman Sea. Phuket Marine Biological Center Special Publication 24: 249–343.

Grube AE (1862) Noch ein Wort über die Capitellen und ihre Stelle im Systeme der Anneliden. Archiv für Naturgeschichte, Berlin, 378 pp. http://www.biodiversitylibrary.org/item/31514#-page/374/mode/1up

Hartman O (1944) Polychaetous annelids from California, including the descriptions of two new genera and nine new species. Allan Hancock Pacific Expeditions 10: 239–307. http://digitallibrary.usc.edu/cdm/ref/collection/p15799coll82/id/12856

Hartman O (1954) Marine annelids from the northern Marshall Islands. Bikini and nearby atolls, Marshall Islands. Geological Survey Professional Paper 260-Q, 619–644. http://pubs.usgs.gov/pp/0260q/report.pdf

Hartman O (1960) Systematic account of some marine invertebrate animals from the deep basins off southern California. Allan Hancock Pacific Expeditions 22: 69–216. http://www.biodiversitylibrary.org/part/92921#/summary

Hartman O (1963) Submarine Canyons of Southern California. Part III. Systematics Polychaetes. Allan Hancock Pacific Expeditions. University of Southern California Press, Los Angeles, 93 pp. http://www.biodiversitylibrary.org/part/4016#/summary

Hartman O (1974) Polychaetous annelids of the Indian Ocean including an account of species collected by members of the International Indian Ocean Expeditions, 1963–64 and a catalogue and bibliography of the species from India. Journal of Marine Biological Association of India 16: 609–644. http://mbai.org.in/php/journal.php?bookid=49&type=0

Hartman O (1976 [issue for 1974]) Polychaetous annelids of the Indian Ocean including an account of species collected by members of the International Indian Ocean Expeditions, 1963–64 and a catalogue and bibliography of the species from India. Journal of Marine Biological Association of India 16: 191–252. http://mbai.org.in/php/journal.php?bookid=49&type=0

Hutchings P (1998) Biodiversity and functioning of polychaetes in benthic sediments. Biodiversity and Conservation 7: 1133–1145. https://doi.org/10.1023/A:1008871430178

Jeong MK, Wi JH, Suh HL (2017) A reassessment of *Capitella* species (Polychaeta: Capitellidae) from Korean coastal waters, with morphological and molecular evidence. Marine Biodiversity vol 20(53): 1–10. https://doi.org/10.1007/s12526-017-0707-2

Read G (2017) Capitellidae. Accessed through: World Register of Marine Species. http://www.marinespecies.org/aphia.php?p=taxdetails&id=921 [Accessed 28 February 2017]

Sars M (1851) Beretning om en i Sommeren 1849 foretagen zoologisk Reise i Lofoten og Finmarken. Nyt Magazin for Naturvidenskaberne 6: 121–211. http://www.biodiversitylibr-ary.org/item/33948#page/129/mode/1up

ZooKeys 685: 105–130 (2017)
doi: 10.3897/zookeys.685.13811
http://zookeys.pensoft.net

RESEARCH ARTICLE

A peer-reviewed open-access journal
ZooKeys
Launched to accelerate biodiversity research

# A revision of *Prespelea* Park (Staphylinidae, Pselaphinae)

Michael S. Caterino[1], Laura M. Vásquez-Vélez[1]

1 *Department of Plant & Environmental Sciences, Clemson University, Clemson, SC 29634 USA*

Corresponding author: *Michael S. Caterino* (mcateri@clemson.edu)

Academic editor: *J. Klimaszewski* | Received 24 May 2017 | Accepted 27 June 2017 | Published 20 July 2017

*http://zoobank.org/4B9905F6-C44E-40AB-9C6B-6E7B49CA3D69*

**Citation:** Caterino MS, Vásquez-Vélez LM (2017) A revision of *Prespelea* Park (Staphylinidae: Pselaphinae). ZooKeys 685: 105–130. https://doi.org/10.3897/zookeys.685.13811

## Abstract

We revise the genus *Prespelea* Park, redefining and redescribing the two previously known species, *P. copelandi* Park and *P. quirsfeldi* Park, and adding ten new species: *P. parki* Caterino & Vásquez-Vélez, **sp. n.**, *P. minima* Caterino & Vásquez-Vélez, **sp. n.**, *P. morsei* Caterino & Vásquez-Vélez, **sp. n.**, *P. divergens* Caterino & Vásquez-Vélez, **sp. n.**, *P. carltoni* Caterino & Vásquez-Vélez, **sp. n.**, *P. myersae* Caterino & Vásquez-Vélez, **sp. n.**, *P. georgiensis* Caterino & Vásquez-Vélez, **sp. n.**, *P. enigma* Caterino & Vásquez-Vélez, **sp. n.**, *P. wagneri* Caterino & Vásquez-Vélez, **sp. n.**, and *P. basalis* Caterino & Vásquez-Vélez, **sp. n.**. The genus is still only known from a relatively small area in the southern Appalachian Mountains, but the diversity is much greater than previously suspected. The new species exhibit considerable diversity in male secondary sexual characters. A preliminary phylogenetic analysis cannot conclusively resolve the polarity of eye and wing reduction across Speleobamini, but the monophyly of Park's subgenus *Fusjugama*, if expanded to include all species with full-eyed and winged males, is not supported, and we therefore synonymize it with *Prespelea s. str*.

## Keywords

Pselaphinae, Speleobamini, brachyptery, leaf litter

## Introduction

Orlando Park (1953) established the genus *Prespelea* for the new species *P. quirsfeldi*. *Prespelea* and the monotypic *Speleobama* Park (1951) were and remain the only genera within the tribe Speleobamini Park (1951), characterized by an unusual synapomorphy of a deeply dorsally constricted neck (Figure 1) that is largely obscured by dense,

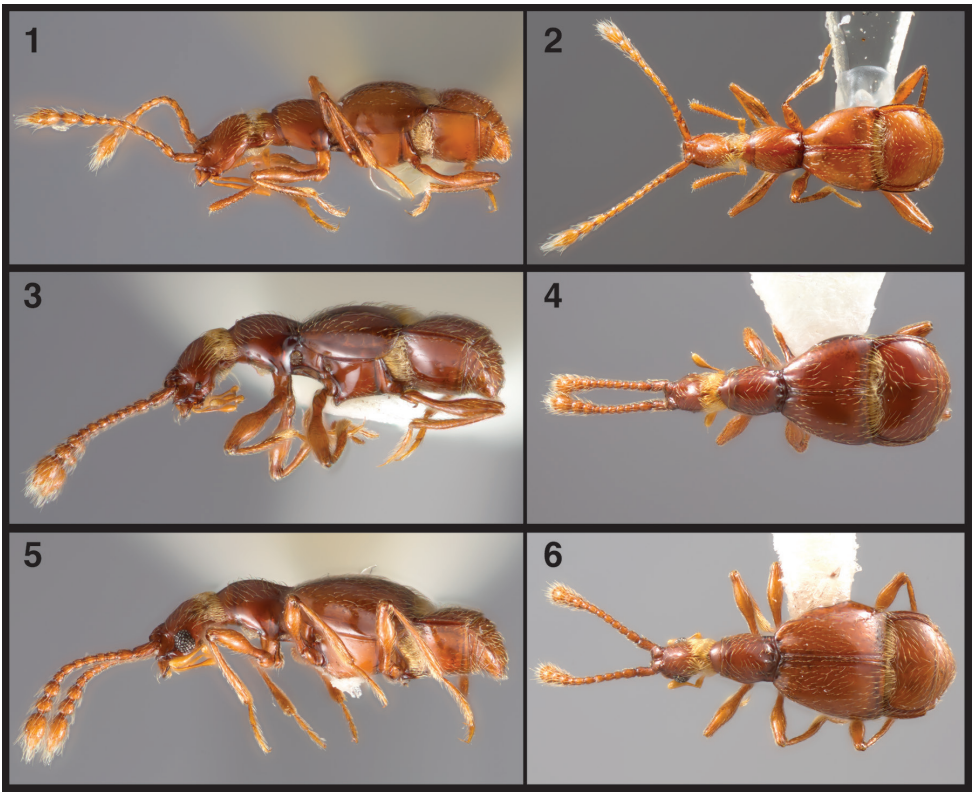


**Figures 1–6.** Dorsal and lateral habitus of Speleobamini. **1–2** *Speleobama vana* **3–4** *Prespelea morsei* **5–6** *Prespelea enigma*.

opposing fringes of setae. *Speleobama vana* Park, lacking eyes and wings, and having generally elongated body and appendages is an obligate troglobite, known only to occur in McClunney (or McCluney according to some sources) Cave in northern Alabama. *Prespelea*, as the name implies, appeared initially (Park 1953) to represent a less specialized but very similar form, retaining eyes (strongly reduced in *P. quirsfeldi*) but lacking wings, and not exhibiting particularly elongated appendages. When Park (1956) described the second known species, *P. copelandi*, however, the diagnosis of *Prespelea* had to be adjusted considerably, as this species has fully developed eyes and wings (in the male only, as we report here).

To the present day, the tribe Speleobamini has contained only three species, representing an apparent grade from minimally to highly troglophilic. However, no additional work has been done on the group, and the true extent of morphological variability and phylogenetic relationships remain obscure. Through our work and that of others, it has become apparent that this group contains considerably more diversity, which could help illuminate the path into troglophily in this lineage. Here we describe ten additional species, discuss the morphology of the females, and provide a preliminary assessment of phylogenetic relationships in the group.

## Materials and methods

Specimens came from our own collections, and through loans from several institutions:

| | |
|---|---|
| **CUAC** | Clemson University Arthropod Collection, Clemson, SC |
| **CNCI** | The Canadian National Collection of Insects, Ottawa, ON |
| **FMNH** | The Field Museum, Chicaco, IL |
| **LSAM** | Louisiana State Arthropod Museum, Baton Rouge, LA |
| **UNHC** | University of New Hampshire Arthropod Collection, Durham, NH |

Morphology was examined using Leica stereomicroscopes, with temporary and permanent slides of selected structures examined using compound microscopes. Males of all morphospecies were dissected in conjunction with attempted DNA extractions (using tissue digestion buffers and proteinase K). For dry mounted specimens the point bearing the specimen was submerged in 100% ethanol for several hours to soften the glue and partially relax the specimen. The specimen was removed from the point and the abdomen was removed by inserting a pin between the metacoxa and 1st visible ventrite. The aedeagus was extracted through the abdominal apex following tissue digestion. Photographs were taken using Visionary Digital's Passport II imaging system (based on a Canon 6D SLR with 65mm MP-E 1-5× macro lens). Drawings were penciled by hand, traced on a drawing pad, and 'inked' in Adobe Illustrator.

Measurements (see Table 1) were taken using a Leica M125 calibrated eyepiece micrometer. Two males and two females of each species were measured, where available. Head length (HL) was measured from the clypeal margin to the upper anterior edge of the neck constriction (ignoring the neck); pronotal length (PnL) was measured along the midline; pronotal width (PnW) was the maximum width, near the midline; elytral length (EL) was measured along the suture from the base of the scutellum to the apex of

**Table 1.** Average measurements (in mm) of important body dimensions. N shows numbers of specimens measured for each species.

| | N | HL | PnL | PnW | EL | EW | T3L | AL | TL |
|---|---|---|---|---|---|---|---|---|---|
| ***P. quirsfeldi*** | 4 | 0.37 | 0.37 | 0.31 | 0.51 | 0.67 | 0.47 | 0.62 | 1.87 |
| ***P. parki*** | 4 | 0.38 | 0.36 | 0.31 | 0.48 | 0.68 | 0.45 | 0.65 | 1.86 |
| ***P. minima*** | 2 | 0.34 | 0.34 | 0.31 | 0.49 | 0.68 | 0.46 | 0.65 | 1.82 |
| ***P. morsei*** | 4 | 0.38 | 0.35 | 0.32 | 0.46 | 0.67 | 0.46 | 0.69 | 1.88 |
| ***P. divergens*** | 3 | 0.38 | 0.35 | 0.31 | 0.48 | 0.69 | 0.46 | 0.71 | 1.93 |
| ***P. carltoni*** | 3 | 0.34 | 0.33 | 0.29 | 0.47 | 0.63 | 0.43 | 0.70 | 1.84 |
| ***P. myersae*** | 4 | 0.36 | 0.34 | 0.30 | 0.44 | 0.61 | 0.42 | 0.58 | 1.73 |
| ***P. georgiensis*** | 4 | 0.35 | 0.33 | 0.30 | 0.46 | 0.62 | 0.41 | 0.60 | 1.74 |
| ***P. copelandi*** | 3 | 0.34 | 0.33 | 0.29 | 0.59 | 0.67 | 0.27 | 0.50 | 1.75 |
| ***P. enigma*** | 4 | 0.37 | 0.33 | 0.31 | 0.53 | 0.65 | 0.39 | 0.60 | 1.83 |
| ***P. wagneri*** | 4 | 0.36 | 0.35 | 0.31 | 0.54 | 0.65 | 0.41 | 0.55 | 1.80 |
| ***P. basalis*** | 1 | 0.39 | 0.31 | 0.29 | 0.59 | 0.67 | 0.28 | 0.51 | 1.80 |

the suture; elytral width (EW) was the maximum width, invariably near the apices; the 1st visible abdominal tergite length (T3L) was measured along the dorsal midline; total abdomen length (AL) was measured laterally in a straight line from the base of the 1st ventrite to the apex of the last tergite (ignoring telescopy and/or curvature); total length (TL) was calculated) as head length + pronotum length + elytral length + abdomen length.

All label data were extracted to an Excel spreadsheet, and coordinates were estimated for all localities. This table appears as an Suppl. material 1, while the species treatments provide only brief locality descriptions (aside from the types). Type localities were selected based on availability of DNA sequence data where possible, to reduce ambiguity for future species assignments. In general single-locality type series were preferred, even where male genitalia seemed consistent across localities. A number of unassociated females were recorded from unique localities. These localities are given in the Suppl. material 1.

In order to understand the origins of various characters, particularly the reduction of eyes, flight ability, and general tendency toward a troglobitic morphology, we conducted phylogenetic analyses utilizing both morphological and molecular characters. In addition to previously and newly described *Prespelea* species, we included *Speleobama vana* (for morphology only), and in order to polarize characters within the tribe, further outgroup representatives from the Valdini and Tychini. We scored all taxa for the following morphological characters:

1. Neck, dorsally: 1. Normal; 2. Deeply cleft and setose.
2. Neck, ventrally: 1. Flattened beneath, weakly to distinctly carinate laterally; 2. convex beneath.
3. Male eyes: 1. Well-developed; 2. Poorly developed; 3. Absent.
4. Male wings: 1. Fully developed; 2. Absent.
5. Male metaventrite: 1. Unmodified; 2. Produced.
6. Male metaventral process: 1. N/A; 2. Simple; 3. Apically emarginate to bifid.
7. Male metatrochanter: 1. Unmodified; 2. Hooked.
8. Male metatrochanteral process: 1. N/A; 2. Hook basal to medial; 3. Hook apical.
9. Antennae: 1. Most basal antennomeres no longer than broad; 2. Basal antennomeres slightly longer than broad; 3. Basal antennomeres distinctly longer than broad.
10. Antennomere 7: 1. Part of gradual sequence; 2. Larger than 6th or 8th.
11. Male 7th ventrite, apex: 1. Shallowly emarginate; 2. Deeply emarginate.
12. Aedeagus, dorsal plate: 1. Present; 2. Absent.
13. Aedeagus, shape: 1. Apically narrowed; 2. Hourglass-shaped.
14. Aedeagus apex, shape: 1. More or less parallel; 2. Expanded.
15. Aedeagus, apical margin: 1. Apical margin truncate; 2. Apical margin emarginate.
16. Aedeagus, apicodorsal ridges: 1. Ending short of margin; 2. Extending to margin.
17. Aedeagus, internal sac: 1. Spineless; 2. With spines.
18. Female pygidium: 1. Broad, apical margin wide; 2. Smaller, apical margin more distinctly tapered.

19. Female pygidium: 1. Apically spinose, often with median carina; 2. Not apically spinose or carinate.
20. Female 7th sternite: 1. With median transverse carina; 2. Without median carina.
21. Female 7th sternite: 1. Concave in apical half; 2. Convex in apical half.

To help assess variability, relationships, and species limits in the group, we also generated a DNA sequence data set for selected, suitably preserved specimens. We attempted to extract DNA from 22 exemplars representing all 12 species of *Prespelea*, using Thermo Scientific's GeneJet kit, and amplified 839 bp of the mitochondrial cytochrome oxidase I gene. Outgroup sequences were obtained from our own specimens, and from an unpublished data set in preparation by Dr. Joseph Parker. These included members of the tribe Amauropini (*Arianops*), Valdini (*Valda*), and Tychini (*Custotychus*, *Ouachitychus*, *Tychus*, *Lucifotychus*, and *Nearctitychus*). These were pruned from the base of (invariably monophyletic) Speleobamini for presentation purposes.

DNA sequences were analyzed alone and together with morphological character states using parsimony, and DNA alone was analyzed via maximum likelihood (using a GTR+I+G model with parameter estimates based on one of the most parsimonious trees) as implemented in PAUP* (Swofford, 2002). We experimented with different combinations of outgroups, which did not reveal any effects on ingroup topologies. The full data matrix in nexus format is available as a supplementary file.

## Results

### Phylogeny

We obtained 15 COI sequences representing 8 putatively distinct species. Successful extractions were almost exclusively specimens that had been recently collected directly into ethanol. A few specimens had been previously mounted, but had come directly from 100% ethanol within the past couple years. Sequences have been deposited in GenBank under accession numbers MF380441-MF380455.

Trees based on separate and combined data differ in some details, but agree on some broad, complicated outlines (see Figs 7–10). First, the species with big-eyed males (corresponding to subgenus *Fusjugama*; i.e. *P. copelandi*, *P. enigma*, *P. wagneri*, and *P. basalis*) do not form a clade in any tree. They are resolved as either a paraphyletic basal grade (morphology; Figs 7, 8) or as a polyphyletic group with various representatives more closely related to either to *P. myersae* (*P. enigma* and *P. wagneri*) or to *P. quirsfeldi* (*P. copelandi* itself). In the combined data (Fig. 10), most big-eyed species group with *P. myersae* (a small-eyed species) and relatives, but not all. This result would make considerable sense in light of the male genitalic morphology, since only some of the '*copelandi*'-like species have well-developed internal sac armature like *P. myersae* and *P. minima* do. The aedeagi of other '*copelandi*'-like species are little distinguishable from that of *P. quirsfeldi*. However, considering only the more conspicuous eye character states, the

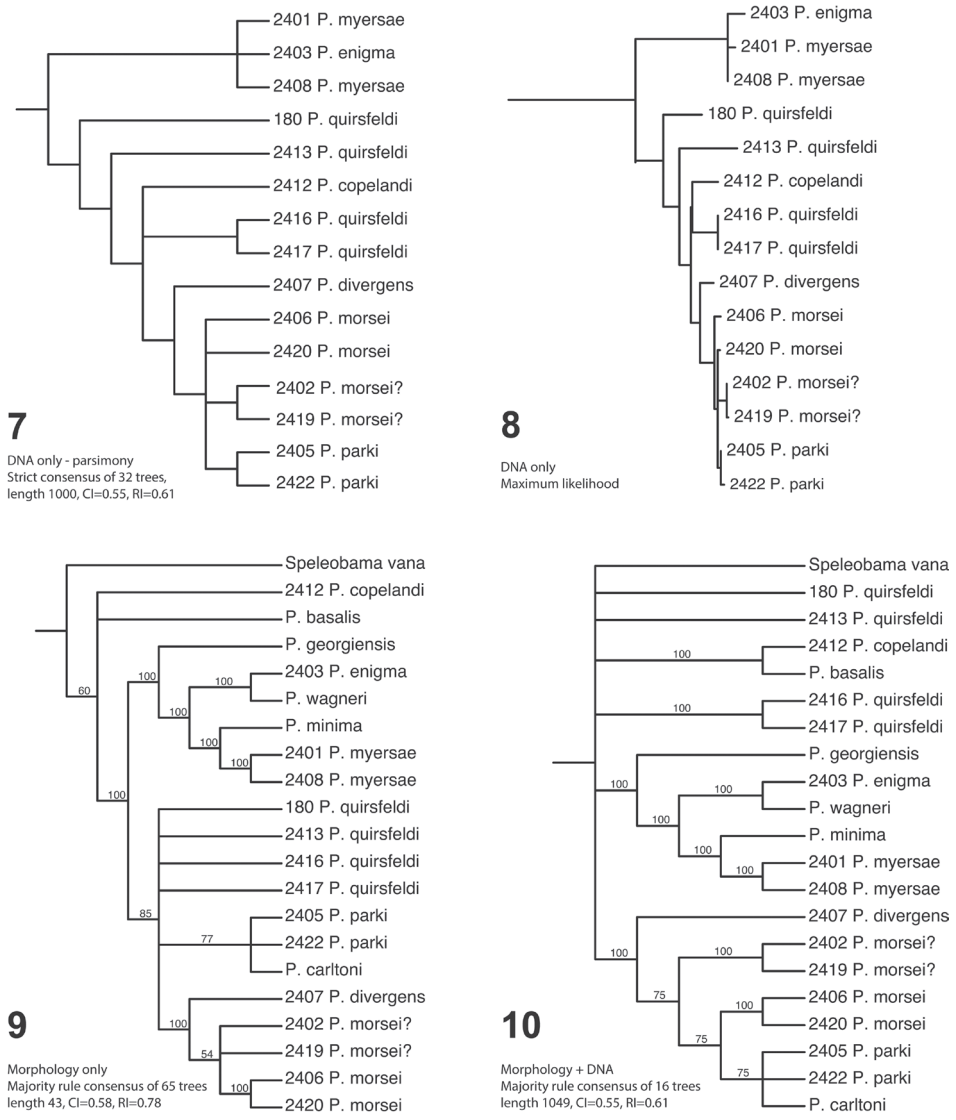


**Figures 7–10.** Phylogenetic hypotheses based on: **7** Parsimony analysis of DNA only **8** Maximum likelihood analysis of DNA only **9** Parsimony analysis of morphology only **10** Parsimony analysis of morphology and DNA combined. Numbers on terminal taxa refer to DNA extraction numbers.

result with this male-fully-eyed group basally paraphyletic with respect to reduced eye species makes much more intuitive sense. Nonetheless, the possibility of more vagility in the development of complete eyes is intriguing. Ultimately, better sampling across these groups for sequenceable specimens will be needed to resolve their relationships.

Among the species with reduced eyes in both sexes, all analyses reconstruct *P. quirsfeldi* as a grade subtending a larger group of populations and species. Referring to morphology only, this larger group only includes other reduced-eye species. However,

molecular data include one representative of a large-eyed species (*P. copelandi*) within this. Furthermore, uncorrected distances within what we've sequenced as *P. quirsfeldi* range to over 6%. Clearly this may suggest that there's more than one species involved. But we cannot find any morphological differences that would support that possibility. This suggests the possibility that what we are treating as *P. quirsfeldi* may be an old, genetically diverse but morphologically homogenous ancestral stock from which a substantial portion of the genus has arisen. It should further be noted that the *P. quirsfeldi* specimens we've sequenced cover a relatively narrow geographical area (as, indeed, the species distribution as a whole does).

The remaining species with reduced-eye males all fall in a well supported clade, most of which are rather minimally divergent in COI (as well as in male genitalia). *Prespelea divergens* falls at the base of this clade in the molecular and combined data trees, consistently 2–3% divergent from the other included taxa. Molecular support for the other morphology-based species (*P. morsei, P. parki*) is considerably weaker, with no divergences exceeding 2%. Although we lack molecular data for *P. carltoni*, morphological data place it within this group as well.

Lacking molecular data, we can say very little about the phylogenetic placement of *Speleobama*. While an assumption of progressive reduction of eyes would suggest its derivation from within *Prespelea* (as is weakly supported by morphological data alone), it is different enough in numerous other characters to cast doubt on this hypothesis. In particular it completely lacks the male secondary characters (metaventrite and metatrochanter) otherwise nearly universal in *Prespelea*. On the other hand, troglobitic habits may be correlated with the absence of distinctive secondary sexual characters in other Pselaphinae (Vásquez-Vélez, unpub. data), for reasons as yet obscure. The male genitalia (as illustrated by Park) are very different from those of any *Prespelea* as well. In the combined data analysis it is equally parsimoniously placed at the base of Speleobamini, what the generic taxonomy would imply, or within a reduced-eye clade, and it is accordingly part of a basal polytomy in the consensus tree.

## Taxonomy

### Tribe Speleobamini Park 1951: 51
### Genus *Prespelea* Park, 1953: 251

***Fusjugama* Park, 1956: 55 (as subgenus), syn. n.**

**Type species.** *Prespelea quirsfeldi* Park (1953: 251), original combination.

**Diagnosis.** Speleobamini can be easily separated from other North American Pselaphinae by the cervical region of head, which is deeply and narrowly constricted, the constriction obscured by dense fringes of opposing setae. *Prespelea* can be separated from *Speleobama*, the tribe's only other genus, by the presence of eyes, and by the maxillary palp, in which the fourth palpomere is tuberculate and bearing a long apical 'cone'; pros-

ternal disk with median setose patch; mesoventrite with well-developed submedian and lateral foveae behind anterior margin; metaventrite with lateral mesocoxal fovea present, small; abdominal ventrite 3 of both sexes with densely setose transverse basal impression; femora obliquely articulated on trochanter so that femur and coxa are relatively close to each other; tarsi of three tarsomeres, the first tarsomere short, the last two very long, the last bearing a single claw; prosternum elongate, without median carina; mesoventrite bisected by strong median carina; procoxae contiguous in confluent cavities; mesocoxae subcontiguous in separate cavities; metacoxae contiguous; males frequently with median metaventral processes and modified metatrochanters; aedeagus large, median lobe elongate, with a long, free style (paramere) on each side that bears four distal setae, and is inserted on the ventral face of the basal capsule.

**Description.** ***Size range*****:** TL 1.54–2.09mm; Max. width (EW) 0.57–0.71mm; **Body.** Integument rufescent, elongate, tapered with prothorax and head narrow; cuticle shining, sparsely setose, most surfaces with moderately long subdecumbent setae, intermixed with longer, finer 'flying' setae (these generally appressed in dry specimens). **Head.** HL 0.31–0.41mm; antennal insertions elevated with shallow median depression between them, broadly open laterally and anteriorly; antennae conspicuously setose, with 11 antennomeres: scape cylindrical, about as long as antennomeres 2 and 3 together; antennomere 2 generally about 1.5× length and width of antennomere 3; antennomeres 3–8 generally similar to each other, variable in length among species; antennomeres 9–11 forming weakly distinct club, with length of antennomere 9 about twice that of 8$^{th}$, length of antennomere 10 1.25× that of 9$^{th}$, and apical antennomere about twice as long as 10$^{th}$, with its sides rounded, tapering to subacute apex; eyes present, situated somewhat ventrolaterally, either of 2–4 facets or >30 (no intermediates known); epistoma broad, somewhat produced, finely elevated along apical margin; labrum rounded laterally and apically, subcircular; mandibles (Fig. 11) apically acute, with row of 5–7 serrate denticles along apical half of inner margin; cardo large, weakly projecting, glabrous; stipes triangular, with single small seta near basolateral corner; lacinia short, with few medially directed apical spines; galea long, digitiform, strongly fimbriate on inner margin; maxillary palp with four palpomeres, all appearing smooth and glabrous, with only few inconspicuous setae, the basalmost palpomere short and elbowed, the second the longest, strongly clavate, the third and fourth slightly shorter than second, subequal, more gradually clavate, the fourth bearing an apical digitiform process; submentum indistinct; mentum subquadrate, slightly elongate, with one or two pairs subapical setae; labial palpifer projecting, bearing three palpomeres, the basalmost palpomere very short, second palpomere about half as long as mentum width, weakly expanded apically, apical palpomere thin and short, bearing pair of apical setae. **Thorax.** PnL 0.31–0.37mm, PnW 0.29–0.33mm; pronotum narrow, sides rounded, widest near middle, slightly narrowed to base and apex, with five deep impressions along basal margin, setae of disk converging anteromedially; pronotosternal sutures absent; prosternum with or without vestigial lateral foveae, disk bearing median cluster of setae; prosternal cavities contiguous, broadly open behind; mesoventrite with well-developed submedian

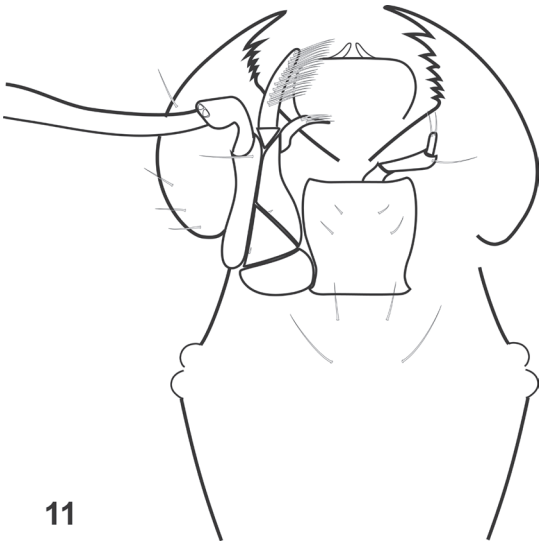


**Figure 11.** Mouthparts of *Prespelea*, based on *P. myersae*. Left maxilla and right labial palpus are omitted for clarity.

and lateral foveae behind anterior margin; metaventrite with lateral mesocoxal fovea present, small; male metaventrite with variably developed process; episterna and epimera concealed. EL 0.39–0.61mm; EW 0.57–0.71mm; elytra strongly narrowed to base (more strongly in wingless forms, including females of all species), each with or without weak pair of basal foveae; sutural stria present; metathoracic wings present (some males) or absent (some males and all females). **Legs.** Femora obliquely articulated on trochanter so that femur and coxa are relatively close to each other; tarsi of three tarsomeres, first short, last two very long, last tarsomere bearing a single claw; males frequently with modified metatrochanters. **Abdomen.** T3L 0.25–0.49; tergite 3 half to two-thirds elytral length (relatively longer in wingless forms), with deep transverse basal impression, densely lined with setae, sides with strong submarginal carina, curving mediad basally; other tergites short, without distinct lateral carinae, only tergites 4 and 5 with distinct paratergites; tergite 7 small and weakly depressed in males, wider and often medially carinate in females; abdominal ventrite 3 of both sexes with densely setose transverse basal impression; ventrites 2 and 3 developed into prominent intercoxal process. **Aedeagus.** Symmetrical, median lobe simple, sides parallel to sinuate to convergent, apex truncate to emarginate, often laterally expanded; apical foramen simple or delimited laterally to subapically by weakly elevated ridges; internal sac simple or bearing spines; parameres elongate, bearing four distal setae, articulated on the ventral face of the basal capsule.

**Distribution.** The genus is only known from the southern Appalachian Mountains.

**Remarks.** Little to nothing is known about the natural history of *Prespelea* species. Although their morphology and relationships to true troglobites seem to suggest deep soil or 'subcave' preferences, our own group's recent collections have been from more

typical litter samples, principally mixed hardwood litters, frequently under evergreen ericaceous shrubs.

We here synonymize the subgenus *Fusjugama* Park since the major phylogenetic divisions in the genus do not support the gross large-eye/small eye division on which that name was based.

**Key to species (males only)**

1 Specimens with one or more of the following: fully developed eyes and wings, and/or (if eyes and wings vestigial) with metatrochanters bearing some form of hook; often also with weak to prominent metaventral processes ..... **2 (Males)**

– Specimens, if small-eyed, then without modified metaventrite or metatrochanters ..... **Females (not keyed further)**

2 With fully developed eyes ..... **3**

– Eyes reduced to a few ommatidia ..... **6**

3 Metaventrite unmodified (Fig. 20) ..... **4**

– Metaventrite modified (Figs 12–19, 21–22) ..... **5**

4 Metatrochanteral processes simple tapered hooks near or beyond middle of metatrochanters (Fig. 31) ..... ***P. copelandi* Park**

– Metatrochanters with rather low, broad hooks near base (Fig. 33) ..... ***P. basalis* sp. n.**

5 Process of metaventrite weakly developed (Fig. 21) ..... ***P. enigma* sp. n.**

– Process of metaventrite prominent (Fig. 22) ..... ***P. wagneri* sp. n.**

6 Metatrochanters apically extended by hooklike process (Figs 25–27, 29 ..... **7**

– Metatrochanters with hooklike process medial, not extending from apices (Figs 23, 24, 28, 30) ..... **10**

7 Metaventral process narrowing to apex (Fig. 14, 15) ..... **8**

– Metaventral process basally constricted (Figs 16, 18) ..... **9**

8 Metaventral process very narrow (Figs 14) ..... ***P. minima* sp. n.**

– Metaventral process broader (Fig. 15) ..... ***P. morsei* sp. n.**

9 Apices of metaventral process divergent (Fig. 16) ..... ***P. divergens* sp. n.**

– Apices of metaventral process not divergent, simply divided (Fig. 18) ..... ***P. myersae* sp. n.**

10 Metatrochanteral processes broad and basal (Fig. 28) ..... ***P. carltoni* sp. n.**

– Metatrochanteral processes narrow and medial to subapical (Figs 23–24, 30) ... **11**

11 Metaventral process narrowing to apex (Fig. 19) ..... ***P. georgiensis* sp. n.**

– Metaventral process broad to apex (Fig. 12–13) ..... **12**

12 Metaventral process produced anterad (Fig. 13); aedeagus broadened apically (Fig. 36) ..... ***P. parki* sp. n.**

– Metaventral process not produced anterad, anterior face angled slightly posterad (Fig. 12); aedeagus more or less parallel-sided to apex (Fig. 34) ..... ***P. quirsfeldi* Park**

***Prespelea quirsfeldi* Park, 1953**
Figs 12, 23, 34–35, Map 48

*Prespelea quirsfeldi* Park, 1953: 251

**Type material.** 1 paratype male (dissected and slide-mounted by Park) from type locality ("North Carolina, Cataloochee Divide nr. 5000 ft. ele., 12.VI.1940, Quirsfeld leg."/"Paratype Prespelia [sic] quirsfeldi Park, 4–59" (FMNH). The Holotype male (USNM), collected at the same locality two days later, was not examined. **Other material:** Three paratype females cannot confidently be assigned to species, given the diversity of species occurring in the same general area; for full details see Suppl. material 1.

**Diagnosis.** Distinguishable only by the following characters of the male: metaventral process rather low, projecting perpendicularly below mesocoxae, apex (in posterior view) broad, subtruncate to very weakly emarginate; metatrochanter with hook subapical, with a moderately broad base tapering to subacute tip; aedeagus with sides convergent from basal third, weakly widening to apex, apex distinctly emarginate, apicodorsal ridges ending short of distal corners; internal sac lacking spines. Female pygidium with weak median process; apical ventrite slightly bilobed. TL 1.83–1.90mm; Max. width (EW) 0.67–0.69mm.

**Distribution.** Known from three somewhat disjunct localities, Cataloochee Divide and Cades Cove within Great Smoky Mountains National Park, and around the Coweeta Hydrological Laboratory south of Franklin, NC.

**Remarks.** This species was described from five specimens, two males and 3 females. The types were collected from 'deep leaf mold in thickets of rhododendrons' (Park, 1953). 'Leaf mold' and 'rhododendron duff' have been mentioned on subsequent specimen labels as well, as has 'nr. rotten wood'. Given the diversity of *Prespelea* now evident, and the difficulty to impossibility of associating females, the paratype females must be considered only tentatively conspecific.

There are unfortunately few subsequently collected specimens that we can definitely attribute to this species. It appears to be somewhat widely distributed, ranging from localities near the type locality along the Cataloochee Divide (Great Smoky Mountains National Park – GSMNP) 60 km west to Cades Cove (also GSMNP) and over 60 km south to the Coweeta area, and it exhibits some variation in metaventral process shape, metatrochanteral hook shape, and even in aedeagal shape. Furthermore, externally many specimens appear almost indistinguishable from those of *P. parki*, which is distinct based on both aedeagal morphology and available sequence data. Therefore there are a number of specimens that we have identified only as '*P. quirsfeldi* or *parki*'. The deep genetic diversity further underscores the need to do further work in this complex to resolve species limits and relationships.

Some of the specimens we cite as 'other material' were initially labeled by John Wagner as types of his manuscript species '*P. steevesi*' and '*P. coweeta*'. We do not believe these constitute distinct species, but have left his labels on the specimens.

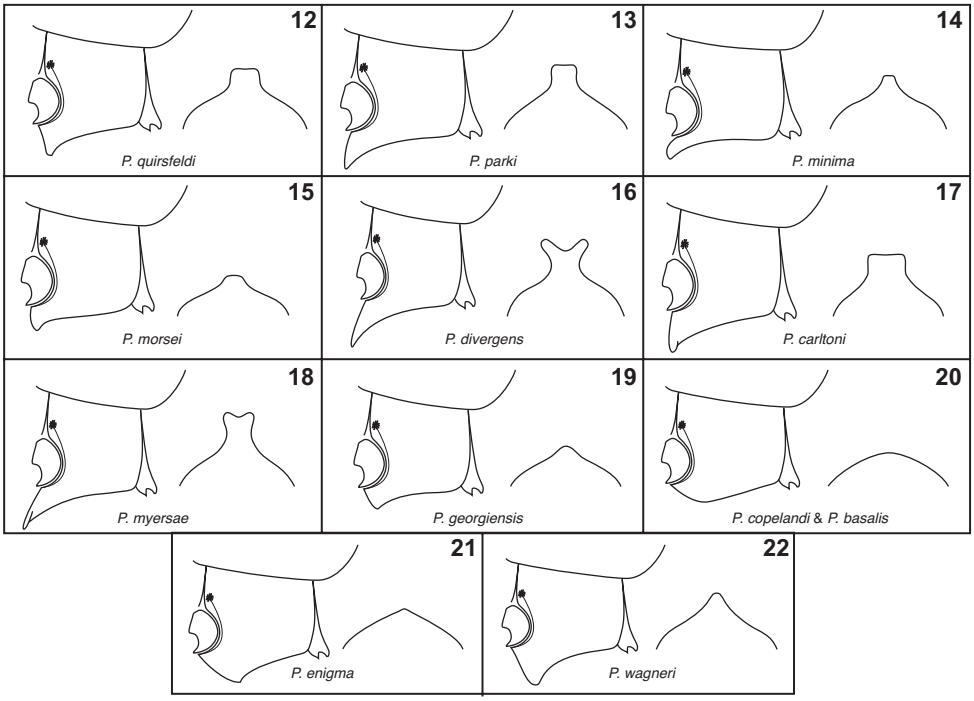


**Figures 12–22.** Metaventrites, lateral (left) and posterior (right) views. **12** *P. quirsfeldi* **13** *P. parki* **14** *P. minima* **15** *P. morsei* **16** *P. divergens* **17** *P. carltoni* **18** *P. myersae* **19** *P. georgiensis* **20** *P. copelandi* and *P. basalis* (indistinguishable in this feature) **21** *P. enigma* **22** *P. wagneri*.

***Prespelea parki* Caterino & Vásquez-Vélez sp. n.**
http://zoobank.org/E211E5FD-6DC6-42A6-852C-D6BB81D2C502
Figs 13, 24, 36, Map 48

**Type material. Holotype male:** NC: Graham County, Joyce Kilmer Memorial Forest, near junction of Indian and Santeetlah Creeks, 35.3451°N, 83.9670°W, vi.24.2015, S. Myers & M. Caterino, sifted litter, CUAC000010972 (DNA extract MSC-2405); deposited in FMNH. **Paratypes (2):** male (CUAC000010948) and female (CUAC000010964; DNA extract MSC-2422) with identical data to type. **Other material:** Macon Co., NC and Union Co., GA; for full details see Suppl. material 1.

**Diagnosis.** Distinguishable from *P. quirsfeldi* only by the following characters of the male: metaventral process more laminate, and slightly more projecting anterad, apically weakly emarginate; metatrochanter with laminate subapical tooth, very similar to that of *P. quirsfeldi* (identical in some, but broader and more flangelike in others, particularly Kilmer specimens); mesofemora somewhat swollen. Aedeagus with sides converging from basal third to near apex, weakly sinuate then strongly divergent to weakly rounded apical corners, apical margin strongly emarginate; apicodorsal ridges strong,

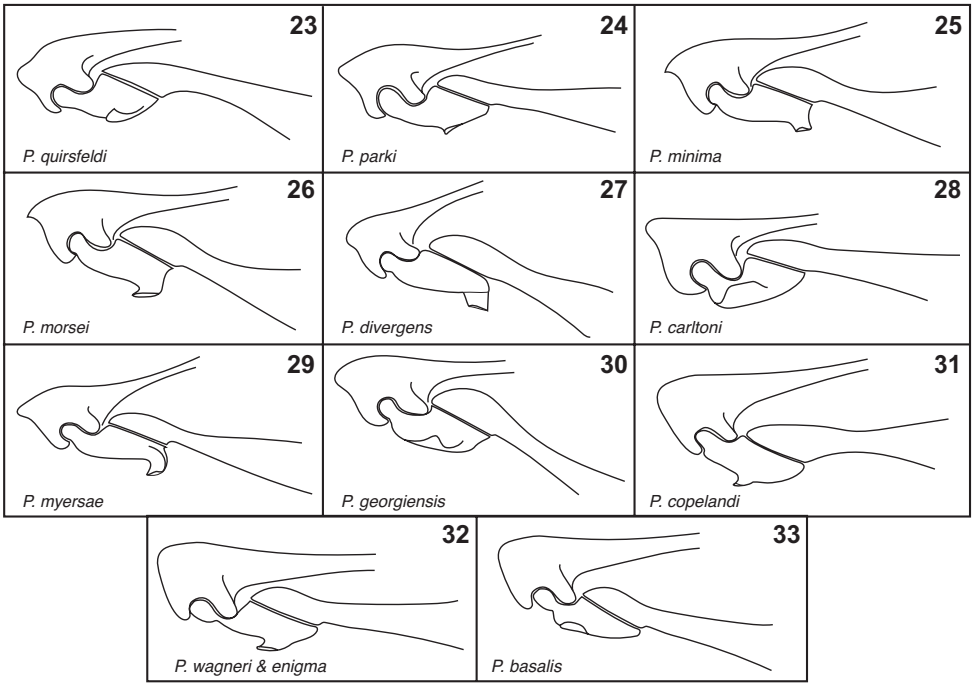


**Figures 23–33.** Metatrochanters, ventral view. **23** *P. quirsfeldi* **24** *P. parki* **25** *P. minima* **26** *P. morsei* **27** *P. divergens* **28** *P. carltoni* **29** *P. myersae* **30** *P. georgiensis* **31** *P. copelandi* **32** *P. basalis* and *P. enigma* (indistinguishable in this feature) **33** *P. wagneri*.

converging toward apex, ending freely (apicodorsal foramen only weakly closed). Female pygidium with median carina increasing to apex, apical ventrite weakly bilobed; neck convex beneath, with distinct median ridge and cluster of postgular setae. TL 1.82–1.91mm; Max. width (EW) 0.66–0.71mm.

**Distribution.** Southwestern North Carolina, extending southwestward to Brasstown Bald in northeastern GA.

**Remarks.** As discussed above, there is a relatively broad range of variation between *P. quirsfeldi* and what we name as *P. parki*, with some specimens falling between. Thus, outside of type material from the Joyce Kilmer Memorial Forest, which we have been able both dissect and sequence, and which is distinct in both morphological and molecular characters, specimens from other localities listed above are merely 'affiliated' with one or the other species. A number of other specimens from localities in and around Great Smoky Mountains National Park cannot be confidently attributed to either (despite dissection). See Suppl. material 1 for additional possible localities.

We name this species for Orlando Park (1901–1969), a leading 20th century specialist in Pselaphinae, and author of the genus. One of the specimens we cite as 'other

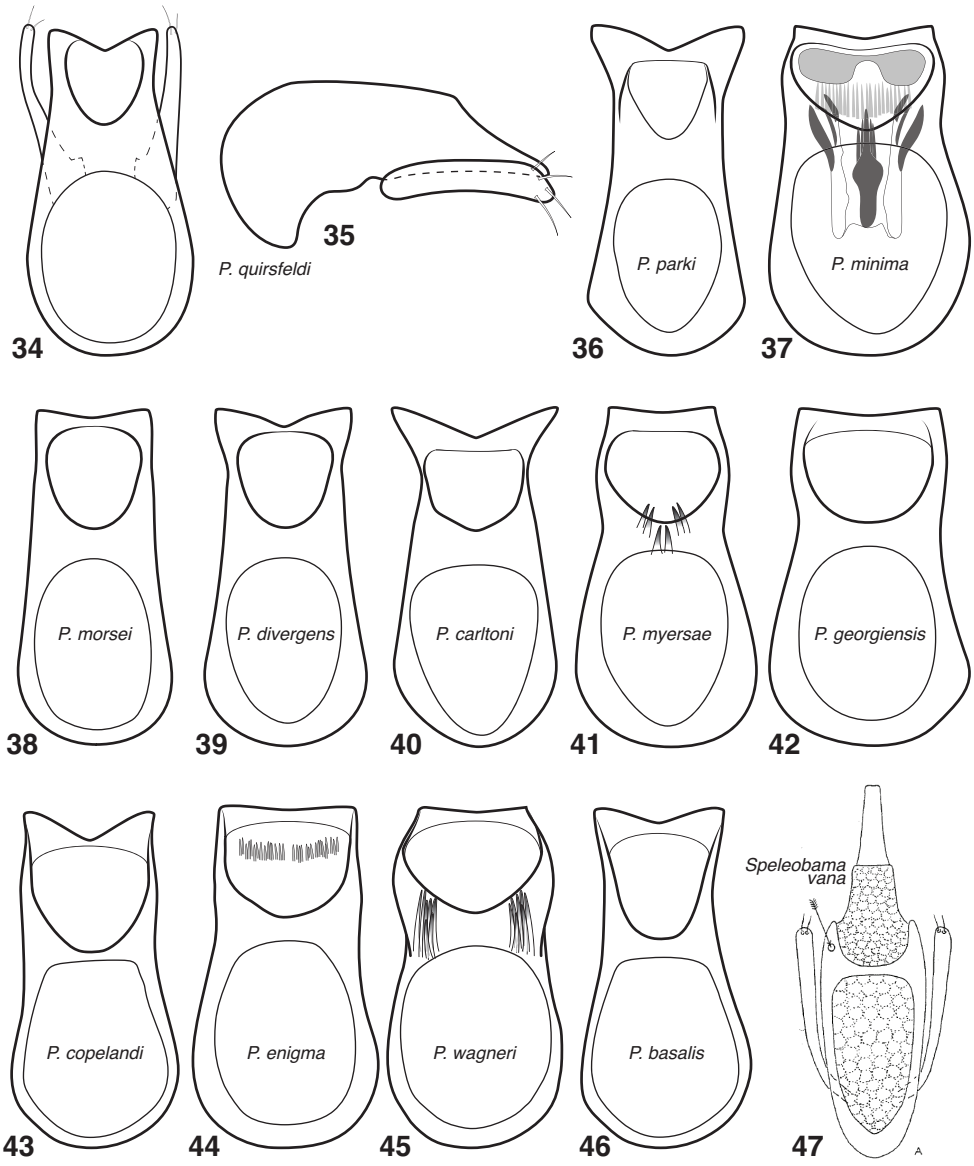


**Figures 34–47.** Aedeagus, mostly dorsal view (except 35). Parameres omitted except from **34, 35** and **47**. **34** *P. quirsfeldi* **35** *P. quirsfeldi*, lateral view **36** *P. parki* **37** *P. minima* **38** *P. morsei* **39** *P. divergens* **40** *P. carltoni* **41** *P. myersae* **42** *P. georgiensis* **43** *P. copelandi* **44** *P. enigma* **45** *P. wagneri* **46** *P. basalis* **47** *Speleobama vana* (from Park, 1951).

material' was initially labeled by John Wagner as a 'type' of his manuscript species '*P. parki*'. While we have used his intended name, but have left his 'labels on the specimen, we exclude this from our type series.

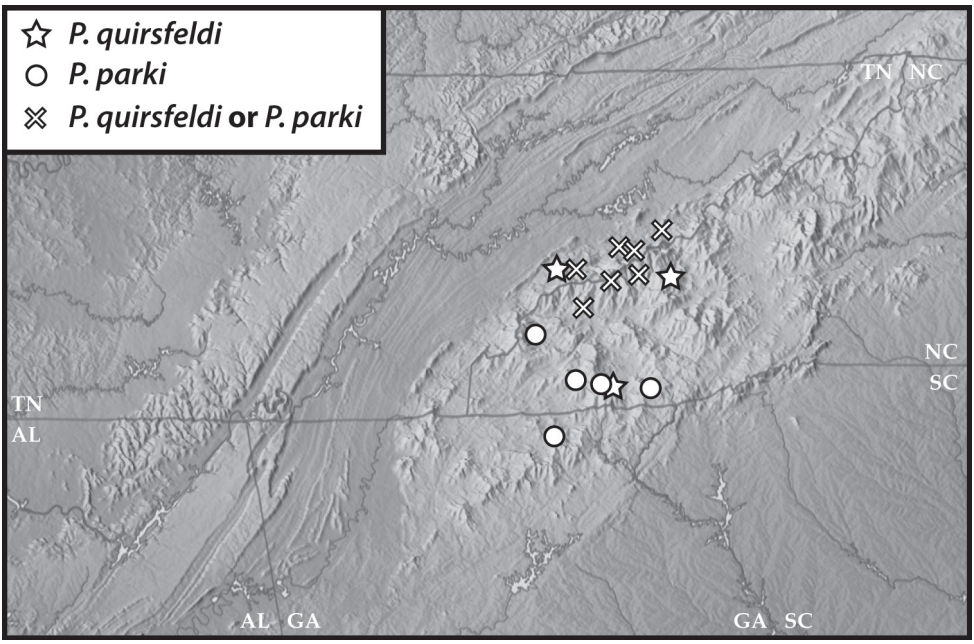


**Figure 48.** Map of southern Appalachia with specimen records for *P. quirsfeldi*, *P. parki*, and for a number of specimens which we cannot positively identify as one or the other.

***Prespelea minima* Caterino & Vásquez-Vélez sp. n.**
http://zoobank.org/CC3AC822-AB1B-4053-898B-A457A5C46035
Figs 14, 25, 37, Map 49

**Type material. Holotype male:** TN: Sevier Co., Great Smoky Mountains National Park, Beech Gap on Clingman Dome Rd. at Appalachian Trail crossing [35.61°N, 83.45°W], 1750m, VI.28.2001, forest litter, C. Carlton, A.K. Tishechkin, & V. Moseley (LSAM0096333); deposited in FMNH. **Paratypes (2):** 1 male: same data as type; 1 male: GSMNP: Chimneys Picnic area (DNA extract MSC-2415); for full details see Suppl. material 1.

**Diagnosis.** Distinguishable only by the following characters of the male: metaventral process rather small, narrowing to subtruncate or weakly emarginate apex (in posterior view), distinctly projecting anterad between mesocoxae; metatrochanters with hooks extending apically, laminate, moderately broad, with truncate apex. Antennae slightly elongate; neck flattened beneath, subcarinate ventrolaterally. Aedeagus broad, sides sinuate, apex emarginate, apicodorsal ridges curving inward at apex; apical foramen with lightly sclerotized plate across apex; internal sac with strong medial and lateral spines, ventrally with ~20 minute spines. TL 1.80–1.84mm; Max. width (EW) 0.67–0.69mm.

**Distribution.** Known only from two localities in the central part of GSMNP.

**Remarks.** Samples were noted to have been taken only from 'forest litter'. Despite an attempted DNA extraction from an older mounted specimen, we have not been successful in generating a DNA sequence for this species.

The species is named for its small metaventral process.

***Prespelea morsei* Caterino & Vásquez-Vélez sp. n.**
http://zoobank.org/C7C58731-D799-4C4D-8C34-A2C4753183F2
Figs 3–4, 15, 26, 38, Map 49

**Type material. Holotype male:** NC: Macon Co., Balsam Mountain Preserve, nr. Sugarloaf Creek, 35.3707°N, 83.1108°W, VI.20.2015, S. Myers, sifted acidic cove litter (CUAC000026234; DNA extract MSC-2406); deposited in FMNH. **Paratypes (13):** several localities within Balsam Mountain Preserve, from oak and mixed oak-hickory litters, all in June 2015; see Suppl. material 1 for details. We also assign two specimens from McDowell Co., NC to this species as nontypes, with some reservation (see remarks).

**Diagnosis.** Distinguishable only by the following characters of the male: metaventral process weaker than in *P. quirsfeldi*, but similar; metatrochanteral hook forming moderately broad flange from apex of trochanter; antennomeres subquadrate, basal antennomeres about as long as wide; aedeagus with sides convergent to near apex, apical margin very weakly emarginate; apicodorsal ridges divergent to apical corners, apicodorsal foramen open. Female pygidium essentially unmodified, with very weak median elevation, almost imperceptible until apex; apical ventrite very weakly bilobed; neck convex beneath, with distinct median ridge (not carina) and cluster of postgular setae. TL 1.74–2.09mm; Max. width (EW) 0.65–0.69mm.

**Distribution.** This species is known only from a relatively small area within the Balsam Mountains of western North Carolina.

**Remarks.** This species is closely related to *P. divergens* and *P. parki*. The two specimens we attribute to this species from Courthouse Falls, in the Pisgah National Forest of McDowell Co., NC, are particularly vexing. These have identical male genitalia to *P. divergens*, but a more moderate metaventral process like *P. morsei*. The male metatrochanter is also more like that of *P. morsei*, lacking the extreme apical point of the *P. divergens*. Molecular data separate these slightly from either species, but place them considerably closer to *P. morsei*.

This species is named to honor Dr. John Morse, the senior author's predecessor as director of the Clemson University Arthropod Collection. All specimens of this species were collected in the vicinity of a property owned by John and his wife Suzanne, and their hospitality and assistance were invaluable in carrying out the work.

***Prespelea divergens* Caterino & Vásquez-Vélez sp. n.**
http://zoobank.org/CE171B75-3141-4860-AFF1-DB83094AD85A
Figs 16, 27, 39, Map 49

**Type material. Holotype male:** SC: Pickens Co., Sassafras Mt., 35.0634°N, 82.7760°W, S. Myers, vi.10.2015, sifted leaf litter (CUAC000025607); deposited in FMNH. **Paratype (1):** male: same general locality and date as type, but at 35.0579°N, 82.7705°W (CUAC000025636; DNA extract MSC-2407). **Other material:** Two specimens from Macon Co., NC also appear to correspond to this species; for full details see Suppl. material 1.

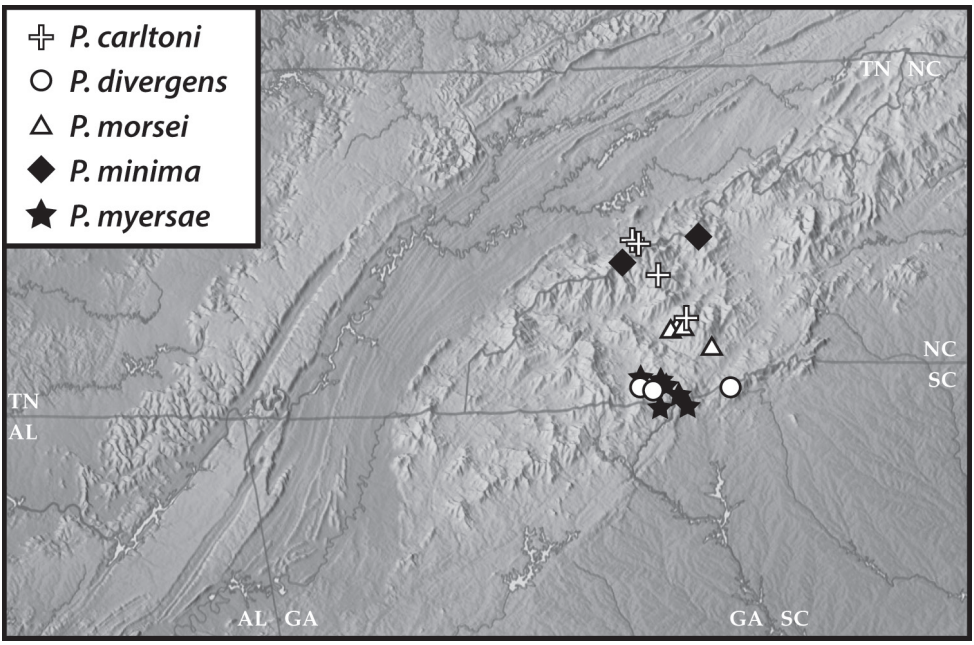


**Figure 49.** Map of southern Appalachia with specimen records for *P. carltoni*, *P. divergens*, *P. morsei*, *P. minima*, and *P. myersae*.

**Diagnosis.** Distinguishable from *P. quirsfeldi* only by the following characters of the male: metaventral process strongly projecting anterad, sublaminate, apically divergent; metatrochanter apically extended, with broad recurved flange whose apical corner is strongly produced and acute; antennae weakly elongate; aedeagus with sides convergent to near apex, then weakly divergent to apical corners, apical margin strongly emarginate; apicodorsal ridges divergent to near apices, apical foramen weakly closed. TL 1.83–2.04mm; Max. width (EW) 0.69–0.71mm.

**Distribution.** This species is only definitely known from Sassafras Mt., South Carolina, the highest point in the state. The other possible locality near Highlands, NC lies about 30 km west.

**Remarks.** This species' morphological distinctness is supported by reasonably clear genetic divergence, at least at the one locality and specimen for which we have sequence data.

***Prespelea carltoni* Caterino & Vásquez-Vélez sp. n.**
http://zoobank.org/89C5ADC1-4DB3-4BD8-B645-A18F5E888754
Figs 17, 28, 40, Map 49

**Type material. Holotype male:** NC: Haywood Co., GSMNP, Cataloochee Rough Ridge Tr., (lower), 306360E, 3940881N [35.5927°N, 83.1374°W], C. Carlton, 7/29/2002, moist berlese (LSAM0092266; DNA Extract MSC-2411); deposited in FMNH. **Paratypes (3):** 1 male same data as type (LSAM0092265); 1 male: NC: Haywood Co., GSMNP,

Cataloochee Rough Ridge Tr., (upper), 305891E, 39040519N [35.5894°N, 83.1415°W], C. Carlton, 7/29/2002, moist berlese (LSAM0060036); 1 male: NC: Jackson Co., Blue Ridge Parkway, nr. Grassy Ridge Mine [35.41°N, 83.05°W], 1520m, A. Smetana (CNC Coleoptera Barcode Voucher 00162876). **Other material:** Two other males (not dissected) from GSMNP, in Cocke Co., TN; for full details see Suppl. material 1.

**Diagnosis.** Distinguishable from *P. quirsfeldi* only by the following characters of the male: metaventral process, broad, elevated, somewhat blunt at middle, with acute distal margins limited to lateral corners, slightly concave behind; metatrochanter with hook broad and basal. Antennae varied, antennomeres 9 and 10 distinctly transverse in some individuals, more equilateral in others. Tegmen tapering from near base to near apex, abruptly widened and bifurcate at apex, with apical corners subacute; apicodorsal ridges moderate, apical foramen broadly open; internal sac without distinct sclerotizations. TL 1.76–1.96mm; Max. width (EW) 0.45–0.49mm.

**Distribution.** This species is only known from a few localities within Great Smoky Mountains National Park.

**Remarks.** This species is most distinctive in its male metatrochanteral process, which is basal and broad. It shows some minor variability in the shape of the metaventral process, which may be weakly emarginate apically or not. Despite an attempted DNA extraction from an older mounted specimen, we have not been successful in generating a sequence for this species.

We name this species for Dr. Chris Carlton of the Louisiana State Arthropod Museum, who collected the types, and who has led efforts to document the beetle fauna of the Smoky Mountains.

***Prespelea myersae* Caterino & Vásquez-Vélez sp. n.**
http://zoobank.org/C58B41FE-7FF1-41BD-8DD3-CC1571A2802F
Figs. 11, 18, 29, 41, Map 49

**Type material. Holotype male:** "USA: SC: Oconee Co., 34.9899°N, 83.0724°W, Indian Camp Ck, V.04.2015, M.Caterino & S. Myers, Sifted leaf litter" (CUAC000010576); deposited in FMNH. **Paratypes (8):** 1 male: "USA:SC: Oconee Co., 34.9886°N, 83.0729°W, Indian Camp Ck, V.04.2015, M.Caterino & S. Myers, Sifted leaf litter" (CUAC000010698, DNA Extract MSC-2408); deposited in CUAC. 2 males and 1 female: "USA:SC: Oconee Co., 34.9903°N, 83.0723°W, Indian Camp Ck, V.04.2015, M.Caterino & S. Myers, Sifted leaf litter" (CUAC000010645, CUAC000010631, CUAC000010647); deposited in FMNH, LSAM & CUAC. 1 female: "USA:SC: Oconee Co., 34.9846°N, 83.1018°W, East Fork, V.04.2015, M.Caterino & S. Myers, Sifted leaf litter" (CUAC000010746); deposited in CUAC. 2 females: "USA:NC: Macon Co., 35.0096°N, 83.1245°W, Ellicott Rock Trail, VII.18.2015, S. Myers, Sifted litter" (CUAC000011201, DNA Extract MSC-2421; CUAC000011216); deposited in CUAC. **Other material:** 13 specimens from Macon & Jackson Cos., NC, and Rabun Co., GA; for full details see Suppl. material 1.

**Diagnosis.** Distinguishable from *P. quirsfeldi* only by the following characters of the male: metaventral process more distinctly laminate and anteriorly projecting than in *P. parki*, weakly to strongly apically cleft; metatrochanter apically produced, with strong, scooplike apical hook; mesofemora somwhat swollen; aedeagus with sides convergent to near apex, then weakly divergent to apical corners; apicodorsal ridges strong, divergent subapically, converging short of apex to weakly closed apical foramen, apical margin subtruncate to weakly emarginate; internal sac with six distinct teeth. Female pygidium weakly depressed, apical ventrite with median transverse carina strongly bilobed, elevated, defining posterior face coplanar with pygidium; neck ventrally flattened, but without median or lateral carinae. TL 1.54–1.84mm; Max. width (EW) 0.57–0.63mm.

**Distribution.** This species is known from a limited area around the point where North Carolina, South Carolina and Georgia meet, centered on the Ellicott Rock Wilderness.

**Remarks.** There is slight variability in the form of the metatrochanteral process in specimens from around Highlands, North Carolina, where its apex is slightly widened and truncate. We have dissected one male from this locality and find its aedeagus to be basically similar in overall shape to that of the type, as well as in the distinctive teeth of the internal sac. There is also considerable variation in the widening and emargination of the metaventral process, even among specimens from near the immediate type locality. The female pygidium of this species shows commonalities with the 'copelandi-like' (fully-eyed) species of the genus, suggesting that the reduction of male eyes may be quite labile. In addition to several 'leaf litter' labels, some specifically mention rhododendron and hemlock as important elements of the sampled microhabitats.

The species is named to recognize the contributions of former Caterino lab postdoc Dr. Shelley Myers, collector of many of the specimens of this and others of the new species described in this paper. Several specimens from the John Wagner collection (FMNH) bear 'type' and 'paratype' labels, and the manuscript name *P. suteri*. We have left these labels on the specimens, though we do not recognize these as types and the name '*P. suteri*' has no formal status.

***Prespelea georgiensis* Caterino & Vásquez-Vélez sp. n.**
http://zoobank.org/A7A7E1D6-5EE8-4B0D-9D9E-332640FC0B66
Figs 19, 30, 42, Map 50

**Type material. Holotype male:** "Cloudland Canyon S.Pk., Dade Co., GA. 7.VII.62, forest floor debris" / "H.R. Steeves Jr. Collection" / "CHNM 1963, H.R. Steeves Jr. Pselaphidae Colln. Acc. Z-13, 288"; deposited in FMNH. **Paratypes (7):** 2 males: same data as type; FMNH. 3 males & 1 female: same locality as type, but collected on ix.3.1961 in 'debris nr. log', by W. Suter & J. Wagner; FMNH & CUAC. 1 female: same locality, but collected on ix.1.1961; FMNH. 1 female: Cloudland Canyon State Park, 34.8152°N, 85.4850°W, ix.17.2006, by Igor Sokolov; LSAM0108983.

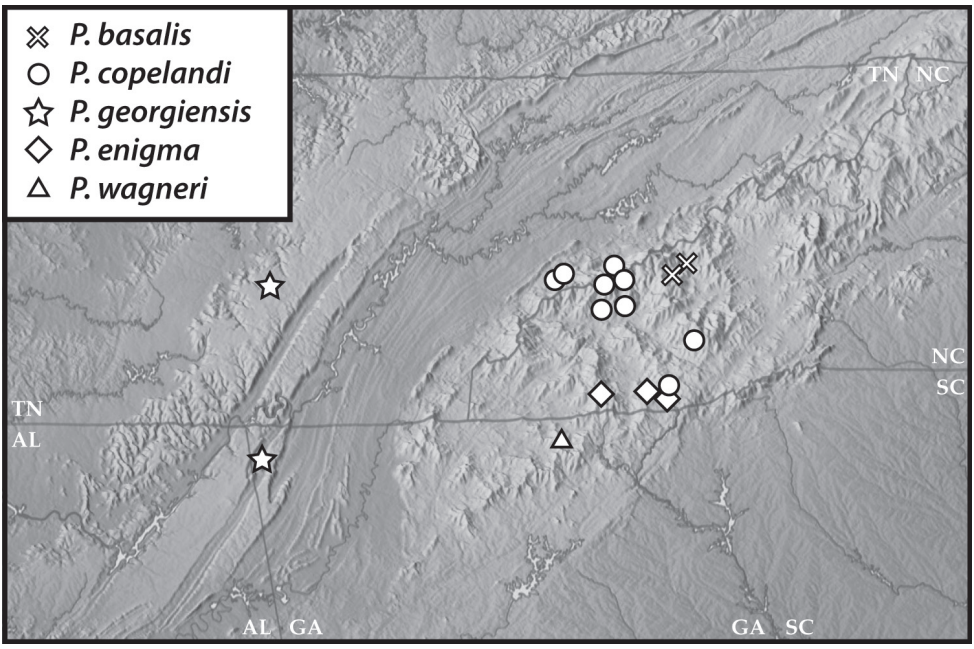


**Figure 50.** Map of southern Appalachia with specimen records for *P. basalis*, *P. copelandi*, *P. georgensis*, *P. enigma*, and *P. wagneri*.

**Other material:** 1 female: TN: Bledsoe Co., Fall Creek Falls St. Park, ix.9.1961, J. Wagner & W. Suter; for full details see Suppl. material 1.

**Diagnosis.** Distinguishable from *P. quirsfeldi* only by the following characters of the male: metaventral process forming low, single, blunt medan point; metatrochanteral point short and medial to subbasal, shorter and more basal than that of *P. quirsfeldi*; antennae relatively short, antennomeres 9 and 10 distinctly wider than long; aedeagus with sides sinuate, widened subapically, then weakly convergent to apical corners, apical margin very shallowly emarginate; apicodorsal ridges weak, converging, weakly closing apical foramen; internal sac lacking teeth. Female pygidium flat, moderately broad, rounded apically; apical ventrite with weak transverse median ridge; neck flattened beneath, subcarinate laterally. TL 1.69–1.81mm; Max. width (EW) 0.59–0.65mm.

**Distribution.** In addition to the type locality, Cloudland Canyon State Park in northwest Georgia, this species may occur about 75 km N in Bledsoe County, Tennessee, but this record is based on a single female, and should be confirmed with more material.

**Remarks.** Despite its small-eyed males, this species shares a number of characteristics with the large-eyed species related to *P. copelandi*. The male metatrochanter is particularly similar to that of *P. enigma*, as is the metaventral process. The flat and broad female pygidium also allies it more closely with *P. copelandi* than with most of the preceding species (with the possible exception of *P. myersae*). Morphological phylogenetic analyses support

this assertion, but it would be good to confirm with molecular data. An attempted DNA extraction from a paratype specimen failed to produce amplifiable DNA.

Some specimens of this species from the John Wagner collection (FMNH) bear 'type' and 'paratype' labels, and we have used his manuscript name for this species. However, though we've left these labels on the specimens, we have selected a different specimen for our primary type than he intended.

### ***Prespelea copelandi*** **Park, 1956**

Figs 20, 31, 43, Map 50

*Prespelea copelandi* Park 1956: 55

**Type material. Holotype male:** "Cades Cove, Blount Co. Tenn. Berlesed, C.D. Copeland"/ "Type"/ "Field Mus. Nat. Hist. Orlando Park Pselaphidae Colln." (FMNH). **Other material:** known from nine non-type specimens from Blount and Sevier Cos., TN, and Swain Co., NC (all within Great Smoky Mountains National Park); and Jackson and Macon Cos., NC, east of GSMNP; for full details see Suppl. material 1.

**Diagnosis.** *Prespelea copelandi* is unique in the genus in lacking male metaventral modifications. The male's metaventrite is slightly more convex than that of the female, but lacks any distinct process. Like several new species, the males exhibit well-developed eyes and wings (associated females of these species all have reduced eyes with 2–4 ommatidia and undeveloped flight wings); metatrochanter with narrow, acute tooth borne slightly basad midpoint; neck moderately flattened beneath, with median ventral carina; aedeagus with weakly sinuate sides and a deeply emarginate apex. Females: none definitely associated. TL 1.72–1.80mm; Max. width (EW) 0.65–0.69mm.

**Distribution.** Known from scattered localities within Great Smoky Mountains National Park, as well as a few locations further east and southeast.

**Remarks.** This species was described from a single undissected male, without associated females. No illustrations were provided. However, the lack of a distinct metaventral process distinguishes it from the other fully-eyed and winged (in males) species we describe below. We assign a few specimens here that do exhibit an extremely minute metaventral denticle, which places them somewhere between this and the next species, and it is this form whose genitalia is illustrated in Fig. 43; we did not risk dissecting the unique type. There is substantial variation, even in male genitalia, with some specimens approaching the shape of *P. quirsfeldi*, with the aedeagus distinctly and evenly narrowed subapically. There is also variation in the depth of the apical emargination of the aedeagus, and this species thus remains poorly characterized. Further material from the type locality (Cades Cove) that can be dissected and sequenced would help define what should and shouldn't be assigned to *P. copelandi*.

***Prespelea enigma* Caterino & Vásquez-Vélez sp. n.**
http://zoobank.org/90333F47-56DC-4539-866F-AA6868E7EE45
Figs 5, 6, 21, 32, 44, Map 50

**Type material. Holotype male**: USA: NC: Macon Co., Jones Gap, 35.0785°N, 83.2923°W, S. Myers, vii.22.2015, sifted litter (CUAC000026531, DNA Extract MSC-2403). **Other material:** 4 males & 6 females, NC: Macon Co., 11 mi. SW Franklin, Back Country info center, VIII-17/21–1990, hardwood litter nr. dead logs, S. O'Keefe; UNHM, FMNH, CUAC. 1 female: NC: Macon Co. Highlands, vi.8.1973, Coker Rhododendron Trail, litter under rhododendron, W. Suter; FMNH.

**Diagnosis.** This species is externally indistinguishable from *P. copelandi* except in the following male characters: metaventrite elevated anteromedially to form small but distinct median tubercle about one-fourth metaventral length behind mesocoxae (Fig. 21), metaventrite moderately flattened behind; posteroapical corner of male metatrochanter produced to form short, incurved flange (Fig. 32), the whole trochanter being somewhat parallelogram-shaped; aedeagus with sides weakly sinuate toward apex, apicodorsal ridges weakly divergent to apical corners; apical margin subtruncate to weakly emarginate; internal sac with broad band of about 18 short, sclerotized teeth. Female not definitely associated. TL 1.76–1.88mm; Max. width (EW) 0.61–0.71mm.

**Distribution.** This species is known from the type locality, a few miles WNW of Highlands, NC, and from a second locality approximately 20 km due west.

**Remarks.** This species is very similar to *P. copelandi*, but the male metaventral process is distinct, being located closer to the meso- than the metacoxae. The metatrochanteral processes of the two are very similar, but that of *P. enigma* is wider and situated at or distad the midpoint of the trochanter's posterior margin. Finally the aedeagus of *P. enigma* is slightly broader and with a much squarer, only weakly emarginate apex, with a distinctly spinose internal sac, which *P. copelandi* lacks. Dissected specimens have the internal sac variably everted, so it is difficult to compare available specimens directly. However, one dissected male excluded from the type series appears to have somewhat better developed (longer) and more numerous spines on the internal sac than the type. The apex of the aedeagus of this specimen is also slightly more emarginate than that of the type. However, generalizations are impossible with such limited material. Our main basis for limiting the type series to the single male from Jones Gap is the availability of molecular data for that specimen. Interestingly, the molecular data suggest that this species may be closely related to *P. myersae*, and this is supported to some extent by the presence of internal sac armature. In external morphology, however, *P. enigma* and *P. myersae* differ greatly, given the males' well-developed eyes and wings in *P. enigma*. Tentatively associated females have the pygidium broad and flat, the apical ventrite with strong transverse carina, concave behind, and the neck flattened beneath, but without median or lateral carinae.

One female specimen cited under 'other material' was initially labeled by John Wagner under his manuscript species '*P. suteri*'. We have not used his intended name, and cannot unequivocally associate the specimen with this species, but have left his label on the specimen.

***Prespelea wagneri* Caterino & Vásquez-Vélez sp. n.**
http://zoobank.org/B692F4FC-D1C8-4320-B5FC-BC954AED38A8
Figs 22, 33, 46, Map 50

**Type material. Holotype male:** "Brasstown Bald, GA, Union Co., 11.VIII.63', El. 2750', B" / "Rhododendron and softwood debris" / "H.R. Steeves, Jr., J.D. Patrick Jr. collectors" / "H.R. Steeves Jr. Collection" / "PARATYPE [not]" / "P. patricki [nom. nud.]"; DNA Extract MSC-2410; deposited in FMNH. **Paratypes (13)**: 2 males, 1 female same data as type, deposited in FMNH, CUAC; 3 males and 3 females, same locality but collected September 8, 1963 from 'forest floor debris', deposited in FMNH; 2 males and 1 female, same locality but collected May 31, 1964 from 'forest floor debris nr. dead wood', deposited in FMNH; 1 female, same locality but collected October 23, 1965 from 'forest floor debris nr rotten wood', deposited in FMNH.

**Diagnosis.** This species is externally indistinguishable from *P. enigma* except in the following male characters: metaventral process broader and more prominent, obviously dentate in lateral view, apically rounded in posterior view, metaventrite very weakly flattened to subconcave behind; metatrochanteral process similar to that of *P. enigma*, with a rather narrow, recurved subapical tooth. Aedeagus with sides distinctly sinuate, wide near apex, thence apically converging, apex shallowly emarginate; apicodorsal ridges not extending to distal corners; internal sac with lateral clusters of ~8 narrow spines. Female pygidium broad, very weakly convex, without median ridge or tooth; apical ventrite with very broadly and weakly bilobed transverse median carina, concave behind. Neck weakly flattened beneath, but not carinate. TL 1.72–1.92mm; Max. width (EW) 0.59–0.69mm.

**Distribution.** This species is known from several collections on Brasstown Bald, Georgia's highest peak (though not apparently near its peak, at a stated 2750 feet on all labels).

**Remarks.** The distinctive internal sac armature of the aedeagus distinguishes this species from all others with fully-eyed males, and may suggest relationships to *P. myersae* and *P. minima*, which also have internal sac armature, though our phylogenetic analyses of morphological data do not unite such a group. Despite the attempted extraction of DNA from one older specimen, we have not been successful at generating a sequence for this species.

The type specimens were initially labeled by John Wagner as 'types' and 'paratypes' of his manuscript species '*P. patricki*'. We have not used his intended name, but have left his labels on the specimens.

***Prespelea basalis* Caterino & Vásquez-Vélez sp. n.**
http://zoobank.org/A9BBBBBB-C42F-47A3-A8C5-A572FD5EFB5F
Figs 20, 32, 45, Map 50

**Type material. Holotype male: "**N.CAROLINA: Haywood Co. GSMNP, Caldwell Fork Tr. at UTM 30897 E 3940883 N. Moist forest Berlese. 3 August 2002. C.Carlton

& N. Lowe" LSAM0091782, DNA Extract MSC-2418; deposited in FMNH. **Paratype male**: NC: Haywood Co., GSMNP, Cataloochee Rough Ridge Tr. [35.5927°N, 83.1374°W], July 29, 2002, C. Carlton, LSAM0092267; deposited in LSAM.

**Diagnosis.** This species is externally indistinguishable from *P. copelandi* except in the following male characters: metaventral process indistinct; metatrochanteral process forming widened flange near basal margin of trochanter; neck convex beneath with weak median carina. Aedeagus very much like that of *P. quirsfeldi*, with sides evenly concave, apices slightly wider, and apical margin shallowly emarginate. Female not associated. TL 1.80mm; Max. width (EW) 0.67mm.

**Distribution.** This species is known only from two localities within Great Smoky Mountains National Park. They are separated by about 5 km in the eastern part of the park.

**Remarks.** This species is most easily distinguished by its broad and basal metatrochanteral flange (to which the species name refers). Otherwise it is extremely similar to *P. copelandi* and *P. enigma*. Its strong similarity in aedeagal shape to *P. quirsfeldi* is surprising, and may suggest the basal/default form for the genus as a whole.

This species name refers to its basally situated metatrochanteral hook.

## Conclusions

This study has revealed an unexpectedly diverse fauna of this formerly small and poorly known genus, which is still known from only a rather limited area. Further litter sampling in new areas may uncover additional species. Molecular study of relationships among known populations would greatly help delimit the species presently known, given the range of variability in many characters. We hope that future studies can obtain fresh material of *Speleobama* for inclusion in a molecular phylogenetic analysis, so that the apparent progressive reduction of several character systems may be more rigorously tested. Finally, aside from some indications of microhabitat preferences for the various species, there is nothing known of the natural history of *Prespelea*. Given their distinct sexual dimorphisms, including wing and eye development, information on their biology will be necessary to put these characters into a proper context.

## Acknowledgments

Several funding bodies helped support this work: USDA National Institute of Food and Agriculture Hatch projects SC-1700527 & SC-1700434; NSF-CSBR grant 1457909; a Clemson University Research Initiation Grant to M. Caterino and S. Myers; and a research grant-in-aid from Highlands Biological Station to S. Myers. We are also grateful to John and Suzanne Morse for facilitating this project in numerous ways. We thank K. Caterino, L. Cushman, A. Deczynski, S. Muñoz, and S. Langton for assistance with fieldwork, and Sumter National Forest, Nantahala National Forest, South Carolina Department of Natural Resources' Heritage Trust Program,

North Carolina State Parks, South Carolina State Parks, and the Balsam Mountain Preserve for collecting permissions. We thank D. Chandler, C. Carlton, B. Owens, P. Bouchard, A. Davies, M. Thayer, and C. Maier for specimens, and J. Parker for sharing unpublished COI sequences.. Finally, we thank D. Chandler and C. Carlton for their comments on an earlier version of this paper. This paper is Technical Contribution No. 6569 of the Clemson University Experiment Station.

## References

Park O (1951) Cavernicolous pselaphid beetles of Alabama and Tennessee, with observations on the taxonomy of the family. Geological Survey of Alabama Museum Paper 31: 1–107.

Park O (1953) New of little known pselaphid beetles of the United States, with observations on the taxonomy and evolution of the family Pselaphidae. Bulletin of the Chicago Academy of Sciences 9(14): 249–283.

Park O (1956) New or little known pselaphid beetles from southeastern United States. Journal of the Tennessee Academy of Science 31(1): 54–100.

Park O (1960) Cavernicolous pselaphid beetles of the United States. The American Midland Naturalist 64(1): 66–104. https://doi.org/10.2307/2422894

Swofford DL (2002) PAUP*. Phylogenetic Analysis Using Parsimony (*and Other Methods). Version 4.0a152. Sinauer Associates, Sunderland, Massachusetts.

## Supplementary material 1

**Specimen data for all material examined**

Authors: Michael S. Caterino, Laura M. Vásquez-Vélez

Data type: occurrence

Explanation note: This Excel file includes verbatim and interpreted (coordinate) data for all specimens of *Prespelea* examined.



Link: https://doi.org/10.3897/zookeys.685.13811.suppl1

## Supplementary material 2

**Phylogenetic character data**

Authors: Michael S. Caterino, Laura M. Vásquez-Vélez

Data type: character state

Explanation note: This nexus file includes morphological and molecular character data for species of Speleobamini and outgroups.



Link: https://doi.org/10.3897/zookeys.685.13811.suppl2

ZooKeys 685: 131–149 (2017)
doi: 10.3897/zookeys.685.13084
http://zookeys.pensoft.net

RESEARCH ARTICLE

A peer-reviewed open-access journal
ZooKeys
Launched to accelerate biodiversity research

# Geometric morphometrics analysis of the hind wing of leaf beetles: proximal and distal parts are separate modules

Jing Ren[1,2], Ming Bai[1], Xing-Ke Yang[1], Run-Zhi Zhang[1], Si-Qin Ge[1]

**1** *Key Laboratory of Zoological Systematics and Evolution, Institute of Zoology Chinese Academy of Sciences, Beijing, China* **2** *University of Chinese Academy of Sciences, Beijing, China*

Corresponding authors: *Run-Zhi Zhang* (zhangrz@ioz.ac.cn); *Si-Qin Ge* (gesq@ioz.ac.cn)

Academic editor: *M. Schmitt* | Received 5 April 2017 | Accepted 13 June 2017 | Published 20 July 2017

*http://zoobank.org/6310CBC5-93FA-4EDE-B8CB-13AEA5C42501*

**Citation:** Ren J, Bai M, Yang X-K, Zhang R-Z, Ge S-Q (2017) Geometric morphometrics analysis of the hind wing of leaf beetles: proximal and distal parts are separate modules. ZooKeys 685: 131–149. https://doi.org/10.3897/zookeys.685.13084

## Abstract

The success of beetles is mainly attributed to the possibility to hide the hindwings under the sclerotised elytra. The acquisition of the transverse folding function of the hind wing is an important event in the evolutionary history of beetles. In this study, the morphological and functional variances in the hind wings of 94 leaf beetle species (Coleoptera: Chrysomelinae) is explored using geometric morphometrics based on 36 landmarks. Principal component analysis and Canonical variate analysis indicate that changes of apical area, anal area, and middle area are three useful phylogenetic features at a subtribe level of leaf beetles. Variances of the apical area are the most obvious, which strongly influence the entire venation variance. Partial least squares analysis indicates that the proximal and distal parts of hind wings are weakly associated. Modularity tests confirm that the proximal and distal compartments of hind wings are separate modules. It is deduced that for leaf beetles, or even other beetles, the hind wing possibly exhibits significant functional divergences that occurred during the evolution of transverse folding that resulted in the proximal and distal compartments of hind wings evolving into separate functional modules.

## Keywords

Chrysomelinae, evolution, variance, venation, wing folding

## Introduction

Coleoptera (known as beetles) are the largest insect order, containing 380,000 named living species classified into more than 160 families (Mckenna et al. 2015); their success is partly attributed to the evolution of a tight exoskeletal shell that leaves no membranous areas exposed (Beutel and Haas 2000, Haas 2006). The fore wings of most beetles are hardened elytra which are not used for flight or to a very minor degree (in Archostemata), but mainly serve to form a protective cover for the hind part of the body (hind wings and abdomen) (Frantsevich 2011). As a part of this essential character complex of Coleoptera, a complicated hind wing folding mechanism has evolved (Beutel and Haas 2000, Haas 2006). As the flight organ, the hind wing must have a certain size to be aerodynamically functional, which makes them distinctly larger than the thickened fore wings (Haas et al. 2000).

Given that large and thin hind wings are vulnerable to damage, they must be folded not only longitudinally but also transversely to be stored below the elytra for protection during ground locomotion and especially when entering narrow spaces. The hind wings unfold only when needed, such as before flying (Muhammad et al. 2010, Truong et al. 2014). With flexed and folded wings, it is easier to hide, use small crevices and shelters against the impact of weather (e.g., wind and rain), and escape predators (Haas 2006). The fitness advantage is so great that transverse wing folding evolved in multiple insect orders (Coleoptera, Dermaptera, and some species of Blattodea) (Forbes 1926, Haas and Beutel 2001, Haas 2006, Beutel et al. 2014). In beetles, longitudinal folding was already present in the earliest stem-lineage representatives of the Lower Permian, whereas transverse folding evolved in the Middle Permian with the formation of a closed subelytral space (Beutel and Haas 2000).

The apical area of beetle's hind wings is folded under elytra when not flying. Transverse folding leads to some morphological changes of hind wings, for example, the wing size, but what additional changes are concomitant? In this study, the morphological variances of beetle hind wings were investigated using geometric morphometrics analysis based on Chrysomelinae beetles. Chrysomelinae beetles could be divided into two tribes, one is Timarchini which are not able to fly, hind wings are reduced or disappeared; the other is Chrysomelini which have functional hind wings (Seeno and Wilcox 1982).Since this study focuses on the wing variance, 96 specimens of tribe Chrysomelini (94 species, 81 genera, eleven subtribes) was collected to observe and analysis the hind wing variance. The typical hind wing of leaf beetles presented in the Figure 1. The hind wing was oblong and venation was simple. Usually, there were two main veins (R and M) and two cells (radial cell and cubitus-anal cell). Apical area is membrane. For some leaf beetles, there was a cross vein cv in the middle area of hind wings (Figure 2C). The wing variance was analysed based on the subtribe level. More importantly, the variation of wing venation caused by the transverse folding function was addressed based on geometric morphometrics analysis results.

Geometric morphometrics analysis approaches have been used successfully in evolutionary biology and systematics (Adams and Funk 1997, Klingenberg and McIntyre

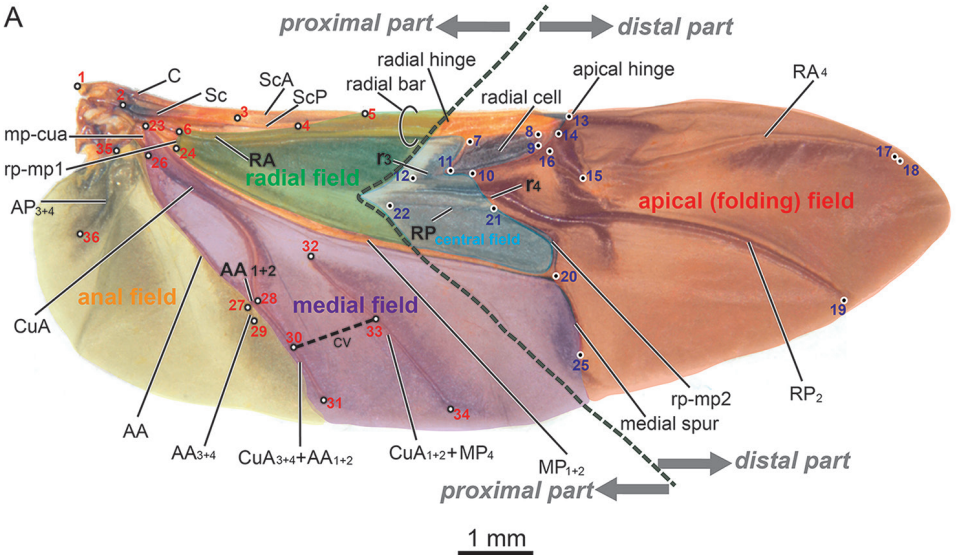


**Figure 1.** Leaf beetle hind wing (*Chrysomela populi* Linnaeus), with landmark locations (the dot with number), vein nomenclature and regional division. The nomenclature of the wing venation follows that of Kukalová-Peck & Lawrence (1993, 2004). Radial area: green, central area: blue, medial area: purple, anal area: yellow, apical (folding) area: red. Proximal part landmarks 1–6, 23, 24, and 26–36 mainly include radial, medial, and anal areas; distal part landmarks 7–22 and 25 include the central area, radial cell, and apical area. Abbreviations: Costa (C), Subcosta (Sc), Subcosta Anterior (ScA), Subcosta Posterior (ScP), Radius Anterior (RA), Radius Posterior (RP), Radial cross veins (r3, r4), Media Posterior (MP), Radio-medial cross veins (rp-mp1, rp-mp2), medial cross vein (cv), Cubitus Anterior (CuA), Medio-cubital Cross-vein or Arculus (mp-cua), Anal Anterior (AA), Anal posterior (AP). "+" indicates fused veins. The sub-number of veins reflects vein branches.

1998, Klingenberg and Zaklan 2000, Shipunov and Bateman 2005, Herrel and O'Reilly 2006, Villemant et al. 2007, Wappler et al. 2012, Catalano et al. 2015, Outomuro and Johansson 2015, Werneburg et al. 2015). Mitteroecker and Gunz (2009) summarised the advances in geometric morphometrics. The geometric morphometric revolution has added to the sophistication of quantitative biological shape analysis while simultaneously simplifying data collection and analysis to answer phenotypic questions, including those related to shape (Mitteroecker and Gunz 2009, Lawing and Polly 2010). Using geometric morphometrics analysis, studies of the morphological variances of insect wings are the most commonplace (Klingenberg and Zaklan 2000, Villemant et al. 2007, Bai et al. 2011, Bai et al. 2012, Wappler et al. 2012, Krosch et al. 2013, Lorenz and Suesdek 2013, McCane 2013, Outomuro et al. 2013a, b). Most of these studies have focused on phylogenetic or taxonomic problems. Examples of geometric morphometrics applied to the morphology-function of wings are few. In this investigation, using geometric morphometrics analysis, Chrysomelinae beetle hind wings were investigated to explore their functional and morphological variances, especially for the apical area.

## Materials and methods

### Samples

This study was based on hind wing images (see Suppl. material 1) of 96 specimens (eleven subtribes, 81 genera, 94 species) of Chrysomelinae (Coleoptera, Chrysomelidae) to obtain landmark data. There were 94 species, 81 genera included in this study; each genus included one to three species. There was two species with two specimens from different geographical locations. There were 96 specimens in 94 species. The leaf beetle specimens were deposited in the Institute of Zoology, Chinese Academy of Sciences. The specimens were examined and dissected to obtain hind wings using a LEICA MZ 12.5 dissecting microscope. Pictures of the wings were obtained with a D500s Nikon camera connected to a stereoscope (Zeiss Stereo Discovery V12). The collection and subtribe information of 96 leaf beetle specimens is presented in Suppl. material 2.

### Landmark digitising

The tpsUtil (Version 1.44, Copyright 2009, F. James Rohlf, Ecology & Evolution, SUNY at Stony Brook) and tpsDig (Version 2.12, Copyright 2008 F. James Rohlf, Ecology & Evolution, SUNY at Stony Brook) software programs were used for digitising landmarks. Figure 1 illustrates the nomenclature of hind wing venation in chrysomelid and the location of 36 landmarks selected for the analysis. The locations of landmarks were chosen based on the intersection of veins or vein base, vein end or apex. The "anterior", "posterior", "proximal", and "distal" veins or plates were used to describe the detailed position of landmarks. If a landmark did not exist on a certain wing, this landmark overlapped with next existing landmark. For example, specimen 70 (*Chrysomela populi* Linnaeus, Figure 1), landmark 30 and 33 didn't not exist, then the landmark 30 overlapped with the next existing landmark 31, landmark 33 overlapped with landmark 34. The position description of landmarks is presented in Table 1. The landmark coordinate data are presented in Suppl. material 3. The nomenclature of the wing venation followed that of Kukalová-Peck and Lawrence (1993, 2004).

### Data analysis

MorphoJ (Version 1.06d) was used for landmark data analyses. MorphoJ is a software package enabling geometric morphometric analysis for two- and three-dimensional landmark data and designed for the analysis of actual biological data (Klingenberg 2011). Prior to further analyses, the landmark data (Suppl. material 3) of wings were imported into MorphoJ, and a complete Procrustes fit was conducted by orthogonal projection to correct size and orientation.

**Table 1.** Landmark position description.

| Landmark # | Position Description |
|---|---|
| 1 | Proximal anterior point of humeral plate (HP) |
| 2 | The crossing point of BSc and Sc |
| 3 | The point of Sc getting to bifurcate into ScA and ScP |
| 4 | The crossing point of ScP and RA |
| 5 | The crossing point of ScA and RA |
| 6 | The crossing point of rp-m1 and RA |
| 7 | Proximal anterior point of radial cell |
| 8 | Distal anterior point of radial cell |
| 9 | Distal posterior point of radial cell |
| 10 | Anterior point of r4 (or the crossing point of r4 and radial cell) |
| 11 | Proximal posterior point of radial cell |
| 12 | Proximal point of r3 |
| 13 | Apical hinge |
| 14 | The anterior point of triangular area of radial cell's distal side |
| 15 | The posterior point of triangular area of radial cell's distal side |
| 16 | The proximal point of triangular area of radial cell's distal side |
| 17 | The distal point of $RA_4$ |
| 18 | The distal point of $RA_1$ |
| 19 | The distal point of $RP_2$ |
| 20 | The point of $MP_{1+2}$ getting to bifurcate |
| 21 | The posterior point of r4, or the crossing point of r4 and rp-mp2 |
| 22 | The proximal point of RP |
| 23 | Anterior point of mp-cua |
| 24 | The crossing point of rm-mp1and MP |
| 25 | The posterior of medial spur |
| 26 | Posterior point of mp-cua |
| 27 | The point of AA getting to bifurcate |
| 28 | The point of $AA_{1+2}$ getting to fuse with $CuA_{3+4}$ |
| 29 | The posterior or distal point of $AA_{3+4}$ |
| 30 | The proximal point of cv |
| 31 | The posterior or distal point of $AA_{1+2}$+$CuA_{3+4}$ |
| 32 | Anterior point of $CuA_{1+2}$+$MP_4$ |
| 33 | The distal point of cv |
| 34 | Posterior point of $CuA_{1+2}$+$MP_4$ |
| 35 | The base point of $AP_{3+4}$ |
| 36 | The posterior point of $AP_{3+4}$ |

Principal component analysis (PCA): PCA is one of the most widely used methods for exploratory multivariate analysis (Klingenberg and McIntyre 1998, Klingenberg and Zaklan 2000). In this study, MorphoJ generates covariance matrices from landmark

datasets of 96 specimens after Procrustes superimposition. Based on the covariance matrices, PCA was used to analyse and display the patterns of covariation of positions of landmarks throughout the wing. Principal components (PCs) are visualised directly as patterns of simultaneous displacements of landmarks in relation to one another.

Canonical variate analysis (CVA): CVA is a method used to find the shape features that best distinguish among multiple groups of specimens (Gumiel et al. 2003, Villemant et al. 2007). Group membership is a known priori. In this study, the subtribe was set as the known *a proiri* to test the phylogenetic implications of the wing features from PCV results. In the current data, there were 89 specimens (76 genera, 88 species) could be definitely divided into eleven subtribes; the left seven specimens (five genera, six species) had no clear subtribe information (Suppl. material 2). CVA based on the 89 specimens was used to explore the wing variance on subtribe level of leaf beetles.

Partial least squares (PLS) analysis: MorphoJ offers an implementation of PLS analysis between blocks of landmarks within the same configuration. This analysis identifies the features of shape variation that most strongly co-vary between the blocks and indicates their relative contribution to the total covariation between blocks (Rohlf and Corti 2000, Klingenberg et al. 2003, Klingenberg 2009). The hind wing was divided into two parts based on the transverse folding function of 96 beetles: landmarks 1–6, 23–24 and 26–36 served as the proximal part; landmarks 7–22 and 25 relevant to apical transverse folding served as the distal part. There were 10,000 permutation test rounds. The *RV* coefficient was used as a measure of overall covariation between blocks; this coefficient is a multivariate analogue of the squared correlation coefficient between two variables. When the *RV* coefficient values (between 0 and 1) are lower (< 0.5), the covariance of the two blocks is weak. The *RV* coefficient provided by this procedure is the same as that in the output from tests of modularity hypotheses (Escoufier 1973; Klingenberg 2009).

Modularity test: MorphoJ implements a method to evaluate hypotheses of modularity (Klingenberg 2009). Modularity is an important principle of organisation in biological systems that is also manifested at the morphological level (Klingenberg 2008). The hypothesis of independent variation in the proximal and distal wing parts as two modules (in terms of PLS analysis) was evaluated. MorphoJ can compare the strength of covariation between two partitions and either all or a large number of the possible alternative partitions with the same numbers of landmarks as in the hypothesised modules (Klingenberg 2009). Similar to PLS analysis, the *RV* coefficient is used as a measure of overall covariation between modules. If the hypothesis of modularity holds, the *RV* coefficient for the partition according to the hypothesis should be the lowest value, or it should at least be close the lower extreme of the distribution of *RV* coefficients for all of the partitions (Klingenberg 2009). Here, based on the two blocks of PLS, the configuration of 36 landmarks was partitioned into two subsets: one subset with 19 landmarks (1–6, 23–24, 26–36) and the other with 17 landmarks (7–22, 25). In our case, the total number of different partitions into subsets was approximately $9\times10^9$ (Klingenberg 2009). However, landmark configurations with more than 20 landmarks may not be computationally feasible (Klingenberg 2009). Therefore, the random parti-

tions of the configuration into subsets of the appropriate number of landmarks can be used instead. The recommended number of random partitions is in the order of $10^4$ for the comparison, which should provide a reasonable characterisation of the distribution of the *RV* coefficient (Klingenberg 2009). In this study, random partitions in the order of 10,000 and 1,000,000 were implemented, with contiguous partitions only.

## Results

### PCA and CVA results

In geometric morphometrics, allometry is widely characterised by multivariate regression of shape on size (usually centroid size or log-transformed centroid size); such regressions often fit the data well and the allometric shape changes tend to affect the entire structures (Klingenberg and Marugán-Lobón 2013). The Procrustes Fit was used to correct the size and orientation of wings. The Procrustes fit procedure adds a data matrix with the Centroid size to the dataset (Figure 2A). Based on Figure 2A, the 36 landmarks were reasonable to analysis the wing variance.

Based on the Procrustes fit data, PCA was carried out based on 96 specimens. The accumulative contribution ratio of the first three components was 68.04%, potentially indicating that the first three components represented the main shape variation of wing venation. Figure 2B shows that the first three PC shape changes. PC1 (with a variance contribution ratio of 45.01%) primarily affected the size of apical area of hind wing. PC1 (-) shows that landmarks 7–16, 20–22, and 25 moved distally, whereas landmarks 17–19 moved proximally, producing a smaller and shorter apical part. In addition, landmarks 1–4, 6, 23–24, 26, and 35 moved proximally, which made the radial and medial area smaller and shorter. Altogether, these changes produced a relatively smaller and shorter apical area of the hind wing. Similarly, PC1 (+) exhibited a relative larger and longer apical area of the hind wing. Therefore, the PC1 is better described as the variation of the relative size of the apical area of the hind wing between a larger and longer or a smaller and shorter apical area. PC2 (with a variance contribution ratio of 12.39%) primarily affected the size of the medial area of the hind wing by movements of landmarks 30 and 33 towards or away between landmarks 28, 32 and 31, 34, which presented the relative location and length of the cross vein cv or whether existed. In addition, landmark 29 exhibited a long variance distance, indicating the length of $AA_{3+4}$. PC3 (with a variance contribution ratio of 10.56%) primarily affected the size of the anal area by the movement of landmarks 20, 22, 25, 29–34 and 36. To different degrees, both PC2 and PC3 affected the relative size of the apical area by moving proximal part landmarks 1–6, 24, 26, and 35 and distal part landmarks 17–19. Thus, when PC1, 2, and 3 are integrated, it was concluded that there were three features of the wing variance of leaf beetles: the relative size of the apical area which could be considered the main feature (variance contribution ratio of 45.01%) to influence of the overall variance of the hind wing, the changes of cross vein cv in the middle area, and relative size of the anal area size.

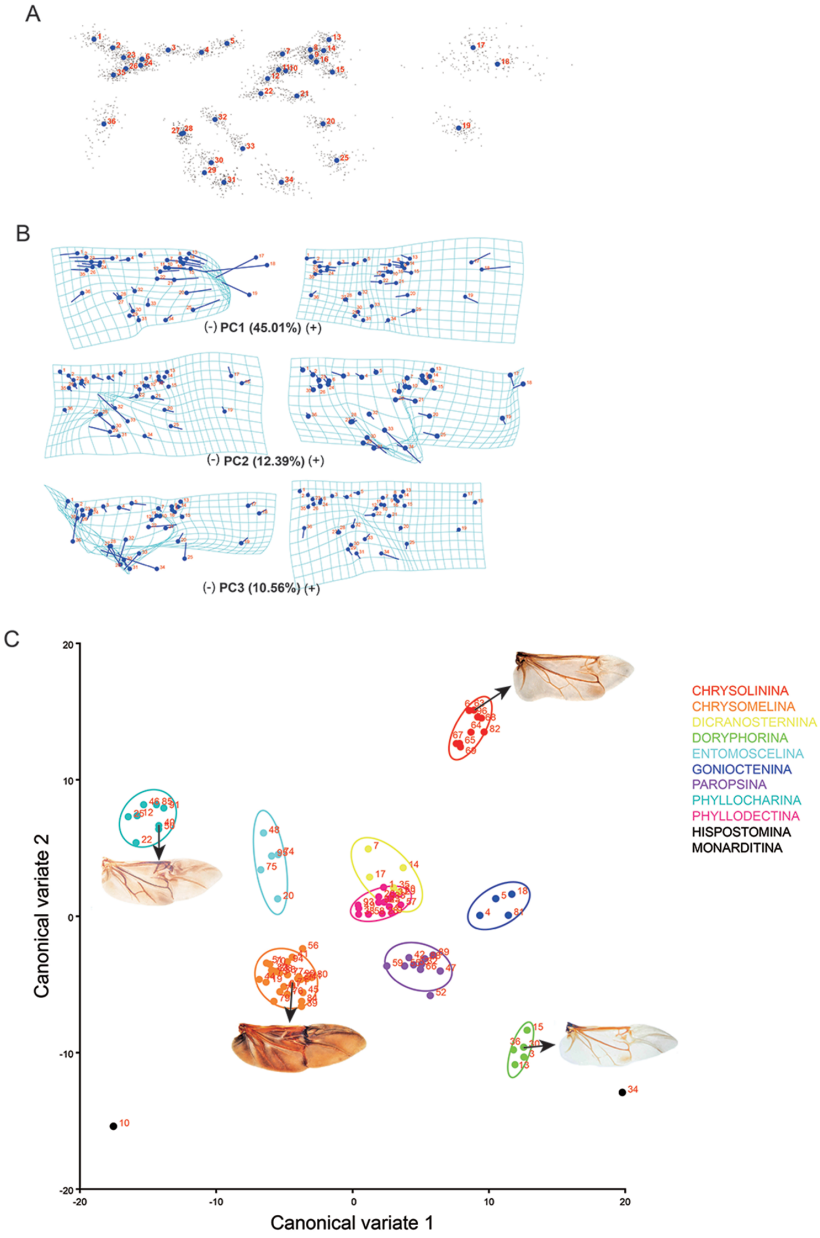


**Figure 2.** PCA and CVA results. **A** Centroid size graph of hind wing landmarks (Procrustes fit) **B** PCA results, the shape changes associated with the first three PCs: the relative size of the apical area which could be considered the main feature (variance contribution ratio was 45.01%) to influence of the overall variance of the hind wing, the changes of cross vein cv in the middle area (variance contribution ratio was 12.39%), and relative size of the anal area size (variance contribution ratio was 10.56%) **C** CVA results, the axis of CV1 and CV2 presented the first two large shape variance of all variance; points with different colours indicated different subtribes' specimens; the ellipse is presented as an equal-frequency ellipse with a given probability level of 90%, which contains approximately 90% of the data points.

Based on the PCA wing variance results, CVA was used to test whether the three features were useful on the distinguishing of the subtribe level. There were eleven subtribes (89 specimens) of Chrysomelinae involved in this study, except subtribe Hispostomina and Monarditina have one specimen for each (sample size is too small, there were no statistical significance); the left have 4–26 specimens for each subtribes. Iin CVA, there were nine subtribes with enough samples to do analysis. As the Figure 2C showed, the axis of CV1 and CV2 presented the first two large shape variance of all variance; points with different colour indicated different subtribes' specimens; the ellipse is presented as an equal-frequency ellipse with a given probability level of 90%, which contains approximately 90% of the data points. The CVA result showed, in the nine subtribes, Dicranosternina and Phyllodectina couldn't be divided based on wing shape data; these two subtribes were overlapped. The other seven subtribes could be divided clearly. Especially for subtribes distributing in the edge of coordinates (with big Mahalanobis distances each other): Chrysolinina, Chrysomelina, Doryphorina, and Phyllocharina, the four subtribes showed big large variances on wing shape. The wing difference between each other could be described as qualitative features. The typical hind wing images of the four subtribes were presented as the Figure 2C showing. Chrysolinina beetles have a shorter apical area and cross vein cv in the middle area; while Chrysomelina beetles have longer apical area and no cross vein cv. Doryphorina beetles have a wide anal area and no cross vein cv; while Phyllocharina have a narrow anal area and cross vein cv in the middle area. Doryphorina and Phyllocharina mainly distributed along the axis of CV1 which had a big variance contribution ratio 40.19%; Chrysolinina and Chrysomelina speciemns mainly distributed along the axis of CV2 which had a second big variance contribution ratio 27.83%. It was concluded that the relative size of the apical area and anal area, and cross vein cv in the middles area, could play an important role in the division of these 4 subtribes. For subtribes Entomoscelina, Gonioctenina, and Paropsina, the wing variance also focused on the apical area, anal area and cross vein cv. These three subtribes distributed in the central region of coordinates (Mahalanobis distances are relatively small between each other); the difference between each other is quantitative and is hard to describe as qualitative features.

**PLS analysis and modularity test of the proximal and distal part of the hind wing**

The apical area of the hind wings of beetles can be folded transversely under elytra (Forbes 1926). Both PCA and CVA showed that the apical area of wings has a large variance. These results prompted us to test whether the apical area had a relatively independent shape change in hind wing shape variances. The apical and central area and radical cells of hind wings (Figure 1) are involved in transverse folding in beetles. The landmarks involving transverse folding were selected as a block; all of the other landmarks composed a second block. PLS analysis of covariation within a configuration of landmarks 1–6, 23–24 and 26–36 as the proximal part and landmarks relevant to transverse folding 7–22 and 25 as the distal part (Figure 1) was performed to test the null hypothesis: no independent shape changes between the proximal and distal parts of the hind wing.

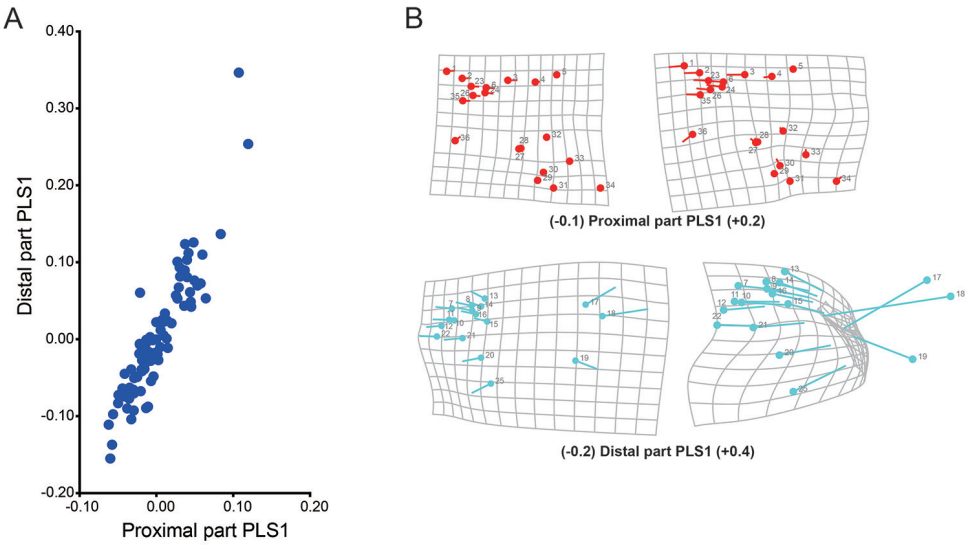


**Figure 3.** PLS analysis results. **A** Scatter plot of the PLS1 of two blocks **B** Shape changes associated with the first PLS axes of two blocks: each diagram shows the block change along the PLS1 in the positive or negative direction, corresponding to Figure 3A.

PLS1 presented 87.22% of the total covariance, indicating that PLS1 represented the main covariance of two blocks. Figure 3A shows scatter plot of the PLS1 of two blocks; Figure 3B presents the shape changes of two blocks based on PLS1 scores. The shape variance of proximal part is more conservative with distal part variance. For PLS1, the pairwise correlation between blocks was up to 0.92 (P=0.0016, 10,000 permutation test rounds), as noted in the plots distributed around the diagonal line of the PLS1 scores coordinate in Figure 3A. However, the *RV* coefficient was only 0.44, indicating that the overall strength of association between blocks was relatively weak (P<0.001, 10,000 randomisation rounds). When the *RV* coefficient values are higher, the covariance of two blocks is stronger. Therefore, the null hypothesis was rejected. Although high correlation was noted between two blocks, the overall strength of association between blocks was weak. From the analysis results, the following was concluded: in beetle hind wings, the distal part, or more precisely the areas relevant to transverse folding (apical area, central area and radial cell of hind wing) exhibits both a certain degree of independence and a high correlation between other parts of wings in the total hind wing shape variances.

Based on the PLS analysis results, a modularity analysis was performed to evaluate whether the proximal and the distal parts of beetle hind wings are separate modules. In the same manner, the landmarks 7–22 and 25 involving transverse folding were extracted as the distal part and the remaining landmarks 1–6, 23–24 and 26–36 as the proximal part, which was our hypothesised partition (Figure 4A). Contiguous partitions were considered with 10,000 and 1,000,000 random partitions. The *RV* coefficient of

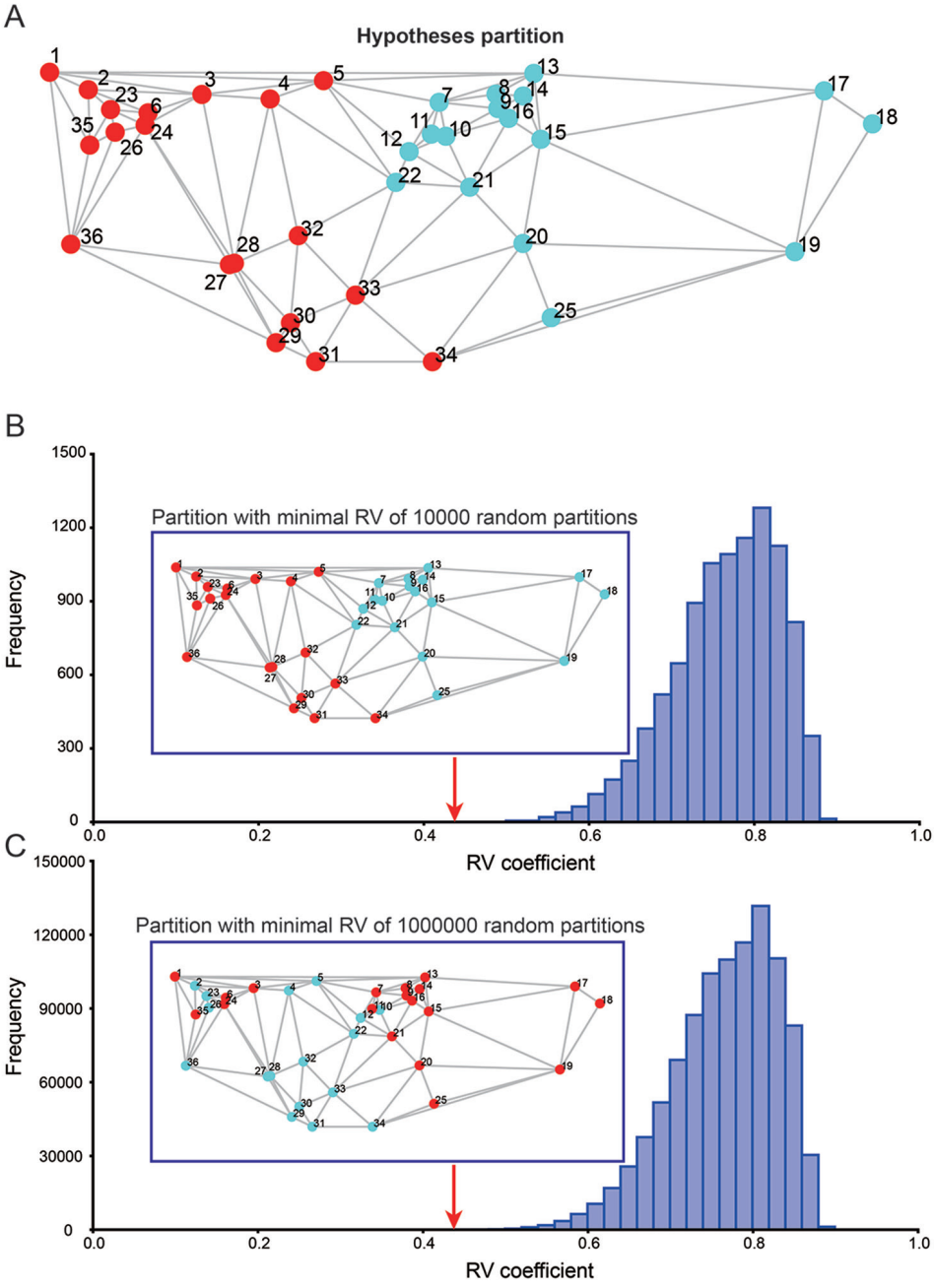


**Figure 4.** Modularity test results. **A** The hypothesized partition: proximal part landmarks 1-6, 23, 24, and 26–36 and distal part landmarks 7–22, 25; different colour presents different modules **B** The partition with minimal covariance in all evaluated $10^4$ partitions by *RV* coefficient **C** The partition with minimal covariance in all evaluated $10^6$ partitions by *RV* coefficient.

the a priori hypothesis partition was 0.44, which was identical to that of the PLS analysis. The 10,000 random partition result showed that there are no partitions with an *RV* less than or equal to the a priori hypothesis. The minimal *RV* coefficient partition of 10,000 random partitions was our hypothesis (Figure 4B). Thus, our null hypothesis partition was not rejected; the proximal and distal parts of the hind wing had minimal covariance in all evaluated 10,000 partitions. The 1,000,000 random partition result revealed ten partitions with a *RV* less than or equal to the a priori hypothesis. The minimal *RV* coefficient of 1,000,000 random partitions was 0.41 (Figure 4C). The partition with minimal *RV* is presented in Figure 4C. However, our null hypothesis was still accepted, because the minimal *RV* was close to the *RV* of the hypothesis partition and because the partition with minimal *RV* was similar to our hypothesis partition. Therefore, the proximal and distal parts of the beetle's hind wing are separate modules.

## Discussion

### Phylogenetic implications

The powerful visualisation tools of geometric morphometrics and the typical large amount of shape variables give rise to a specific exploratory style of analysis, allowing the identification and quantification of previously unknown shape features (Mitteroecker and Gunz 2009).

In this study, it was mainly focused on the wing variance of different species based on subtribe level of leaf beetles. Three main features of leaf beetle's hind wing variance based on PCA results (Figure 2B) were concluded. All the three features were useful phylogenetic features on subtribe level by CVA testing. Based on PCV and CVA results, the apical area of hind wing presented large variance and could be useful morphological features to distinguishing the subtribe Chrysolinina and Chrysomelina. The anal area was also useful to distinguishing the subtribe Doryphorina and Phyllocharina. The changes of cross vein cv in the middle area were also useful in the subtribe level distinguishing.

The PCA results presented three phylogenetic features of hind wings of leaf beetles, and the changes of apical area was the most obvious (variance contribution ratio was 45.01%, Figure 2B). Subtribe Chrysolinina beetles have a very short apical area in their hind wings (Figure 2C). Compare with Chrysolinina, subtribe Chrysomelina beetles have a long and big apical area in their hind wings (Figure 2C). What is the role of apical area in wing evolution is still unclear. It's worth to pay more attentions on the apical area of hind wings to explore answers.

### Functional and morphological implications

In our study, PLS analysis showed that the distal part of hind wing, which is involved in transverse folding and includes the apical area, central area, and radial cell, exhib-

ited independent shape variance in the total variance of the hind wing (Figure 3). A modularity test was used to confirm that are the distal and proximal parts of the hind wing consisted of two modules (Figure 4). Modules are units exhibiting a high degree of integration from many or strong interactions but relative independence from other such units (Klingenberg 2008, 2009, 2011). For a morphometric analysis, these interactions should be manifested as strong covariation among parts within modules and weak covariation between modules (Klingenberg 2009, 2014); thus, the PLS analysis is reasonable in our study. The PLS analysis suggests that proximal and distal parts of chrysomelid hind wings have weak between-module integration (i.e., a low *RV* coefficient of 0.44) but strong within-module integration (i.e., a high correlation of 0.92). Based on the PLS analysis results, a modularity test to verify the hypothesis regarding partitioning as noted in Figure 4A was performed. The partition with a minimal *RV* coefficient of all evaluated partitions does fit with our hypothesised partition: the proximal and distal parts of hind wing are separate modules.

Various studies of *Drosophila*'s wings using morphometric approaches have addressed the question of whether anterior and posterior wing compartments are distinct modules reflecting phenotypic and genetic variation (Thompson and Woodruff 1982, Cavicchi et al. 1985, Cowley and Atchley 1990, Guerra et al. 1997, Baylac and Penin 1998, Klingenberg and Zaklan 2000). Based on correspondences to distinct cell lineages and domains of gene expression (Escoufier 1973, Lawrence and Morata 1976), the subdivision of wings into anterior and posterior compartments has been given special attention in *Drosophila*. However, Klingenberg and Zaklan (2000) used geometric morphometrics analysis and found that the covariation between landmarks in the anterior and posterior compartments are not weaker than expected for an arbitrary partition of the wing into two subsets of landmarks. This finding clearly contrasts with the conclusions of earlier studies that support the hypothesis that the anterior and posterior compartments are separate developmental modules.

What is the nature of the modularity interactions of hind wings? Generally, it can be developmental, functional, or genetic (Klingenberg 2008, 2009, 2011). Here, all of our hypotheses are based on the transverse folding function of the beetle hind wing. It's thus concluded that the proximal and distal parts of hind wings are separate functional modules and that this separation is caused by the transverse folding function of a beetle's hind wing. The veins of the distal part of the hind wings are mainly radial veins ($RA_4$, RP, $RP_2$ and radial cell, see Figure 1), and some veins of the proximal part are also radial veins (RA and radial bar, see Figure 1). Thus, the landmarks of both proximal and distal compartments are mainly derived from radial veins, indicating that the two compartments of hind wings are rarely separate developmental or genetic modules. This finding is likely related with the necessity to fold the hind wings transversely for complete storage below the elytra.

The separate modules of proximal and distal parts of Chrysomelid hind wings have been tested. The main reason of the separate modules could be attribute to its special function: transverse folding in hind wings of beetles. Although there were only 96 chrysomelid beetles considered in our study, it could be believed that other beetles feature the same modularity of hind wings, given that the transverse folding of the hind

wing is a common feature of beetles. However, more data are needed to confirm this hypothesis. Here, the apical part of the hind wings of leaf beetles has an important influence on hind wing shape variance by PCA (Figure 2B). The shape variance of the apical part of the hind wing in all beetles (not exclusively leaf beetles) should be given more attention in studies of wings or flight. In particular, what effect could the relative size of the apical part have on beetle flying, folding function or phylogeny? What type of role does it play in wing evolution? These questions require more work to find the answers.

## Conclusion

Taking the PCA, CVA, PLS analyses and the modularity test into account, it was concluded that areas of the beetle hind wing relevant to transverse folding importantly influence hind wing shape variances and are relatively independent. In addition, the proximal and distal parts of a beetle's hind wing are separate modules. The changes of apical area, anal area and middle area of hind wings were useful features to distinguishing subtribe level of leaf beetles. For beetles, hind wing folding is a morphological and functional compromise between fore wing evolution to elytra and the maintenance of hind wing flying function. This separate function modules could allow the hind wings to be folded at rest and to unfold when flying. In addition, the separate function could explain why beetles are the most prosperous animals in evolution. Our discovery could provide the theoretical basis and a new perspective for studies of the morphological evolution of wings and wing folding mechanisms.

## Author contributions

Experiments were planned by Jing Ren, Si-Qin Ge, and Run-Zhi Zhang. Species identification was completed by Si-Qin Ge. Experiments were conducted by Jing Ren. Analysis and interpretation of the results was performed by Jing Ren, Ming Bai, Run-Zhi Zhang, and Xing-Ke Yang. The paper was written by Jing Ren, Si-Qin Ge, and Run-Zhi Zhang.

## Conflict of interest

All authors declare there are no potential competing interests.

## Acknowledgements

We are very grateful to Professor Christian Peter Klingenberg (Faculty of Life Sciences, University of Manchester, Manchester, United Kingdom) for providing technical guidance

of MorphoJ software and are very grateful to Adam Ślipiński (CSIRO Ecosystem Sciences, Australian National Insect Collection, Canberra, Australia) and Mauro Daccordi (Museo Civico di Storia Naturale, Verona, Italy) for loaning a portion of the research specimens. The project is partly supported by grants from the National Science Foundation of China (Grant Nos. 31472028, 31672345, 31672347).

## References

Adams DC, Funk DJ (1997) Morphometric inferences on sibling species and sexual dimorphism in *Neochlamisus bebbianae* leaf beetles: multivariate applications of the thin-plate spline. Systematic Biology 46(1): 180–194. https://doi.org/10.1093/sysbio/46.1.180

Bai M, Beutel RG, Song KQ, Liu WG, Malqin H, Li S, Hu XY, Yang XK (2012) Evolutionary patterns of hind wing morphology in dung beetles (Coleoptera: Scarabaeinae). Arthropod Structure & Development 41(5): 505–513. https://doi.org/10.1016/j.asd.2012.05.004

Bai M, McCullough E, Song KQ, Liu WG, Yang XK (2011) Evolutionary constraints in hind wing shape in chinese dung beetles (Coleoptera: Scarabaeinae). PLoS One 6 (6): e21600. https://doi.org/10.1371/journal.pone.0021600

Baylac M, Penin X (1998) Wing static allometry in *Drosophila simulans* males (Diptera, Drosophilidae) and its relationships with developmental compartments. Acta Zoologica Academiae Scientiarum Hungaricae 44(1-2): 97–112.

Beutel RG, Friedrich F, Yang X-K, Ge S-Q (2014) Insect morphology and phylogeny: A textbook for students of entomology. Walter de Gruyter GmbH, Berlin/Boston, 115–146.

Beutel RG, Haas F (2000) Phylogenetic relationships of the suborders of Coleoptera (Insecta). Cladistics 16(1): 103–141. https://doi.org/10.1006/clad.1999.0124

Catalano SA, Ercoli MD, Prevosti FJ (2015) The more, the better: the use of multiple landmark configurations to solve the phylogenetic relationships in musteloids. Systematic Biology 64(2): 294–306. https://doi.org/10.1093/sysbio/syu107

Cavicchi S, Guerra D, Giorgi G, Pezzoli C (1985) Temperature-related divergence in experimental populations of *Drosophila melanogaster*. I. Genetic and developmental basis of wing size and shape variation. Genetics 109: 665–689.

Cowley DE, Atchley WR (1990) Development and quantitative genetics of correlation structure among body parts of *Drosophila melanogaster*. American Naturalist 135(2): 242–268. https://doi.org/10.1086/285041

Escoufier Y (1973) Le traitement des variables vectorielles. Biometrics 29: 751–760. https://doi.org/10.2307/2529140

Forbes WT (1926) The wing folding patterns of the Coleoptera. Journal of the New York Entomological Society 34(1): 42–68.

Frantsevich L (2011) Mechanisms modeling the double rotation of the elytra in beetles (Coleoptera). Journal of Bionic Engineering 8(4): 395–405. https://doi.org/10.1016/s1672-6529(11)60045-0

Guerra D, Pezzoli MC, Giorgi G, Garoia F, Cavicchi S (1997) Developmental constraints in the *Drosophila* wing. Heredity 79(6). https://doi.org/10.1038/sj.hdy.6882490

Gumiel M, Catalá S, Noireau F, Rojas De Arias A, García A, Dujardin JP (2003) Wing geometry in *Triatoma infestans* (Klug) and *T. melanosoma* Martinez, Olmedo & Carcavallo (Hemiptera: Reduviidae). Systematic Entomology 28(2): 173–180. https://doi.org/10.1046/j.1365-3113.2003.00206.x

Haas F (2006) Evidence from folding and functional lines of wings on inter-ordinal relationships in Pterygota. Arthropod Systematics & Phylogeny 64(2): 149–158.

Haas F, Beutel RG (2001) Wing folding and the functional morphology of the wing base in Coleoptera. Zoology 104(2): 123–141. https://doi.org/10.1078/0944-2006-00017

Haas F, Gorb S, Blickhan R (2000) The function of resilin in beetle wings. Proceedings of The Royal Society B-Biological Sciences 267(1451): 1375–1381. https://doi.org/10.1098/rspb.2000.1153

Herrel A, O'Reilly CJ (2006) Ontogenetic scaling of bite force in lizards and turtles. Physiological and Biochemical Zoology 79(1): 31–42. doi: doi:10.1086/498193

Klingenberg CP (2008) Morphological integration and developmental modularity. Annual Review of Ecology, Evolution, and Systematics 39: 115–132. https://doi.org/10.1146/annurev.ecolsys.37.091305.110054

Klingenberg CP (2009) Morphometric integration and modularity in configurations of landmarks: Tools for evaluating a priori hypotheses. Evolution & Development 11(4): 405–421. https://doi.org/10.1111/j.1525-142x.2009.00347.x

Klingenberg CP (2011) Morphoj: An integrated software package for geometric morphometrics. Molecular Ecology Resources 11(2): 353–357. https://doi.org/10.1111/j.1755-0998.2010.02924.x

Klingenberg CP, Marugán-Lobón J (2013) Shape variation in outline shapes. Systematic Biology 62(1): 134–46. https://doi.org/10.1093/sysbio/sys080

Klingenberg CP (2014) Studying morphological integration and modularity at multiple levels: concepts and analysis. Philosophical Transactions of the Royal Society B: Biological Sciences 369(1649): 20130249. https://doi.org/10.1098/rstb.2013.0249

Klingenberg CP, McIntyre GS (1998) Geometric morphometrics of developmental instability: analyzing patterns of fluctuating asymmetry with procrustes methods. Evolution 52: 1363–1375. https://doi.org/10.2307/2411306

Klingenberg CP, Mebus K, Auffray JC (2003) Developmental integration in a complex morphological structure: how distinct are the modules in the mouse mandible? Evolution & Development 5(5): 522–531. https://doi.org/10.1046/j.1525-142X.2003.03057.x

Klingenberg CP, Zaklan SD (2000) Morphological integration between developmental compartments in the *Drosophila* wing. Evolution 54(4): 1273–1285. https://doi.org/10.1554/00-14-3820(2000)054[1273:mibdci]2.0.co;2

Krosch MN, Schutze MK, Armstrong KF, Boontop Y, Boykin LM, Chapman TA, Englezou A, Cameron SL, Clarke AR (2013) Piecing together an integrative taxonomic puzzle: microsatellite, wing shape and aedeagus length analyses of *Bactrocera dorsalis s.l.*(Diptera: Tephritidae) find no evidence of multiple lineages in a proposed contact zone along the Thai/Malay Peninsula. Systematic Entomology 38(1): 2–13. https://doi.org/10.1111/j.1365-3113.2012.00643.x

Kukalová-Peck J, Lawrence JF (1993) Evolution of the hind wing in Coleoptera. Canadian Entomologist 125(02): 181–258. https://doi.org/10.4039/ent125181-2

Kukalová-Peck J, Lawrence JF (2004) Relationships among Coleopteran suborders and major endoneopteran lineages: Evidence from hind wing characters. European Journal of Entomology 101(1): 95–144. https://doi.org/10.14411/eje.2004.018

Lawing AM, Polly PD (2010) Geometric morphometrics: recent applications to the study of evolution and development. Journal of Zoology 280(1): 1–7. https://doi.org/10.1111/j.1469-7998.2009.00620.x

Lawrence P, Morata G (1976) Compartments in the wing of *Drosophila*: a study of the engrailed gene. Developmental Biology 50(2): 321–337.

Lorenz C, Suesdek L (2013) Evaluation of chemical preparation on insect wing shape for geometric morphometrics. American Journal of Tropical Medicine and Hygiene 89(5): 928–931. https://doi.org/10.4269/ajtmh.13-0359

McCane B (2013) Shape variation in outline shapes. Systematic Biology 62(1): 134–146. https://doi.org/10.1093/sysbio/sys080

Mckenna DD, Wild AL, Kanda K, Bellamy CL, Beutel RG, Caterino MS, Farnum CW, Hawks DC, Ivie MA, Jameson ML (2015) The beetle tree of life reveals that Coleoptera survived end-Permian mass extinction to diversify during the Cretaceous terrestrial revolution. Systematic Entomology 40(4): 835–880.

Mitteroecker P, Gunz P (2009) Advances in geometric morphometrics. Evolutionary Biology 36(2): 235–247. https://doi.org/10.1007/s11692-009-9055-x

Muhammad A, Nguyen QV, Park HC, Hwang DY, Byun D, Goo NS (2010) Improvement of artificial foldable wing models by mimicking the unfolding/folding mechanism of a beetle hind wing. Journal of Bionic Engineering 7(2): 134–141. https://doi.org/10.1016/s1672-6529(09)60185-2

Outomuro D, Adams DC, Johansson F (2013a) The evolution of wing shape in ornamented-winged damselflies (Calopterygidae, Odonata). Evolutionary Biology 40(2): 300–309. https://doi.org/10.1007/s11692-012-9214-3

Outomuro D, Adams DC, Johansson F (2013b) Wing shape allometry and aerodynamics in calopterygid damselflies: a comparative approach. BMC Evolutionary Biology 13(1): 118. https://doi.org/10.1186/1471-2148-13-118

Outomuro D, Johansson F (2015) Bird predation selects for wing shape and coloration in a damselfly. Journal of Evolutionary Biology 28(4): 791–799. https://doi.org/10.1111/jeb.12605

Rohlf FJ, Corti M (2000) Use of two-block partial least-squares to study covariation in shape. Systematic Biology 49(4): 740–753. https://doi.org/10.1080/106351500750049806

Seeno TN, Wilcox JA (1982) Leaf beetles genera (Coleoptera: Chrysomelidae).Entomography publications. Sacramento, California, 71–76.

Shipunov AB, Bateman RM (2005) Geometric morphometrics as a tool for understanding *Dactylorhiza* (Orchidaceae) diversity in European Russia. Biological Journal of the Linnean Society 85(1): 1–12. https://doi.org/10.1111/j.1095-8312.2005.00468.x

Thompson Jr J, Woodruff R (1982) Polygenic analysis of pattern formation: interdependence among veins in the same compartment of the *Drosophila* wing. Genetica 60(1): 71–76. https://doi.org/10.1007/bf00121460

Truong Q-T, Argyoganendro BW, Park HC (2014) Design and demonstration of insect mimicking foldable artificial wing using four-bar linkage systems. Journal of Bionic Engineering 11(3): 449–458. https://doi.org/10.1016/s1672-6529(14)60057-3

Villemant C, Simbolotti G, Kenis M (2007) Discrimination of *Eubazus* (Hymenoptera, Braconidae) sibling species using geometric morphometrics analysis of wing venation. Systematic Entomology 32(4): 625–634. https://doi.org/10.1111/j.1365-3113.2007.00389.x

Wappler T, De Meulemeester T, Murat Aytekin A, Michez D, Engel MS (2012) Geometric morphometric analysis of a new Miocene bumble bee from the Randeck Maar of southwestern Germany (Hymenoptera: Apidae). Systematic Entomology 37(4): 784–792. https://doi.org/10.1111/j.1365-3113.2012.00642.x

Werneburg I, Wilson LA, Parr WC, Joyce WG (2015) Evolution of neck vertebral shape and neck retraction at the transition to modern turtles: an integrated geometric morphometric approach. Systematic Biology 64(2): 187–204. https://doi.org/10.1093/sysbio/syu072

## Supplementary material 1

**Images of hind wings.**

Authors: Jing Ren, Ming Bai, Xing-Ke Yang, Run-Zhi Zhang, Si-Qin Ge

Data type: Species data



Link: https://doi.org/10.3897/zookeys.685.13084.suppl1

## Supplementary material 2

**Sample information.**

Authors: Jing Ren, Ming Bai, Xing-Ke Yang, Run-Zhi Zhang, Si-Qin Ge

Data type: Specimens data



Link: https://doi.org/10.3897/zookeys.685.13084.suppl2

## Supplementary material 3

**Coordinates data of landmarks.**

Authors: Jing Ren, Ming Bai, Xing-Ke Yang, Run-Zhi Zhang, Si-Qin Ge

Data type: Distribution data



Link: https://doi.org/10.3897/zookeys.685.13084.suppl3

ZooKeys 685: 151–159 (2017)
doi: 10.3897/zookeys.685.13398
http://zookeys.pensoft.net

RESEARCH ARTICLE

A peer-reviewed open-access journal
ZooKeys
Launched to accelerate biodiversity research

# Further records of the deep-sea pandalid shrimp *Heterocarpus chani* Li, 2006 (Crustacea, Decapoda, Caridea) from southern India

Chien-Hui Yang[1], Appukuttannair Biju Kumar[2], Tin-Yam Chan[1,3]

**1** *Institute of Marine Biology, National Taiwan Ocean University, Keelung 20224 Taiwan, R.O.C.* **2** *Department of Aquatic Biology & Fisheries, University of Kerala, Thiruvananthapuram 695581, Kerala, India* **3** *Center of Excellence for the Oceans, National Taiwan Ocean University, Keelung 20224, Taiwan, R.O.C.*

Corresponding author: *Tin-Yam Chan* (tychan@ntou.edu.tw)

Academic editor: *S. De Grave* | Received 25 April 2017 | Accepted 2 June 2017 | Published 20 July 2017

*http://zoobank.org/CA6F790F-91F7-4BF1-8909-E5861EBBB735*

**Citation:** Yang C-H, Kumar AB, Chan T-Y (2017) Further records of the deep-sea pandalid shrimp *Heterocarpus chani* Li, 2006 (Crustacea, Decapoda, Caridea) from southern India. ZooKeys 685: 151–159. https://doi.org/10.3897/zookeys.685.13398

## Abstract

The commercial deep-sea caridean shrimp *Heterocarpus gibbosus* Spence Bate, 1888 has long been recorded from India and constitutes an important part of the catches in the context of the further development of deep-sea fisheries in India. A recent survey in some deep-sea fishing ports in southern India, however, revealed that all material previously reported as "*H. gibbosus*" is actually a misidentification of its closely related species *H. chani* Li, 2006, which has only recently been reported from India. More detailed comparisons allowed the discovery of more distinctive characters between *H. chani* and *H. gibbosus*.

## Keywords

*Heterocarpus chani*, deep-sea, shrimp, India

## Introduction

The commercial deep-sea caridean shrimp *Heterocarpus gibbosus* Spence Bate,1888 was thought to be widely distributed in the Indo-West Pacific (Chace 1985, Crosnier 1988) and in some areas as being rather abundant (Holthuis 1980, Chan and Yu 1987). Recently, however, this species was split into four species (Li 2006, Yang et al. 2010) mainly based on the height of the rostral crest, the development of the boss on the third abdominal somite

and the length of the exopod of the third maxilliped. Specimens previously referred to this species from the western Pacific are not the true *H. gibbosus* but are instead *H. abulbus* Yang, Chan & Chu, 2010 and *H. corona* Yang, Chan & Chu, 2010. These two western Pacific species are rather different from *H. gibbosus* in having either a much lower or higher rostral crest (the low crest species, *H. abulbus* also has an indistinct abdominal boss). The other recently described species, *H. chani* Li, 2006, is very similar to *H. gibbosus* but with a much shorter exopod of the third maxilliped (Li 2006, Yang et al. 2010) and is currently mainly known from the South China Sea and the Philippines (Li and Chan 2013) as well as a short report from India (Kuberan et al. 2015). Other than co-occurring together with *H. chani* in the South China Sea and the Philippines, *H. gibbosus* is presumed to be the main species of this species complex in the Indian Ocean.

*Heterocarpus gibbosus* has long been reported from India (e.g., Wood-Mason and Alcock 1892, Alcock 1901, Kemp and Swell 1912, George and Rao 1967, Suseelan 1976, Radhakrishnan et al. 2012, Samuel et al. 2016, see also synonymy list in Fransen 2006) and now forms a major part of the catch in the deep-sea fisheries of India (e.g., Rajan et al. 2001, Kurup et al. 2008, Radhika Rajasree and Madhusoodana Kurup 2011, Rajool Shanis et al. 2012, 2014). However, recently a brief local technical report recorded *H. chani* from southern India (Kuberan et al. 2015). A visit of the third author (TYC) to the deep-sea fishing ports in southern India also found that the abundant materials identified there as "*H. gibbosus*" are actually all *H. chani*. The present work reports this finding. Detailed comparisons of these two species also revealed more differences between them. The material examined is deposited in the Department of Aquatic Biology and Fisheries, University of Kerala (DABFUK), National Taiwan Ocean University (NTOU), Lee Kong Chian Natural History Museum, Singapore (ZRC) and Oxford University Museum of Natural History (OUMNH). Additional materials for comparisons are those reported from the Philippines in Li and Chan (2013) and deposited in NTOU, with 69 specimens of *H. gibbosus* and 66 specimens of *H. chani*. Size measurements given are carapace length (cl) measured dorsally from the postorbital margin to the posterior margin of the carapace. Partial sequences of mitochondrial cytochrome c oxidase I (COI) gene data were generated by following the methods outlined in Yang et al. (2010).

## Taxonomy

**Family Pandalidae Haworth, 1825**
**Genus *Heterocarpus* A. Milne-Edwards, 1881**

***Heterocarpus chani* Li, 2006**
Figs 1–3

*Heterocarpus chani* Li, 2006: 362, figs 1–4 (type locality: Philippines).—Yang et al. 2010: 207, fig. 5E.—De Grave and Fransen 2011: 442.—Li and Chan 2013: 133, fig. 1B.—Kuberan et al. 2015: 27, fig. 1.

(?) *Heterocarpus gibbosus*—George and Rao 1967: 331.—Suseelan 1974: 50, fig. 2-Heterocarpus gibbosus. (*non* Spence Bate, 1888)

(?) *Heterocarpus* ? *gibbosus*—Wood-Mason & Alcock, 1892: 368, fig. 6. (*non* Spence Bate, 1888)

**Material examined.** Sakthikulangara fishing harbor, Kollam district, Kerala, 20 March 2017, 1 ♂ cl 28.65 mm, 2 ovigerous ♀♀ cl 29.9–31.2 mm (NTOU M02049); 1 ♂ cl 33.3 mm, 3 ovigerous ♀♀ cl 26.8–35.8 mm (NTOU M02050), 1 ovigerous ♀ cl 30.0 mm, 1 ♀ cl 24.2 mm (ZRC 2017.0892); 1 ♂ cl 21.3 mm (DABFUK/AR-DEN-30), 1 ovigerous ♀ cl 26.2 mm (DABFUK/AR-DEN-31); 1 ♂ cl 23.0 mm, 1 ovigerous ♀ cl 23.8 mm (OUMNH). Muttom fishing harbor, Tamil Nadu, 21 March 2017, 1 ♀ cl 20.6 mm (NTOU M02051).

**Diagnosis.** Rostrum far overreaching scaphocerite, 0.6–1.0 times as long as carapace. Rostrum dorsally armed with 7–10 teeth including 4–5 teeth on carapace posterior to orbital margin, ventrally armed with 10–16 teeth along entire length but with distal 2–3 teeth obscure. Rostral crest moderately elevated. Two lateral carinae on carapace, postorbital carina extending posteriorly almost to posterior margin of carapace and distinctly recurved downwards at posterior end. Branchiostegal carina sharp and extending posteriorly to 75–80% of carapace length (Figs. 2A–B). Abdominal tergites without spine, boss on third somite distinct and with lateral borders somewhat carinate, width 0.2–0.3 and length 0.7–0.8 times as long as somite (Fig. 3C); only pleura IV and V bearing posteroventral tooth. Telson bearing 4 pairs of dorsolateral and 3 pairs of distal spines. Maxilliped III with exopod very short, 0.2–0.3 times as long as antepenultimate segment (Fig. 2C). Pereiopod III with carpus and ischium bearing 0–2 spines, merus with 1–6 mesial and 10–15 lateral spines, dactylus 0.2–0.4 times as long as propodus. Pereiopod IV with carpus bearing 1–2 spines, merus with 1 distinct apical spine and 10–13 lateral spines, ischium with 2 spines. Pereiopod V with carpus bearing 0–1 spines, merus with 10–13 lateral spines, ischium without any spine (Fig. 2D–F).

**Coloration.** Body generally orange red to rose red, rostrum whitish in anterior half but with tip often reddish. Eyes dark brown. Basal parts of antennular and antennal flagella whitish (more so in former). Scaphocerite with distal part whitish. Ventral lateral carina of carapace sometimes whitish except at tip (i.e. branchiostegal spine). Posterior border of carapace and anterior margin of abdominal somite I whitish. Maxilliped III with penultimate segment and sometimes also distal part of antepenultimate segment whitish. Pereiopod I with posterior part of carpus and sometimes also anterior part of merus whitish. Longer pereiopod II with chela, carpus and anterior part of merus whitish. Shorter pereiopod II only with basal carpus and distal merus whitish. Pereiopods III with propodus, carpus and anterior 1/2-1/3 of merus whitish. Pereiopods IV and V with propodus, carpus, merus and sometimes even entire pereiopod whitish except for reddish dactylus. Eggs greenish brown.

**Distribution.** Only known with certainty from the South China Sea, Philippines and southern India, at depths of 382 (perhaps as shallow as 200 m, see Kuberan et al. 2015) to 888 m.

**Figure 1.** *Heterocarpus chani* Li, 2006, Sakthikulangara fishing harbor, SW India, ovigerous ♀ cl 29.9 mm (NTOU M02049).

**Remarks.** Although *Heterocarpus gibbosus* Spence Bate, 1888 (type locality: Bohol Sea, The Philippines, see Li et al. 2007, Anonymous 2009) has long been reported from India, going back to soon after the original description of the species (Wood-Mason and Alcock 1892). Although recently considered as an important catch in the local deep-sea fishery (e.g., Rajan et al. 2001, Kurup et al. 2008, Rajasree and Kurup 2011, Rajool Shanis et al. 2012, 2014), the abundant specimens observed in three deep-sea fishing ports in southern India (Sakthikulangara, Muttom and Tuticorin, only specimens kept as vouchers were listed in Material examined) all actually represent *H. chani* without exception. Thus, the brief record of *H. chani* in India by Kurberan et al. (2015) is confirmed. The southern Indian material of *H. chani* agrees well with that reported from the South China Sea and the Philippines (Li 2006, Li and Chan 2013). The only observed difference is the length of the rostrum being more frequently shorter in the Indian population. About half of the Indian specimens have the rostrum 0.6–0.7 times as long as the carapace in contrast to only about 1/10 of the comparative Philippines material with a shorter rostrum. Comparison of the COI sequences (657 bps) between the short (GenBank accession nos. MF149971–MF149973) and long rostral (MF149974) forms in the Indian material shows only 0.2–0.6% divergence, while genetic divergences between the Indian and Philippine materials (GQ302748, GQ302750, GQ302752, GQ302754) are 2.1–2.7 %. COI sequence divergences of less than 3% are generally considered to be intraspecific in decapod crustaceans (e.g.

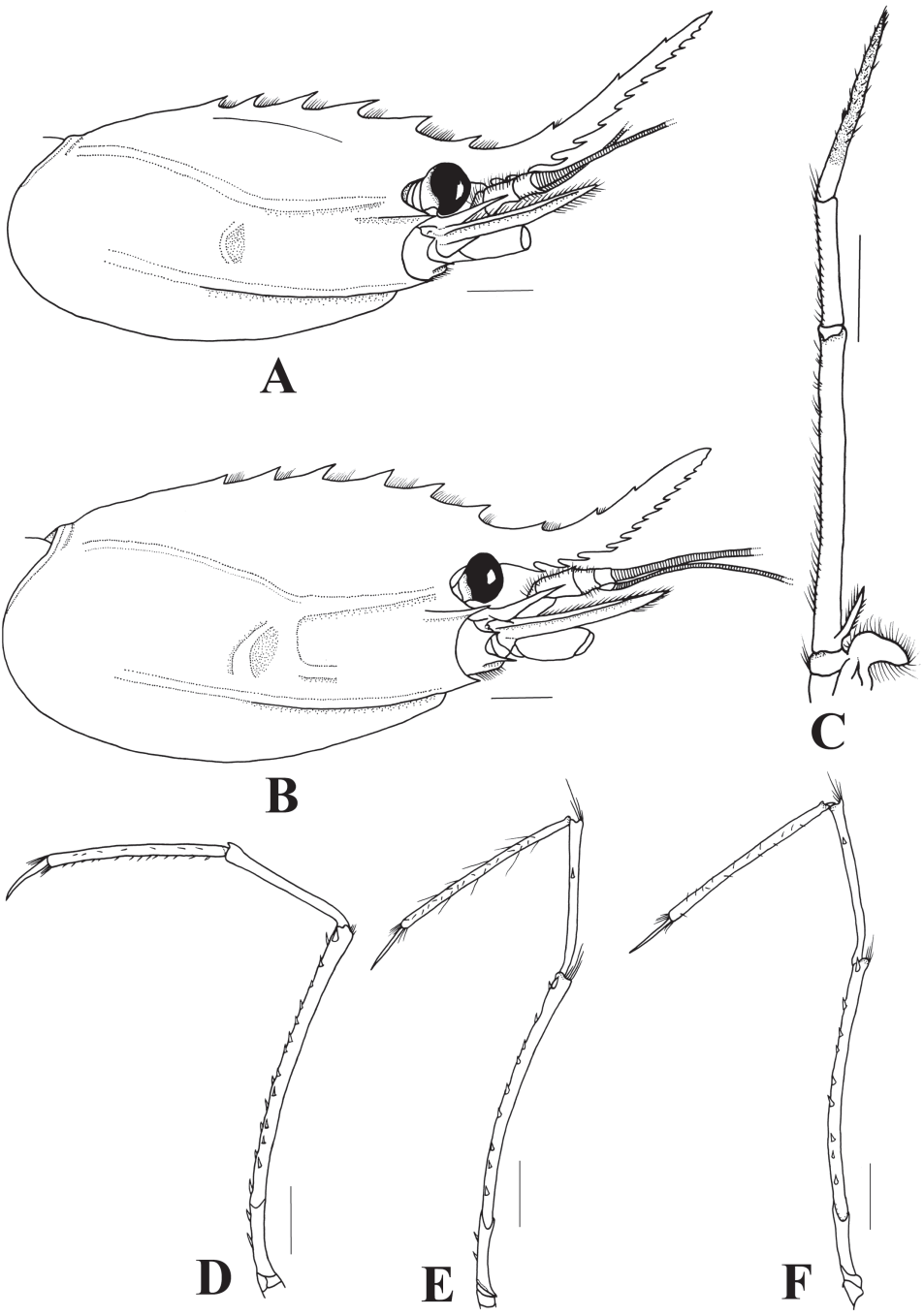


**Figure 2.** *Heterocarpus chani* Li, 2006, Sakthikulangara fishing harbor, SW India. **A, C–F** ovigerous ♀ cl 26.8 mm (NTOU M02050) **B** ovigerous ♀ cl 31.4 mm (NTOU M02050) **A–B** Carapace, lateral **C** right maxilliped III **D** right pereiopod III **E** right pereiopod IV **F** right pereiopod V. Scales = 5 mm.

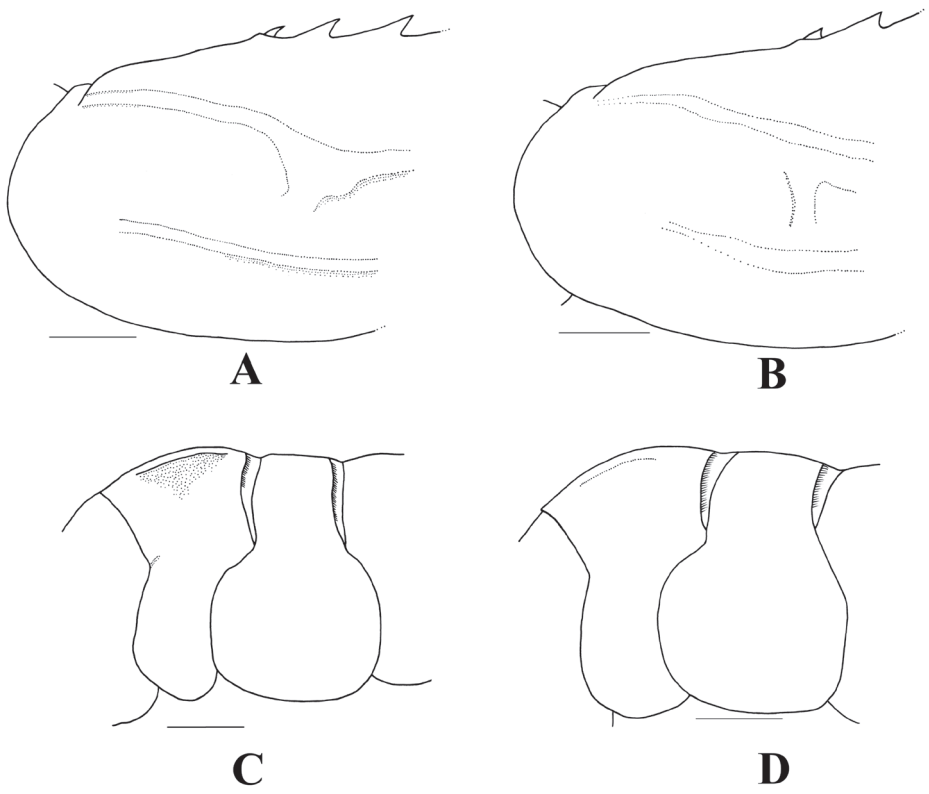


**Figure 3. A, C** *Heterocarpus chani* Li, 2006, Sakthikulangara fishing harbor, SW India, ovigerous ♀ cl 26.8 mm (NTOU M02050) **B, D** *H. gibbosus* Spence Bate, 1888, the Philippines, PANGLAO 2005, stn CP 2359, ♂ cl 25.9 mm (NTOU M00792) **A–B** posterior carapace, lateral **C–D** abdominal somites II and III, lateral. Scales = 5 mm.

Darling 2011, Vergamini et al. 2011, Yang et al. 2016). The coloration of the Indian material also generally agrees with that from the Philippines (Fig. 1, Li 2006: fig. 4, Yang et al. 2010: fig.5E, Li and Chan 2013: fig. 1B).

While *H. chani* exhibits a high genetic divergence from *H. gibbosus* (GQ302740, GQ302742, GQ302744, GQ302746, with 10.0–11.5% COI sequence divergence, also see Yang et al. 2010), the two species are morphologically very similar and mainly differ in the relative length of the exopod on the third maxilliped (Li 2006). More careful comparison of the present material reveals that there are three more, somewhat, subtle differences between these two species. The posterior end of the postorbital carina is distinctly ridged and recurved downwards in *H. chani* (Fig. 3A), but becomes rather indistinct and not bending downwards in *H. gibbosus* (Fig. 3B). The abdominal boss is more distinct and with the lateral borders ridged in *H. chani* (Fig. 3C) whilst in *H. gibbosus*, the abdominal boss is relatively less distinct and with the lateral borders not forming ridges (Fig. 3D). The posterior pereiopods each have a distinct red band on the anterior part of the merus in *H. gibbosus* (Li 2006: fig. 6, Yang et al. 2010: fig. 5B, Li

and Chan 2013: fig. 1C), while such red bands are lacking in *H. chani* (Fig. 1, Li 2006: fig. 4, Yang et al. 2010: fig. 5E, Li and Chan 2013: fig. 1B; Kuberan et al. 2015: fig. 1).

Although more differences are now enumerated between *H. chani* and *H. gibbosus*, it still cannot be deduced if the numerous reports of *H. gibbosus* from India in reality refer to that species or indeed solely represent *H. chani*, because all these records are too brief or did not list nor discuss any of the above distinctive characters. However, the "*H. gibbosus*" specimens from SW Cochin reported by George and Rao (1967) were described as having an abdominal boss with rather prominent median carination, and therefore likely represent *H. chani* instead. The "*Heterocarpus* ? *gibbosus*" illustrated by Wood-Mason and Alcock (1892: fig. 6), though lacking an abdominal boss, likely also represents *H. chani* since it has a shorter rostrum and with the posterior end of the postorbital carina sloping downwards. The rough line-drawing of "*Heterocarpus gibbosus*" provided in Suseelan (1974: fig. 2) also shows a posteriorly recurved downward postorbital carina. Thus, whether *H. gibbosus* truly occurs in India continues to be in need of confirmation.

## Acknowledgements

Grateful acknowledgement is extended to Peter K.L. Ng of the Lee Kong Chian Natural History Museum, Singapore for arranging the third author (TYC) to visit southern India and making the present study possible. This work was supported by grants from the Ministry of Science and Technology, Taiwan, R.O.C.

## References

Alcock A (1901) A Descriptive Catalogue of the Indian Deep-Sea Crustacea Decapoda Macrura and Anomala, in the Indian Museum. Being a Revised Account of the Deep-Sea Species Collected by the Royal Indian Marine Survey Ship "Investigator", 286 pp., 3 Pls., Calcutta (Indian Museum).

Anonymous (2009) Opinion 2217 (Case 3389) *Heterocarpus gibbosus* Bate, 1888 (Crustacea, Decapoda, Pandalidae): replacement of the holotype by a neotype. Bulletin of Zoological Nomenclature 66(1): 91–92. https://doi.org/10.21805/bzn.v66i1.a11

Chace FA Jr (1985) The caridean shrimps (Crustacea: Decapoda) of the Albatross Philippine Expedition, 1970–1910, part 3: Families Thalassocarididae and Pandalidae. Smithsonian Contribution to Zoology 411: 1–143. https://doi.org/10.5479/si.00810282.411

Chan TY, Yu HP (1987) On the *Heterocarpus* shrimps (Crustacea: Decapoda: Pandalidae) from Taiwan. Bulletin of the Institute of Zoology Academia Sinica 26(1): 53–60.

Crosnier A (1988) Sur les *Heterocarpus* (Crustacea, Decapoda, Pandalidae) du sud-ouest de l'océan Indien. Remarques sur d'autres espèces ouest-pacifiques du genre et description de quatre taxa nouveaux. Bulletin du Muséum National d'Histoire Naturelle, Paris. 4(10): 57–103, Pls.1–4.

Darling JA (2011) Interspecific hybridization and mitochondrial introgression in invasive *Carcinus* shore crabs. PLoS ONE 6(3): e17828. https://doi.org/10.1371/journal.pone.0017828

De Grave S, Fransen CHJM (2011) Carideorum Catalogus: The recent species of the dendrobranchiate, stenopodidean, procarididean and caridean shrimps (Crustacea: Decapoda). Zoologische Mededelingen 85: 195–589.

Fransen CHJM (2006) Pandalidae (Crustacea: Decapoda) of the SONNE, VALDIVIA and METEOR expeditions 1977–1987 to the Red Sea and the Gulf of Aden. Senckenbergiana maritima 36(1): 51–82. https://doi.org/10.1007/BF03043702

George MJ, Rao PV (1967) On some Decapod Crustaceans from the south-west coast of India. In: Symposium Series of the Marine Biological Association of India. No. 2. Proceedings Symposium on Crustacea, Part 1: 327–336, Tabs. 1–2.

Holthuis LB (1980) FAO species catalogue, Vol.1. Shrimps and prawns of the world. An annotates catalogue of species of interest to fisheries. FAO Fisheries Synopsis, 125/1, Rome, 261 pp.

Kemp S, Seweli RBS (1912) Notes on Decapoda in the Indian Museum. III. "The Species obtained by R.I.M.S.S. 'Investigator' during the Survey Season, 1910-11. Records of the Indian Museum 7: 15–32, PI. 1.

Kuberan G, Chakraborty RD, Purushothaman GM (2015) A new record of deep-sea caridean shrimp *Heterocarpus chani* (Decapoda: Pandalidae) from southern coast of India. Marine Fisheries Information Service; Technical and Extension Series 226: 27.

Kurup BM, Rajasree R, Venu S (2008) Distribution of deep sea prawns off Kerala. Journal of the Marine Biological Association of India 50(2): 122–126.

Li X (2006) Additional pandaloid shrimps from the South China Sea (Crustacea: Decapoda: Caridea), with description of new species. The Raffles Bulletin of Zoology 54(2): 36–372.

Li X, Chan TY (2013) Pandalid shrimps (Crustacea, Decapoda, Caridea) collected from the Philippines PANGLAO 2005 deep-sea expedition. In: Ahyong ST, Chan TY, Corbari L, Ng PKL (Eds) Tropical Deep-Sea Benthos 27, Muséum national d'Histoire naturelle, Paris, 129–154.

Li X, Chan TY, Ng PKL (2007) *Heterocarpus gibbosus* Bate, 1888 (Crustacea, Decapoda, Pandalidae): proposed replacement of the holotype by a neotype. Bulletin of Zoological Nomenclature 64(3): 155–159.

Radhakrishnan EV, Deshmukh VD, Maheswarudu G, Josileen J, Dineshababu AP, Philipose KK, Sarada PT, Pillai SL, Saleela KN, Chakraborty R, Dash G, Sajeev CK, Thirumilu P, Sridhara B, Muniuyappa Y, Sawant AD, Vaidya NG, Johny RD, Verma JB, Baby PK, Unnikrishnan C, Ramachandran NP, Vairamani A, Palanichamy A, Radhakrishnan M, Raju B (2012) Prawn fauna (Crustacea: Decapoda) of India – An annotated checklist of the Penaeoid, Segestoid, Stenopodid and Caridean prawns. Journal of Marine Biological Association of India 54(1): 50–72.

Rajan KN, Nandakumar G, Chellappan K (2001) Innovative exploitation of deepsea Crustacean along the Kerala coast. Marine Fisheries Information Service; Technical and Extension Series 168: 1–11.

Rajasree SRR, Kurup BM (2011) Food and feeding habits of deepsea pandalid prawns *Heterocarpus gibbosus*, Bate 1888 and *Heterocarpus woodmasoni*, Alcock off Kerala, south India. Indian Journal of Fisheries 58(3): 45–50.

Rajool Shanis CP, Akhilesh KV, Manjebrayakath H, Ganga U, Pillai NGK (2012) Shrimps of the family Pandalidae (Caridea) from Indian waters, with new distributional record of *Plesionika adensameri* (Balss, 1914). Journal of the Marine Biological Association of India 54(1): 45–49.

Rajool Shanis CP, Salim SS, Manjebrayakath H, Ganga U, Manjusha U, Pillai NGK (2014) Deep-sea shrimp fishery operations in Kerala coast: problems and prospects. International Journal of Fisheries and Aquatic Studies 1(6): 237–242.

Samuel VKD, Sreeraj CR, Krishnan P, Parthiban C, Sekar V, Chamundeeswari K, Immanuel T, Shesdev P, Purvaja R, Ramesh R (2016). An updated checklist of shrimps on the Indian coast. Journal of Threatened Taxa 8(7): 8977–8988. https://doi.org/10.11609/jott.2628.8.7.8977-8988

Spence Bate, C (1888). Report on the Crustacea Macrura collected by the Challenger during the years 1873-76. Report on the Scientific Results of the Voyage of H.M.S."Challenger" during the years 1873–76 24: i-xc-1–942, Plates 1–157.

Suseelan C (1976) Observations on the deep-sea prawn fishery off the South-West coast of India with special references to pandalids. Journal of the Marine Biological Association of India 16: 491–511, figs 1–7.

Vergamini FG, Pileggi LG, Mantelatto FL (2011) Genetic variability of the Amazon River prawn *Macrobrachium amazonicum* (Decapoda, Caridea, Palaemonidae). Contributions to Zoology 80(1): 67–83.

Wood-Mason J, Alcock A (1892) Natural History Notes from H. M. Indian Marine Survey Steamer 'Investigaotr', Commander R.F. Hoskyn, R.N., commanding. Ser. II, No. 1. On the Results of Deep-sea Dredging during the Season 1890-91. Annals and Magazine of Natural History 9(6): 265–275, 358–370, Pls. 14-15, figs 1–6.

Yang CH, Chan TY, Chu KH (2010) Two new species of the "*Heterocarpus gibbosus* Bate, 1888" species group (Crustacea: Decapoda: Pandalidae) from the western Pacific and north-western Australia. Zootaxa 2372: 206–220.

Yang CH, Tsuchida S, Fujikura K, Fujiwara Y, Kawato M, Chan TY (2016) Connectivity of the squat lobsters *Shinkaia crosnieri* (Crustacea: Decapoda: Galatheidae) between cold seep and hydrothermal vent habitats. Bulletin of Marine Science 92(1): 17–31. https://doi.org/10.5343/bms.2015.1031